Aspects of epimuscular myofascial force transmission

a physiological, pathological and comparative-zoological approach

Hanneke J.M. Meijer

VRIJE UNIVERSITEIT

Aspects of epimuscular myofascial force transmission

a physiological, pathological and comparative-zoological approach

ACADEMISCH PROEFSCHRIFT

ter verkrijging van de graad Doctor aan
de Vrije Universiteit Amsterdam,
op gezag van de rector magnificus
prof.dr. L.M. Bouter,
in het openbaar te verdedigen
ten overstaan van de promotiecommissie
van de faculteit der Bewegingswetenschappen
op donderdag 29 november 2007 om 13.45 uur
in de aula van de universiteit,
De Boelelaan 1105

door

Hanneke Johanna Maria Meijer

geboren te Beek en Donk

promotor: prof.dr. P.A.J.B.M. Huijing

Contents

1

Introduction

In vertebrates, locomotion is the resultant of force transmission from the muscle fibre on to the bone. Upon activation of a muscle, active muscle force is generated by the cycling of cross-bridges between the actin and myosin filaments in the sarcomeres. Sarcomeres are connected to each other in series at the Z-lines, forming long myofibrils. At least at one end of the muscle fibre, tendon collagen fibres attach to invaginations of the sarcolemma-basal lamina complex. Via transsarcolemmal molecules and the cytoskeleton, this complex is attached to the thin filaments of the final sarcomeres of the myofibril. Such 'myotendinous' junctions (MTJ) (Tidball 1991; 1985; Trotter 2002) ensure the transmission of muscle force onto the tendon and are the most recognized pathway for transmission of muscle force onto the bony skeleton. However, recent work has shown that additional pathways exist via which muscle force is transmitted eventually onto the bone. Such transmission is referred to as *myofascial force transmission* (Huijing *et al.* 1998).

Pathways of myofascial force transmission

i) Intramuscular myofascial force transmission

Force generated by sarcomeres is transmitted also onto the actin filaments of the subsarcolemmal cytoskeleton by structural proteins such as desmin at the Z-band. Two types of molecules connect the cytoskeleton to two types of transsarcolemmal protein complexes (Berthier & Blaineau 1997; Huijing & Jaspers 2005; Rando 2001). Figure 1 gives a generalized schematic overview of the two transsarcolemmal pathways. (1) Via dystrophin, the sub-sarcolemmal cytoskeleton is connected to the transsarcolemmal sarcoglycans. This system is referred to as the dystroglycan complex. (2) Talin connects the sub-sarcolemmal cytoskeleton to the integrins at the sarcolemma. The dystroglycan complex as well as the integrins is connected to laminin of the basal lamina. Laminin is also connected to the collagen IV reinforcement of the basal lamina. The latter in its turn is connected to the endomysial-perimysial network via structural proteins and collagen fibrils (Huijing & Jaspers 2005; Passerieux *et al.* 2006).
It is by shearing of these connections that force is transmitted via these pathways onto the endomysium (Huijing 2007; Street & Ramsey 1965; Street 1983). The endomysium enveloping the muscle fibre has been shown to be continuous with the endomysia of adjacent fibres, as well as with the perimysium and epimysium (Jarvinen *et al.* 2002; Nishimura *et al.* 1996a; Nishimura *et al.* 1996b; Trotter & Purslow 1992). Together they form a network of connective tissue within the muscle in which the muscle fibres, fascicles and whole muscle are embedded (Passerieux *et al.* 2006). Thus, when muscle force is transmitted from the muscle fibre onto the endomysium, it may be transmitted throughout the entire muscle. Such transmission is referred to as *intramuscular myofascial force transmission* (Huijing 1999a).

Huijing (Huijing *et al.* 1998) showed the occurrence of such transmission by cutting the different distal tendons of rat extensor digitorum longus muscle (EDL). After tenotomising selected heads of EDL muscle, active force exerted by the different heads could be only transmitted at the part of the muscle that still was connected to the force transducer. Consequently, muscle force generated within the muscle fibres can be transmitted myofascially onto the muscles' tendon via the intramuscular network of connective tissue, and thus without passing at least one of the muscle fibres' myotendinous junctions.
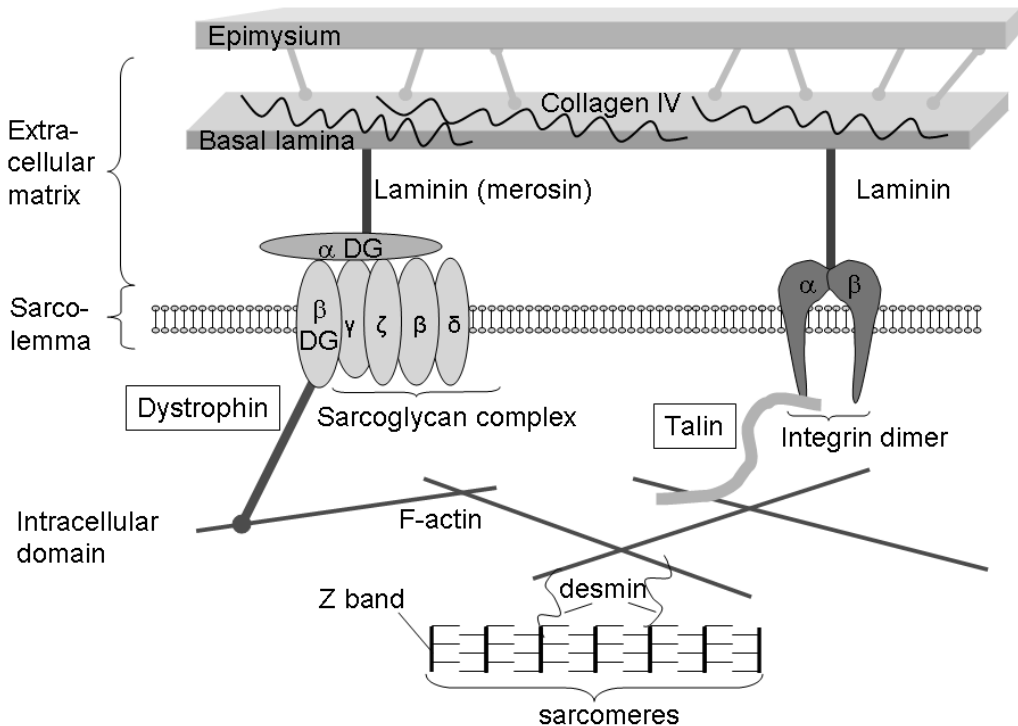
Figure 1. Schematic generalized overview of supramolecular organization of transsarcolemmal connections between the cytoskeleton and the endomysium. Two parallel pathways connect the cytoskeleton to the endomysium: 1) via dystrophin, the cytoskeleton is connected to the dystroglycan complex, and 2) via talin the cytoskeleton is connected to the integrin complex. Both the dystroglycan and integrin complex are connected to the basal lamina.

For a muscle isolated from surrounding tissues, muscle fibre force can only be transmitted via myotendinous or intramuscular myofascial pathways to the proximal and distal tendons. However, *in vivo,* muscles are embedded within connective tissues. At the epimysium, the muscles' intramuscular stroma is continuous with that of other muscles as well as with other non-muscular connective tissues. Thus, via the epimysium, muscle fibre force may be transmitted onto surrounding connective tissues and muscles via the continuous

stroma of connective tissues. This is referred to as *epimuscular myofascial force transmission* (Huijing 2007*)*. Two potential pathways for epimuscular myofascial force transmission can be distinguished:

ii) Intermuscular myofascial force transmission

Anatomical investigations on the rat lower limb have shown that the intramuscular myofascial stroma from adjacent muscles is continuous; the epimysium of a muscle is connected to the epimysia of neighbouring synergistic muscles. Cross-sections of the rat anterior crural compartment (Maas *et al.* 2001) show that the intramuscular connective tissue of tibialis anterior muscle (TA) is continuous with, and can not be easily distinguished from, that of EDL. The continuous intermuscular network at the interface between the muscles becomes visible by softly pulling muscles apart. Often, these structures are referred to as 'loose' connective tissue because they appear weak and can be easily broken by blunt dissection (Huijing & Baan 2001a). However, myofascial force transmission is hypothesized to occur due to shearing of myofascial connections. During shearing, the direction and magnitude of force applied to myofascial connections is different from that during blunt dissection. Therefore it is hypothesized that the intermuscular myofascial connections are sufficiently stiff during shearing to transmit forces. Thus, intermuscular myofascial connections enable force to be transmitted directly between adjacent (synergistic) muscles via their epimysia. Such transmission is referred to as *intermuscular myofascial force transmissions* (Huijing & Baan 2001a)

iii) Extramuscular myofascial force transmission

When muscle force is transmitted from a muscle onto or via non-muscular connective tissue structures, it is classified as *extramuscular myofascial force transmission* (Huijing & Baan 2001b*)*. Examples of such extramuscular connective tissue structures are structures delimiting the compartment, such as compartment and general fasciae, intermuscular septa, periost, interosseal membranes, epitendinous tissues and connective tissues reinforcing delicate nerves, lymph and blood vessels (Huijing 2007; Rijkelijkhuizen *et al.* 2005; Yucesoy *et al.* 2003a). Particularly the latter category of extramuscular connections is of special importance: the collagen reinforcement of blood and lymph vessels and nerves, referred to as the neurovascular tract, is connected to the muscles' intramuscular stroma (Huijing 2003; Maas *et al.* 2001). Such continuity indicates that the connective tissues of a compartment should be considered as unit, and that force can be transmitted between muscle fibres located in different muscles via inter- as well as extramuscular myofascial pathways.

Functional consequences of myofascial force transmission

For active or passive muscles within their natural context of connective tissue, loads are exerted on the muscle via inter- and extramuscular myofascial pathways. These myofascially transmitted forces act on the muscle in addition to myotendinous ones. Consequently, forces exerted at the origin and insertion of the muscle usually are not equal (Huijing *et al.* 1998). For the rat anterior crural compartment, it was found that force exerted at the origin and insertion of EDL within an intact compartment is unequal at most muscle lengths (Huijing & Baan 2001b; Maas *et al.* 2004). Therefore, a difference in forces exerted at the origin and insertion of a muscle is taken as evidence for epimuscular transmission of forces (*i.e.* via non-myotendinous pathways). However, for a muscle within an intact compartment, the individual contributions of inter- and extramuscular myofascial pathways can only be estimated by removing one pathway.

Via myofascial pathways, force has been shown to be transmitted between synergistic muscles in the rat anterior crural compartment (Huijing & Baan 2003; Maas *et al.* 2004). More recently, it was shown that myofascial force transmission also occurs between antagonistic muscles (Huijing *et al.* 2007), even if located in compartments at opposites sides of the lower leg (Rijkelijkhuizen *et al.* 2007). Such transmission indicates that morphologically defined muscles, both synergists and antagonists, can not be considered as independent actuators.

The work of Huijing, Yucesoy and Maas has shown that the magnitude and direction of the myofascially transmitted load(s) are co-determined by muscle length and the position of the muscle relative to its surroundings (Huijing & Baan 2003; Maas *et al.* 2001; Maas *et al.* 2003a; Maas *et al.* 2003c; Maas *et al.* 2004; Yucesoy *et al.* 2002b; Yucesoy *et al.* 2006) as these parameters affect the stiffness and possibly orientation of the myofascial pathways. The exertion of a myofascial load on a muscle means that shortening of the sarcomeres is not only limited by the loads imposed on them by sarcomeres in series, but also by loads exerted by myofascial connections. These myofascial loads are not distributed equally on all sarcomeres within the muscle fibres or on all muscle fibres of the muscle. Therefore, the exertion of myofascial loads on the muscle is hypothesized to create or enhance distributions in sarcomere lengths within the muscle fibre as well as the distribution of mean fibre sarcomere lengths throughout the muscle, (*i.e.* parallel distribution in sarcomere length, Maas *et al.* 2003a; Yucesoy *et al.* 2003a; Yucesoy *et al.* 2005). Changes in distributions in sarcomere lengths will affect length-force characteristics by affecting the range of active force exertion. An increase in the serial distribution in sarcomere lengths, as well as an enhanced parallel distribution in sarcomere length have been associated with an increase in the length range of active force exertion and a decrease in optimal force (Ettema & Huijing 1994b; Willems & Huijing 1994). Finite element modelling of muscles with inter- and extramuscular myofascial pathways using a linked fibre-matrix mesh model (Yucesoy *et al.* 2002a) has shown that enhanced distributions in sarcomere lengths may arise as a result of myofascial force transmission via inter- and extramuscular connective tissues (Yucesoy *et al.* 2002b; Yucesoy *et al.* 2003a; Yucesoy *et al.* 2006). Altered length-force characteristics have been observed for

muscles within an intact compartment (Huijing & Baan 2001b; Huijing *et al.* 2003; Maas *et al.* 2003c) and are therefore hypothesized to result from myofascially induced increased distributions in sarcomere lengths.

Clinical implications of myofascial force transmission

In clinical studies, considering muscles as units capable of mechanical interaction with other muscles via myofascial pathways has proven fruitful. In transfer surgeries to alleviate undesirable joint positions, muscles are detached from their insertion and reattached to another location, to alter the range of movement around the joint. Smeulders and Kreulen (Kreulen *et al.* 2003; Smeulders & Kreulen 2007) investigated the implications of tendon transfer surgery in patients with cerebral palsy. After severing the distal tendon of the flexor carpi ulnare (FCU), they found that shortening of the muscle was only minimal upon stimulation, but was increased after the muscle belly was partially dissected free from its surroundings. In addition, tenotomised FCU is lengthened as the wrist is extended (Kreulen *et al.* 2003). This indicates that via epimuscular myofascial pathways forces are exerted on the muscle that affect the range of movement, even after tenotomy. Also, Riewald and Delp (1997) found that after detachment of the rectus femoris muscle from the patella and reattachment to a flexor site of the knee, the muscle still generated a knee extension moment on stimulation. Such surprising results can only be described in myofascial terms; myofascial connections between the rectus femoris muscle belly and adjacent synergists still enables the transmission of an extension moment on the knee.

The above described experimental evidence and clinical observations on the effects of myofascial force transmission on muscles have shown unequivocally that muscles are not independent actuators, but are capable of significant mechanical interaction. The functional relevance of such mechanical interaction between muscles via myofascial paths *in vivo* is unknown. Therefore, the main aim of this thesis is to gain more insight in the functional relevance of epimuscular myofascial force transmission by analyzing effects of factors that are thought to be of importance in the *in vivo* situation. Secondly, as myofascial force transmission depends upon an intact network of connective tissue, the effect of a lack of elements constituting the chain between contractile apparatus and the collagen reinforcement of the extracellular matrix on myofascial force transmission are investigated. Thirdly, the presence of epimuscular myofascial force transmission is investigated from a comparative-zoological perspective in a group of animals thought to possess very few connective tissues, the insects. This research is inspired by Pond (1982), who noted that "[for adult insects] each muscle was anatomically distinct and only very loosely attached to adjacent muscles. Even its constituent fibres could easily be teased apart, and each one could, and apparently in life often did, contract independently of its neighbours." This would suggest

that myofascial force transmission is of less importance in insects, an assumption that is inconsistent with our current knowledge on myofascial force transmission.

Thesis outline

-In **Chapter 2**, the origin of the myofascial interaction between synergistic EDL and TA+EHL in the rat anterior crural compartment is investigated by progressively dissecting the myofascial pathways.

-Effects of submaximal stimulation frequencies on myofascial force transmission are investigated for anterior crural muscles within the rat lower limb in **Chapter 3**.

-In **Chapter 4**, effects of lengthening of the whole group of anterior crural muscles on myofascial force transmission between synergistic EDL and TA+EHL, as well as on myofascial force transmission between anterior crural muscles and antagonistic peroneal muscles were investigated.

-In **Chapter 5**, myofascial force transmission between submaximally active synergistic and antagonistic muscle groups is investigated for lengthening of the anterior crural muscle group.

-In **Chapter 6**, myofascial force transmission is investigated in dystrophin-deficient (*mdx*) mice. In contrast to human patients suffering from dystrophin-deficiency (Duchenne Muscular Dystrophy (DMD)), *mdx* mice display increased levels of utrophin. Utrophin is a dystrophin homolog and upregulation of utrophin is reported to result in a less severe dystrophic phenotype. However, despite the milder phenotype, *mdx* mice show signs of muscle degeneration. It is therefore hypothesized that *mdx* muscles suffer from a decreased importance of myofascial force transmission due to less stiff intramuscular myofascial pathways.

-A further exploration of myofascial force transmission in mice is the subject of **Chapter 7,** in which the effects of length of the TA+EHL complex on myofascial force transmission in EDL are investigated for healthy mice. These results are compared to those of added lengthening of TA+EHL in rats.

-Chapter 8 discusses the presence and extent of myofascial force transmission in insects. It has been suggested by Pond (1982) that insects posses very little connective tissue, and therefore questions have arisen regarding the significance of myofascial force transmission in invertebrates. Therefore, in this chapter it is investigated whether myofascial force transmission affects the flight muscles of the desert locust *Schistocerca gregaria*.

-Finally, in **Chapter 9,** the experimental results of this thesis are reviewed, as well as their implications for our understanding of force exertion of healthy and pathological muscles. In addition, the possible evolutionary origin and functions of myofascial force transmission will be dealt with. Finally, in an attempt at integrating multiple scientific disciplines, the role of myofascial force transmission in reconstructing animals long gone extinct (the field of vertebrate palaeontology, one of the major interests of the author) will be discussed.

2

Intermuscular interaction between synergists in rat originates from both intermuscular and extramuscular myofascial force transmission

Huub Maas, Hanneke J.M. Meijer & Peter A. Huijing

Abstract

The purpose of the present study is to investigate the origin of mechanical interactions between the rat extensor digitorum longus (EDL) muscle and the grouped tibialis anterior and extensor hallucis longus muscles (TA+EHL). The proximal and distal tendons of EDL as well as the tied distal tendons of TA+EHL were transacted and connected to force transducers. Connective tissues at the muscle bellies of the anterior crural compartment were left intact. Supramaximal stimulation of the common peroneal nerve activated all muscles maximally and simultaneously. Length-isometric force characteristics of distal TA+EHL were assessed. Simultaneously, forces exerted at the proximal and distal tendons of EDL, kept at constant muscle-tendon complex length and position, were measured. Intermuscular interaction was tested in two conditions: (a) after full longitudinal compartmental fasciotomy, and (b) after blunt dissection of the intermuscular connective tissue linkages between EDL and TA+EHL. Note that in the latter condition, intermuscular myofascial pathways were eliminated. In the initial condition, lengthening TA+EHL by 12 mm increased proximal (by 0.14 N, i.e. 9.5%) and decreased distal EDL force (by 0.21 N, i.e. 11.8%), despite the fact that EDL muscle-tendon complex length was kept constant. Blunt dissection decreased TA+EHL and distal EDL forces at low TA+EHL lengths only, while proximal EDL force decreased for all TA+EHL lengths tested. The dissection caused no changes in the TA+EHL length effects on proximal EDL force. In contrast, the amplitude of change in the distal EDL force curve decreased significantly (by 39%) subsequent to blunt dissection. It is concluded that mechanical interaction between synergists originates from both intermuscular as well as extramuscular connective tissues. The highest contribution, however, should be ascribed to the extramuscular pathway.

Abbreviations used in this paper

EDL   m. extensor digitorum longus
EHL   m. extensor hallucis longus
FCU   m. fl exor carpi ulnaris
Fma   active force
Fmp   passive force
lm+t   muscle-tendon complex length
TA   m. tibialis anterior

Introduction

Recently, it was shown that adjacent synergistic muscles do not function as independent units with regard to force transmission. A substantial difference between force exerted at the origin and force exerted at the insertion of the rat extensor digitorum longus muscle (EDL), embedded within an intact compartment, was reported (Huijing & Baan 2001b; Maas *et al.* 2001). Length changes as well as changes in the relative position of a single muscle-tendon complex did not only result in force changes in the muscle that was manipulated, but also in differences in force exerted at the tendons of adjacent fixed synergists (Maas *et al.* 2001) (Huijing & Baan 2003; Maas *et al.* 2003b; Maas *et al.* 2004). The underlying mechanism for such mechanical interaction of a muscle with its direct environment is force transmission to the bone via pathways other than the muscular origin and insertion, i.e. myofascial force transmission (Huijing 1999a). Two separate pathways for such force transmission have been distinguished (Huijing 1999b; Huijing & Baan 2001b): intermuscular and extramuscular. If force is transmitted between the stromata of two adjacent muscles via the continuous connective tissue at their muscle belly interface (Huijing & Baan 2001a; Huijing *et al.* 2003; Maas *et al.* 2001), it is classified as intermuscular myofascial force transmission. Although this connective tissue can be easily broken by blunt dissection and has been characterized as 'loose', it appears to be stiff and strong enough to transmit force if loaded under physiological conditions (e.g. shear). If force is transmitted between the intramuscular connective tissue network of a muscle and non-muscular structures within a compartment, it is classified as extramuscular myofascial force transmission. Examples of extramuscular connective tissues (Huijing & Baan 2001b; Huijing & Baan 2003; Huijing *et al.* 2003; Maas *et al.* 2001; Rijkelijkhuizen *et al.* 2005) are: (1) Connective tissues that reinforce the nerves and blood vessels (i.e. the neurovascular tract) and connect them to the compartment walls. It has been shown that these extramuscular structures within the anterior crural compartment are sufficiently stiff to transmit force between EDL muscle and bone (Maas *et al.* 2003a). (2) Fascia forming the compartmental borders. Fasciotomy causes major changes in the origin-insertion EDL force difference (Huijing *et al.* 2003) (3) Epitendinous connective tissues, i.e. tissues around the tendons. Recently, even after substantial dissection to isolate the rat medial gastrocnemius muscle except for its interface with plantaris muscle, extramuscular force transmission via epitendinous tissues to the calcaneal bone was shown to be substantial for rat plantaris muscle (Rijkelijkhuizen *et al.* 2005). The term epimuscular myofascial force transmission is used to indicate transmission via inter- or extramuscular pathways, without distinction, as each involves force transmission via the muscle belly surface (i.e. the epimysium). The aim of the present study is to investigate the pathways of the mechanical interactions between muscles reported previously for rat EDL muscle and TA+EHL, i.e. tibialis anterior (TA) and extensor hallucis longus (EHL) muscles combined (Maas *et al.* 2001; Maas *et al.* 2004). Mechanical interaction is defined as changes in force exerted at the tendons of a fixed muscle due to changes in

muscle-tendon complex length of a synergistic muscle. It may appear obvious to describe this as intermuscular myofascial force transmission. However, preliminary results in rats have indicated such a mechanical interaction between antagonistic muscles that are located within adjacent compartments (Huijing 2002; Huijing 2004). The two compartments (anterior crural compartment and peroneal compartment) are separated by the anterior intermuscular septum (Huijing & Baan 2001a; Huijing 2003) and, thus, direct intermuscular connections between the muscular stromata of these muscles are not present. Therefore, such antagonistic intermuscular interaction must be classified as extramuscular myofascial force transmission. These results suggest that the mechanical interactions between EDL and TA+EHL may also be mediated by extramuscular myofascial pathways. In addition to intermuscular connections, EDL and TA+EHL are also connected to each other via extramuscular connective tissues (Huijing *et al.* 2003; Maas *et al.* 2001). Within an intact muscle compartment, the individual role of each pathway and each structure cannot be determined experimentally. Therefore, in the present experiment mechanical interactions between EDL and TA+EHL were assessed for two conditions of the anterior crural compartment: (1) with intact intermuscular connective tissue, as well as intact extramuscular connective tissues, except for the cut compartmental fascia, and (2) after disruption of the intermuscular EDL and TA+EHL interface, with only intact extramuscular connective tissues.

Materials and Methods

Surgical and experimental procedures were in strict agreement with the guidelines and regulations concerning animal welfare and experimentation set forth by Dutch law, and approved by the Committee on Ethics of Animal Experimentation at the Vrije Universiteit Amsterdam.

Male Wistar rats, *Rattus norvegicus albinus* (n = 8, body mass 298.8 g SD 4.4), were anesthetized using intraperitoneally injected urethane (initial dose 1.2 ml/100 g body mass, 12.5% urethane solution, extra doses were given if necessary, maximally 1.5 ml). To prevent hypothermia during surgery and data collection, the animals were placed on a heated water pad at approximately 37 ° C. Muscle temperature was controlled by an airflow (Holland Heating) around the muscle of 22 ° C (SD 0.5) and 80% (SD 2) humidity. Dehydration of muscle and tendon tissue was prevented by regularly irrigating the tissue with isotonic saline.

Surgical Procedures
Removing the skin and most of the biceps femoris muscle from the left hind limb exposed the anterior crural compartment, which envelopes the TA, EDL and EHL muscles. The anterior crural compartment was opened by full lateral fasciotomy (i.e. longitudinal section). Connective tissues between the muscle bellies of TA, EHL and EDL were left intact. The retinaculae at the ankle (i.e. the transverse crural ligament and the crural cruciate ligament) were severed to dissect the distal

tendons of EDL, TA and EHL. As it is difficult to measure force exerted by each tendon individually without friction between them, the four distal EDL tendons as well as the distal tendons of TA and EHL were tied together using polyester thread, with the knee and ankle joint at 90° and the metatarsophalangeal angle at 180°. The latter complex will be referred to as TA+EHL. The foot was firmly attached to a plastic plate using tie wraps. The femoral compartment was opened to position a metal clamp on the femur to secure the rat in the experimental apparatus. In addition, a small piece of the epicondylus lateralis, representing the origin of the EDL muscle, of the femur was cut to attach it to Kevlar thread. Within the femoral compartment, the tibial nerve and the sural branch of the sciatic nerve were cut as proximally as possible. The sciatic nerve with only the peroneus communis nerve branch left intact was dissected and cut.

Mounting the Animal in the Experimental Apparatus

The rat was placed on a platform in between force transducers which were mounted on single axis micropositioners. A metal clamp was used to secure the femur at a knee angle of approximately 100°. The foot was positioned in such a way that the ankle angle was 180°. The proximal tendon and the complex of distal tendons of EDL muscle as well as the distal tendons of the TA+EHL complex were connected to force transducers (BLH Electronica Inc., maximal output error ! 0.1%, compliance of 0.0162 mm/N) with Kevlar thread (diameter = 0.5 mm, tensile modulus = 58 GPA, 3.7% extension to breaking; Goodfellow). All tendons were connected directly to the force transducers which were positioned in the line of pull (fig. 1). Experimental data indicating that differences in force measured at the two force transducers of 1 0.7% cannot be ascribed to this measurement system have been reported previously [Maas et al., 2001].
The sciatic nerve was placed on a pair of silver electrodes. The nerve was prevented from dehydrating by covering it with paper tissue, saturated with isotonic saline, and covered by a thin piece of latex. Branches of the intact peroneus communis nerve innervate EDL, TA and EHL muscles and stimulation will therefore activate all three muscles simultaneously. In all experimental conditions, the sciatic nerve was stimulated supramaximally with the electrodes connected to a constant current source (3 mA, pulse width 100 ms).

Isometric Length-Force Characteristics of TA+EHL

Timing of stimulation of the nerve and A/D conversion (12-bit A/D converter, sampling frequency 1,000 Hz, resolution of force 0.01 N) were controlled by a special purpose microcomputer. Before acquiring data, the TA+EHL muscle complex was preconditioned by several isometric contractions (for stimulation protocol see below) at high length (i.e. near optimum length as indicated by a passive force) of TA+EHL until isometric forces at low (i.e. 7 mm below the high length) and high TA+EHL length were reproducible (Huijing & Baan 2001b). Values that deviated less than 4% were considered reproducible; a mean of 3.73% was measured.

For all experimental conditions, the EDL muscle-tendon complex was kept at a constant moderately low length. The proximal tendon of the EDL muscle was set to a position corresponding to a knee joint angle of approximately 100°. The distal tendons were brought to a position yielding a force of approximately 75% of distally measured optimal force (i.e. 1.8 N), which corresponds to approximately optimum length –3 mm (Maas *et al.* 2003c). Due to inter-individual variation in both muscle-tendon complex length (Δlm+t), as well as muscle relative position (Huijing & Baan 2003; Maas *et al.* 2004), rather large differences in the initial level of EDL forces occurred between experiments (1.19–1.64 N for EDL proximal and 1.60–1.90 N for EDL distal at Δlm+t TA+EHL = –10 mm). This introduces high standard deviations, but does not affect the statistical analysis, as ANOVA for repeated measures was used (see Treatment of Force Data and Statistics).

To collect length-force data, TA+EHL was lengthened distally with 1 mm increments starting at the muscle active slack length (i.e. the lowest length at which active force approaches zero) until approximately 2 mm over optimum length. Before each contraction, passive TA+EHL as well as EDL were brought to the desired length and relative position by moving their force transducers. Two twitches were evoked (200 ms apart) and passive force was determined approximately 200 ms after the second twitch. 100 ms later, the muscle was excited tetanically (pulse train 400 ms, frequency 100 Hz). Isometric force was measured during the tetanic contraction of the muscles. After each contraction, all muscles were allowed to recover below active slack length for minimally 2 min. The first set of length-force data was collected with the anterior crural compartment in the initial condition (fig. 1 A): i.e. after full lateral compartmental fasciotomy. Two sets of measurements were performed: (1) With the intermuscular connective tissues between the muscle bellies intact. If fasciotomy would have been performed within the experimental set-up there is a risk of also disrupting intermuscular connective tissue. As for the aim of the present study it is important to keep this tissue intact in the initial condition, fasciotomy was carried out before the animal was mounted in the experimental apparatus. Consequently, the contribution of the compartmental fascia to intermuscular interaction could not be investigated here. (2) After blunt dissection (see Surgical Procedures) had been performed on the intermuscular connective tissue linkages between the EDL muscle and TA+EHL, separating the muscle belly of EDL. This was done by inserting a small blunt-ended steel rod from laterally between the muscle bellies and moving it proximo-distally between the muscles so that intermuscular connections were severed. In the vicinity of the neuromuscular tract, extra care was taken not to damage this tract.
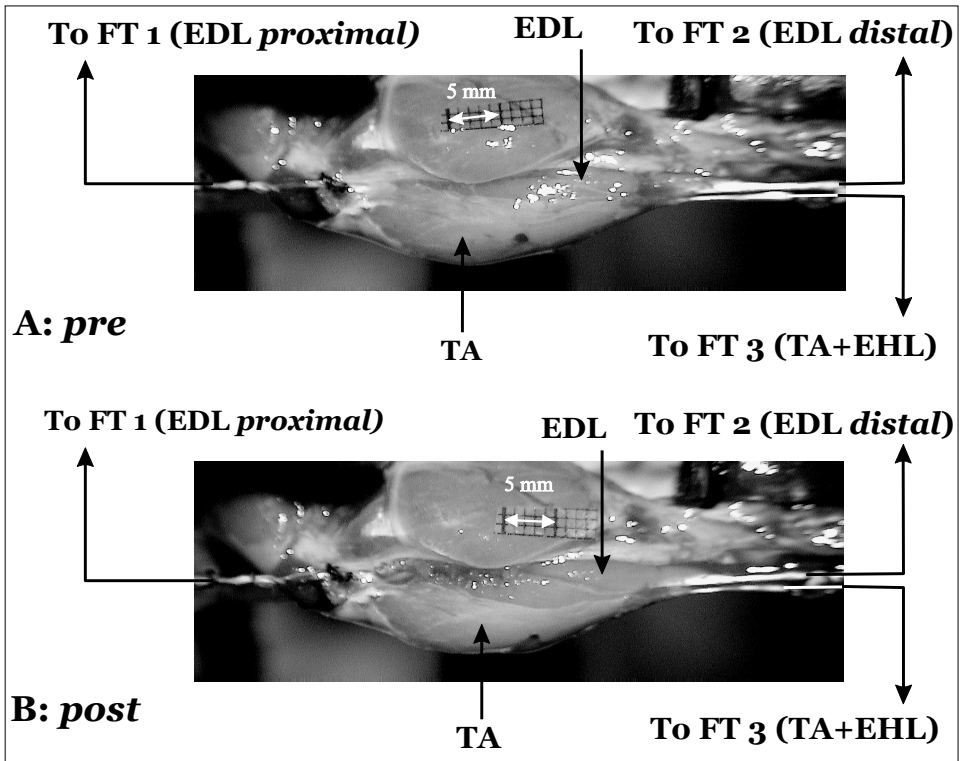
Figure 1 Lateral view of the anterior crural compartment of the left hind limb as in the experimental set-up before (A) and after (B) blunt dissection. For the initial condition (A), the skin and most of the biceps femoris muscle were removed and the anterior crural compartment was opened by full lateral fasciotomy (i.e. longitudinal section). Connective tissues between the muscle bellies of TA, EHL and EDL were left intact. Due to effects of gravity, TA muscle moved downward and, consequently, a part of the latero-dorsal aspect of EDL muscle was exposed when the rat was placed in the experimental set-up. For condition B, blunt dissection was performed on the intermuscular connective tissue linkages between the EDL and TA+EHL muscles, separating the muscle belly of EDL. This was done by inserting a small blunt-ended steel rod between the muscle bellies and moving it proximo-distally between the muscles, so that any intermuscular connective tissue connections were severed. As a consequence, a larger part of the EDL muscle belly surface was exposed and the distal part was visibly separated from TA. The Kevlar threads connecting the different tendons to force transducers are indicated. FT 1 indicates the force transducer connected to the proximal tendon of EDL muscle, FT 2 indicates the force transducer connected to the distal tendon of EDL muscle, and FT 3 indicates the force transducer connected to the tied distal tendons of TA and EHL muscles (TA+EHL). Various muscle-tendon complex lengths of TA+EHL were obtained by repositioning FT 3. Double arrows = 5 mm.

The blunt dissection allows passive EDL to sag a little. As a consequence, a larger part of the EDL muscle belly surface was exposed and the distal part was clearly separated from TA+EHL (fig. 1b). Most of the myofascial connections of EHL belly to the intermuscular septum were also severed in the process of blunt dissection. To keep the experimental conditions similar for the two conditions, the surgical intervention was performed with the rat remaining in the experimental set-up.

Treatment of Force Data and Statistics

For all force data, the mean and standard deviations (SD) were calculated. Although the forces exerted at the distal tendons of EDL and TA+EHL are in the opposite direction to the forces exerted at the proximal tendon of EDL, all forces will be presented as positive values. The difference between proximal and distal EDL force is defined as: F EDLprox – F EDLdist. This force difference is a direct measure of the magnitude of net epimuscular myofascial force transmission. A positive value indicates net force transmission via inter- and/or extramuscular myofascial pathways to the proximal tendon of EDL muscle. A negative value indicates such force transmission to the distal tendons (Maas *et al.* 2004).To test for effects of TA+EHL distal length on force exerted at the proximal and distal tendons of the EDL muscle, a two-way ANOVA for repeated measures was performed (factors: TA+EHL length and location of EDL force measurement). Two-way ANOVA's for repeated measures were also performed to test for the effect of blunt dissection on TA+EHL and EDL forces (factors: TA+EHL length and surgical intervention). For the ANOVAs, p values of < 0.05 were considered significant. If significant main effects were found, Bonferroni post-hoc tests were performed to locate significant differences.

Results

Acute Effects of Distal TA+EHL Lengthening after Compartmental Fasciotomy

TA+EHL Force (fig. 2 A)

Passive force (Fmp) was 0 at low TA+EHL lengths and increased exponentially after distal lengthening TA+EHL (Fmp, peak = 0.88 N, SD 0.30). Optimal force of the TA+EHL complex was 8.11 N (SD 0.29).

EDL Forces (fig. 2 B)

Since EDL muscle was kept at a constant moderately low length, proximally as well as distally measured passive force remained negligible. Despite the fact that the EDL muscle-tendon complex was kept at a constant length, ANOVA indicated significant effects of TA+EHL length on EDL active force (Fma) exerted at the proximal and distal tendon. Proximal EDL active force increased as a function of TA+EHL length (from 1.45 N (SD 0.14) at Δlm+t = –10 mm to a maximum of 1.59 N (SD 0.13) at Δlm+t = –4 mm). In contrast, distal EDL active force decreased as a function of TA+EHL length (from 1.74 N (SD 0.10) at Δlm+t = –10 mm to 1.54 N (SD 0.14) at Δlm+t = +2 mm). Note that the major changes in proximal as well as distal EDL forces were found at low lengths of TA+EHL (= –10 ≤ lm+t ≤ 4 mm). Only for the lowest TA+EHL lengths (= –10 ≤ lm+t ≤ –7 mm), ANOVA indicated significant differences between active force exerted at the distal tendon and active force exerted at the proximal tendon of the EDL muscle (ΔFma, max = –0.29 N (SD 0.09), which corresponds to 17% of the distal EDL force at the same TA+EHL length). Such proximo-distal force differences are direct measures of the

magnitude of net inter- and extramuscular myofascial force transmission. Lengthening TA+EHL decreased this proximo-distal EDL force difference (see also fig. 6 B). EDL proximal and distal forces did attain similar values that were persistent at several higher TA+EHL lengths (Δlm+t = –5 through +2 mm). These results clearly indicate mechanical interactions between EDL and TA+EHL.

Effects of Disrupting the Connective Tissue TA+EHL – EDL Interface on Isometric Forces

TA+EHL Force

After blunt dissection, passive as well as active length-force characteristics of the TA+EHL complex were altered significantly (ANOVA): passive forces as well as active forces were decreased (fig. 3). However, a significant interaction between factors (TA+EHL length and surgical intervention) was found for active force only. Post-hoc analysis revealed a significant force decrease at Δlm+t = –8 to –6 mm (between 0.37 and 0.44 N, i.e. between 9.0 and 15.7% of pre-blunt dissection values at the same length). However, optimal force (i.e. Fma = 8.04 N, SD 0.29) as well as optimal length were unchanged. These results indicate that interfering with connective tissues at the interface of TA+EHL and EDL muscle bellies alters the length-active force characteristics of TA+EHL within the low to moderate length range.

Proximal EDL Force

Significant main effects on active force exerted at the proximal tendon of EDL muscle were found (ANOVA, factors: blunt dissection and TA+EHL length; fig. 4 A). For all TA+EHL lengths tested, proximal EDL force decreased slightly (on average by 0.03 N (SD 0.01), i.e. 1.9%). However, no significant interaction between these factors was found, indicating that the curves could statistically not be distinguished from being parallel. Pre and post blunt dissection (i.e. removing intermuscular connective tissues) length changes in TA+EHL caused similar changes in proximal EDL force (fig. 4 B). Thus the effects of TA+EHL lengthening on changes in proximal EDL force are mediated predominantly by extramuscular connective tissues. The overall force decrease, although very small, suggests the presence of force transmission between the proximal tendon of EDL and TA+EHL via intermuscular connective tissue.
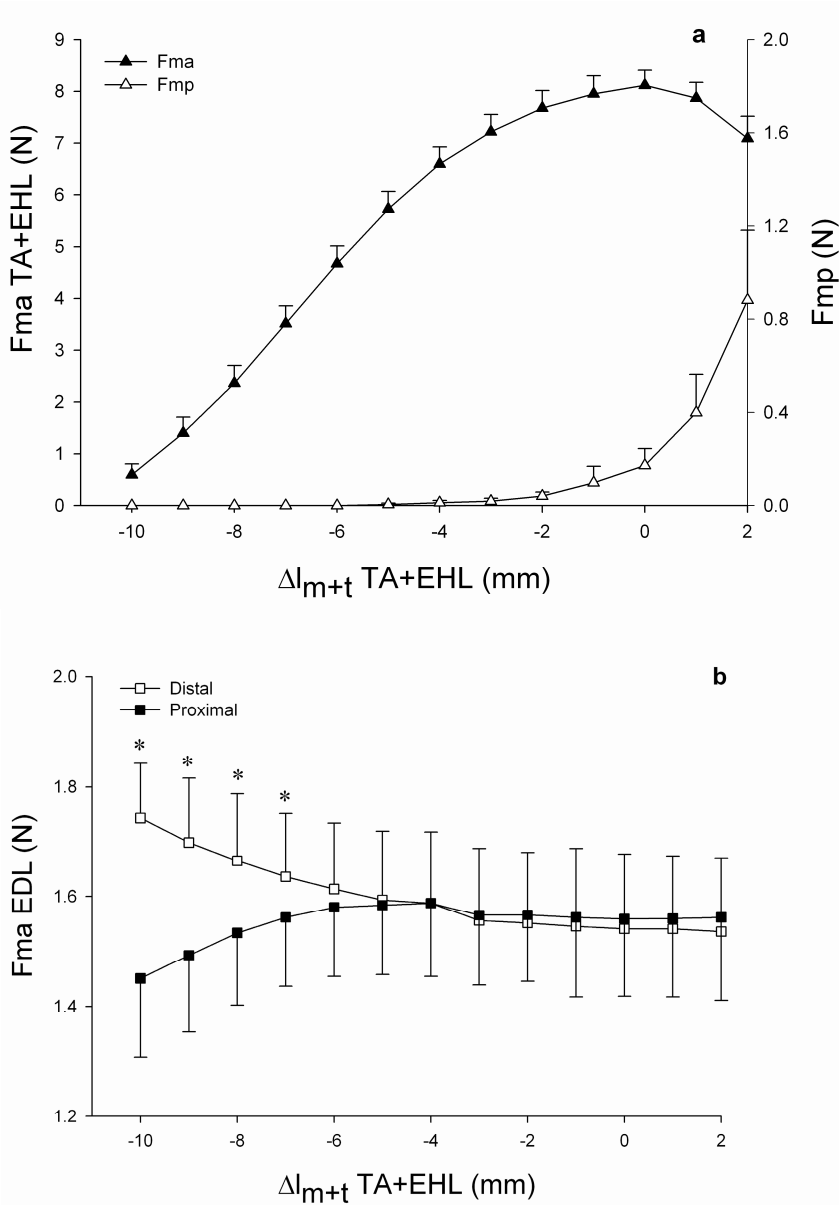
Figure 2. Length – distal force of the TA+EHL complex and the simultaneously measured forces exerted at the proximal and distal tendons of EDL muscle, kept at constant muscle-tendon complex length, after previous full longitudinal fasciotomy of the anterior crural compartment (i.e. initial condition). (A) Active (Fma) and passive (Fmp) forces exerted at the distal tendons of TA+EHL. Muscle-tendon complex length is expressed as the deviation (Δlm+t) from optimum length of TA+EHL. (B) Active forces exerted at the proximal and distal tendons of EDL plotted as a function of TA+EHL muscle-tendon complex length (Δlm+t). Note that proximally as well as distally measured EDL passive forces (not shown) were negligible at all TA+EHL lengths tested. Significant differences (Bonferroni post-hoc) between proximal and distal EDL forces are indicated (*). Values are shown as mean + or $^-$ SD (n = 8).
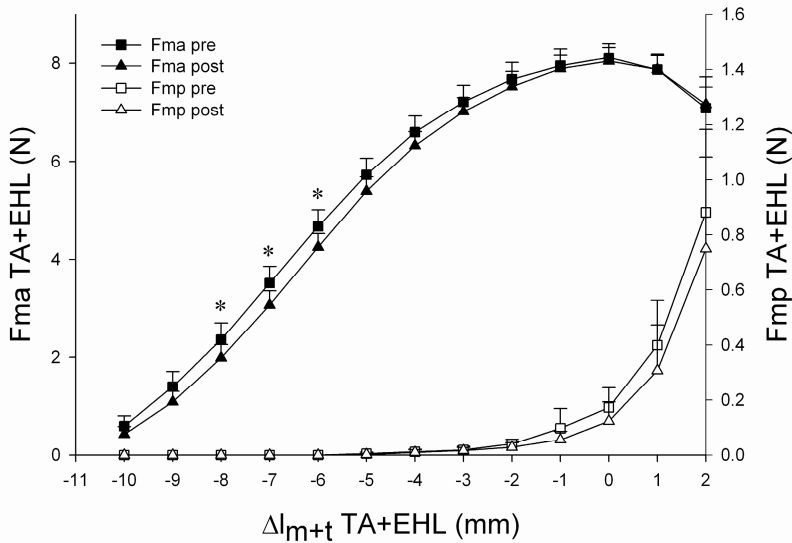
Figure 3. Effects of blunt dissection on length – force characteristics of TA+EHL. Active (Fma) as well as passive (Fmp) forces before (pre) and after (post) disruption of intermuscular connective tissues are plotted. Significant differences (Bonferroni post-hoc) between pre and post forces are indicated (*). Muscle-tendon complex length is expressed as the deviation (Δlm+t) from optimum length of TA+EHL. Values are shown as mean + or – SD (n = 8).

Distal EDL Force

For distal EDL force, ANOVA indicated significant main effects for blunt dissection, as well as for increasing TA+EHL length, and also a significant interaction between these factors. At low TA+EHL lengths (Δlm+t = –10 and –9 mm), active force exerted at the distal tendon of EDL decreased significantly due to blunt dissection: by 0.08 N (SD 0.07) i.e. 4.4%, and by 0.06 N (SD 0.06) i.e. 3.2%, respectively (fig. 5 A). However, at high TA+EHL lengths no differences in EDL distal force between pre and post blunt dissection were found. Furthermore, the amplitude of change in the TA+EHL length – distal EDL force curve (fig. 5 B) decreased subsequent to blunt dissection (from 0.20 N (SD 0.05) to 0.12 N (SD 0.02), i.e. a decrease of 39%). These results indicate that disruption of intermuscular connective tissues causes a substantial decrease in the degree of interaction between TA+EHL and distal sarcomeres within EDL, but more than half of the interaction effect is still present. As only connective tissues of the neurovascular tract as well as remnants of the compartmental fascia were left intact, the sustained intermuscular mechanical effects should be ascribed to extramuscular myofascial force transmission.
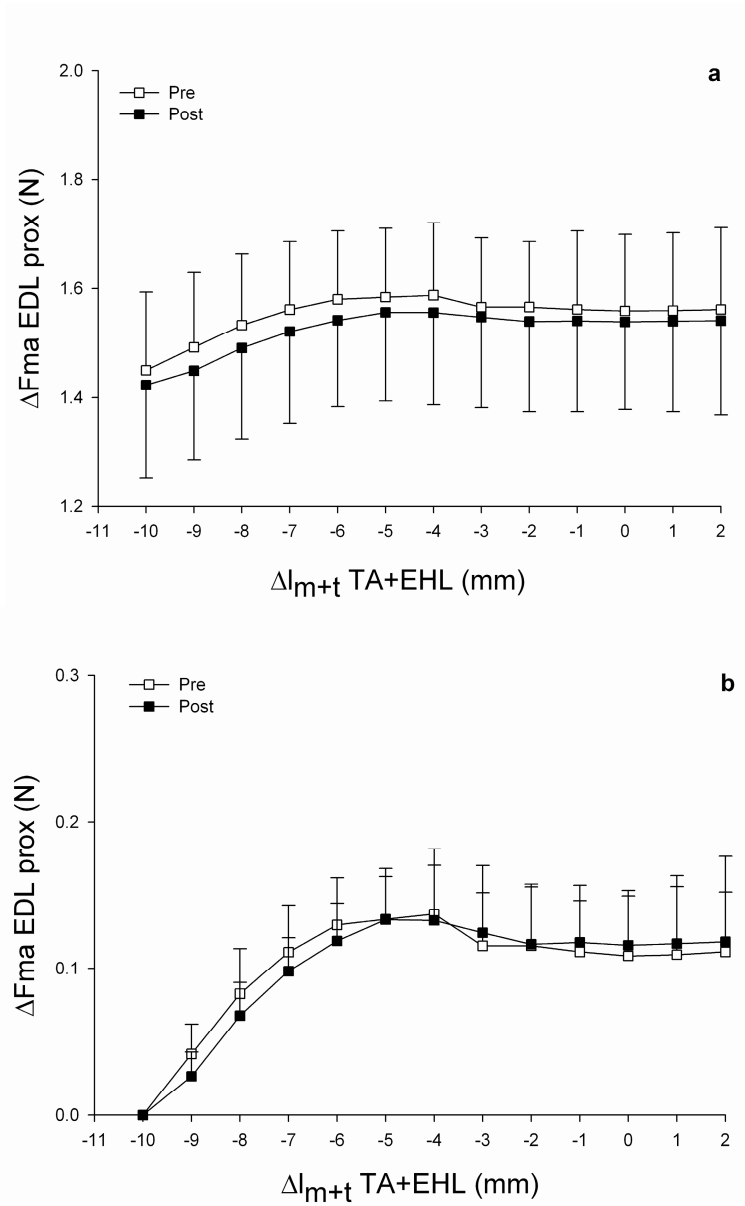
Figure 4. Effects of blunt dissection on force exerted at the proximal tendon of EDL. Forces are plotted as a function of TA+EHL muscle-tendon complex length (Δlm+t) before (pre) and after (post) disrupting intermuscular connective tissues. **(A)** Absolute values of active (Fma) force and **(B)** forces expressed as the deviation (ΔFma) from the value at low TA+EHL length (Δlm+t = −10 mm): Fma, pre = 1.45 N (0.14) , Fma, post = 1.42 N (0.17). Note that EDL muscle is kept at a constant muscle-tendon complex length. Values are shown as mean + or − SD (n = 8).
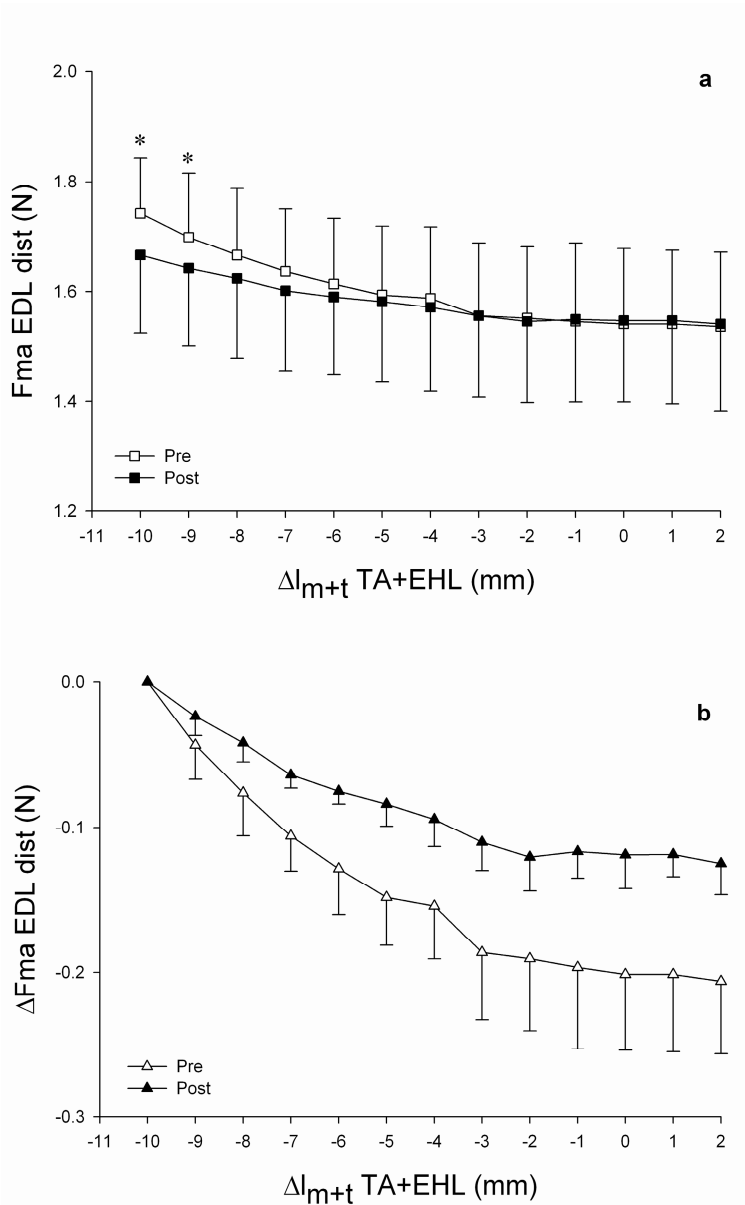
Figure 5. Effects of blunt dissection on force exerted at the distal tendon of EDL. Forces are plotted as a function of TA+EHL muscle-tendon complex length (Δlm+t) before (pre) and after (post) disrupting intermuscular connective tissues. **(A)** Absolute values of active (Fma) force and **(B)** forces expressed as the deviation (ΔFma) from the value at low TA+EHL length (Δlm+t = 10 mm): Fma, pre = 1.74 N (0.10) , Fma, post = 1.67 N (0.14). Note that EDL muscle is kept at a constant muscle-tendon complex length. Significant differences (Bonferroni post-hoc) between pre and post forces are indicated (*). Values are shown as mean + or ⁻ SD (n = 8).
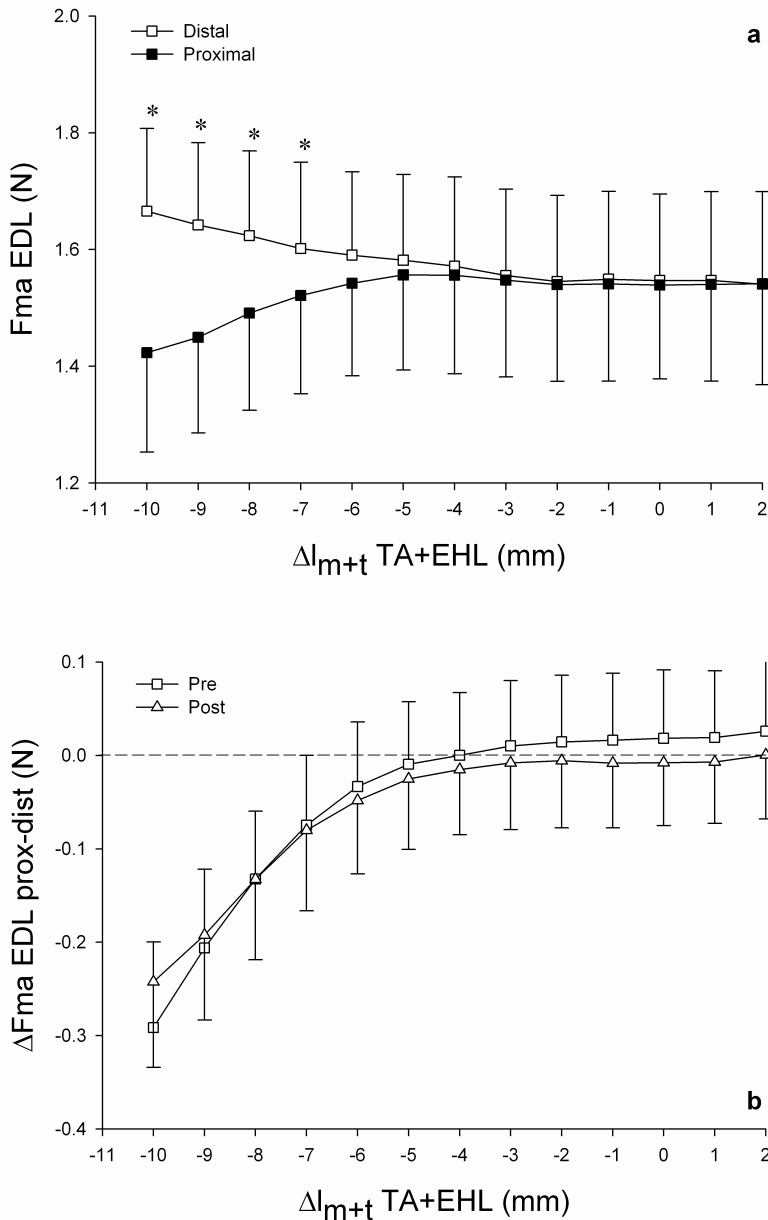
Figure 6. Effects of blunt dissection on the difference between proximal and distal EDL forces. **(A)** Proximal and distal EDL active (Fma) forces after disruption of intermuscular connective tissues plotted as a function of TA+EHL muscle-tendon complex length (Δlm+t). **(B)** The proximo-distal force difference before (pre) and after (post) blunt dissection. A positive value indicates net force transmission via inter- and/or extramuscular myofascial pathways to the proximal tendon of EDL muscle. A negative value indicates such force transmission to the distal tendons. Significant differences (Bonferroni post-hoc) between pre and post forces are indicated (*). Values are shown as mean + or – SD (n = 8).

Proximo-Distal Force Difference

After blunt dissection, significant differences between the proximal and distal EDL forces remained (fig. 6 A) for the lower TA+EHL lengths (Δlm+t = –10 through –7 mm), as a result of extramuscular myofascial force transmission. Furthermore, significant effects of blunt dissection on the curve describing the proximo-distal force difference as a function of TA+EHL length were found (fig. 6 B). Note that the effects varied with muscle-tendon complex lengths of TA+EHL. For the lowest length (Δlm+t = –10 mm), the EDL force difference decreased (by 0.05 N (SD 0.03), i.e. 17%). At this length, proximal as well as distal EDL forces decreased, but the latter to a greater extend (fig. 4 A, 5 A). For higher TA+EHL lengths (= –3 ≤ Δlm+t ≤ +2 mm), the EDL force difference switched signs: a small positive value turned to a small negative value after blunt dissection. As at these lengths no effects on distal EDL force were encountered, this is explained by the decrease in force exerted at the proximal tendon of EDL muscle (fig. 4 A).

These results show that the effects of blunt dissection on net force transmission via non-myotendinous pathways of EDL muscle are small but significant. This can be explained in two ways: either (1) net intermuscular myofascial force transmission was minor, or (2) net extramuscular myofascial force transmission increased following the disruption of intermuscular connective tissues.

Discussion

Two separate pathways, other than the muscular origin and insertion, are distinguished for force transmission from muscle to neighbouring tissues: intermuscular and extramuscular connective tissues. The aim of the present study was to investigate the contribution of each pathway to mechanical interactions between EDL and TA+EHL of the rat. Mechanical interaction was operationalized as changes in force exerted at the tendons of a synergistic muscle kept at constant length due to changes in an agonistic muscle-tendon complex. The major findings of the present study are that disruption of intermuscular connective tissues by means of blunt dissection (1) did not change the interaction between TA+EHL and the proximal tendon of EDL muscle, but caused a partial decrease (i.e. 39%) in TA+EHL – distal EDL interaction, (2) yielded a decrease in both active and passive TA+EHL forces, but (3) had only minor effects on net epimuscular (i.e. summed inter- and extramuscular) myofascial force transmission from and onto the EDL muscle. Although the purpose was to investigate the origin of mechanical interactions between EDL and TA+EHL reported previously (Maas *et al.* 2001; Maas *et al.* 2004), it should be noted that there is a major difference between the muscle conditions of the present experiment and the conditions under which these muscles function in vivo. In this study, the length of TA and EHL muscles was changed while EDL was kept at a constant muscle-tendon complex length. During normal movements, ankle joint movements will involve length changes in all synergists. However, also in vivo substantially different length changes in synergistic muscles and, thus, relative motions of muscle bellies do occur

(Asakawa *et al.* 2002; Bojsen-Moller *et al.* 2004). In a previous paper, we estimated for the rat that within in vivo ranges of knee and ankle joint angles, changes in EDL length can deviate up to 3 mm from changes in TA+EHL length (Maas *et al.* 2004). Furthermore, the position of (parts of) a muscle relative to nonmuscular fixed structures within a compartment (e.g. bone, septa) will alter with each change in joint angle. The functional relevance of myofascial force transmission is further dependent on the physiological significance of the effects found. A 12-mm change in TA+EHL length altered the proximal EDL force by 0.14 N and distal EDL force by 0.20 N. This corresponds to 5.4 and 7.7% of the maximal EDL force (i.e. 2.60 N), as assessed previously in rats with similar body mass (Maas *et al.* 2001). In addition, this caused a change in the difference between proximally and distally measured EDL force of 0.32 N (i.e. from –0.29 to +0.03 N), corresponding to 12.3% of the maximal EDL force. If such physiologically relevant effects are also present during in vivo changes in muscle length remains to be elucidated.

It is concluded, however, that this study clearly indicated that myofascial interaction effects between adjacent synergists originate from both intermuscular and extramuscular connective tissues. The highest contribution should be ascribed to the extramuscular pathway. Several previous studies in humans as well as in different animal species have indicated mechanical interactions between adjacent muscles (Asakawa *et al.* 2002; Bender & Hawkins 2004; Huijing 1999b; Kreulen *et al.* 2003; Maas *et al.* 2001; Maas *et al.* 2003b; Maas *et al.* 2004; Yucesoy *et al.* 2003a). However, this is the first systematic study that distinguishes the contribution of separate pathways to such intermuscular interactions.

Effects of Blunt Dissection on Forces Exerted at the tendons of EDL and TA+EHL

In one of our previous experiments, the interaction between EDL and TA+EHL was studied using similar experimental procedures (Maas *et al.* 2001). Forces exerted at the proximal and distal tendons of the EDL muscle, which was kept at a low constant muscle-tendon complex length, were measured while changing the length of TA+EHL. In contrast to the present study, the anterior crural compartment was kept as intact as possible, i.e. no fasciotomy or blunt dissection was performed. Those results are in agreement with our present figure 2. Changes in proximally and distally measured EDL forces were explained (Maas *et al.* 2001) by changes in the configuration (i.e. angle and length) of inter- and extramuscular connective tissues. At low TA+EHL length, the configuration thought to be such that some force is transmitted from TA and EHL muscle fibres via intermuscular connections to distal sarcomere-extracellular matrix units of EDL muscle and then further onto the distal tendon by either intramuscular myofascial or myotendinous transmission. This can explain why distal force is higher than proximal force of EDL. As TA+EHL is lengthened: force previously exerted at the distal tendons of EDL is exerted at the distal tendons of TA+EHL. Opposite changes in distribution of force occur at the origin of EDL and TA+EHL. The absence of a proximo-distal force difference at high TA+EHL lengths was explained by inter- and extramuscular myofascial forces in opposite directions.

Based on such a view, severing EDL – TA+EHL linkages at low TA+EHL lengths would result in a decrease in distal EDL force, an increase in proximal EDL force, as well as an increase in distal TA+EHL force. In the present study, not only did distal EDL force decrease (fig. 5 A), but also proximal EDL force (fig. 4 A), as well as distal TA+EHL force did (fig. 3). Furthermore, the view presented above would predict that severing EDL – TA+EHL intermuscular connections at high TA+EHL lengths should increase distal EDL force, but decreases proximal EDL force as well as distal TA+EHL force. In the present study, proximal EDL force decreased (fig. 4 A), but distal EDL force (fig. 5 A) as well as distal TA+EHL force (fig. 3) were unchanged. These conflicting results between predictions and experimental observations indicate that additional mechanisms are active simultaneously and interact with the myofascial effects. Using a finite-element model of the rat anterior crural compartment, it was shown that inter- and extramuscular connective tissues affect serial and parallel distributions of lengths of sarcomeres (within the same and different muscle fibres, respectively) (Maas *et al.* 2003a; Yucesoy *et al.* 2003a). Changes in such distributions alter the muscle length range of active force exertion (i.e. the length range between the minimum and maximum length at which the muscle can still exert force) as well as optimal force (Huijing 1995). The effects of blunt dissection on EDL forces, as found in the present study, can be explained by opposing effects of a shift in active slack length as well as optimum length to a higher length, as found for EDL muscle in a previous study after excising TA and EHL muscles (Huijing & Baan 2001b). Such a shift results in a decrease in active force at the ascending limb of the length-force curve and, thus, for the EDL muscle in this study. At low TA+EHL lengths, this counteracts the predicted increase in proximal EDL force. At high TA+EHL lengths, this counteracts the predicted increase in distal EDL force.

For TA+EHL, blunt dissection decreased active force at the low to moderate length range, but it did not alter optimum length as well as optimal force (fig. 3). Such a change in the length-force curve is more compatible with a decrease in the compliance of elastic components in series with the sarcomeres (Kawakami & Lieber 2000).

Importance of Inter- and Extramuscular Connective Tissues for Muscle Function

Several experiments have investigated the role of different connective tissue structures for muscle function with regard to force transmission. This has been done by progressively dissecting muscles free from surrounding tissues: longitudinal compartmental fasciotomy followed by blunt dissection or surgical dissection and, finally, removal of adjacent muscles to isolate the muscle as much as possible.

Fasciotomy

For dog hind limbs, it has been shown that partial fasciotomy decreased force (by 10%) exerted at the distal tendon of the tibialis cranialis muscle (Garfin *et al.* 1981). In the rat, full longitudinal fasciotomy at the lateral aspect of the anterior crural compartment caused: (1) major changes in the proximally measured length-force

characteristic of the EDL muscle; (2) a decrease in force exerted at the proximal tendon of EDL (by up to 14%); (3) a decrease in the proximo-distal force difference (from 14 to 5% of the proximal force), and (4) an increase in force exerted at the distal tendons of TA+EHL (Huijing *et al.* 2003). In addition, fasciotomy of the antebrachial compartment significantly affected length-force characteristics of the rat flexor carpi ulnaris (FCU) muscle: active force at low lengths decreased (by up to 40%) and optimum length shifted to higher lengths (Smeulders *et al.* 2002). It appears that fasciotomy decreases epimuscular myofascial force transmission by (1) decreasing the stiffness of the compartmental fascia itself and/or (2) indirectly by decreasing the stiffness of other inter- and extramuscular pathways. A decreased stiffness of intermuscular connective tissue may diminish its contribution to the mechanical interaction between EDL and TA+EHL. Therefore, the relative contribution of inter- and extramuscular myofascial force transmission, as found after fasciotomy in the present study, may be different within a fully intact compartment. The effects of fasciotomy on mechanical interaction between adjacent muscles could not be investigated in the present study. Based on the studies described above, it is concluded that the compartmental fasciae are an important structure for muscular force transmission.

Blunt Dissection

Intermuscular myofascial force transmission implies that force is transmitted between the intramuscular stromata of two adjacent muscles via direct connective tissue linkages at their muscle belly interface. Blunt dissection has been performed to disrupt such intermuscular connective tissue. It has been shown that such an intervention alters length-force characteristics of proximally measured EDL muscle (Huijing & Baan 2001a): active force decreased at almost all lengths tested (up to 10%), but active slack length and optimum length remained unchanged. In contrast to the present experiment, blunt dissection was performed with an intact fascia of the anterior crural compartment. As a consequence, it could not be checked visually if all or a portion of intermuscular connections had been severed. Partial dissection of the distal half of rat FCU muscle (including partial fasciotomy) has been reported to decrease distally measured optimal force by 8% without significant changes in the length range of active force exertion (Smeulders *et al.* 2002). Transmission of force between adjacent muscles via intermuscular connective tissue and onto the tendon prior to dissection may explain the effects of such intervention. Note that in both of the above described studies forces were measured at only one tendon of a single muscle. In agreement with the results of the present studies, their results indicate that intermuscular connective tissue mediates muscular force transmission.

Muscle 'Isolation'

The muscle is dissected free from its surrounding tissues by fully removing adjacent muscles. Isolation cannot be complete as, for physiological measurements, innervation and blood supply need to be kept intact. Under such conditions, the only remaining pathway for extramuscular myofascial force

transmission is the connective tissue that reinforces the nerves and blood vessels. After removal of TA and EHL muscles, proximal and distal EDL active forces were reported to be equal at all lengths tested (Huijing & Baan 2001b; Huijing *et al.* 2003). In contrast, the proximally measured passive force of EDL muscle was higher than distally measured passive force. In a recent study, clear proof of force transmission via the neurovascular tract was found (Maas *et al.* 2003a). Substantial proximo-distal differences were reported for both passive and active forces of isolated EDL muscle. The magnitude changed as a function of the position of EDL relative to its fixed surroundings (e.g. tibia, anterior intermuscular septum). Such an effect of muscle relative position on force transmission via the neurovascular tract was recently confirmed for fully dissected rat medial gastrocnemius muscle (Rijkelijkhuizen *et al.* 2005). The effects of muscle relative position have been explained by changes in the configuration of the connective tissues (Maas *et al.* 2004). Preliminary data have shown length changes, as well as position changes in the peripheral nerves of the lower limb in human cadavers as a function of ankle, knee and hip joint movements (Babri *et al.* 2003). Therefore, the lack of a proximo-distal active force difference in the fully dissected EDL of previous studies (Huijing & Baan 2001b; Huijing *et al.* 2003) must be attributed to different experimental conditions, specifically different muscle relative positions. Several clinical surgical interventions include manipulation of muscle or its surrounding connective tissues. Fasciotomy is applied in order to reduce the intracompartmental pressure in patients with compartment syndrome (Almdahl & Samdal 1989). Tendon transposition surgeries to improve the range of motion of the affected joints in patients with cerebral palsy involve opening the compartment (i.e. partial fasciotomy) and dissecting the distal portion of the target muscle free from its environment (i.e. blunt dissection) (Kreulen *et al.* 2003). Therefore, knowledge of the acute, as well as long-term, effects of disrupting connective tissues has important implications for surgical practice.

Conclusions

The present study shows that intermuscular interaction between the adjacent synergists within the anterior crural compartment of rat originates from intermuscular as well as extramuscular myofascial force transmission.

The actual ratio of stiffnesses determines the fraction of force transmitted via each path. Intermuscular connective tissues, which can be easily broken by blunt dissection and has been characterized as 'loose', as well as extramuscular connective tissues, which were allotted other functions such as protecting nerves and blood vessels, play a substantial role in muscle function. This has implications not only for surgical practice, but also for biomechanical modelling, neuromuscular control of movements and the etiology of muscle disorders.

3

Myofascial force transmission is increasingly important at lower forces: firing frequency-related length-force characteristics of rat extensor digitorum longus

Hanneke J.M. Meijer, Guus C. Baan & Peter A. Huijing

- Chapter 3

Abstract

Aim: Effects of submaximal stimulation frequencies on myofascial force transmission were investigated for rat anterior crural muscles with all motor units activated.

Methods: Tibialis anterior and extensor hallucis longus (TAEHL) muscles were kept at constant muscle – tendon complex length, but extensor digitorum longus muscle (EDL) was lengthened distally. All muscles were activated simultaneously at 10, 20, 30 and 100 Hz within an intact anterior crural compartment.

Results: At lower frequencies, significant proximo-distal EDL force differences exist. Absolute EDL proximo-distal active force differences were highest at 100 Hz ($\Delta F_{dist-prox}$ =0.4 N). However, the normalized difference was highest at 10 Hz ($\Delta F_{dist-prox}$ =30%F_{dist}). Firing-frequency dependent shifts of the ascending limb of the EDL length-force curve to higher lengths were confirmed for a muscle within an intact compartment, although effects of firing frequency assessed at proximal and distal EDL tendons differed quantitatively. As EDL was lengthened distally, TAEHL distal isometric active force decreased progressively. The absolute decrease was highest for 100 Hz ($\Delta F_{from\ initial}$=-0.25 N). However, the highest normalized decrease was found for 10 Hz stimulation ($\Delta F_{from\ initial}$ = -40%).

Conclusions: At submaximal stimulation frequencies, myofascial force transmission is present and the fraction of force transmitted myofascially increases with progressively lower firing frequencies. Evidently, the stiffness of epimuscular myofascial paths of force transmission decreases less than the stiffness of serial sarcomeres and myotendinous pathways. It is concluded that low firing frequencies as encountered *in vivo* enhance the relative importance of epimuscular myofascial force transmission with respect to myotendinous force transmission.

Keywords: myofascial force transmission, connective tissue, anterior crural compartment, firing frequency, extensor digitorum longus muscle, tibialis anterior muscle, length force characteristics.

- Chapter 3

Introduction

In addition to myotendinous force transmission (Tidball 1991; Trotter *et al.* 1985; Trotter 2002), force exerted by sarcomeres is transmitted via alternative pathways (Street & Ramsey 1965; Street 1983). Via the muscle fibre cytoskeleton, which is connected to the basal lamina, a fraction of the force exerted by sarcomeres is transmitted onto the connective tissue within the muscle (myofascial force transmission). This intramuscular connective tissue is connected to the intermuscular connective tissues and to similar stromata of other muscles, as well as to extramuscular connective tissues. Proof of the existence of such epimuscular myofascial force transmission is a difference in force exerted at the origin and insertion of a muscle (Huijing 1998; Huijing & Baan 2001a; Huijing & Baan 2001b; Huijing & Baan 2003). Such transmission has been shown for muscles within the anterior crural compartment of the rat (Huijing & Baan 2001b), and in gradually dissected rat medial gastrocnemius muscle (Rijkelijkhuizen *et al.* 2005), the rat flexor carpi ulnaris (FCU) muscle (Smeulders *et al.* 2002) as well as human FCU in patients with cerebral palsy (Kreulen *et al.* 2003; Kreulen *et al.* 2004). One of the important factors affecting muscle length-force characteristics is the level of muscular excitation. The effects of stimulation frequencies on muscle length-force characteristics, of fully dissected *in situ* muscles, have been recognized since the observations of Rack and Westbury (1969): at low stimulation frequencies, the length-force curves of muscles are not scaled versions of their curves at 100 Hz. Using pulse trains with a constant asynchronous stimulation frequency (CSF), it was shown that the ascending limb of the length-force curve of cat soleus muscle shifted to higher muscle length as stimulation frequency was lowered (Brown *et al.* 1999; Rack & Westbury 1969; Roszek & Huijing 1997).

The major mechanisms by which length-force characteristics are altered are predominantly intracellular ones, such as the length-dependent calcium sensitivity of force; increasing sarcomere length results in an enhanced sensitivity to calcium (Stephenson & Williams 1982; Stephenson & Wendt 1984). The question arises whether such effects, of intracellular origin, on length-force characteristics are recognizable also in muscle that is still embedded within its natural context of connective tissues, or that such effects are modified by higher levels of tissue organisation (as argued as a possibility by Huijing (2003) and Huijing & Jaspers (2005)). Major distributions in sarcomere lengths due to myofascial force transmission (Maas *et al.* 2003a; Yucesoy *et al.* 2002a) could be a factor in such potential modifications. Low muscular firing frequencies play an important role in the *in vivo* motor control. For example firing frequencies in rat muscle vary between 10 and 60 Hz (Hennig & Lomo 1985). Therefore, it is necessary to assess the presence and importance of epimuscular myofascial force transmission at physiological stimulation frequencies. This thought is also inspired by work by Hugo Kronecker and Theodore Cash (1880), who, after noting effects of a passive muscle on an actively shortening neighbouring muscle, reported that at intermediate levels of stimulation of the muscle, the neighbouring active muscle was not impeded significantly. This may suggest that although myofascial force

transmission is highly important at maximal stimulation, this may not be the case at submaximal levels of stimulation. Therefore, the aim of this study is twofold: (1) to assess the presence of epimuscular myofascial force at low firing frequencies, and if present at significant levels, its relative importance compared to that at high firing frequencies, (2) and if present, to asses if myofascial force transmission modifies the frequency-related effects on muscle length-force characteristics.
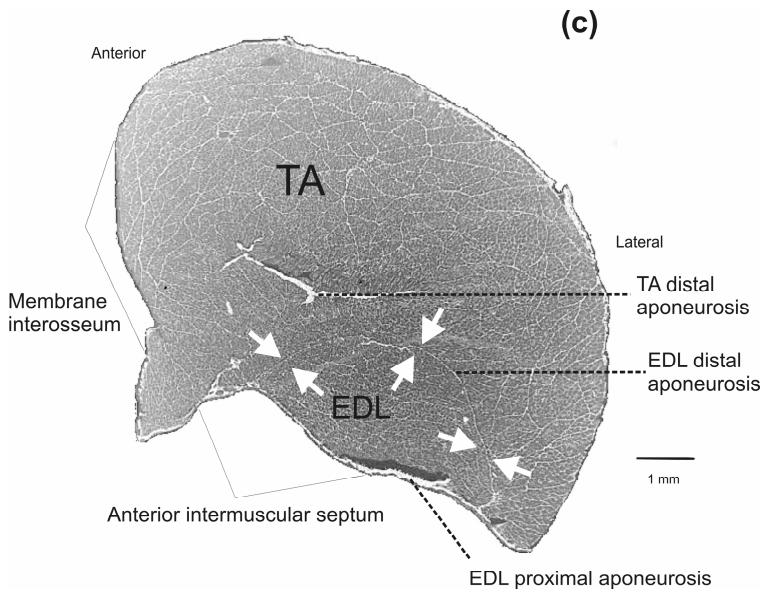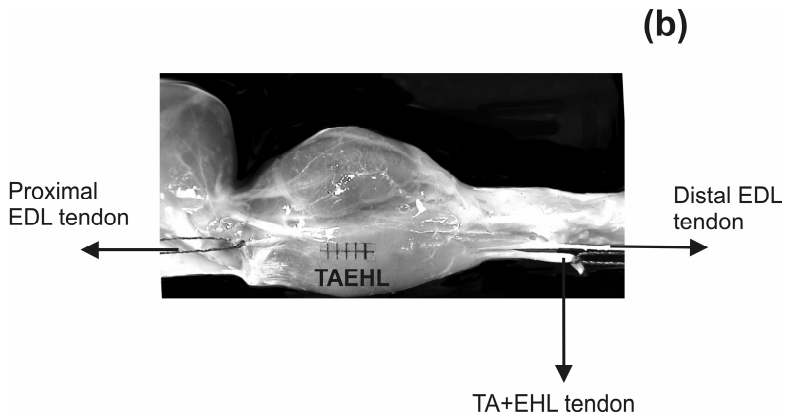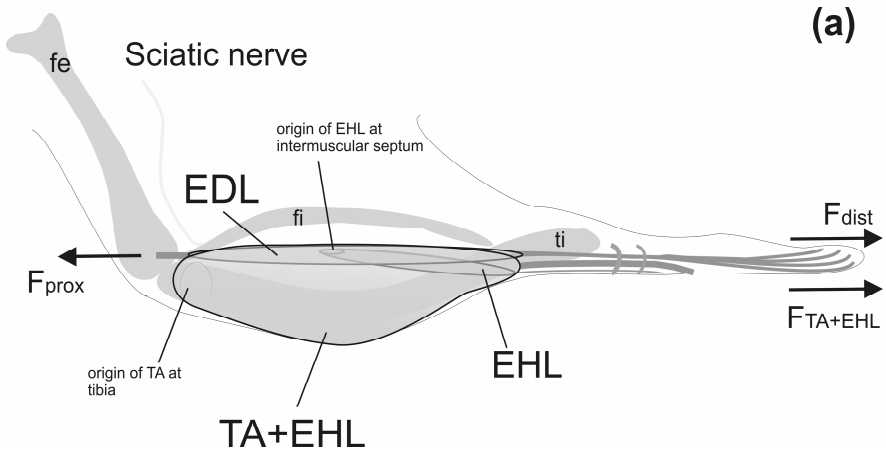
Methods

Surgical and experimental procedures were in agreement with the guidelines and regulations concerning animal welfare and experimentation set forth by Dutch law, and approved by the Committee on Ethics of Animal Experimentation at the Vrije Universiteit. Immediately after all experiments, animals were killed using an overdose of urethane solution, and double-sided pneumothorax was performed.

Surgical procedures

Seven male Wistar rats (*Rattus norvegicus* (Berkenhout, 1769)) with a mean body mass of 303.4 gr. (S.D. = 11.80) were anaesthetized using intraperitoneally injected urethane solution (1.5 g kg-1 body mass). Extra doses were given if necessary (maximally 1.5 ml.). During surgery and data collection, the rats were placed on a heated water pad of approximately 37°C, to prevent hypothermia.

The anterior crural compartment, which envelopes tibialis anterior (TA), extensor digitorum longus (EDL) and extensor hallucis longus (EHL) muscles (see Fig 1), was exposed by removing the skin and most of the biceps femoris muscle from the left hind limb. Connective tissue at the muscle bellies of TA, EHL and EDL was left intact. However, the transverse crural ligament and the crural cruciate ligament were severed and limited fasciotomy was performed to dissect the distal tendons of EDL, TA and EHL. As it is difficult to measure force exerted by each EDL tendon individually, without friction between neighbouring tendons, the four EDL tendons were tied together using polyester thread. For the same reasons, the distal tendons of TA and EHL as well as the distal tendons of peroneal muscles (PER) were tied to each other, creating a complex of these muscles. Two pieces of the epicondylus lateralis of the femur were cut, representing the origin of EDL muscle and of the lateral collateral ligament. Both pieces of bone were attached to metal rods using 100% polyester yarn. Markers were placed on the gastrocnemius muscle, representing the original proximo-distal position of the origin of the EDL muscle and lateral collateral ligament. Screws were inserted in to the medial surface of the tibia and used for tibia fixation. The foot was firmly fixed to a plate. Both tibia and footplate were fixed within a rigid frame in such a way that the muscles were aligned with the force transducer.

(a)

Sciatic nerve

fe

EDL

origin of EHL at
intermuscular septum

fi

ti

F_{dist}

F_{prox}

origin of TA at
tibia

EHL

F_{TA+EHL}

TA+EHL

(b)

Proximal
EDL tendon

TAEHL

Distal EDL
tendon

TA+EHL tendon

(c)

Anterior

TA

Lateral

TA distal
aponeurosis

EDL distal
aponeurosis

Membrane
interosseum

EDL

1 mm

Anterior intermuscular septum

EDL proximal aponeurosis

Figure 1 (previous page). Representation of the experimental set up and muscle anatomy of the rat anterior crural compartment. **(a)** Schematic lateral view of the rat anterior crural compartment after removal of the skin and biceps femoris muscle. Connective tissue at the muscle bellies was left intact. Origins and insertions of muscles are shown. Proximally, the EDL tendon attaches at the lateral condyle of the femur and the TA originates from the antero-proximal face of the tibia. The TA+EHL complex is made transparent in the image to allow showing of the position of the EDL and the EHL originating at the anterior intermuscular septum. The distal tendons of EDL insert on the four toes. Both distal TA and EHL tendons curve medially to insert on metatarsal I. The proximal EDL tendon was severed and attached to a force transducer using a metal rod (represented by an arrow). Distally, the tendons of EDL as well as of the TA+EHL complex were connected to separate force transducers using metal rods (represented by arrows). Both tibia and foot were fixed within a rigid frame so that the muscles were aligned with the force transducers. **(b)** Lateral view of gross muscle anatomy after removal of the skin and biceps femoris muscle. After limited fasciotomy, the distal and proximal tendon of EDL and the distal tendon of TA+EHL were severed. EDL muscle is covered completely by TA+EHL muscle and GM muscle, except for both proximal and distal tendons. **(c)** Inverted image of a cross-section of the rat anterior crural compartment at 50% of the proximo-distal length of the EDL muscle belly, showing tibialis anterior muscle (TA) enveloping a large part of extensor digitorum muscle (EDL). The EHL is only present more distally. The TA-EDL connective tissue interface is indicated by white arrows. Bar indicates 1 mm.

Within the femoral compartment, the tibial nerve and the sural branch of the sciatic nerve were cut as proximally as possible. The sciatic nerve was dissected free of its surroundings. Only the peroneus communis nerve branch was left intact, other branches were denervated. Branches of the intact common peroneal nerve innervate EDL, TA and EHL muscles. Stimulation of the nerve will, therefore, activate all three muscles simultaneously.

The experimental apparatus

The rat was placed on a platform. The footplate was positioned in such a way that the ankle angle was in extreme plantar flexion to make room for free passage of the distal tendons (Fig. 1). The knee was kept at a 110° angle. All three distal tendon complexes as well as the proximal EDL tendon and the collateral lateral ligament (the latter two still attached to pieces of bone) were connected to force transducers (BLH Electronica Inc., maximal output error < 0.1 %, compliance of 0.0162 mm/N) using stainless steel rods to ensure isometric contractions. The force transducers were mounted on single axis micropositioners. The sciatic nerve was placed in a pair of electrodes (supramaximal current).

Experimental conditions

The nerve was prevented from dehydration by covering it with paper tissue saturated with isotonic saline and covered by a thin piece of latex. Ambient temperature (22°C ± 0.5 °C) and air humidity (70 ± 2%) were kept constant by a computer controlled air-conditioning system (Holland Heating, Waalwijk, the Netherlands). Muscle and tendon tissue was further prevented from dehydration by regularly irrigating the tissue with isotonic saline. Timing of stimulation of the nerve and A/D conversion (12-bit A/D converter, sampling frequency 1000 Hz, resolution of force 0.01N) were controlled by a special purpose microcomputer. Before each contraction, the EDL muscle was brought to the desired length

passively by moving the distal force transducer exclusively. The TAEHL complex and the peronei muscles were kept at constant length set to exert an initial force of respectively 3N and 5 N. The collateral lateral ligament was kept at a position equivalent to its in situ position corresponding to the knee angle imposed. The original proximal EDL position was determined by using the corresponding marker position on the gastrocnemius muscle. The proximal EDL position was subsequently placed at a length which was 2 mm shorter than the original marker position. The experimental stimulation protocol consisted of two twitches (at t = 200ms and t = 400ms), followed by a pulse train (at t = 600ms) with a staircase complex of ascending stimulation frequencies (ASF) of 10, 20, 30 and 100 Hz (Fig 2), and a final twitch at t = 1800ms. The successive pulse frequency phases were equal in duration (250 ms) and total stimulation time was 1000 ms. After each contraction, the muscles were allowed to recover near active slack length for 2 minutes. Before acquiring data, EDL muscle was preconditioned by isometric contractions alternatively at high and low lengths of EDL until forces at low length were reproducible, i.e. effects of previous activity at high lengths are removed (Huijing & Baan 2001a; Huijing & Baan 2001b). Isometric contractions were performed at different EDL lengths starting near muscle active slack (i.e. the smallest muscle length at which muscle active force approaches zero). The muscle-tendon complex was distally lengthened with 1.0 mm increments. Results are plotted for a length range to 3 mm over 100 Hz optimum length. Passive isometric muscle force was measured just prior to the tetanic contraction, and total isometric muscle force was measured during the tetanic plateau of the muscle force.

Treatment of data and statistics

Passive muscle force was fitted using an exponential curve $y = \exp(ax + b)$, where y represents passive muscle force, x represents muscle length and 'a' and 'b' are fitting constants. Active EDL muscle force (F_{ma}) was estimated by subtracting passive force (F_{mp}) for the appropriate muscle length from total force (F_m). Active EDL length-force data were then fitted with a stepwise polynomial regression procedure. In this procedure, the curve fit is determined by increasing the order (max. of 6) of the polynomial as long as this yields a significant improvement to the description of the length-active force data, as determined by one-way analysis of variance (ANOVA). The polynomial: $y = b0 + b1x + b2x2 + \ldots Bnxn$, where y represents active muscle force, x represents active muscle force length and b0 …..bn are fitting constants. Optimum muscle length was defined for each curve as the active muscle length at which the fitted curve showed maximal active muscle force (F_{mao}). Using the selected polynomials, mean and standard errors of active muscle force were calculated for a given EDL length. In order to estimate more accurately the distal active slack length, data of muscle length and active muscle force ($F_{ma} < 0.3 \times F_{mao}$) were selected. The data points were then extrapolated with a fitted curve where $y = \exp(b0 * x + b1) + b2$. Active slack length was determined by solving the roots for this equation.

Two-way ANOVA's for repeated measures were performed to test for the effects of stimulation frequency (four levels: 10, 20, 30 and 100 Hz) and EDL muscle

length on the force exerted at the proximal and distal tendons of EDL muscle as well as TAEHL complex forces. In addition, a two-way ANOVA was used to test for the effects of stimulation frequency and EDL muscle length on the distally and proximally measured optimum muscle length (L_{mao}). To test for the presence of a proximo-distal EDL force difference, one-way ANOVA was performed. If significant effects were found, post hoc tests were performed using the Bonferroni procedure for multiple pair wise comparisons to locate differences. Main and interaction effects as well as differences were considered significant at $P < 0.05$.
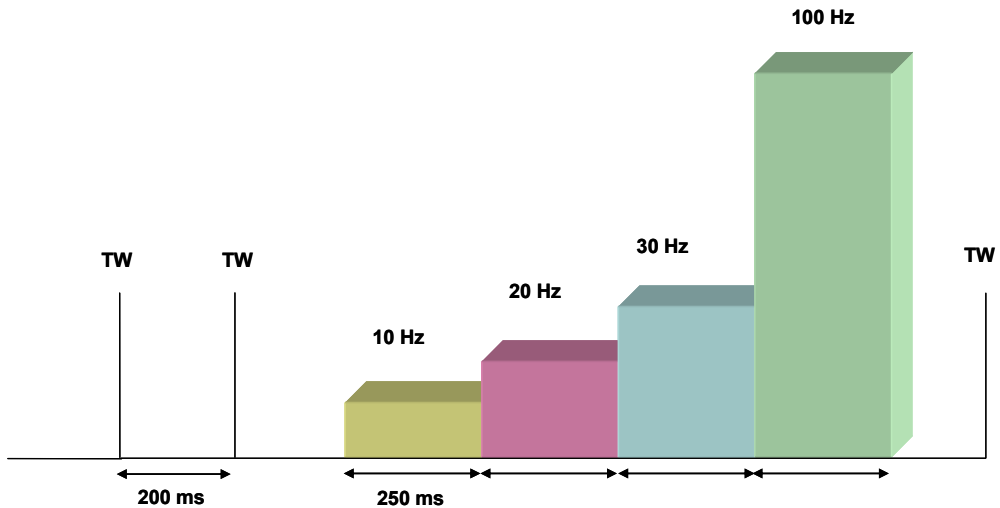
Figure 2. Schematic representation of the ascending stimulation frequency (ASF) protocol. The protocol started with two twitches (TW), followed by an ascending staircase of 10, 20, 30 and 100 Hz stimulation, and ended by a twitch.
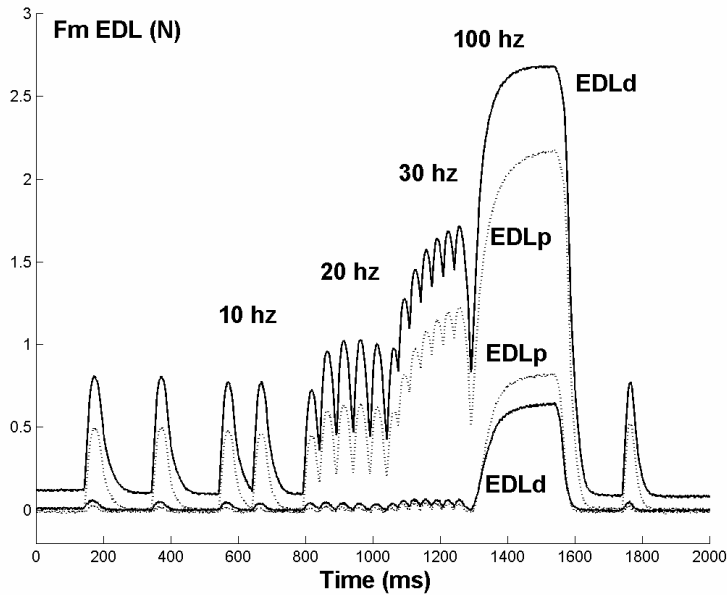
Figure 3. Representative proximal and distal time-force traces obtained by applying the ascending frequency stimulation protocol. **a)** Near active slack length (lower traces), **b)** near optimum muscle length (upper traces). 'EDLd' indicates distal EDL force; 'EDLp' indicates proximal EDL force.

Results

Effects of stimulation frequency on length-force characteristics of EDL muscle

Representative time – EDL force traces of the ascending frequency stimulation protocol are shown in Fig. 3. The protocol started with two twitches followed by 10 Hz stimulation. In three steps, the stimulation frequency was increased to 100 Hz and EDL force increases with it. Note that at low as well as at high muscle length, the tetani are not completely fused for stimulation frequencies of 10 – 30 Hz. At low muscle length, EDL forces are low. Note that EDL proximal force is higher than EDL distal force. Both forces reach the plateau phase simultaneously. At higher muscle length, EDL distal force reaches the tetanus plateau earlier than EDL proximal force. EDL distal force is now higher than EDL proximal force.

For distal EDL active force, ANOVA indicates significant main effects of stimulation frequency and EDL length as well as an interaction between these factors (Fig. 4a). The ascending frequency protocol (ASF) was attended by significantly higher muscles force. Force enhancement was length dependent ($P < 0.05$) and force decreased at muscle lengths over the optimum length. Distal active force increases with increasing length in two major ways: (1) a flatter region; the length range from active slack length to $\Delta l_{m+t} \approx$ -7 to -8, and (2) a steeper region; the length range between $\Delta l_{m+t} \approx$ -7 and optimum lengths. No significant shifts of distal active slack lengths (estimated by extrapolation) could be shown.

43

Extrapolation to zero force of proximal length-force data was unreasonable because of high levels of proximal force remaining as well as the shape of the curve. For lower frequencies, optimum muscle length shifted substantially to higher muscle length (e.g. for 10 Hz the shift equalled 2.4 mm, see figure 5b). Distal passive force increased exponentially as a function of EDL muscle length. Note that a rise in passive force starts well below optimum length (i.e. $\Delta l_{m+t} \approx$ -5). For proximal active force (Fig. 4b), ANOVA indicates significant effects of stimulation frequency and muscle length, as well as an interaction between these factors. Proximal active force also increased as a function of EDL muscle length in two phases, but the length ranges seem different from those of distal EDL active force: for the lower stimulation frequencies, the slower increase ends at higher lengths (i.e. -6 < Δl_{m+t} < -5) but for 100 Hz this phase ends at lower lengths ($\Delta l_{m+t} \approx$ -8). At lower stimulation frequencies, optimum muscle length of proximal active force was shown to have shifted significantly to higher lengths (e.g. 2.6 mm at 10 Hz stimulation, see figure 5b). Proximal passive force increased exponentially with lengthening of EDL. Note that proximal passive force does not increase substantially until optimum length is attained.

Proximo-distal EDL force differences and effects of stimulation frequency

Figure 5a shows examples of the length-force curves of EDL proximal and distal active force at 20 and 100 Hz stimulation. Proximal and distal EDL active forces differ as a function of muscle-tendon complex lengths and stimulation frequency. Note that distal EDL passive force is also significantly higher than proximally measured EDL passive force. For 10 and 100 Hz stimulation frequency, optimum length measured at the proximal tendon of EDL differs from optimum length measured at the distal tendon (Fig. 5b), but not for 20 and 30 Hz stimulation.

A plot of proximo-distal force differences (Fig. 6a) shows that except for 100 Hz stimulation, proximal and distal active forces are similar at low muscle lengths (-9 < l_{m+t} < -5). However, for l_{m+t} > -5, distal active force is dominant over proximal active force. The proximo-distal EDL active force difference increased until well over optimum length (Fig. 6a). The absolute difference in active force between the proximal and distal tendon is highest for 100 Hz stimulation (ΔF = 0.36 N), and is lowest at 10 Hz stimulation (ΔF = 0.2 N). At low muscle lengths, (-9 < l_{m+t} < -5), proximal and distal passive forces are equal. The passive proximo-distal force difference starts to increase exponentially for l_{m+t} > -5 and eventually becomes larger than the active proximo-distal force difference.
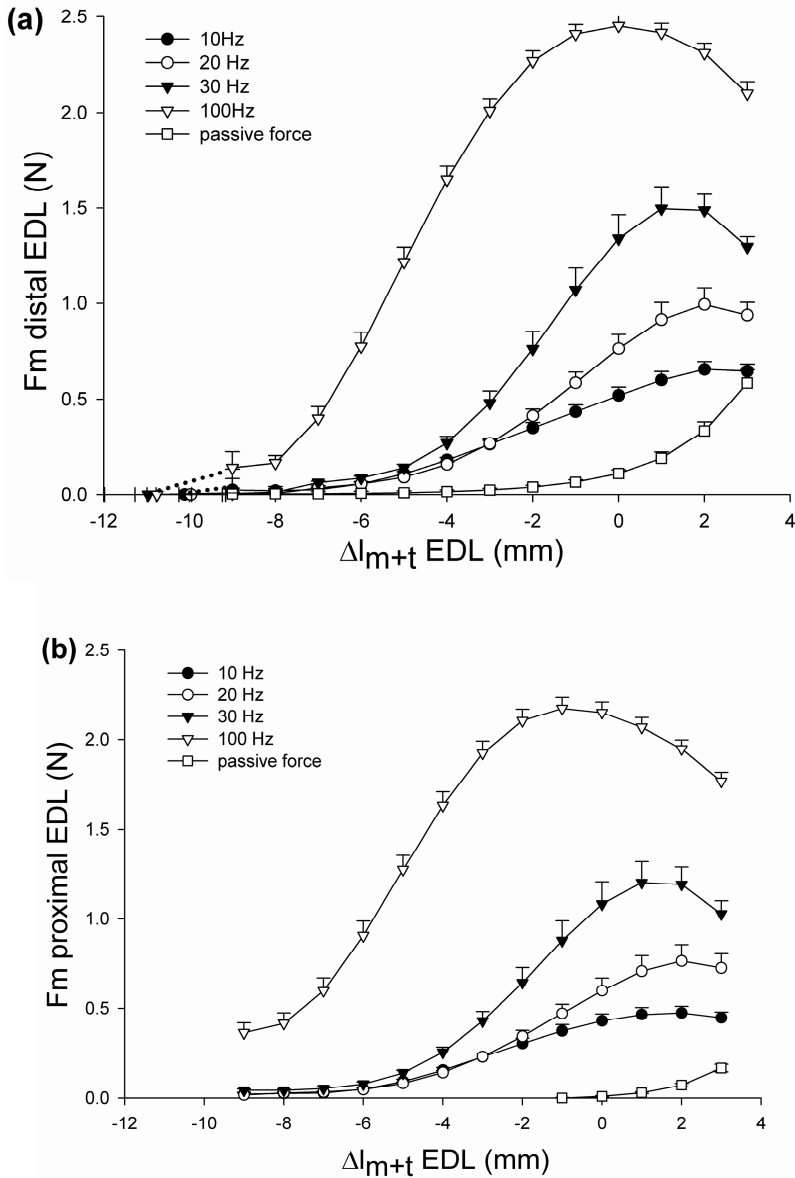
Figure 4. Effects of firing frequency on EDL length-force characteristics. All values are shown as means + standard error, n = 6. **(a)** length force characteristics as measured at the distal tendon, **(b)** length force characteristics as measured at the proximal tendon. EDL length, increased by distal EDL lengthening (Δlm+t EDL dist), is expressed as deviation from distal optimum length for 100 Hz stimulation.
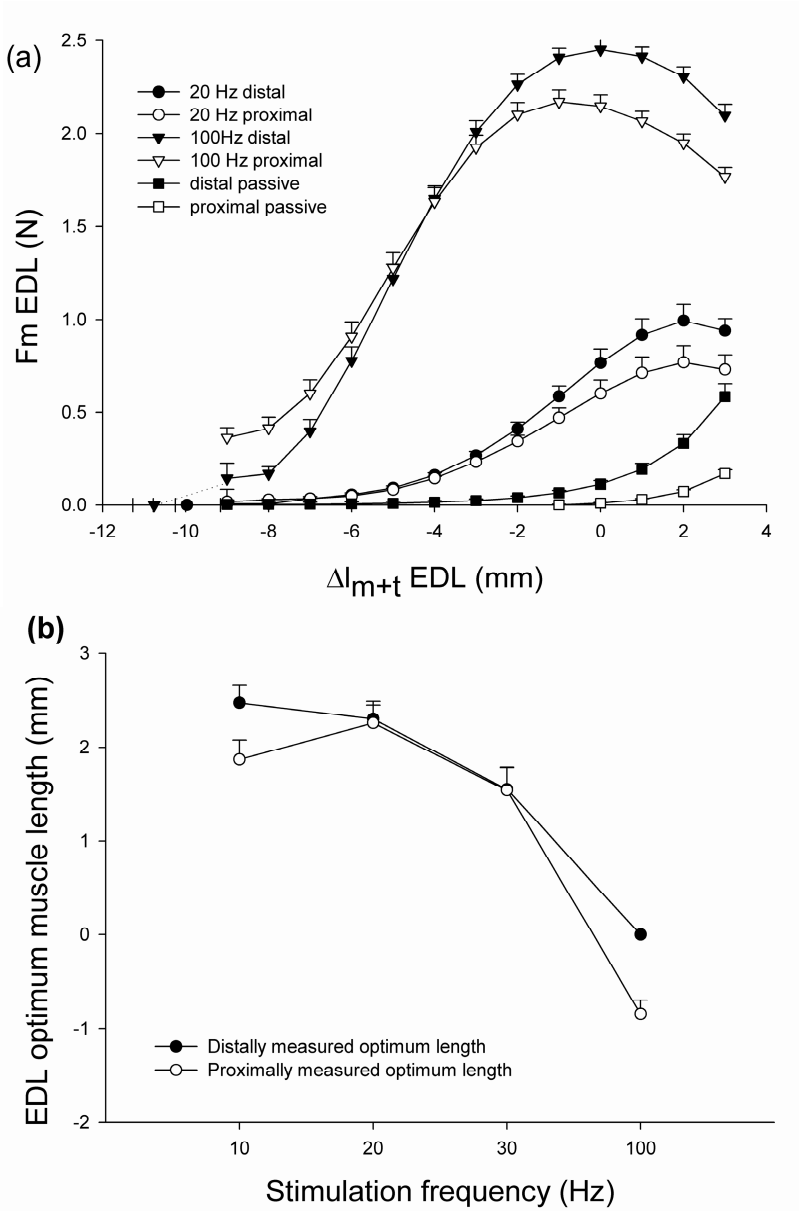
Figure 5. Comparison of EDL proximal and distal length force characteristics at different stimulation frequencies. All values are shown as means + standard error, n = 6. **(a)** length-force characteristics of EDL muscle-tendon complex length, increased by distal EDL lengthening (Δlm+t EDL dist), expressed as deviation from 100 Hz distal optimum length, **(b)** Proximal and distal optimum muscle lengths (lmao) vs. stimulation frequency.

In contrast, for a certain length range ($-3 < \Delta l_{m+t} < 0$), force differences, normalized for distal optimum force per frequency, are quite similar for different stimulation frequencies (Fig. 6b). For other length ranges, substantial differences were found. At higher lengths, 10 Hz stimulation caused the highest normalized difference (up to 30 % F_{mao}) and 100 Hz stimulation the lowest (up to $\pm$ 15 % F_{mao}). At low lengths, only major normalized proximo-distal force differences were found for 100 Hz ($\pm$ -20 %) stimulation. The normalized passive force difference equals zero at low muscle lengths, but shows an exponential increase at $l_{m+t} > -5$. The increase of a significant proximo – distal force difference with lower stimulation frequencies, suggest that the transmission of force by epimuscular myofascial pathways increases relatively with respect to myotendinous force transmission at low frequency stimulation.

Effects of EDL length and stimulation frequency on TAEHL complex force

ANOVA showed significant main effects of EDL muscle-tendon complex length and stimulation frequency on TAEHL active force, as well as an interaction between these factors, on TAEHL active force (Fig. 7). TAEHL active force increased significantly with firing frequency. Distal lengthening of the EDL muscle tendon complex caused the TAEHL active force to decrease significantly despite the fact that TAEHL muscle-tendon complex length was left unchanged.

Fig. 7b shows that the decreases in force normalized for the initial levels are substantial (e.g. 10 Hz active force dropped approx. 40 %).Note that normalized force decrease is lowest for 100 Hz and highest for 10 Hz. Note also that decreasing TAEHL active force coincides with increasing EDL proximo-distal active force difference, particularly at higher lengths. This is taken as an indication that, as EDL is lengthened, at least part of TAEHL active force is exerted at the distal tendon of EDL through myofascial pathways.
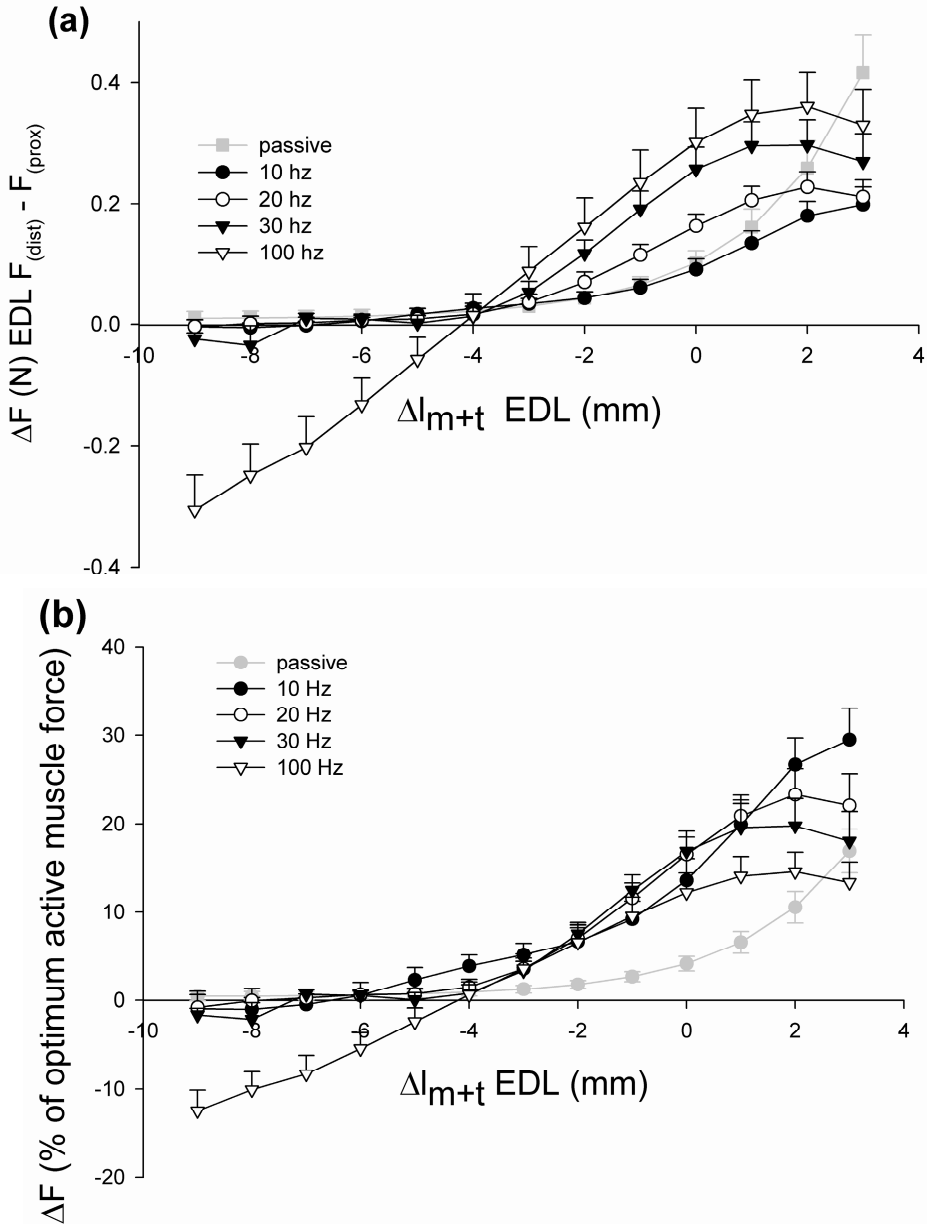
Figure 6. Effects of stimulation frequency and EDL muscle tendon complex length, increased by distal EDL lengthening (Δlm+t EDL dist), on the proximo-distal force difference. Values are shown as means + standard error, n = 6. **(a)** ΔF, absolute difference between distal and proximal active and passive force. **(b)** ΔF, normalized for distal optimum active force per frequency (Fmao (f)) and passive force, (normalized for distal 100 Hz optimum force). Both graphs are plotted as a function of muscle – tendon complex length (Δlm+t) of EDL. EDL muscle-tendon complex length is expressed as a deviation from 100 Hz distal optimum length.
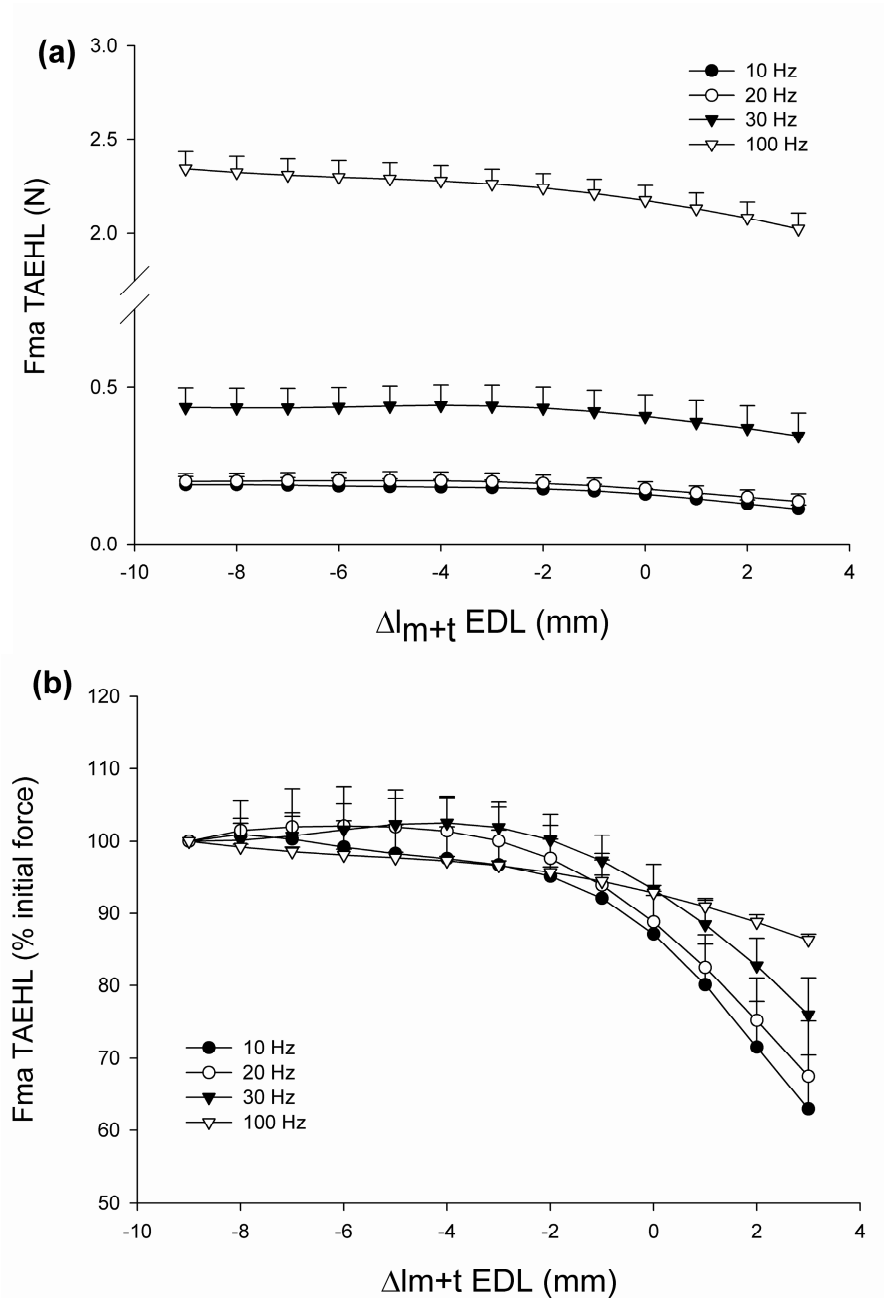
Figure 7. Effects of distal EDL lengthening (Δlm+t EDL dist) on TA+EHL forces. Values are shown as means + standard error, n = 6. **(a)** TA+EHL active forces , **(b)** TAEHL active forces expressed as a percentage of the initial active force. Both graphs are plotted as a function of EDL muscle – tendon complex length (Δlm+t EDL dist). EDL muscle-tendon complex length is expressed as a deviation from 100 Hz distal optimum length.

Discussion

EDL proximo-distal force differences and myofascial force transmission

At submaximal firing frequencies, isometric force exerted at the proximal and distal tendons of EDL muscle was found to differ as a function of EDL length. These findings are in agreement with those of previous studies on epimuscular myofascial force transmission in maximally activated muscle (Huijing *et al.* 1998; Maas *et al.* 2001). Any such proximo-distal force difference indicates that net forces, additional to myotendinous ones, act as a load on the muscle. Intact inter- and/or extramuscular connections surrounding the EDL muscle mediate this myofascial force transmission (Huijing & Baan 2001a). The effects of such force transmission do not arise from innate characteristics of the muscle fibre, but can be best understood on the basis of changes in length, direction of applied length changes, as well as relative positions of muscles and concomitant changes in the configuration of extra- and intermuscular connective tissues connecting EDL and the TA+EHL complex (Huijing & Baan 2001a; Huijing & Baan 2001b; Maas *et al.* 2003c). It indicates that, when considering a muscle active within an intact organism, an integrative approach is needed (Huijing 2003), which also accounts for changes in muscle characteristics as a result of interaction with tissues at higher levels of organisation.

The decrease in active force exerted by TAEHL while kept at constant muscle tendon complex length (Fig. 7a), can be seen as a direct effect of epimuscular myofascial force transmission due to changes in the configuration of the connective tissue between EDL and TA+EHL (Huijing *et al.* 1998; Maas *et al.* 2001). As EDL is distally lengthened, myofascial connections at the interface between TA+EHL and EDL lengthen and forces generated by sarcomeres within the TA+EHL will be exerted on the distal EDL tendon.

Myofascial force transmission at lower firing frequencies

Although the absolute magnitude of EDL active force transmitted through epimuscular myofascial connections (i.e. the difference between distally and proximally measured forces) peaked at 100 Hz (Fig. 6a), the normalized force difference (proximo-distal force difference normalized for distal optimum force per frequency) was highest at 10 Hz (Fig. 6b). For TA+EHL active forces (Fig. 7), the normalized decrease in active force was also found to be enhanced at lower firing frequencies. This indicates that, as stimulation frequency decreases, a larger fraction of the force is transmitted via epimuscular myofascial connections. Apparently, as stimulation frequency was lowered, the stiffness of the myofascial pathways (not containing serial sarcomeres) decreased less than the stiffness of the sarcomeres in series - myotendinous pathway. The decreased stiffness of the serial sarcomeres, which affected our results in a major way, is a function of the decreased number of cross-bridges binding to actin filaments. In fully dissected rat muscles it was found that for each stimulation frequency, a typical force stiffness curve existed (Ettema & Huijing 1994a), indicating a lower serial stiffness for sarcomeres - myotendinous pathway at lower forces.

- Chapter 3

Effects of stimulation frequency on length-force characteristics

The dependence of length-force characteristics on stimulation frequency is a well-known phenomenon for fully dissected muscle since the observations of Rack and Westbury (1969). For fully dissected muscles at submaximal levels of stimulation, shifts in muscle optimum length arise from the length-dependent Ca-sensitivity of force (Rack & Westbury 1969; Stephenson & Wendt 1984). At sarcomere lengths higher than optimum length of maximal activation, the effects of decreased filament overlap are counteracted by a higher force exerted per unit [Ca^{++}]. These two counteracting effects create new optimal conditions for active force at higher lengths. The use of both synchronous stimulation as well as a distributed stimulation of groups of motor units at variable stimulation frequencies by Rack & Westbury (1969) showed that at low firing frequencies, a distributed stimulation protocol provides smoother tetani than synchronous stimulation, and is thus one step closer to physiological conditions. However, the firing frequency dependence of length-force characteristics still holds true during synchronous stimulation (Mela *et al.* 2002). In addition to shifts in muscle optimum lengths, muscle active slack length was found to shift to higher muscle lengths as firing frequency is decreased (Rack and Westbury, 1969; Roszek and Huijing,1997; Brown *et al.*,1999)

Effects of myofascial force transmission on firing frequency-related shifts in optimum muscle length

In accordance with results of Rack and Westbury (1969; for fully dissected cat soleus muscle), Brown *et al.* (1999; for dissected feline caudofemoralis muscle), and Roszek and Huijing (1997; for fully dissected rat GM muscle), our present results show that also for a muscle within an intact compartment, lower stimulation frequencies are always accompanied by a progressive shift of optimum EDL length to higher lengths (Fig. 5). However, this shift is not equal for distally and proximally measured forces (Fig. 5b), indicating effects of additional factors.

It should be noted however, that optimum length cannot be measured directly, since only passive force and total force is measured experimentally. As active force is calculated by subtracting passive force before or after the tetanic contraction from total force, only an estimate of optimum length for whole muscle is obtained (MacIntosh & MacNaughton 2005). Therefore, the actual shifts in optimum lengths will be enhanced compared to our present results; passive force becomes relatively more important at higher muscle lengths and the underestimation of optimum length will increase.

In fully dissected and maximally activated muscle the following additional factors determine muscle optimum length (length of maximal active force exertion): (1) effects of pennation, (2) elastic effects of series elastic structures and (3) the serial distribution in sarcomere lengths. For muscles within its *in vivo* context of connective tissues, this reasoning has to be extended to include effects of an enhanced parallel distribution of sarcomeres lengths (or fibre mean sarcomeres length (Huijing 1996)), distinguishing proximal and distal fibre populations of muscle fibres within the muscle. Finite element modelling of muscle with

connections to the extracellular matrix (Yucesoy *et al.* 2003a) shows that substantial differences in fibre mean sarcomere lengths are to be expected between proximal and distal parts of the muscle, which are affected by asymmetries of muscle geometry and asymmetries of stiffness of myofascial connections.

Our present results also provide indirect evidence for the presence of a serial distribution of sarcomeres lengths within muscle fibres: Near optimum lengths (Figs. 3 and 5a) absolute EDL active force exerted at the distal tendon is higher than at the proximal tendon. There are two, mutually exclusive, alternative explanations for this phenomenon:

(a) Individual sarcomeres within the distal segment of EDL muscle fibres are active on the descending limb of their length force curves. Therefore, if they exert higher active forces, they would be active at lower lengths than the proximal sarcomeres within the same fibres. In accordance with results of (Julian & Morgan 1979), who related directly measured sarcomeres dynamics to the duration of creep, the enhanced creep in the proximal force traces (Fig. 3) would indicate the increased sarcomeres dynamics within muscle fibres at higher lengths. In such a case, the lower optimum length found for proximal EDL at 10 and 100 Hz firing frequencies would be explained by such serial distribution of sarcomeres length.

(b) Individual sarcomeres within the distal segment of EDL muscle fibres are active on the ascending limb of their length force curves. Therefore, they would be active at higher lengths than the proximal sarcomeres within the same fibres. This view is supported by finite element model results that explained well the principle of epimuscular myofascial force transmission and its experimentally found effects on muscle length force characteristics (Yucesoy *et al.* 2003a).

To discriminate between these two alternative explanations the following arguments are used: (1) on activation, the degree of shortening of sarcomeres is determined by the compliance of the series elastics elements. Within single muscle fibres (Julian & Morgan 1979), serial sarcomeres and their myotendinous connections and thus intersarcomere dynamics are the determining factor because of the comparatively low stiffness of the (remnants of) endomysium. In contrast for sarcomeres of muscle acting within its in vivo context of connective tissues, the length and compliance series elastic components (serial sarcomeres and remnants of the endomysium) are not affected predominantly by the sarcomeres of the muscle fibre considered, but also by sarcomeres as well as connected endo- and perimysial stromata of muscle fibres adjacent with in the muscle (and given epimuscular myofascial force transmission even by more distant structures). In such a case, additional forces are exerted on the myofascial series elastic elements. Consequently, these series elastic elements are expected to be at higher lengths and thus stiffer and stable equilibrium sarcomere lengths are expected to be attained faster than in single muscle fibres (Yucesoy *et al.* 2003a). These authors showed that the experimentally determined creep duration showed no direct relation to the calculated serial distribution of fibre strain (being an estimate for sarcomeres length). In contrast to single fibre results, high equilibrium serial distributions would be preceded by low creep durations. (2) For the passive muscle a higher force is indicative of higher sarcomere lengths. This means that,

prior to stimulation at different frequencies, the distal sarcomeres within muscle fibres of EDL are at higher lengths than their proximal counterparts. In such conditions, a reversal of serial sarcomeres length distribution upon activation is highly unlikely as the shorter proximal sarcomeres within EDL muscle fibres would be exposed to more compliant series elastic elements and would shorten more than their distal counterparts. Therefore, we conclude that the second explanation is the more likely one: Near optimum lengths, distal sarcomeres attain a higher length than the proximal ones within the same muscle fibres.

If for all muscle fibres of EDL the same serial distribution of sarcomeres length would be present, for all firing frequencies one would expect distally determined EDL optimal force to occur at lower muscle lengths than proximally determined EDL optimal force. However, our present results indicate either no effect (Fig 5b: 20 and 30 Hz) or an opposite effect (Fig. 5b: 10 Hz). Therefore, we hypothesize that an parallel distribution of fibre mean sarcomeres length, enhanced by epimuscular myofascial force transmission caused net differences between proximally and distally determined optimum muscle lengths (at 10 and 100Hz) and just compensated opposing effects at intermediate firing frequencies. This happens because additional forces transmitted via epimuscular connections are not exerted equally on all muscle fibres. For example, the neurovascular tract giving off branches of nerves and blood vessels to the muscles while coursing through the compartment in distal direction becomes smaller in diameter and les stiff.

Effects of myofascial force transmission on frequency- related shifts in active slack lengths

In contrast to the findings on fully dissected muscle (Rack and Westbury, 1969; Roszek and Huijing,1997; Brown *et al.*,1999) in which a lowered firing frequency shifted muscle active slack length progressively to higher muscle lengths, no significant firing frequency related shifts of distal active slack length were found in our current study (Fig. 4a). Muscle active slack length is the muscle length at which no active force is exerted by sarcomeres within a fibre on structures outside of the muscle. Therefore, muscle active slack length is not attained until the last sarcomere exerting force did shorten to its active slack length. In addition to elastic and pennation effects, serial or parallel distributions of sarcomere lengths may affect the muscle length at which this condition is fulfilled. Firing frequency-related shifts of active slack length in fully dissected muscles are thought to be due to intracellular mechanisms related to the lower sensitivity to calcium at lower lengths (Rack and Westbury, 1969; Roszek and Huijing, 1997; Brown *et al.*,1999). Therefore, one would expect a shift in active slack length to be present also for a muscle within an intact compartment, unless a compensating effect is created by the presence of such myofascial connections. Such a compensation of a shift in active slack length is not likely to be the result of a serial distribution of sarcomere lengths; at lower firing frequencies, the serial distribution is negligible (ΔF EDL approaches zero). Therefore, it is hypothesised that at lower firing frequencies, the increased role of myofascial force transmission causes an increased parallel distribution in sarcomere lengths (i.e. enhanced distribution in fibre mean sarcomere lengths). In order to compensate the frequency-related shift in active

slack length to higher muscle lengths, this increased parallel distribution should be characterized by an increased incidence of higher lengths of the sarcomeres still exerting force at low muscle lengths.

In conclusion, epimuscular myofascial force transmission becomes increasingly important at low stimulation frequencies, indicating that the relative stiffness of the serial sarcomeres-myotendinous path decreased more than that of the myofascial paths. The firing frequency dependent effects on length-force characteristics are modified by myofascial force transmission and create different effects at opposite ends of the muscle. Such effects should be taken into account for muscles operating within their *in vivo* context of connective tissues. Changes of distributions of sarcomere lengths (particularly parallel distributions) are hypothesised to play a major role in these effects.

4

Myofascial force transmission between antagonistic rat lower limb muscles: effects of single muscle or muscle group lengthening

Hanneke J.M. Meijer, Josina M. Rijkelijkhuizen & Peter A. Huijing

Abstract

Effects of lengthening of the whole group of anterior crural muscles (tibialis anterior and extensor hallucis longus muscles (TA+EHL) and extensor digitorum longus (EDL)) on myofascial interaction between synergistic EDL and TA+EHL muscles, and on myofascial force transmission between anterior crural and antagonistic peroneal muscles, were investigated. All muscles were either passive or maximally active. Peroneal muscles were kept at a constant muscle tendon complex length. Either EDL or all anterior crural muscles were lengthened so that effects of lengthening of TA+EHL could be analyzed. For both lengthening conditions, a significant difference in proximally and distally measured EDL passive and active forces, indicative of epimuscular myofascial force transmission, was present. However, added lengthening of TA+EHL significantly affected the magnitude of the active and passive load exerted on EDL. For the active condition, the direction of the epimuscular load on EDL was affected; at all muscle lengths a proximally directed load was exerted on EDL, which decreased at higher muscle lengths. Lengthening of anterior crural muscles caused a 26% decrease in peroneal active force.

Extramuscular myofascial connections are thought to be the major contributor to the EDL proximo-distal active force difference. For antagonistic peroneal complex, the added distal lengthening of a synergistic muscle increases the effects of extramuscular myofascial force transmission.

Keywords:

Introduction

In the last decade, studies have shown that morphologically defined muscles are not independent actuators, but are capable of mechanical interaction via their connective tissue structures (Huijing *et al.* 1998; Huijing & Baan 2001a; Maas *et al.* 2001; Smeulders *et al.* 2002; Yucesoy *et al.* 2003c). The concept of myofascial force transmission is based on the ability to transmit forces between muscles fibres and fascial connective tissues. Chains of molecules, including, trans-sarcolemmal molecules enable forces, generated by sarcomeres within a muscle fibre, to be transmitted via the basal lamina onto the surrounding endomysium and from there onto other intramuscular connective tissue structures (Street 1983; Tidball 1991; Trotter & Purslow 1992). The intramuscular stromata of adjacent muscles are continuous. Via those connections, muscle force can be transmitted from a muscle, without passing, and thus parallel to, the muscle tendon. Consequently, sarcomeres are not only loaded by forces via the myotendinous pathways and sarcomeres in series, but also by forces transmitted by myofascial connections. Note that if the force is transmitted from muscle via its epimysium, force transmission is referred to as *epimuscular* myofascial force transmission (Huijing *et al.* 1998; Huijing & Baan 2001a). For a muscle within its natural context of connective tissue, it has been shown that force measured at the origin of a muscle is not necessarily equal to the force exerted at its insertion. With the transmission of forces via epimuscular myofascial connections, additional loads act on the muscle. A difference in forces measured at the muscles' origin and insertion is an unequivocal indication for *net* epimuscular myofascial force transmission (Huijing & Baan 2001b). As epimuscular myofascial force transmission is mediated by connective tissues, the fraction of force transmitted myofascially has been found to depend on muscle length as well as the muscle's position relative to its surrounding structures (Huijing & Baan 2003; Maas *et al.* 2003a; Maas *et al.* 2003c).

So far, experimental studies in which only the muscle-tendon complex length of one muscle was changed have demonstrated the importance of myofascial force transmission between synergistic muscles (Maas *et al.* 2001; Maas *et al.* 2005b) as well as antagonistic muscles (Huijing 2002; Huijing & Jaspers 2005) . Although this unequivocally shows the mechanical interaction between muscles via myofascial pathways, such experimental conditions differ from the *in vivo* conditions. Besides for pathological conditions such as cramp or cerebral palsy, (Huijing 2007; Malaiya *et al.* 2007; Smeulders & Kreulen 2007; Yucesoy & Huijing 2007) *in vivo* movement involves simultaneous lengthening of a group of synergistic muscles. Such movement will yield big changes in relative position between antagonistic muscles. Since relative position of muscles is an important determinant of myofascial force transmission (Maas *et al.* 2004), effects on transmission between antagonistic muscles may be expected. The aim of this paper is twofold: 1) to investigate the effect of lengthening of the whole anterior crural muscle group and test whether the added lengthening of tibialis anterior and extensor hallucis longus muscles (TA+EHL) alters myofascial interaction between synergistic extensor digitorum longus (EDL) and TA+EHL muscles, compared to myofascial

force transmission for exclusive lengthening of EDL, and 2) to asses the effects of added lengthening of TA+EHL on the myofascial force transmission between anterior crural and antagonistic peroneal muscles.

Methods

Surgical and experimental procedures were in agreement with the guidelines and regulations concerning animal welfare and experimentation set forth by Dutch law, and approved by the Committee on Ethics of Animal Experimentation at the Vrije Universiteit. Immediately after all experiments, animals were killed using an overdose of urethane solution, and double-sided pneumothorax was performed.

Surgical procedures

Male Wistar rats (for lengthening of EDL n=7, for added lengthening of TA+EHL, n = 6, with mean body masses of 303.4 (S.D. 11.80) and 302.6 gr. (S.D. 16.2)) were anaesthetized using intraperitoneally injected urethane solution (1.5 g kg $^{-1}$ body mass, 12,5% urethane solution). Extra doses were given if necessary (maximally 1.5 ml). During surgery and data collection, the animals were placed on a heated water pad of approximately 37°C to prevent hypothermia. The skin and the biceps femoris muscle of the left hind limb were removed, exposing the anterior crural compartment which confines extensor digitorum longus (EDL), extensor hallucis longus (EHL) and tibialis anterior (TA) muscles. Connective tissue near the muscle bellies within the anterior crural compartment was left intact. Only limited distal fasciotomy was performed to severe the retinaculae (i.e. the transverse crural ligament and the crural cruciate ligament), and subsequently dissect the distal tendons of EDL, EHL and TA. For the added lengthening of TA+EHL, the original position of TA+EHL relative to the EDL in the reference position (i.e. corresponding to a knee angle of 110° and ankle angle of 180° plantar flexion) was preserved by aligning the markers on the distal TA, EHL and EDL tendons. In both experiments, the four distal tendons of EDL were tied together at the reference position using polyester yarn. After uniting, these tendons were severed distally to the knot. The distal tendons of TA and EHL muscles as well as the distal tendons of peroneal muscles were tied together and subsequently severed, and will be referred to as TA+EHL and peroneal complex respectively. The position of the proximal EDL tendon in the reference position (knee angle of 110°) was marked with a small pin on the epicondylus lateralis of the femur, before cutting a small piece of the bone with the proximal attachment of the EDL muscle. All tendons were connected to metal rods using 100% polyester yarn. The sciatic nerve was dissected free from the upper limb muscles and severed as proximally as possible. The foot was firmly fixed to a plastic plate.
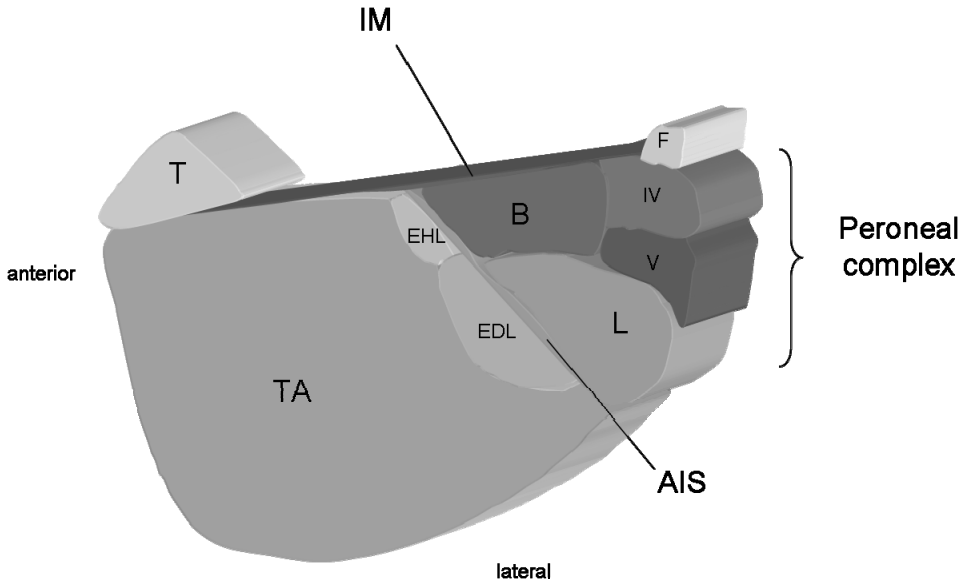
Figure 1. Schematic representation of a cross-section of the anterior crural and peroneal compartment in the rat lower limb, at approximately the middle of the EDL muscle belly. The anterior crural muscle group consists of tibialis anterior muscle (TA) enveloping extensor digitorum longus (EDL) and extensor hallucis longus (EHL) muscles. The anterior crural compartment is bordered medially by the interosseal membrane (IM) spanning the distance between the tibia (T) and (f) fibula. The peroneal muscle group, separated from the anterior crural compartment by the anterior intermuscular septum (AIS), consists of the peroneus longus (L), peroneus brevis (B), peroneus quarti (IV) and peroneus quinti (V) muscles.

Experimental set-up

The rat was placed on a heated platform (37°C) to prevent hypothermia, with the femur clamped to ensure a knee angle of 110°. The foot, attached to the plate, was firmly fixed into a rigid frame with the ankle in extreme plantar flexion (180°), with the metal rods passing over and under the foot (Fig. 2). All tendons were connected to force transducers (BLH Electronics Inc., Canton MA, compliance 16.2 $\mu m \cdot N^{-1}$, mounted on single-axis micropositioners) by the metal rods, which were aligned with the muscles' line of pull. The sciatic nerve was placed on a pair of silver electrodes and prevented from dehydration by covering it with paper tissue saturated with isotonic saline and which was covered by a thin piece of latex.

Experimental conditions

Ambient temperature (22° C ± 0.5) and air humidity (70 ± 2%) were kept constant by a computer-controlled air-conditioning system (Holland Heating, Waalwijk, the Netherlands). Muscle and tendon tissue was further prevented from dehydration by regularly irrigation with isotonic saline. The peroneal complex, deep flexors and triceps surae were kept at a constant muscle tendon complex length. The peroneal complex was set at such a length as to exert an initial force of

5 N. For lengthening of only EDL, TA+EHL was kept at a constant length, set to exert a force of 3N. The proximal EDL position was set to correspond to the marker on the femur, and was subsequently placed at a length which was 2 mm shorter than the original marker position. In the experiments in which TA+EHL was lengthened as well, the marker at the distal EDL tendon was aligned with the marker on the distal TA+EHL tendon. This relative position was maintained during the experiment by moving both distal force transducers equal distances.

Prior to excitation, all muscles were brought to their desired length and position passively by moving the force transducers. Before acquiring data, EDL, and in the added lengthening of TA+EHL experiment also TA+EHL, were preconditioned by isometric contractions at alternating high and low lengths, until forces at low length were reproducible (i.e. effects of previous activity at high length, Huijing & Baan 2001b) are removed). For the length-force curve, isometric contractions were performed at different EDL and TA+EHL lengths. Both TA+EHL and EDL muscles were lengthened distally with 1 mm increments. Two twitches were evoked, followed by a tetanic contraction at 100 Hz. All muscles studied were activated by stimulation of the sciatic nerve (with sureal and tibial branches denervated for the EDL lengthening experiment) with a constant current (3 mA) and a stimulation frequency of 100 Hz (pulse width 0.1 ms). Timing of stimulation of the nerve and A/D conversion (12-bit A/D converter, sampling frequency 1000 Hz) were controlled by a special purpose microcomputer. After each contraction, the muscles were allowed to recover near active slack length for 2 minutes. Passive isometric force was measured prior to the tetanic contraction and total force was measured during the tetanic plateau of the muscle force.

Data treatment

Passive muscle force was fitted using an exponential curve

$$y = e^{(ax + b)}$$

where y represents passive muscle force, x represents muscle-tendon complex length and 'a' and 'b' are fitting constants. Active EDL muscle force (F_{ma}) was estimated by subtracting the calculated passive force (F_{mp}) using the fitted function, from total force (F_m) for the appropriate muscle length. Active EDL length-force data were then fitted with a stepwise polynomial regression procedure (see statistics). The polynomial

$$y = b_0 + b_1x + b_2x^2 + \ldots B_nx^n$$

where y represents active muscle force, x represents active muscle force length and b_0 through b_n are fitting constants. Using the selected polynomials, mean and standard errors of active muscle force were calculated for given EDL lengths.

Optimum muscle length was defined for each individual curve as the active muscle length at which the fitted active force curve showed maximum force (F_{mao}).
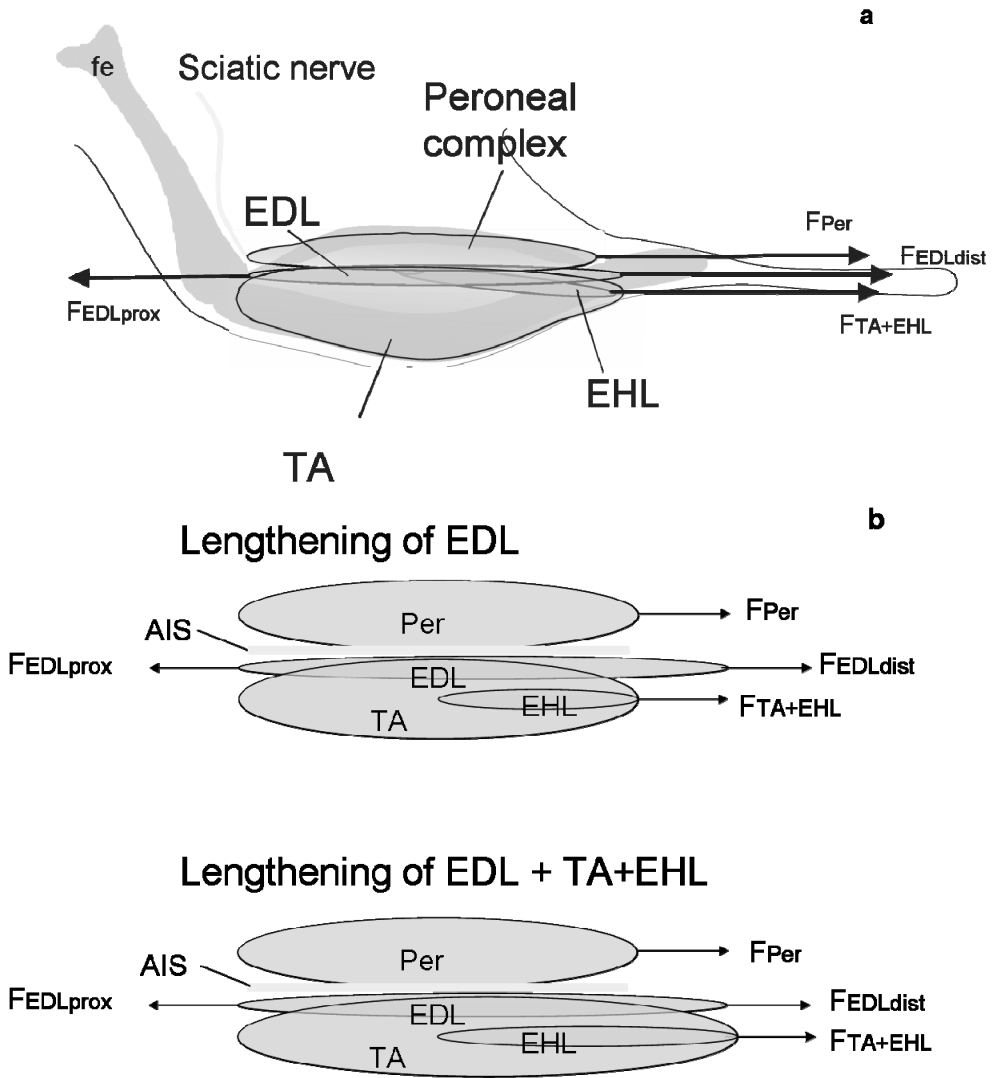
Figure 2. Schematic representation of the experimental setup and lengthening conditions.
(a) Lateral view of the rat lower limb after removal of the skin and biceps femoris muscle. The origin of extensor digitorum longus muscle (EDL) at the lateral condyle of the femur (fe) and the insertions of tibialis anterior (TA), extensor hallucis longus (EHL), EDL and peroneal muscles (Per) on the foot are severed and connected to force transducers (represented by arrows). Both femur and foot were fixed within a rigid frame in the reference position which corresponds to a knee angle of 110° and the ankle at 180° plantar flexion. **(b)** The two imposed lengthening conditions. Arrows indicate force transducers. For lengthening of EDL exclusively (upper panel), extensor digitorum longus muscle was lengthened distally by 1 mm increments, while the peroneal complex and tibialis anterior and extensor hallucis longus muscles were kept at a constant length. For synergist lengthening (lower panel), EDL and TA+EHL muscles were lengthened distally by 1 mm increments, while the peroneal complex is left at a constant muscle tendon complex length. The peroneal complex is separated from the anterior crural muscles by the anterior intermuscular septum (AIS).

In order to estimate more accurately the distal active slack length, data of muscle length and active muscle force ($F_{ma} < 0.3 \times F_{mao}$) were selected. The data points were then extrapolated with a fitted curve;

$$y = b_0 + b_1 x + b_2 \, {}^{exp(x)}$$

Active slack length was determined by solving this equation.

Statistics

In the active muscle force fitting procedure, the curve fitting starts with a first order polynomial and the power was increased up to maximally a sixth order, as long as this yields a significant improvement to the description of the length-active force data, as determined by one-way analysis of variance (ANOVA)(Neter *et al.* 1990). Two-way ANOVA's for repeated measurements were used to test for the effects of EDL muscle-tendon complex length and location of force measurement on EDL forces, to test for effects of EDL muscle-tendon complex length and lengthening condition (lengthening of EDL or synergistic lengthening of TA+EHL and EDL) on distal and proximal EDL forces, the proximo-distal force differences (for the interval $-7 \leq \Delta l_{m+t} \leq 3$) and peroneal active forces. One-way ANOVA's were used to test for the effect of EDL muscle-tendon complex length on TA+EHL as well as peroneal forces, and to test for differences between distally and proximally assessed optimum muscle lengths. Independent samples T-tests were performed to test for differences in active slack length and distal and proximal optimum muscle lengths between EDL lengthening and the added lengthening of TA+EHL. If significant effects were found, post hoc tests were performed using the Bonferroni procedure for multiple pair wise comparisons to locate differences. Main and interaction effects as well as differences were considered significant at $P < 0.05$. Values are plotted mean + SE, and muscle length is expressed as a deviation of distal EDL optimum muscle length.

Results

Effects of EDL lengthening and lengthening of synergists on length-force characteristics of EDL forces

Distal EDL forces

For distal EDL active forces (Fig. 3a), ANOVA showed significant effects of EDL length and lengthening condition, as well as interaction. At the ascending limb of the length-force curve, EDL distal active force during EDL lengthening is higher than for the added lengthening of TA+EHL. Optimal forces for both conditions are equal (2.4 N), and are similar for lengths over optimum muscle length. The length range of distal EDL active force exertion for the added lengthening of TA+EHL is smaller than for lengthening of EDL exclusively, as active slack length differed significantly (-8.3 mm and -10.7 mm for EDL + TA+EHL and EDL respectively).

For distal EDL passive forces, ANOVA also showed significant effects of muscle-tendon complex length and lengthening condition, as well as interaction. Below optimum muscle length, lengthening of synergistic muscles resulted in a lower distal passive force than lengthening of EDL. Passive forces increased exponentially with muscle-tendon complex length. Note that for both conditions, distal passive force starts to increase from well below distal optimum muscle length.

It is concluded that, the added lengthening of synergistic TA+EHL causes distal EDL length-force characteristics to be different from those during distal lengthening of EDL exclusively.
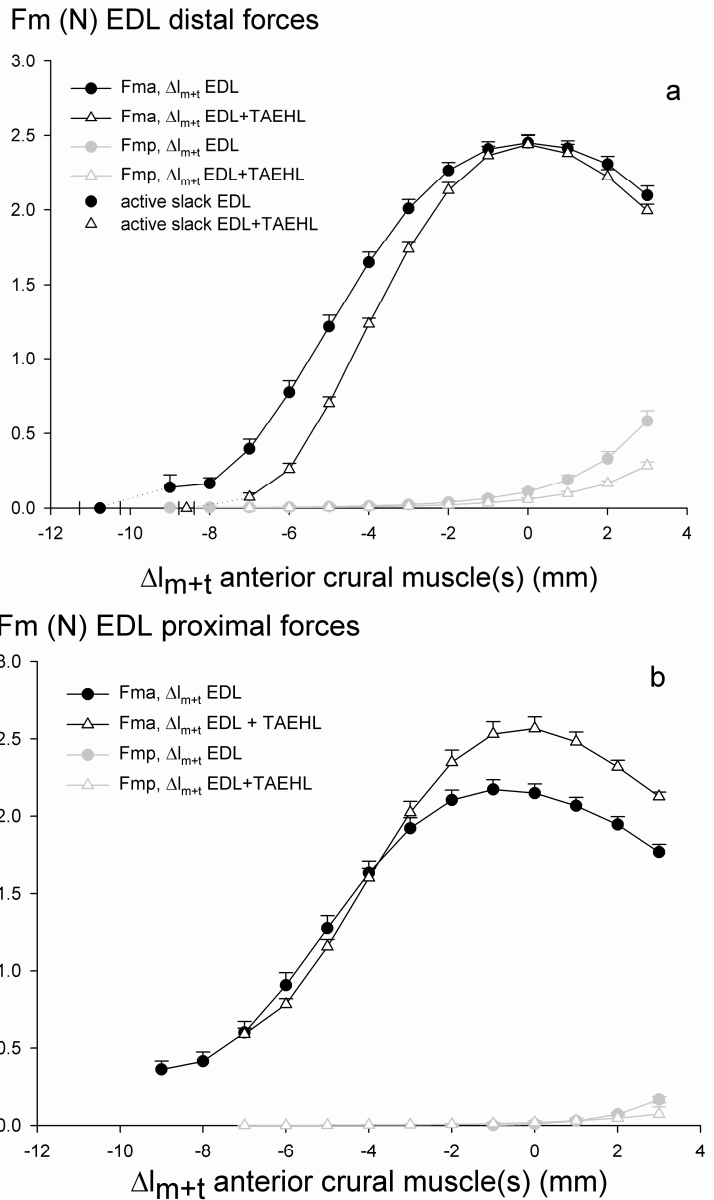
Proximal EDL forces

ANOVA showed significant effects of muscle-tendon complex length of EDL and lengthening condition on EDL proximal active forces (Fig. 3b), as well as an interaction between these factors. ANOVA also showed a significant difference in proximal optimum muscle lengths for these conditions. At low muscle lengths ($\Delta l_{m+t} \leq -4$), proximal active forces do not differ for EDL and synergistic muscles. At higher muscle lengths ($-3 \leq \Delta l_{m+t}$), proximal active force for lengthening of synergistic muscles is higher than proximal active force measured during lengthening of EDL exclusively. Proximal passive forces increased significantly and exponentially as a function of EDL muscle length, but passive forces did not differ significantly for the two conditions.

In conclusion, also for proximal active forces, the added lengthening of TA+EHL alters the EDL active length-force characteristics compared to lengthening of EDL only.

Effects of the added lengthening of TA+EHL on proximo-distal EDL force differences

Differences between proximally and distally exerted EDL forces were found for both lengthening of EDL exclusively and lengthening of synergistic muscles (Fig. 4). Such differences indicate that EDL is loaded also by myofascial loads. Note that a negative value for this difference indicates that EDL is loaded myofascially in distal direction. The additional load is resisted by EDL active force and in this case the load is integrated into the force exerted at the proximal tendon. Conversely, a positive proximo-distal active force difference represents myofascial loading of EDL in proximal direction and integration of that load in distal EDL active force.

ANOVA showed effects of muscle-tendon complex length and location of lengthening for active and passive EDL force differences, but no interaction was found for active force. The effects of added lengthening of TA+EHL shift down the whole curve describing proximo-distal active force difference as a function of length (Fig. 4). As a consequence, the reversal of the direction of loading seen for lengthening of EDL exclusively, is removed, as an effect of added TA+EHL lengthening. In this case EDL is loaded myofascially in distal direction at all lengths.

Figure 3. Proximal and distal active and passive EDL forces. **(a)** Length-force characteristics of distally measured EDL forces as a function of distal EDL muscle tendon complex length or muscle tendon complex length of EDL + TA+EHL. **(b)** Length-force characteristics of proximally measured forces of EDL as a function of distal EDL muscle tendon complex length or muscle tendon complex length of EDL + TA+EHL. (All values are shown as means + SE, n = 7 for lengthening of EDL, n = 6 for the added lengthening of TA+EHL).

At higher lengths, a smaller myofascial load is imposed than at lower lengths (Fig. 4). In the passive condition, EDL is always loaded myofascially in proximal direction. The added lengthening of TA+EHL does not shift the whole curve, but lowers the magnitude of the load at higher lengths (Fig. 4).

It is concluded that proximo-distal differences in EDL force exists also when a group of synergistic muscles are lengthened. However, the synergistic distal lengthening of TA+EHL and EDL alters the magnitude and direction of myofascial force transmission, especially at high muscle lengths.

TA+EHL forces for the two lengthening conditions

Fig. 5 shows the TA+EHL active and passive length force curve for as a function of the length the anterior crural muscles.

Distal lengthening of EDL exclusively caused a significant decrease in TA+EHL active force (Fig. 5, filled circles), despite the fact that TA+EHL was kept at a constant muscle-tendon complex length. TA+EHL active force decreased by 0.32 N (i.e. by 13%). Part of this decrease in TA+EHL active force should be ascribed to history effects, as control contractions after determining the EDL length-force curve indicate a force decrease of 5,7%. At the set length of TA+EHL, a relatively low muscle length, passive force is negligible, regardless of EDL length.
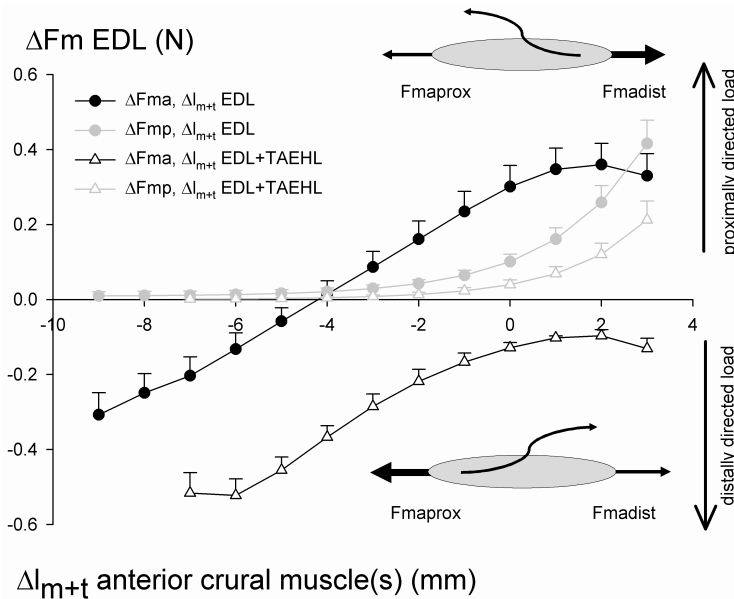
Figure 4. EDL proximo-distal force differences in the two lengthening conditions. Active (ΔFma) and passive (ΔFmp) force differences (Fdist – Fprox) are shown as means + SE (n = 7 for lengthening of EDL, n = 6 for the added lengthening of TA+EHL). Icons indicate direction of the net epimuscular load for positive and negative force differences. Note that an effect of added lengthening of TA+EHL is to remove the change in direction of the epimuscular load.
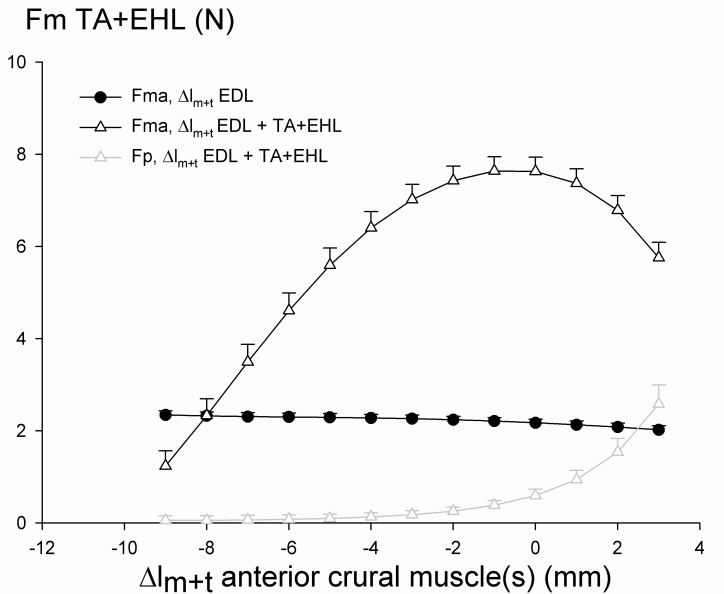
Figure 5. TA+EHL active and passive forces as a function of EDL + TA+EHL lengthening. Lengthening was obtained by moving the distal force transducers. As a reference, the decreasing active TA+EHL force with this complex at constant length is shown also. All values are shown as means + SE, n = 7 for lengthening of EDL, n = 6 for the added lengthening of TA+EHL.

*Effects of lengthening of synergistic anterior crural muscles on peroneal force*

During distal lengthening of EDL exclusively, peroneal active force (Fig. 6a, filled circles) decreased significantly ($P < 0.05$) despite the fact that peroneal muscles were kept at a constant length. Active force decreased by a relative small amount (maximally 0.25N or 6 %, Fig. 6b, filled circles).

Also after the added lengthening of TA+EHL, Bonferroni post-hoc tests showed a significant effect of EDL + TA+EHL muscle-tendon complex length on peroneal active force (Fig. 6a, open triangles); peroneal active force decreased significantly, despite the fact that peroneal muscles were kept at constant length. Peroneal active force decreased from 3.36N at Δl_{m+t} = -9 with 0.87N to 2.48N at Δl_{m+t} = 3. Expressed as a percentage of the initial active force level (Fig. 6b, open triangles), peroneal active force decreases with 26% as EDL + TA+EHL are lengthened by 12 mm.

The above results show that the added distal lengthening of a synergistic muscle has significant effects on active forces exerted by the antagonistic peroneal complex: force decrease in antagonistic peroneal muscles is much enhanced as a consequence of the added lengthening of TA+EHL.
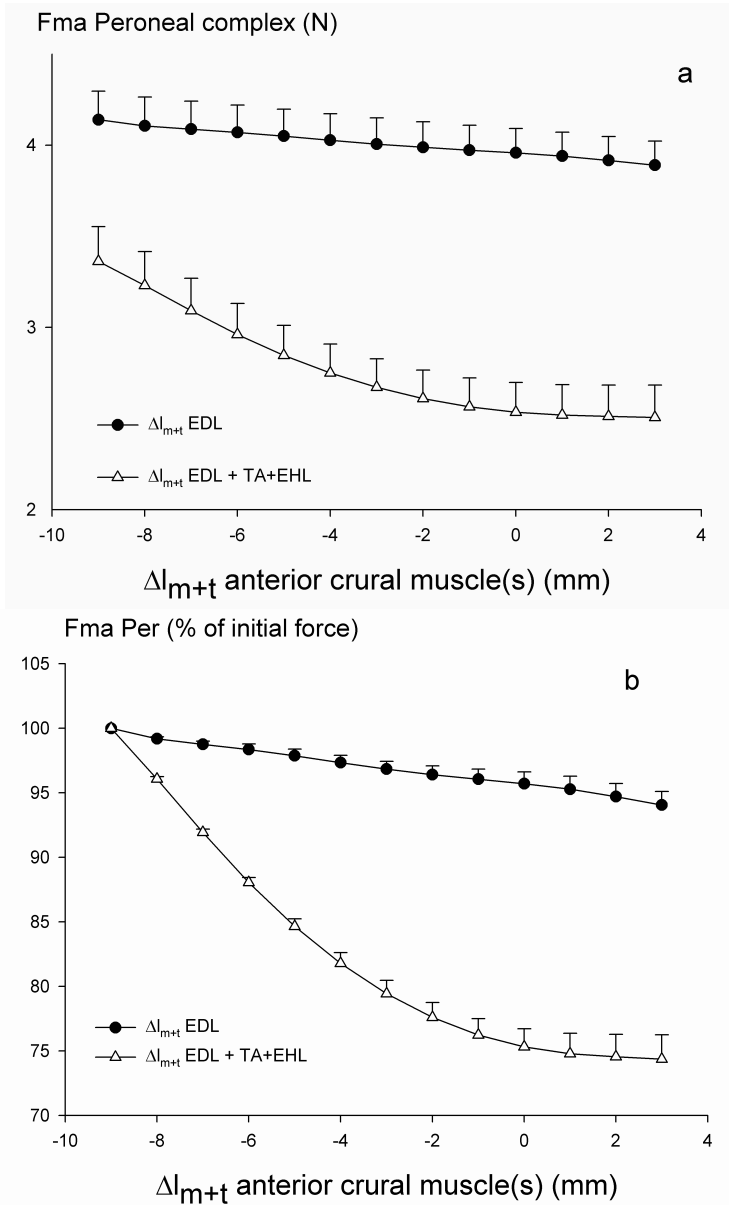
Figure 6. Effects of anterior crural lengthening condition on antagonistic peroneal forces.
(a) Peroneal active force as a function of muscle-tendon complex length of either EDL exclusively or EDL + TA+EHL. **(b)** Normalized peroneal active force, expressed as percentage of the initial force as a function of muscle-tendon complex length of either EDL exclusively or EDL + TA+EHL. All values are shown as means + SE, $n = 7$ for lengthening of EDL, $n = 6$ for the added lengthening of TA+EHL.

Discussion

Epimuscular myofascial force transmission

Effects of added lengthening of TA+EHL on the EDL proximo-distal force difference

Distal lengthening of the extensor digitorum longus muscle, as well as distal lengthening of synergistic EDL + TA+EHL within an intact anterior crural compartment results in length-dependent differences in active and passive forces exerted at the proximal and distal EDL tendons (Fig. 3). Such proximo-distal force differences are indicative of epimuscular myofascial force transmission (Huijing *et al.* 1998; Huijing & Baan 2001a). The present results are in agreement with previous studies on maximally activated rat extensor digitorum longus muscle within an intact anterior crural compartment (Huijing & Baan 2003; Maas *et al.* 2001; Maas *et al.* 2003a). However, the present study is a novel demonstration of the effects of length of a whole muscle group of synergistic muscles on epimuscular myofascial force transmission between synergistic muscles, as well as antagonistic muscles and the comparison of effects of length of a single muscle. For other new studies involving muscle group lengthening and antagonistic myofascial force transmission see elsewhere within this issue (Huijing 2007; Rijkelijkhuizen *et al.* 2007).

Both the magnitude as well as the direction of the *net* epimuscular force on EDL is affected after the added lengthening of TA+EHL (Fig. 4). Whereas for lengthening of EDL exclusively the proximo-distal active force difference reverses from a negative value at low muscle lengths to a positive value at high muscle lengths. The added lengthening of TA+EHL shifts the whole curve downwards, resulting in a negative active force difference that decreases with increasing lengths. According to our sign definitions, for the added lengthening of TA+EHL a *net* epimuscular load in distal direction is now exerted on active EDL at all muscle lengths. After lengthening of EDL exclusively, this distally directed load is only found at lower lengths: the sign of the proximo-distal active force difference reverses at higher muscle lengths. This is ascribed to changes in relative position between TA+EHL and EDL occurring during EDL lengthening and concomitant length and stiffness changes in their intermuscular connections. It should be noted that, after the added lengthening of TA+EHL, such changes in relative position between TA+EHL and EDL are absent and as a result, a reversal in the direction of the epimuscular force is prevented. Note that, in contrast to the EDL active force differences after added lengthening of TA+EHL, a positive passive proximo-distal force difference for EDL is found at high muscle lengths. This indicates that for the passive state of the muscles, the *net* epimuscular load on EDL is exerted in proximal direction, but that it changes into a *net* distally directed epimuscular force upon activation of the muscles.

The dominance of proximal active EDL force at low muscle tendon complex lengths for both lengthening conditions shows that even at low EDL forces, epimuscular connections are sufficiently stiff to allow myofascial loading of the

proximal EDL segment. Such 'prestrained' epimuscular connections ((Yucesoy *et al.* 2005), see also Yucesoy and Huijing (2007)) were found for EDL at a reference length (i.e. a length corresponding to a knee angle of 100° and an ankle angle of 90°), as well as for proximal lengthening of EDL. It is concluded that myofascial force transmission between EDL and TA+EHL is present for lengthening of EDL as well as for the added lengthening of TA+EHL. However, magnitude and direction of the net epimuscular force have changed as a result of the added lengthening of TA+EHL.

Effects of anterior crural muscle group length on peroneal active force

After distal lengthening of EDL exclusively, as well as after the added lengthening of TA+EHL, peroneal active force is always decreased significantly, despite the fact that this muscle group is kept at a constant muscle-tendon complex length. For lengthening of EDL exclusively, a decrease in peroneal active force was also reported by Huijing and Huijing & Jaspers in preliminary reports (2002; 2005) . In the present work, after the added lengthening of TA+EHL, the decrease in peroneal active force is almost 25%. Note that EDL and TA+EHL are located within the anterior crural compartment and separated from the peroneal compartment by the anterior intermuscular septum. The only connections between these muscle groups are myofascial ones, and therefore, the effect of lengthening anterior crural muscles on the peroneal active force is mediated by extramuscular myofascial force transmission, i.e. force transmission via non-muscular structures. For lengthening of EDL, the decrease in peroneal force is accompanied by an increase in distal EDL active force, which suggests that part of the EDL active force exerted at the distal tendon originates from the peroneal muscles. For the added lengthening of TA+EHL, it is hypothesized that the force exerted at the epimuscular connections between peroneal and TA+EHL muscles is increased, and therefore, more force will be transmitted from peroneal muscles onto TA+EHL muscles via this path. As a consequence, the force transmitted by epimuscular connections between peroneal muscles and the EDL is smaller, as this pathway is then comparatively less stiff. At higher muscle lengths, the added lengthening of TA+EHL reduces the epimuscular force transmission onto EDL (Fig. 4).

For the conditions of our present study, the added lengthening of TA+EHL significantly increases myofascially transmitted forces between antagonists. Therefore, for interaction between antagonists, muscle size (e.g. cross sectional area) is one determinant of the magnitude of epimuscular myofascial force transmission (Yucesoy *et al.* 2005).

Pathways of myofascial force transmission

Epimuscular myofascial force transmission is mediated by connective tissue structures surrounding the muscles, and is therefore susceptible to changes in muscle relative position as well as muscle length (Huijing & Baan 2003). Potential epimuscular connections are (1) direct connections between the intramuscular stromata of two adjacent muscles. Force transmitted via such pathways is referred

to as *intermuscular myofascial force transmission* (Huijing & Baan 2001a). Within the anterior crural compartment, intermuscular myofascial force transmission is known to occur at the EDL + TA+EHL muscle-belly interface (Maas *et al.* 2001; Maas *et al.* 2004). A recent study by Maas et al. (2005b) reported that after compartmental fasciotomy and subsequent blunt dissection, distal lengthening of TA+EHL resulted in a significant EDL proximo-distal active force difference, despite the fact that EDL was kept at a constant length. These results suggest that conditions exist in which the contribution of intermuscular myofascial connections to the proximo-distal force difference is small. In our current study, changes in relative position of intermuscular myofascial connections between EDL and TA+EHL are absent, and the added lengthening of TA+EHL creates different conditions for these intermuscular connections, compared to exclusive lengthening of EDL. Therefore, it is hypothesized that the contribution of the intermuscular connections to the proximo-distal EDL active force difference during added lengthening of TA+EHL is small.

When force is transmitted between the muscle and (2) connections between the intramuscular stromata and extramuscular connective tissue structures, such as connective tissues reinforcing nerves and blood vessels, intermuscular septa, the interosseal membrane, compartmental fascia and epitendinous tissues (Rijkelijkhuizen *et al.* 2005), we refer to it as *extramuscular myofascial force transmission* (Huijing & Baan 2001b). Previous studies (Huijing & Baan 2001b; Maas *et al.* 2003a; Rijkelijkhuizen *et al.* 2005; Yucesoy *et al.* 2003a) have shown that the most likely candidate for extramuscular myofascial force transmission in the rat lower limb is the neurovascular tract, a collagen reinforced complex supporting the nerves as well as blood and lymph vessels, see also discussion and images elsewhere in the present journal issue (Huijing 2007). The neurovascular tract passes between the peroneal compartment and the anterior crural compartment via a fenestration in the anterior intermuscular septum (Huijing & Baan 2001a) and branches within the anterior crural compartment (Maas *et al.* 2001). Note that the rather stiff connective fasciae are anchored to epimysia and compartmental walls and allow forces to be transmitted (Yucesoy *et al.* 2003b). In addition to the neurovascular tract, an indirect extramuscular linkage of anterior crural muscles with peroneal muscles exists because of the connections of both the anterior crural muscles' and peroneal muscles' intramuscular stromata to the anterior intermuscular septum (Huijing 2002).

For distal lengthening of EDL exclusively, it is hypothesized that the EDL branch of the neurovascular tract lengthens and consequently increases in stiffness, thereby exerting a proximally directed load on to EDL particularly at low lengths. This load is integrated in the force exerted at the distal EDL tendon and results in a higher distal than proximal EDL active force. The added lengthening of TA+EHL is expected to increase the total loading of the neurovascular tract, thereby increasing the stiffness of the extramuscular pathway between TA+EHL and peroneal muscles. More force (maximally 26%, Fig. 6b) is then transmitted from the peroneal muscles via the neurovascular tract onto the anterior crural compartment. However, such an increased proximal load exerted on EDL fails to

explain a (albeit decreasing) negative EDL active force difference for the added lengthening of TA+EHL. Note that the proximo-distal force differences represent the *net* epimuscular load exerted on EDL. This means that a net negative EDL proximo-distal active force difference can exist in the simultaneous presence of a high proximally directed as well as a slightly higher distally directed load. One likely myofascial structure to impose such a distally directed load is the fasciae covering the distal segment of the TA muscle belly and tendons (Fig. 7). These fasciae, consisting of general fascia and the epimysia of biceps femoris muscle, are attached medially onto the tibial crest and run laterally over the TA muscle belly and its epimysium, and continue towards and are connected to the antagonistic compartment walls. At low TA lengths, these distal fasciae are lengthened and exert a distally directed load on TA. As EDL is connected to TA+EHL via epimuscular myofascial connections, a fraction of this distally directed load is also exerted onto EDL, resulting in a negative active force difference. Lengthening of TA+EHL shortens the distal fasciae and decreases the distal load exerted on EDL. For passive muscles at any given length, this distal load is smaller than during the active state, as the displacement of the active muscle belly lengthens the distal fasciae and increases their stiffness. Therefore, it is possible for a net proximally directed myofascial load to be exerted onto passive EDL, while a net distally directed load is exerted upon activation.

It is concluded that different pathways of extramuscular myofascial force transmission are major determinants of the EDL proximo-distal active force difference. Both the neurovascular tract and the distal fasciae are hypothesized to be of major importance for extramuscular force transmission between the anterior crural compartment and antagonistic peroneal muscles.

Effects of myofascial force transmission on sarcomere length distributions

It has been argued that for a muscle with epimuscular myofascial connections, distributions of sarcomere lengths within the muscle fibres are altered (Maas *et al.* 2003a; Yucesoy *et al.* 2003a). Myofascially transmitted forces are not exerted equally on all muscle fibres within the muscle and as a consequence, sarcomeres at different locations within the muscle are allowed to shorten to a different degree. This leads to distributions in mean fibre sarcomere lengths, i.e. parallel distribution in sarcomere lengths (Huijing 1996). Finite element modelling of a muscle with intact myofascial connections supports such concept (Yucesoy *et al.* 2002a; Yucesoy *et al.* 2003a). An decreased distribution of mean fibre sarcomere lengths is hypothesized to explain the differences in the active length ranges between lengthening of EDL and the added lengthening of TA+EHL (Fig.3). The fact that a major difference in EDL active length range is found only for distal force may be explained by the fact that distal lengthening of EDL in the higher length range has location specific effects: (1) It enhances the change in relative position of the distal half of the while EDL muscle more than of its proximal half, (2) It enhances the change in relative position of the distal segments of EDL more than of the proximal segments of the same EDL fibres.
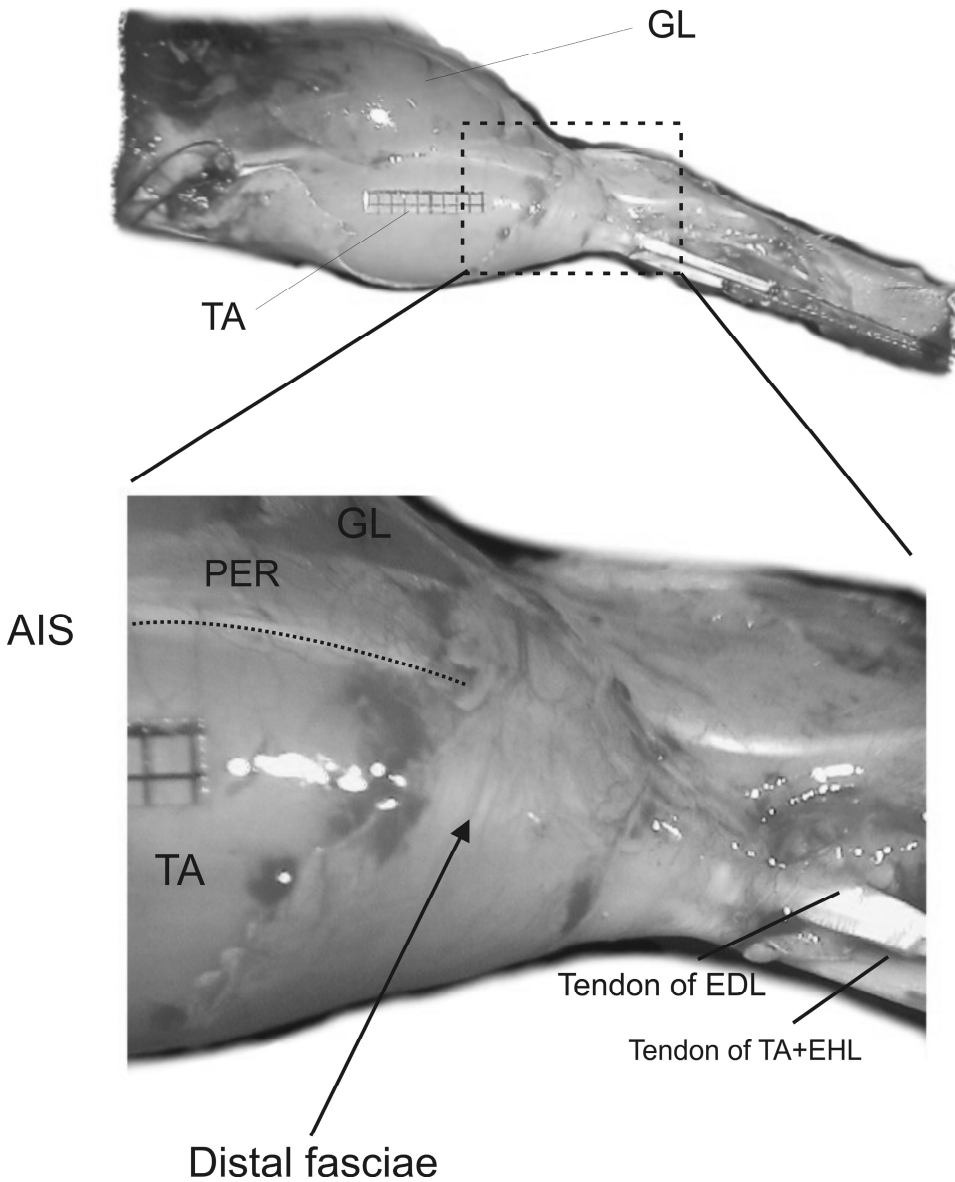
Figure 7. Lateral view of the rat lower leg after removal of the skin and biceps femoris muscle showing the distal fasciae. The distal EDL and TA+EHL tendons as well as the proximal origin of the EDL are cut from their attachment and connected to Kevlar threats. Note that the distal fasciae run from the tibial crest over the TA muscle belly towards the peroneal and triceps surae compartments. Via these fasciae, it is thought that a distally directed force is exerted onto the anterior crural muscles. TA indicates the tibialis anterior muscle, GL indicates the lateral gastrocnemius muscle, PER indicates the peroneal muscles, and AIS indicates the anterior intermuscular septum.

These factors combined have consequences for the magnitude of the parallel distribution of EDL sarcomere lengths (i.e. distribution of mean sarcomere lengths of the distal fibre segments). On the added lengthening of TA+EHL, the epimuscular load on EDL is distributed more evenly particularly in the distal muscle fibre segments, because the effects of intermuscular relative position are decreased or removed. Simultaneously, also the extramuscular load on TA+EHL is increased which tends to unload EDL.

Note that the added lengthening of TA+EHL causes distal EDL passive force to be higher than proximal passive force, indicating that the passive distal sarcomeres are at higher length than their proximal counter parts. However, this is reversed upon activation of the muscle, as proximal EDL active force is higher than distal active force. A reversal of sarcomere length distribution can only occur when, upon activation, the more proximal sarcomeres within muscle fibres are exposed to higher loading than distal ones. Such enhanced distal loading of TA does occur via the distal fasciae (Fig. 7). As the muscle is activated the muscle belly will shorten from its passive condition, because of elastic effects on the distal tendon, and the distal compartmental fasciae are stretched. It is hypothesized that this distal load is, at least in part, myofascially transmitted onto EDL.

It is concluded that simultaneous lengthening of a group of synergistic muscles increases extramuscular myofascial force transmission between antagonistic muscles. Intermuscular myofascial force transmission between synergists is altered by different muscle relative positions within the compartment. Such major effects should be taken into account when studying muscles within an *in vivo* context.

5

Effects of firing frequency on length-dependent myofascial force transmission between antagonistic and synergistic muscle groups

Introduction

In recent years, it has been shown that muscle force is not only transmitted via tendinous connections (Tidball on the frog semitendinous (1991), and Trotter et al. (1985) on mouse gastrocnemius muscle) but also via connective tissue structures within and surrounding the muscle (i.e. myofascial force transmission,Huijing *et al.* 1998; Huijing & Baan 2001b; Maas *et al.* 2001; Yucesoy *et al.* 2003a).

Via myofascial connections, a fraction of the muscle force can be transmitted from one muscle onto another, without passing one of its tendons. Any difference in force measured at the origin and insertion of a muscle is therefore an indication of myofascial force transmission between a muscle and its surrounding tissues. As a consequence, sarcomeres are not only loaded by forces transmitted via the myotendinous pathways and sarcomeres in series, but also by forces transmitted by myofascial connections. The direction and magnitude of these myofascially transmitted forces has been found to depend upon muscle length as well as the muscle's position relative to its surroundings (Huijing & Baan 2003; Maas *et al.* 2003a; Maas *et al.* 2003c; Yucesoy *et al.* 2006). At low firing frequencies, which are common for *in vivo* muscle functioning (Hennig & Lomo 1985), myofascial force transmission between synergistic muscles was found to be relatively more important (Meijer *et al.* 2006).

Myofascial force transmission between muscles is not limited to synergistic muscles, but also occurs between antagonistic muscles, (Huijing & Jaspers 2005; Huijing 2007; Rijkelijkhuizen *et al.* 2007). Meijer et al. (2007) showed that lengthening of a whole group of maximally active synergistic muscles significantly increases effects of extramuscular myofascial force transmission between antagonistic muscles. To enhance understanding of the physiological relevance of such myofascial interactions between antagonists, it is important to assess the effects of submaximal firing frequencies on extramuscular myofascial force transmission between antagonistic muscles.

Therefore, main aims of this study are (1) to quantify effects of stimulation frequency on myofascial force transmission between antagonistic and synergistic muscles of the rat lower hind leg at different lengths of anterior crural muscles and (2) test the hypothesis that anterior crural muscle length force curves are affected by such transmission at different firing rates.

Methods

Surgical and experimental procedures were in agreement with the guidelines and regulations concerning animal welfare and experimentation set forth by Dutch law, and approved by the Committee on Ethics of Animal Experimentation at the Vrije Universiteit. Immediately after all experiments, animals were killed using an overdose of urethane solution, and double-sided pneumothorax was performed.

Surgical procedures

Male Wistar rats (n = 6, with mean body mass of 302.6 gr. (S.D. 16.2)) were anaesthetized using intraperitoneally injected urethane solution (1.5 g kg $^{-1}$ body mass, 12,5% urethane solution). Extra doses were given if necessary (maximally 1.5 ml). During surgery and data collection, the animals were placed on a heated water pad of approximately 37°C to prevent hypothermia. The skin and the biceps femoris muscle of the left hind limb were removed, exposing the anterior crural compartment. This compartment contains extensor digitorum longus (EDL), extensor hallucis longus (EHL) and tibialis anterior (TA) muscles. Connective tissue near the muscle bellies within the anterior crural and peroneal compartments was left intact. Limited fasciotomy in the foot was performed to severe the distal tendons of peroneal and triceps surae muscles, as well as the transverse crural ligament and the crural cruciate ligament in order to subsequently dissect the distal tendons of EDL, EHL and TA. The original position of the TA+EHL muscles relative to the EDL in the reference position (i.e. corresponding to a knee angle of 110° and ankle angle of 180° plantar flexion) was recorded by placing aligned markers on the distal TA, EHL and EDL tendons. The position of the proximal EDL tendon in the reference position was marked with a small pin on the epicondylus lateralis of the femur. The four distal tendons of EDL were tied together at the reference position using polyester thread. After tying these tendons, they were severed distally to the knot. The distal tendons of TA and EHL muscles, as well as the distal tendons of triceps surae and peroneal muscles were tied together and these complexes will be referred to as TA+EHL, triceps surae and peroneal complex respectively. The proximal EDL tendon was freed by cutting a small piece of the bone with the proximal attachment of the EDL muscle. All severed tendons were connected to metal rods using 100% polyester yarn. The sciatic nerve was dissected free and severed as proximally as possible. The foot was firmly fixed to a plastic plate.

Mounting the animal in the experimental set-up

The rat was placed on a heated platform (37°C) to prevent hypothermia. The femur was clamped to ensure a knee angle of 110°. The foot, attached to the plate, was firmly fixed into a rigid frame with the ankle in extreme plantar flexion (180°). Before each experiment, all force transducers (BLH Electronics Inc., Canton MA, compliance 16.2 μm $\cdot$N^{-1}, mounted on single-axis micropositioners) to be used in the experiments were calibrated within the experimental setup. To eliminate differences between the force transducers, the proximal force transducer was calibrated vertically by the use of weights, while the distal force transducer was calibrated against the proximal force transducer while attached to the proximal one via a compliant spring. All tendons were connected to the force transducers by the metal rods. The metal rods of triceps surae and peroneal muscles passed dorsally over the foot, whereas the metal rods of TA+EHL and distal EDL passed ventrally under the foot (Fig. 1b). All metal rods were visually aligned with the muscles' line of pull. The sciatic nerve was placed on a pair of silver electrodes

and prevented from dehydration by covering it with paper tissue (saturated with isotonic saline) and by a thin piece of latex.

Experimental conditions

Ambient temperature (22° C ± 0.5) and air humidity (70 ± 2%) were kept constant by a computer-controlled air-conditioning system (Holland Heating, Waalwijk, the Netherlands). Muscle and tendon tissue was further prevented from dehydration by regular irrigation with isotonic saline. The peroneal complex and triceps surae muscles were kept at a constant muscle tendon length, set to exert an initial force of 5 N and 11 N respectively. At these muscle lengths, passive forces were very small. Note that the initial values of peroneal and triceps surae active forces in figures 2 and 3 are lower than the forces set at the start of the experiment. These initial force levels were determined when all other muscles were at their active slack lengths. Distal lengthening of the other muscles increases the myofascial load on the muscles, with a consecutive decrease in force exerted at the distal tendons. The proximal EDL position was set to correspond to the marker on the femur, and was subsequently placed at a length which was 2 mm shorter than the original marker position. The original position of TA+EHL relative to the EDL in the reference position was preserved by aligning the markers on the distal TA, EHL and EDL tendons. This relative position was maintained during the experiment by moving EDL and TA+EHL distal force transducers equal distances. Prior to excitation, all muscles were brought to their desired length and position passively by moving the force transducers. Before acquiring data, EDL and TA+EHL were preconditioned by isometric contractions at alternating high and low lengths, until forces at low length were reproducible (i.e. effects of previous activity at high length (Huijing & Baan 2001b) are removed). For the length-force curve, TA+EHL and EDL muscles were lengthened distally with 1 mm increments and isometric contractions were performed at different EDL and TA+EHL lengths. All muscles studied were stimulated through the sciatic nerve with a constant current (3 mA). The stimulation protocol started with two twitches (at t=200 and t=400ms), followed by a pulse train (at t=600 ms) with a staircase complex of ascending stimulation frequencies of 10, 20, and 30 and 100 Hz (pulse width 0.1 ms, total stimulation time 1000 ms), and a final twitch at t=1800 ms (Fig. 1a). Timing of stimulation of the nerve and A/D conversion (12-bit A/D converter, sampling frequency 1000 Hz, resolution of force 0.01N) were controlled by a special purpose microcomputer. After each contraction, the muscles were allowed to recover near active slack length for 2 minutes. Passive isometric force was measured prior to the tetanic contraction and total force was measured during the tetanic plateau of the muscle force (see Figure 1a).

Data treatment

Passive muscle force was fitted using an exponential curve

$$y = \exp^{(ax + b)} + C$$

where y represents passive muscle force, x represents muscle-tendon complex length and 'a' and 'b' are fitting constants. Active muscle force (F_{ma}) was estimated by subtracting the calculated passive force (F_{mp}) using the fitted function, from total force (F_m) for the appropriate muscle length. Active length-force data were then fitted with a stepwise polynomial regression procedure (see statistics). The polynomial

$$y = b_0 + b_1x + b_2x^2 + \ldots b_nx^n$$

where y represents active muscle force, x represents active muscle force length and b_0 through b_n are fitting constants. Using the selected polynomials, mean and standard errors of active muscle force were calculated for given muscle lengths. Optimum muscle length was defined for each individual curve as the active muscle length at which the fitted active force curve showed maximum force (F_{mao}). Active slack length for TA+EHL and distal EDL was estimated by selecting data of muscle length and active muscle force ($F_{ma} < 0.3x\ F_{mao}$) and extrapolated with a fitted curve where

$$y = \exp (b_0\ x + b_1) + b_2.$$

Active slack length was determined by solving the roots for this equation and is plotted with horizontal error bars.

For EDL, the differences in total, passive and active force between the distal and proximal tendon (respectively $\Delta Fm_{dist\text{-}prox}$, $\Delta Fmp_{dist\text{-}prox}$ and $\Delta Fma_{dist\text{-}prox}$) were calculated by subtracting proximal force from distal force. The normalized active force difference was calculated for each frequency by expressing the absolute active force difference as a percentage of the optimum distal active force for that frequency. Normalized peroneal and triceps surae active forces were calculated by expressing active forces as a percentage of the initial active force per frequency.

Statistics

In the active muscle force fitting procedure, the curve fitting starts with a first order polynomial and the power was increased up to a sixth order, as long as this yields a significant improvement to the description of the length-active force data, as determined by one-way analysis of variance (ANOVA)(Neter *et al.* 1990). Two-way ANOVA's were used to test for the effects of anterior crural muscle length and firing frequency on absolute and normalized peroneal and triceps surae active forces. In addition, two-way ANOVA's were used to test for the effects of stimulation frequency and anterior crural muscle length on EDL proximal and distal active and passive forces, TA+EHL active forces, the EDL proximo-distal active force differences as well as proximally and distally measured optimum muscle length (L_{mao}). One-way ANOVA's were used to test for the effects of firing frequency on distal EDL and distal TA+EHL active slack lengths and to test for the effects of anterior crural muscle length on TA+EHL passive force and the EDL proximo-distal difference in passive forces. A one sample t-test was used to test

whether EDL ΔFma was significantly different from zero. If significant effects were found, Bonferroni post-hoc tests for multiple pair wise comparisons were used to locate differences. Main and interaction effects were considered significant at $P < 0.05$.
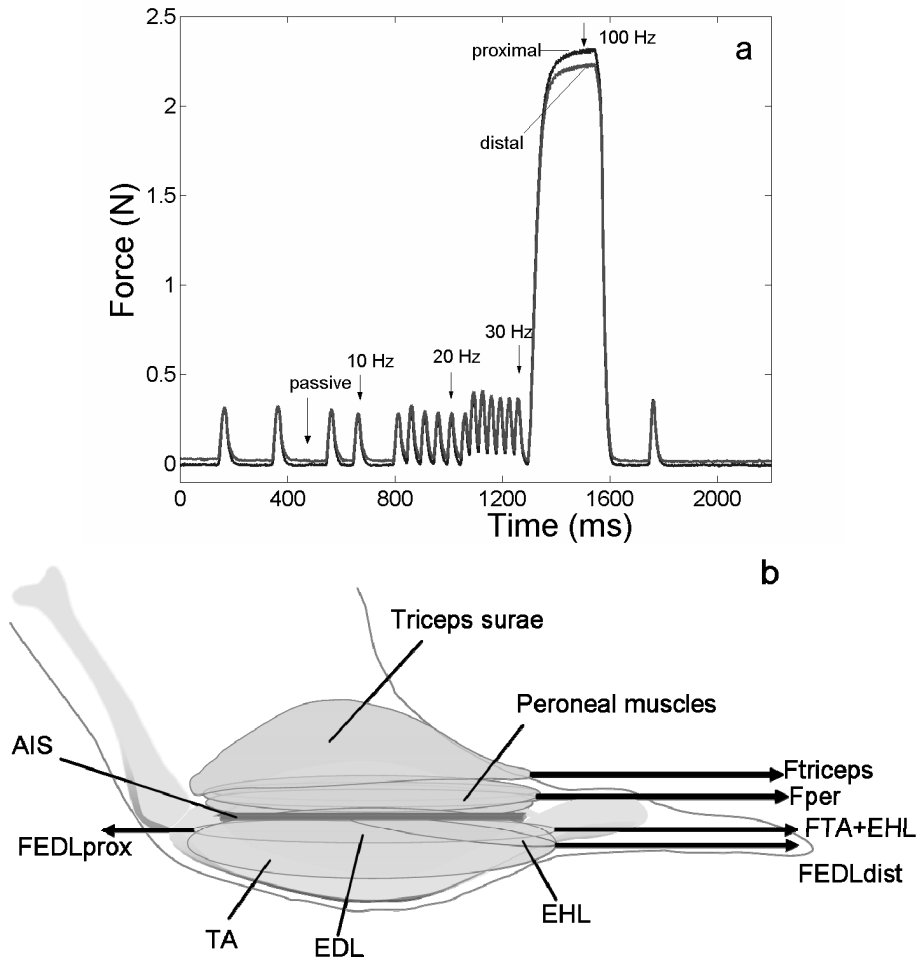
Figure 1. (a) Example of proximal as well as distal time-force traces of EDL muscle. An ascending stimulation frequency protocol of 10, 20, 30 and 100 Hz was applied to the nerve innervating the muscle. The example shows results for a contraction near optimum length. Arrows indicate the locations where active and passive force is measured. **(b)** Schematic view of the experimental set up of the rat lower leg. Lateral view of the rat anterior crural, peroneal and triceps surae compartments after removal of the skin and m. biceps femoris. Connective tissues at the muscle bellies were left intact. The m. tibialis anterior and m. extensor hallucis longus complex (TA+EHL) and m. triceps surae muscles are shown transparent to allow showing of the position of the underlying m. extensor digitorum longus (EDL), m. extensor hallucis longus (EHL) and peroneal muscles (PER). Note that EHL originates at the anterior intermuscular septum (AIS). The proximal origin of the extensor digitorum longus (EDL) as well as the distal tendons of the triceps surae, peroneal, EDL and TA+EHL muscles were severed and connected to force transducers using metal rods. The forces measured are represented by arrows. Both tibia and foot were fixed within a rigid frame in such a way that the muscles were aligned with the force transducers.

Definitions of myofascial force transmission via different pathways

Three types of myofascial force transmission are distinguished. [1] Muscle force generated by the sarcomeres can be transmitted onto the basal lamina and the endomysium (Bloch & Gonzalez-Serratos 2003; Street & Ramsey 1965; Street 1983). From that point, the intramuscular stroma of connective tissue enables the transmission of force onto the perimysium as well as the epimysium. This is referred to as *intramuscular myofascial force transmission* (Huijing 2003). [2] For muscles within their natural context of connective tissue, the continuity of intramuscular stromata of adjacent muscles creates pathways for the transmission of force between these muscles. Such transmission is referred to as *intermuscular myofascial force transmission* (Huijing & Baan 2001a; Maas *et al.* 2001). Third, when force is transmitted between the epimysium of a muscle and a non-muscular structure, such as connective tissues reinforcing nerves and blood vessels, intermuscular septa, the interosseal membrane, compartmental fascia and epitendinous tissues (Rijkelijkhuizen *et al.* 2005), it is referred to as *extramuscular myofascial force transmission* (Huijing & Baan 2001b). Note that when muscle force is transmitted via the epimysium, it is generally referred to as *epimuscular myofascial force transmission* until further distinction of pathways is possible.

Results

A. Mechanical interaction between antagonistic muscle groups

1. Effects of stimulation frequency and anterior crural muscle length on peroneal active forces

Figure 2 shows effects of stimulation frequency on peroneal active forces as a function of anterior crural muscle length. Note that the peroneal group consists of antagonistic muscles with respect to the muscles that are lengthened. Passive forces were small (Fmp < 0.04N) and therefore not plotted. ANOVA showed significant effects of anterior crural muscle length as well as stimulation frequency on peroneal active forces, but no interaction effect. Peroneal active force increased with higher firing frequency. However, despite the fact that the peroneal complex was kept at a constant muscle-tendon complex length for each stimulation frequency, peroneal active force decreased as a function of anterior crural muscle length (Fig. 2a). The absolute decrease in peroneal active force is highest for 100 Hz stimulation (ΔFmax = 0.87N). The smallest decrease is found for 20 Hz stimulation (ΔFmax = 0.14N).

For normalized peroneal forces (i.e. peroneal active force expressed as percentage of the initial force for each frequency, Fig. 2b), ANOVA showed significant effects of stimulation frequency and anterior crural muscle length, as well as interaction. Normalized peroneal active forces decreased as a function of anterior crural muscle-tendon complex length. The decrease in normalized peroneal force occurs in three phases: 1) for $\Delta l_{m+t} \leq -4$, normalized peroneal force at 100 Hz stimulation decreases more than at the submaximal stimulation frequencies; 2) for $-3 \leq \Delta l_{m+t}$,

this patterns changes and submaximal stimulation result in a similar (10 – 20 Hz) or even higher (30 Hz) deviation of initial peroneal force than for 100 Hz; 3) ultimately, at Δl_{m+t} = +3, the peak decrease for 10 and 20 Hz stimulation (approx. 34%) are similar to that of 30 Hz stimulation, but higher than for 100 Hz (ΔFma = approx. 26%).

These results show that distal lengthening of synergistic anterior crural muscles significantly affects antagonist peroneal complex distal active forces. For submaximal stimulation frequencies, the fraction of force transmitted this way is similar or larger at certain muscle lengths than for maximally active muscle. It is concluded that muscle tendon complex length of synergistic muscle is a co-determinant of active force exerted by adjacent antagonistic muscles.

2. Effects of stimulation frequency and anterior crural muscle length on triceps surae active forces
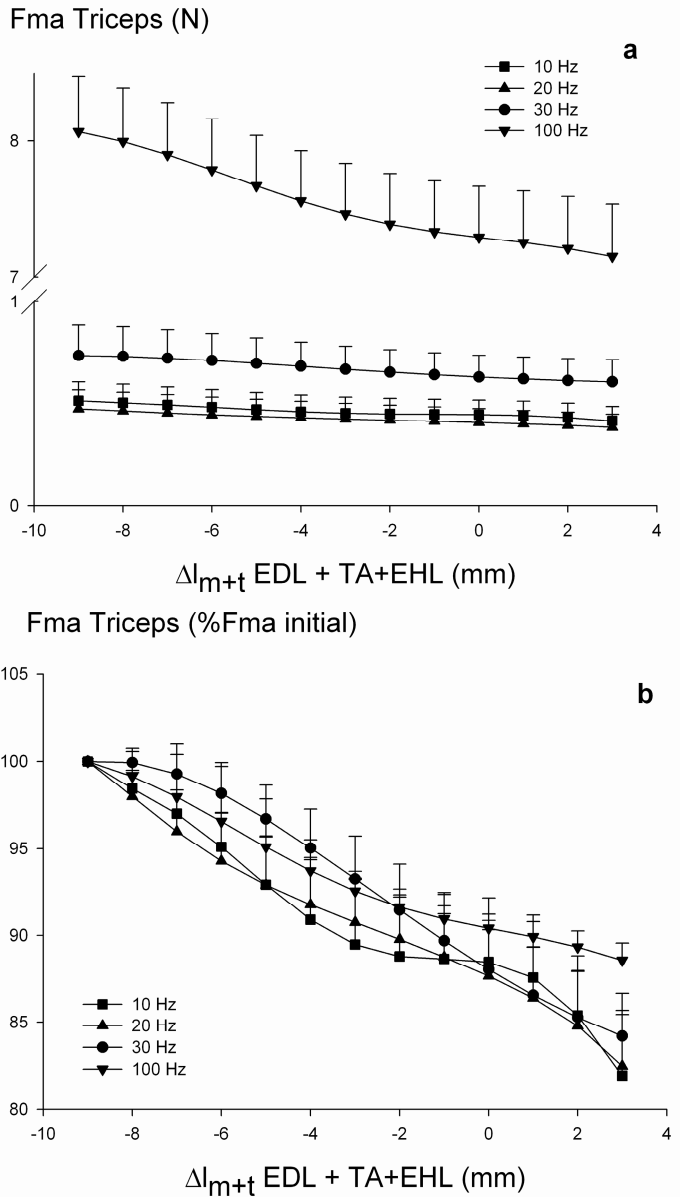
The effects of stimulation frequency on triceps surae active forces are plotted as a function of anterior crural muscle length (Fig. 3). Passive forces were small (Fmp < 0.05N) and therefore not shown. ANOVA showed significant effects of stimulation frequency, as well as anterior crural muscle length on triceps surae active forces (Fig. 3a), but no interaction was shown. Triceps surae active force increased significantly with the ascending stimulation frequencies. However, distal lengthening of anterior crural muscles caused significant decreases in triceps surae active force, despite a constant triceps surae muscle length. The maximal absolute decrease in active force is highest for 100 Hz stimulation (0.92N). The smallest decrease in triceps surae active force is found for 20 Hz stimulation (0.09N).

For normalized triceps surae active force (Fig. 3b), ANOVA showed significant effects of anterior crural muscle length and stimulation frequency, but no interaction effect was shown. For each stimulation frequency, normalized triceps surae active forces decreased as all anterior crural muscles were lengthened distally. The decrease in normalized triceps surae forces with increasing anterior crural muscle-tendon complex length shows two patterns 1) at low muscle lengths ($\Delta l_{m+t} \leq$ -2), the curve for 100 Hz normalized triceps surae force is intermediate between the submaximal firing frequencies; 2) for higher muscle lengths, $\Delta l_{m+t} \geq$ -1, the decrease in normalized force is highest for submaximal firing frequencies. Ultimately, 10 and 20 Hz stimulation yield the highest decrease (ΔFma = approx. 18%), while 100 Hz stimulation shows the smallest decrease (ΔFma = 11 %). This pattern differs from that seen for normalized peroneal force.

It is concluded that even distant antagonistic muscles within the same segment are not independent actuators: distal lengthening of the anterior crural muscles significantly affects antagonistic muscles even if they are located on the other side of the leg. Depending on length, the fraction of force transmitted myofascially is similar to that in maximally activated muscles or even higher at some submaximal stimulation frequencies.
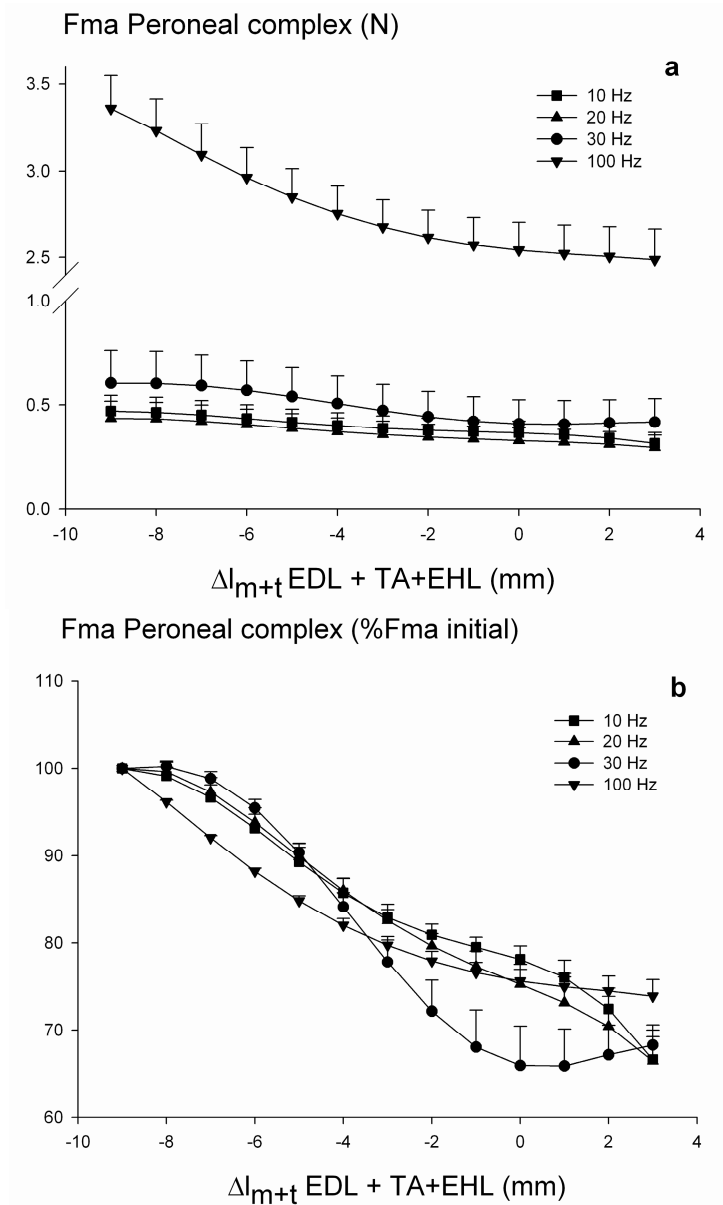
Figure 2. Effects of stimulation frequency on forces exerted distally by peroneal muscles at constant length. **(a)** Peroneal active forces during the tetanic plateau at 10, 20, 30 and 100 Hz stimulation as a function of lengths of the anterior crural muscles. **(b)** Peroneal active forces, normalized for initial force level per frequency, as a function of lengths of anterior crural muscles. Anterior crural muscle-tendon complex (Δl_{m+t}) length is expressed as a deviation from 100 Hz distal EDL optimum length. Values are shown as mean + SE, n = 6.

Fma Triceps (N)

Fma Triceps (%Fma initial)

Figure 3. Effects of stimulation frequency on forces exerted distally by triceps surae muscles kept at constant length. (a) Triceps surae active forces during the tetanic plateau at 10, 20, 30 and 100 Hz stimulation as a function of length of anterior crural muscles. (b) Triceps surae active forces, normalized for initial force level per frequency, as a function of length of anterior crural muscles. Lengthening of the anterior crural muscles was performed by moving the distal force transducers of EDL and TA+EHL only, and anterior crural muscle-tendon complex length (Δlm+t) is expressed as a deviation from 100 Hz distal EDL optimum length. Values are shown as mean + SE (n = 6).
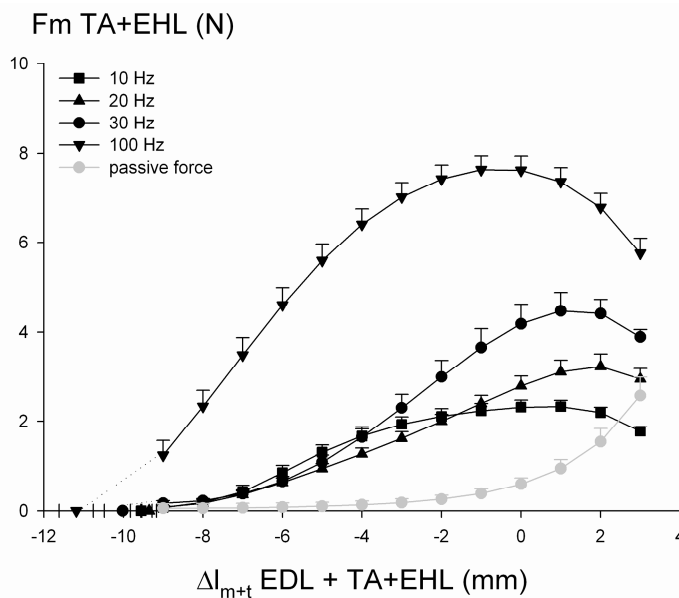
B. Effects of stimulation frequency on length-force characteristics

1. TA+EHL.

ANOVA showed significant main effects of anterior crural muscle length and firing frequency on TA+EHL active forces (Figure 4), as well as an interaction effect. Passive forces showed a length-dependent increase ($P < 0.05$).

In general, higher firing frequencies cause significantly higher active forces, and this force increase is quite length dependent. TA+EHL 100 Hz optimum length occurs at significantly lower muscle lengths compared to 20 and 30 Hz stimulation (ANOVA). In contrast, results for 10 Hz showed some aspects that deviate very much from expectations based on intrinsic mechanisms: (a) 10 Hz optimum length could not shown to be significantly different from that of the other stimulation frequencies, and thus did not fit the expected pattern of decreasing optimum lengths with increasing firing frequencies. (b) For the length range $-7 < \Delta l_{m+t} < -2$, 10 Hz active forces were actually higher or equal to 20 Hz forces! These two results combined indicate that TA+EHL forces are much increased with respect to expectations over a considerable length range (possibly range $-7 < \Delta l_{m+t} > +2$).

Active slack length was also shown to significantly shift to lower muscle lengths with increasing stimulation frequency. Bonferroni post-hoc tests showed significant differences in active slack length between 100 Hz and the three submaximal firing frequencies, but not within the submaximal firing frequencies.

Figure 4. Effects of stimulation frequency on TA+EHL length-force characteristics. TA+EHL passive and active forces at 10, 20, 30 and 100 Hz stimulation as a function of lengthening of the anterior crural muscles.(by moving the distal force transducers of EDL and TA+EHL only). Anterior crural muscle-tendon complex length ($\Delta lm+t$) is expressed as a deviation from 100 Hz distal EDL optimum length. Distal active slack length was estimated by extrapolation of active muscle force to zero and displays horizontal standard errors (SE). All values are shown as mean + SE (n = 6).

2. EDL

Figure 5a shows length-force curves for proximal and distal EDL forces at 10, 20, 30 and 100 Hz stimulation. For both distal and proximal active forces, ANOVA showed significant effects of anterior crural muscle length and stimulation frequency, as well as interaction between these two factors. For high lengths (Δl_{m+t} > -2), EDL proximal and distal active forces increased at higher stimulation frequency, and this force increase is length-dependent ($P<0.05$).

For 10, 30 and 100 Hz, ANOVA showed that proximal and distal EDL active forces differ significantly and proximal active force is higher than distal active force at all muscle lengths. In contrast, for 20 Hz, ANOVA showed no significant effect of location of force measurement (i.e. at the proximal or distal tendon) on EDL active forces. For 100 Hz, ANOVA showed an interaction between effects of location of force measurement and length, indicating that proximal and distal EDL active forces vary in an individual way as a function of anterior crural muscle length.

Note that EDL optimum lengths measured at the proximal tendon did not differ significantly from optimum lengths measured at the distal tendon. As expected, for 20, 30 and 100 Hz, EDL optimum length shifted to lower muscle lengths as firing frequency was increased (e.g. for 100 Hz, the shift in optimum muscle length equalled approximately 3 mm with respect to 20 Hz).

Also for EDL 10 Hz active force deviating patterns were observed, but they were smaller than effects for TA+EHL: (a) EDL optimum muscle length for 10 Hz could not be shown to differ significantly from that at 20 and 30 Hz, but differed significantly from 100 Hz optimum length. (b) For a considerable length range (i.e. $-5<\Delta l_{m+t} < +1$) 10 Hz and 20 Hz forces were quite similar. These two results combined also indicate for EDL that 10 Hz forces are enhanced in some way over a considerable length range.

Distal active slack lengths were shown (ANOVA) to differ significantly as a function of firing frequency. However, Bonferroni post-hoc tests showed that distal active slack length between the three submaximal stimulation frequencies did not differ significantly.

3. Effects of stimulation frequency on EDL proximo-distal force differences

The presence of any difference in proximally and distally measured forces is indicative of epimuscular myofascial force transmission. A negative value for this difference indicates a *net* myofascial loading of EDL in distal direction. This additional load is resisted by EDL force and the net load is integrated into the force exerted at the proximal tendon, causing proximally measured force to be higher than distally measured force.

The proximo-distal differences in total EDL force ($\Delta Fm_{dist-prox}$) represent the *net* myofascial load exerted on EDL during activation (Fig. 5b). ANOVA showed effects of anterior crural muscle length and firing frequency, as well as an interaction. Bonferroni posthoc-tests showed that $\Delta Fm_{dist-prox}$ is not significantly different for the submaximal firing frequencies. In addition, $\Delta Fm_{dist-prox}$ for 100 Hz stimulation differs significantly from $\Delta Fm_{dist-prox}$ at the submaximal firing frequencies. Initially, $\Delta Fm_{dist-prox}$ attains negative values for submaximally as well

as maximally active EDL, which indicates that a *net* total myofascial load is exerted on EDL in the distal direction. For the submaximal firing frequencies, this distally directed myofascial load is small, whereas the distally directed load on maximally active EDL is substantial (0.5N). At $\Delta l_{m+t} \geq -1$, the net myofascial load exerted at submaximally active EDL is reversed as the $\Delta Fm_{dist-prox}$ becomes positive and increases with increasing anterior crural muscle length. However, for maximally active EDL, $\Delta Fm_{dist-prox}$ initially decreases with increasing anterior crural muscle length, only to become positive at $\Delta l_{m+t} > 1$. Note that at high muscle lengths, the proximally directed myofascial loads are largest for the submaximal firing frequencies (0.2N). The proximo-distal difference in total EDL force are unequivocal evidence for the exertion of myofascially transmitted loads on maximally, as well as submaximally active EDL.

To allow a more thorough analysis of the contributions of the muscles' active and passive forces, the myofascial load exerted on EDL is analyzed for these conditions (Fig. 5c). Note however that proximo-distal differences in EDL active force can at best be only estimates, as active force is not measured directly, but calculated by subtracting passive force (measured before the tetanic plateau) from total force (measured during the tetanic plateau) (MacIntosh & MacNaughton 2005).

For all muscle lengths studied, EDL proximo-distal differences in active force ($\Delta Fma_{dist-prox}$) are negative (Fig. 5c). Bonferroni post-hoc tests showed that $\Delta Fma_{dist-prox}$ at the submaximal stimulation frequencies differs significantly from that at 100 Hz stimulation, but no significant difference in $\Delta Fma_{dist-prox}$ is found between the submaximal firing frequencies. $\Delta Fma_{dist-prox}$ for 10, 20 and 30 Hz is quite small ($\Delta Fma_{dist-prox} = 0.03N$ or 5% of F_{mao}). Note, however, that this value is significantly different from zero (one sample t-test on average values). In addition, no significant effect of anterior crural muscular length could be shown on $\Delta Fma_{dist-prox}$ at submaximal firing frequencies. In contrast, for 100 Hz firing frequency, the $\Delta Fma_{dist-prox,}$ and thus the *net* active myofascial load, is length-dependent and is highest at low muscle lengths but decreases after anterior crural muscles are lengthened distally. Note that at the lowest lengths, this value represents all of the active force exerted by EDL.

The normalized proximo-distal active force differences (i.e. $\Delta Fma_{dist-prox}$ normalized for distal EDL optimum force at each frequency) represent the fraction of EDL active force transmitted myofascially (Fig. 5d). For this variable, ANOVA showed effects of length, as well as of firing frequency, but no interaction. Bonferroni posthoc tests showed that normalized $\Delta Fma_{dist-prox}$ for maximal stimulation is significantly different from the submaximal stimulation frequencies; particularly at low muscle lengths, normalized $\Delta Fma_{dist-prox}$ for 100 Hz is significantly higher than for the submaximal firing frequencies. No significant differences between the three submaximal firing frequencies could be shown. For the absolute proximo-distal differences in passive EDL force, ANOVA showed significant effects of anterior crural muscle length and of stimulation frequency on the EDL proximo-distal active force difference, but no significant interaction effect was shown.
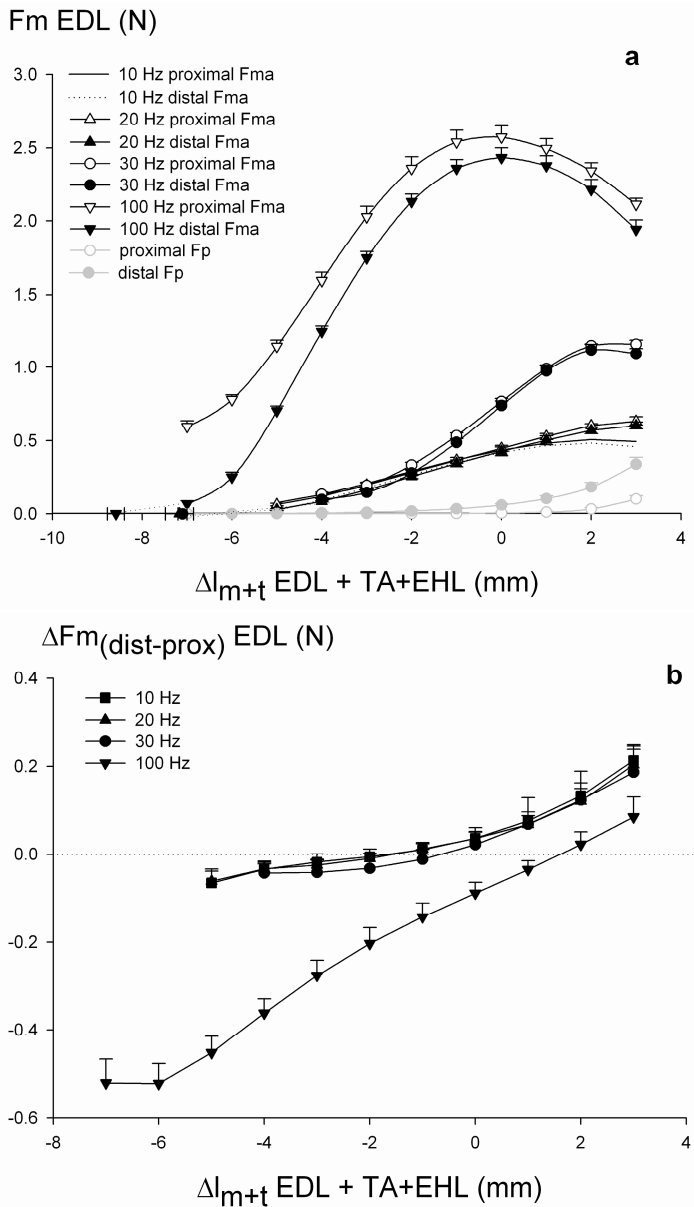
Figure 5. EDL proximal and distal length-force characteristics and proximo-distal force differences.
(a) EDL passive and active length-force characteristics at 10, 20, 30 and 100 Hz stimulation as a function of distal length of the anterior crural muscles (EDL + TA+EHL), expressed as a deviation from EDL 100 Hz distal optimum length. **(b)** The difference in proximally and distally exerted EDL total force, $\Delta Fm_{dist-prox}$, as a function of anterior crural muscle length (expressed as a deviation from EDL 100 Hz distal optimum length). The proximo-distal force difference was calculated by subtracting proximal force from distal force for any given muscle length. The negative value for the EDL proximo-distal difference in force indicates the presence of a *net* distally directed load exerted onto EDL, a positive value indicates a proximally directed *net* myofascial load.
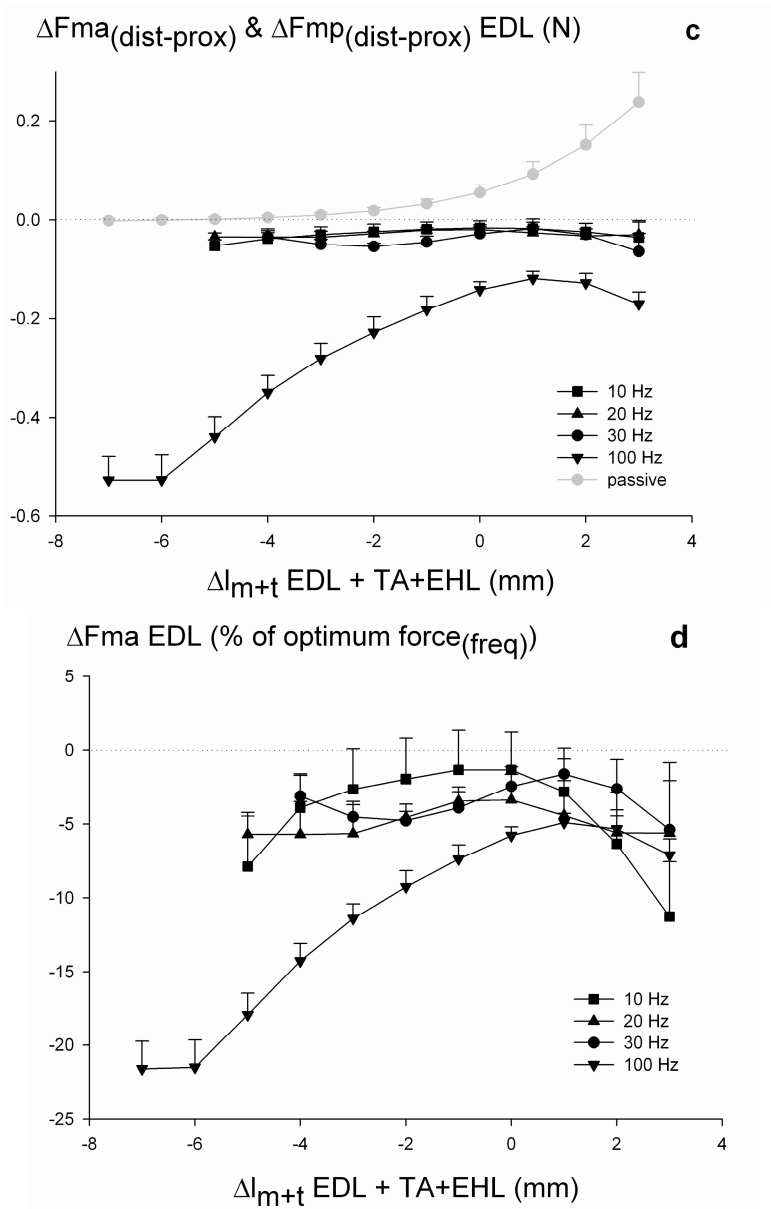
Figure 5. **(c)** EDL proximo-distal differences in active (ΔFma$_{dist-prox}$) and passive (ΔFmp$_{dist-prox}$) forces for 10, 20, 30 and 100 Hz stimulation, as a function of anterior crural muscle lengthening. Anterior crural muscle-tendon complex length is expressed as a deviation from EDL 100 Hz distal optimum length. **(d)** EDL proximo-distal force differences in active forces, ΔFma$_{dist-prox}$, normalized for distal optimum active force per frequency as a function of anterior crural muscle length. Values are shown as mean ± SE, n = 6.

Discussion

Extramuscular myofascial force transmission between antagonistic muscle groups

The main two findings of this study are: (1) the presence of significant mechanical interaction between antagonistic muscle groups despite being kept at a constant muscle tendon-complex length, maximally, as well as submaximally stimulated peroneal and triceps surae muscles decrease in active force as a function of distal lengthening of all anterior crural muscles. (2) The more limited effects of firing frequencies (compared to those of single muscle lengthening of Meijer *et al.* 2006) on this interaction. As firing frequency is lowered, and thus active force exerted at the triceps surae and peroneal distal tendons decreases, the fraction of the force transmitted via extramuscular myofascial connections (Fig. 2b and 3b) is equal to or even higher than for maximal stimulation. In any case, the conclusion is warranted that mechanical interaction between antagonistic muscles via extramuscular myofascial force transmission is substantial, even at submaximal firing frequencies. Such importance of myofascial force transmission at submaximal stimulation frequencies is in agreement with previous conclusions regarding synergistic myofascial force transmission between EDL and TA+EHL for distal lengthening of EDL exclusively (Meijer *et al.* 2006).

Peroneal muscles are located within a compartment adjacent to the anterior crural one, and separated from it by the anterior intermuscular septum. A very small part of the lateral gastrocnemius muscle is adjacent to the anterior crural and peroneal compartments, but the major part of the triceps surae muscle mass is located at the opposite site of the anterior crural compartment within lower leg (Fig. 6). All connections between anterior crural and antagonistic peroneal and triceps surae muscles are extramuscular myofascial connections, such as compartmental fasciae, the neurovascular tract or epitendinous tissues. Via these extramuscular myofascial connections, force is transmitted from the peroneal and triceps surae muscles onto other muscles within the same or other compartments, joint capsules and ligaments, and ultimately bones. For maximally stimulated muscles, such transmission is in agreement with previous studies on extramuscular myofascial force transmission between antagonists (Huijing *et al.* 2007; Rijkelijkhuizen *et al.* 2007). In fact in a combination of studies, for all rat lower hind leg muscle groups (anterior crural, peroneal, deep flexors, and triceps surae) such transmission has been shown for conditions of maximal activation (Huijing 2007; Meijer *et al.* 2007).

It should be noted that in our current and previous experiments, the length and position of only one muscle or muscle group were changed simultaneously, with all other muscles kept at constant muscle- tendon complex lengths to be able to unequivocally demonstrate the myofascial effects. However, *in vivo* movement will involve simultaneous and opposite length changes of antagonistic muscle groups (particularly anterior crural and triceps surae muscles). Therefore, changes in relative position of these antagonistic muscles will be more pronounced. As a consequence, it is expected that *in vivo,* myofascial force transmission between

submaximally active antagonistic muscle groups will even attain higher maximal values than in our present work.

A fraction of the force transmitted from peroneal and triceps surae muscles is exerted onto anterior crural muscles via extramuscular pathways. Potentially important extramuscular myofascial pathways between anterior crural muscles and triceps surae and peroneal muscles are judged to be the collagenous stromata that reinforce the blood vessels and nerves of the lower leg (Fig. 6). Such complexes are referred to as the neurovascular tract. Within the rat lower leg, the neurovascular tract connects the anterior crural compartment and triceps surae and peroneal compartments in two ways; 1) the neurovascular tract itself forms a direct connection between antagonistic muscles, as the anterior tibial artery and vein descend from the triceps surae compartment via the deep flexor compartment into the peroneal and anterior crural compartments, where it is joined by the deep peroneal nerve, entering from the peroneal to the anterior crural compartment and 2) via the attachment of the neurovascular tract to both sides of the anterior intermuscular septum, as well as to the epimysia of individual muscles and general fascia bordering all compartments. Distal lengthening of the anterior crural muscles will shear the neurovascular tract and results in stiffer extramuscular myofascial connections between peroneal and triceps surae and anterior crural muscles. Maas *et al.* (2005b) suggested that for muscles within the anterior crural compartment, this extramuscular collagen-reinforced system is the major contributor to epimuscular myofascial force transmission between synergistic muscles. Our current work implies that the neurovascular tract is also an important candidate pathway for intercompartmental myofascial force transmission between multiple antagonistic compartments.

Extramuscular myofascial force transmission and deviating length-force characteristics of EDL and TA+EHL

Any proximo-distal difference in force is taken as an indication for epimuscular myofascial force transmission (Huijing *et al.* 1998; Huijing & Baan 2001a; Huijing & Baan 2001b; Maas *et al.* 2001). For submaximal firing frequencies, the difference in proximally and distally determined EDL forces is small (Fig. 5c), suggesting that the effects of epimuscular myofascial force transmission on EDL may be negligible. Also, in contrast to earlier work on submaximally active EDL (Meijer *et al.* 2006), a firing-frequency related increase in the fraction of the force transmitted myofascially, indicative of an enhanced importance of myofascial force transmission at low firing frequencies, is absent (Fig. 5d). However, it should be kept in mind that the proximo-distal force difference represents only the *net* result of oppositely directed myofascial loads (Huijing 2007; Meijer *et al.* 2007).
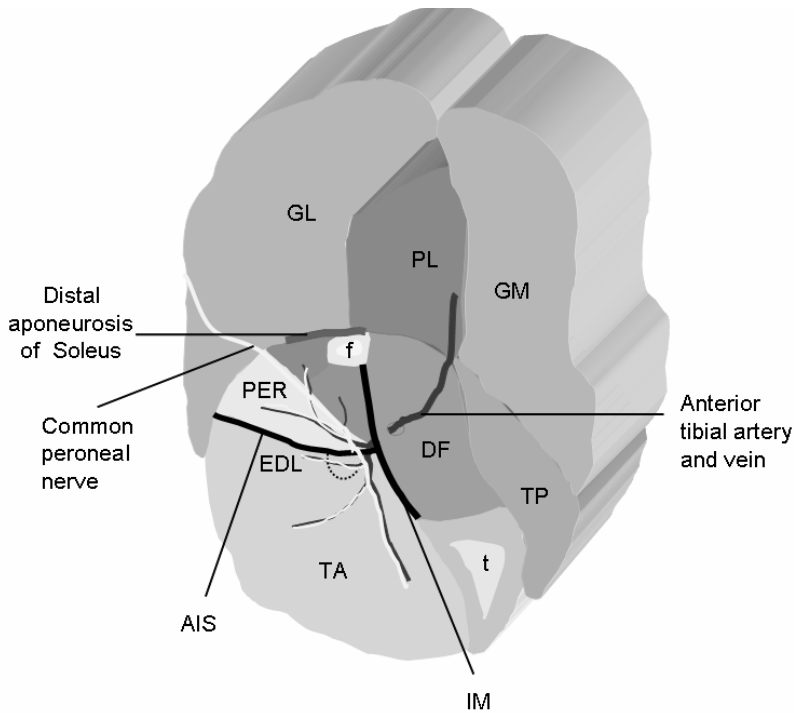
Figure 6. Schematic representation of a cross-section of the rat lower leg with the biceps femoris muscle removed. Most of the cross-section represents the anatomy at approximately 1/3 of the length of the EDL muscle belly from its origin. Note that the course of the common peroneal nerve and major blood vessels (anterior tibial artery and vein) is projected upon the cross-section from different levels. The EHL is only present more distally, but its position with respect to EDL and TA+EHL is indicated by a dotted line. Of the soleus muscle (SOL), only the distal aponeurosis is visible yet. GL indicates the lateral gastrocnemius muscle, GM indicates the medial gastrocnemius muscle, PL indicates the plantaris muscle, PER indicates the peroneal muscles, DF indicates the deep flexor muscles, TP indicates the tibialis posterior muscle, f denotes the fibula, t indicates the tibia, IM represents the interosseal membrane and AIS indicates the anterior intermuscular septum.

This becomes particularly evident when considering the total proximo-distal difference (Fig. 5b) at high muscle lengths; although the *net* total myofascial load on EDL is proximally directed, the separate active and passive myofascial loads on EDL are oppositely (i.e. distally and proximally respectively) directed (Fig. 5c). Therefore, a small proximo-distal force difference may actually represent multiple large myofascial loads being exerted on the muscle. Such conditions should have significant consequences for length force characteristics. As our present results contain such effects we argue that despite the small proximo-distal EDL active force differences, large extramuscular myofascial loads are exerted on anterior crural muscles. This is most evident for 10 Hz firing frequency, for which TA+EHL and EDL length-force characteristics do not fit within the firing

frequency-related pattern described for either fully dissected muscles (i.e. with only the nerve and blood supply left intact) or single muscle fibres. Work on fully dissected muscle (Rack & Westbury (1969) on cat m. soleus; Roszek & Huijing on rat m. gastrocnemius (1997); Brown et al (1999) on cat caudofemoralis) and on skinned single muscle fibres (Stephenson & Wendt 1984) did show that as stimulation frequency or concentration of Ca^{++} is lowered, optimum length and, for dissected muscle also active slack length, shift progressively to higher muscle lengths. In agreement with previous work from our laboratory (Meijer *et al.* 2006) we conclude that for a muscle within an intact compartment, intrinsic properties and mechanisms alone do not suffice to explain firing frequency-related changes of length -force characteristics, because myofascial loads are integrated into the force exerted at the tendons. It should be noted that to explain higher distally exerted forces for 10 Hz firing a proximally directed load has to be exerted near to the distal end of the EDL and TA+EHL muscle-tendon complexes. The contrast between such a load and the observed net distally directed load illustrates the complexity of myofascial loading of muscle. In the present experimental conditions, proximally directed myofascial loads are expected to be exerted on anterior crural muscles by peroneal and triceps surae muscles via the neurovascular tracts. For conditions of maximal activation, it was recently shown (Huijing 2007) that a distal load is a common feature of a distally shortened muscle and that distal lengthening of all anterior crural muscles decreases the distally directed load exerted onto EDL (Meijer *et al.* 2007). For anterior crural muscles this distally directed load is imposed by the distal segments of compartmental and general fasciae of the anterior crural compartment, which attach to the tibial crest, run laterally over the TA muscle belly, attach to its epimysium and continue towards to the antagonistic muscles (Meijer *et al.* 2007). A fraction of this distally directed myofascial load exerted on TA+EHL is exerted on EDL via epimuscular myofascial connections between EDL and TA+EHL. At low firing frequencies, for any given muscle length, lower forces are exerted at the series-elastic structures, i.e. the myotendinal and the myofascial pathways, and consequently the force transmitted via these pathways may be reduced. It should be realized that imposing such loads at different locations on the muscle fibres and within the muscle will lead to (enhanced) distributions serial and parallel distribution in sarcomere lengths (Yucesoy *et al.* 2003a).

In conclusion, for muscles active within their natural context of connective tissues, mechanical interaction between antagonistic muscles via extramuscular myofascial pathways is also substantial at submaximal stimulation frequencies. Antagonistic muscles need not be adjacent for such interaction. They interact even if located at opposite sites of the lower leg. Such extramuscular myofascial force transmission between antagonistic compartments significantly modifies the effects of firing frequency on muscle length-force characteristics.

6

A comparison of epimuscular myofascial force transmission in healthy and mdx mice: A preliminary analysis

Introduction

In Duchenne Muscular Dystrophy (DMD), the absence of dystrophin, a protein hypothesized to mechanically stabilize the membrane during shear stress, especially in eccentric contractions (Hoffman & Dressman 2001; Pasternak *et al.* 1995; Petrof *et al.* 1993; Williams & Bloch 1999) results in rapidly progressing muscle degeneration, fibrosis, and death as the disease ultimately affects vital muscles.

Most of our current knowledge regarding the pathological consequences of the absence of dystrophin result from research on the *mdx* mouse (Bulfield *et al.* 1984; Gillis 1996), a line of mice with a point mutation in the dystrophin gene eliminating the expression of dystrophin (Sicinski *et al.* 1989). *Mdx* muscle fibres are dystrophin-deficient, but unlike Duchenne patients, display elevated levels of utrophin. Utrophin is a dystrophin homolog that in healthy skeletal muscle confined to the postsynaptic membrane at the neuromuscular junction (Blake *et al.* 1996). The upregulation of utrophin has been reported to improve the functional performance of the muscle (i.e. force development and resistance to stretch) and results in a milder dystrophic phenotype (Deconinck *et al.* 1997; Grady *et al.* 1997; Tinsley *et al.* 1998). Nonetheless, despite the compensation of dystrophin by utrophin, *mdx* muscle show characteristics of muscle degeneration and regeneration, i.e. centrally nucleated cells, presence of inflammatory cells, necrotic fibres and elevated serum creatine kinase levels (Gillis 1999; Pastoret & Sebille 1993).

Dystrophin is part of the supramolecular chain linking cytoskeleton to the extracellular matrix. Via such connections, muscle force is transmitted from the muscle fibre onto the intramuscular connective tissue stroma. From there, it may be transmitted onto any other muscle within the limb segment, and possibly even beyond, via inter- and extramuscular connective tissue pathways. Such transmission via non-myotendinous structures is referred to as epimuscular myofascial force transmission (Huijing *et al.* 1998; Huijing & Baan 2001b; Maas *et al.* 2005b; Yucesoy & Huijing 2007). Such transmission has been shown to be inherent to the integration of the muscle in a higher level organization of the body. As dystrophin is potentially part of the myofascial pathway, its absence is expected to weaken the intramuscular myofascial connections. Therefore, it is hypothesized that dystrophic muscle may suffer from a decreased importance of myofascial force transmission.

The aim of this study is to test the hypothesis that in *mdx* mice, epimuscular myofascial force transmission is decreased due to less stiff intramuscular myofascial pathways.

Material and Methods

Surgical and experimental procedures were in compliance with the guidelines and regulations concerning animal welfare and experimentation set forth by Dutch law, and approved by the Committee on Ethics of Animal Experimentation at the Vrije Universiteit.

Immediately after all experiments, animals were killed using Euthesate (sodium pentobarbital solution), and double-sided pneumothorax was performed.

Surgical procedures

Experiments were performed on six-week old C57BL10/10ScSn-Dmd[mdx]/J mice (six males, one female, body mass of 26.2 gr., SE = 0.96), donated by the Leiden University Medical Centre (LUMC) and age matched male control (C57BL10/ScSN) mice obtained from Charles River Laboratories (n = 6, body mass of 24.5 gr., SE = 0.56). The mice were first sedated with 0.15cc Nembutal (6mg/ml) and then anaesthetized with urethane (12.5% solution, 125mg/ml, 1.2 ml/100 g body mass). Additional doses of Nembutal (0.3cc) were given when necessary, but after several hours, urethane injections were given to maintain deep anaesthesia. During surgery and data collection, animals ware placed on a heated water pad of approximately 37 °C to prevent hypothermia.

The anterior crural compartment from the left hind limb was exposed by removing the skin and the biceps femoris muscle. Limited fasciotomy was performed distally to expose the distal tendons of the m. tibialis anterior (TA), m. extensor hallucis longus (EHL) and m. extensor digitorum longus (EDL), and to severe the retinaculae (i.e. the transverse crural ligament and crural cruciate ligament). The connective tissue at the muscle bellies was left intact.

In the reference position (corresponding to a knee angle of 100° and ankle angle of 180° plantar flexion), the original position of the proximal tendon of EDL on the epicondylus lateralis of the femur was marked by placing corresponding markers on the proximal EDL tendon and lateral collateral ligament. A small piece of the epicondylus lateralis comprising the origin of the EDL muscle was then cut. Subsequently, the distal tendons of EDL were tied together (Ethilon surgical suture) and severed distally of the knot. Also, the distal tendons of TA and EHL were tied (polyester yarn) and severed from their insertions. Below, this complex will be referred to as TA+EHL complex.

To be able to insert a small clamp on the femur, small insertions were made in the musculature located anteriorly and posteriorly of the femur. The sciatic nerve was dissected free from surrounding tissues and severed as proximally as possible. The foot was firmly fixed to a plastic plate.

Experimental set-up

The animal was mounted in the experimental set-up, and the femur was clamped to at a knee angle of 100° (Fig. 1). The foot, attached to a plastic plate, was firmly attached into a rigid frame with the ankle in extreme plantar flexion to allow free passage of the distal tendons of EDL and TA+EHL at the ankle. The distal tendons

of TA+EHL and EDL as well as the proximal EDL tendon were connected to force transducers (ME-Meßsysteme GmbH, Germany, compliance of 0.025 mm/N) mounted on single-axis micropositioners by Kevlar threads (4% elongation at a break load of 800N) and metal rods. The line of pull of EDL and TA+EHL was aligned with the line of pull of the force transducers.

The sciatic nerve was placed on a pair of silver electrodes and prevented from dehydration by covering it with paper tissue saturated with isotonic saline and a thin piece of latex.
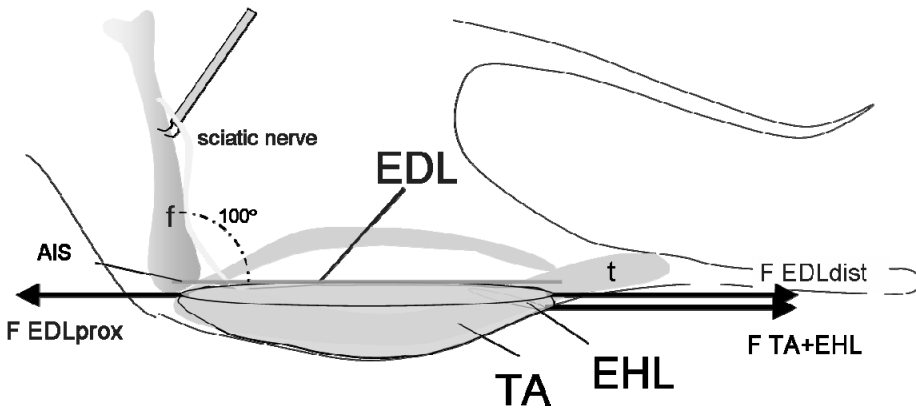
Figure 1. Schematic lateral view of the rat anterior crural compartment after removal of the skin and m. biceps and representation of the experimental set-up. Connective tissues at the muscle bellies were left intact. The m. tibialis anterior (TA) is shown as being transparent to allow showing of the position of the underlying m. extensor digitorum longus (EDL), m. extensor hallucis longus (EHL). Note that EHL originates at the anterior intermuscular septum (AIS). The origin of the extensor digitorum longus muscle (EDL) at the femur (f), as well as the distal tendons of EDL and TA+EHL muscles were severed and connected to force transducers using Kevlar threads attached to metal rods. t denotes the tibia. The forces measured are represented by arrows. Both femur and foot were fixed within a rigid frame, in such a way that the muscles were aligned with the force transducers.

Experimental conditions

Ambient temperature (22° C ± 0.5) and air humidity (70 ± 2%) were kept constant by a computer-controlled air-conditioning system (Holland Heating, Waalwijk, the Netherlands). Muscle and tendon tissue was further prevented from dehydration by regular irrigation with isotonic saline. The proximal EDL tendon was set at a position 1 mm distal of the reference position (i.e. shorter muscle).

Before acquiring length-force data, EDL was preconditioned by isometric contractions at alternating high (Δl_{m+t} = 0) and low (Δl_{m+t} = -3) muscle lengths, until active forces at low length were reproducible (i.e. effects of previous activity at high length (Huijing & Baan 2001b) are minimized).

TA+EHL optimal active force (F_{mao}) was determined by performing contractions at different muscle-tendon complex lengths to find the length of maximal active

force exertion. This value was used to set TA+EHL complex at a constant muscle-tendon complex length corresponding to an active force $1/3F_{mao}$. Note that the initial values for TA+EHL active force differ for dystrophic and healthy mice (Fig. 4a). Prior to excitation, all muscles were brought passively to the desired length and position by moving the distal force transducers. All muscles were activated simultaneously by supramaximal stimulation of the sciatic nerve with a constant current (3 mA) and a stimulation frequency of 100 Hz (pulse width 0.5 ms). Two twitches were evoked, followed by a tetanic contraction of 300 ms. Timing of stimulation of the nerve and A/D conversion (12-bit A/D converter, sampling frequency 1000 Hz) was controlled by a special purpose microcomputer. After each tetanic contraction, the muscles were allowed to recover near active slack length for 2 minutes. Passive isometric force was measured at a point prior to the tetanic contraction and total force was measured at a point during the final quarter of the tetanic plateau of the muscle force.

Data treatment

Passive muscle force was fitted with an exponential curve using a least-squares criterion:

$$y = \exp(ax + b) + C$$

where y represents passive muscle force, x represents muscle-tendon complex length and a, b and C are fitting constants.
Active muscle force (F_{ma}) was estimated by subtracting the calculated passive force (F_{mp}) for the appropriate muscle length using the fitted function, from total force (F_m) measured. Active length-force data were obtained then fitted applying a stepwise polynomial regression procedure (also see statistics)

$$y = b_0 + b_1 x + b_2 x^2 + \ldots b_n x^n$$

where y represents active muscle force, x represents active muscle force length and b_0 through b_n are fitting constants. Using the selected polynomials, mean and standard errors of active muscle force were calculated for given muscle lengths. Optimum muscle length was defined for each individual muscle as the muscle length at which the fitted active force curve showed a maximum (F_{mao}).
EDL distal active slack lengths were estimated by selecting data at lower muscle lengths ($F_{ma} < 0.3x\ F_{mao}$) and extrapolated using the fitted curve;

$$y = \exp(b_0 x + b_1) + b_2 ,$$

where y represents muscle active force, x represents active muscle force length and b_0 through b_n are fitting constants. For each individual muscle, active slack length was calculated by solving the roots for this equation. The group mean of active slack length is calculated and plotted with horizontal error bars.

For EDL, the differences in passive and active force exerted at the distal and proximal tendon ($\Delta Fmp_{dist-prox}$ and $\Delta Fma_{dist-prox}$ respectively) were calculated by subtracting proximal force from distal force.

Statistics

For curve fitting of active length-force data, the procedure starts with a first order polynomial and the power was increased up to a sixth order, as long as this yields a significant improvement of the statistical description of the length-active force data, as determined by one-way analysis of variance (ANOVA) (Neter *et al.* 1990). Two-way ANOVA's were used to determine effects of EDL length and mouse strain (control and dystrophin-deficient (*mdx*)) on (1) on distally exerted EDL active forces (2) on proximally exerted EDL active forces, (3) on distally exerted EDL passive forces, and (4) on proximally exerted EDL passive forces. Also, two-way ANOVA's were used to determine effects of EDL length and mouse strain on (1) the proximo-distal in active EDL force, (2) the proximo-distal difference in passive EDL force, and (3) the TA+EHL active force. One sample t-tests were used to test for differences in distal EDL active slack length of control and *mdx* mice.

Results

A comparison of effects of EDL length on EDL forces in dystrophic and control mice

i) Distal EDL forces

ANOVA showed significant main effects (mouse strain and EDL length) on distal EDL active force, as well as significant interaction between these factors. At the lower part of the ascending limb of the length-force curve ($\Delta l_{m+t} < -1.5$), distally exerted active EDL force for dystrophic mice is higher than for control mice (Fig. 2a). Beyond this length, active EDL force is highest for control mice. Optimum muscle force for dystrophic mice is lower than in control mice (0.29N vs. 0.35N respectively). Distally determined active slack length is significantly different for dystrophic and control mice: for dystrophic mice, active slack is estimated to occur at $\Delta l_{m+t} = -5.3$, whereas for control mice, active that value is $\Delta l_{m+t} = -4.6$. This means that for dystrophic mice the length range between optimum and active slack length is increased. For distally exerted passive forces, ANOVA showed significant main effects of mouse strain and EDL length, as well as interaction between these factors. At $\Delta l_{m+t} > -2.5$, distal passive EDL force for dystrophic mice increases exponentially to much higher values than for control mice (Fig. 2b, peak values of 0.15N and 0.033N respectively).

It is conclude that active, as well as passive, EDL length-distal force characteristics are affected substantially by the deficiency in dystrophin and the simultaneous replacement of that molecule by utrophin in *mdx* mouse.

ii) Proximal EDL force

Note that EDL proximal active and passive forces are in general more variable in dystrophic mice (as judged from the standard error of the mean) than distal EDL forces. For proximally exerted active EDL forces, ANOVA only could show an effect of EDL length (Fig. 3a) but not of mouse strain. No interaction between these two factors was shown. Proximal active EDL force increases to peak values 0.10N and 0.14N for dystrophic and control mice. In contrast, ANOVA did show a main effect of mouse strain on proximal passive EDL forces (Fig. 3b), but did not indicate a significant effect of length. No interaction between these two factors was shown. Posthoc tests showed that particularly at higher lengths ($-1 < \Delta l_{m+t} < 1$) proximal passive EDL forces are significantly higher for dystrophic than for control mice.

In contrast to distal EDL active force, we do not have sufficient evidence to conclude that proximal EDL active force is affected substantially by the deficiency in dystrophin and the simultaneous replacement of that molecule by utrophin in *mdx* mouse. However, for proximal EDL passive forces such a conclusion is still warranted.
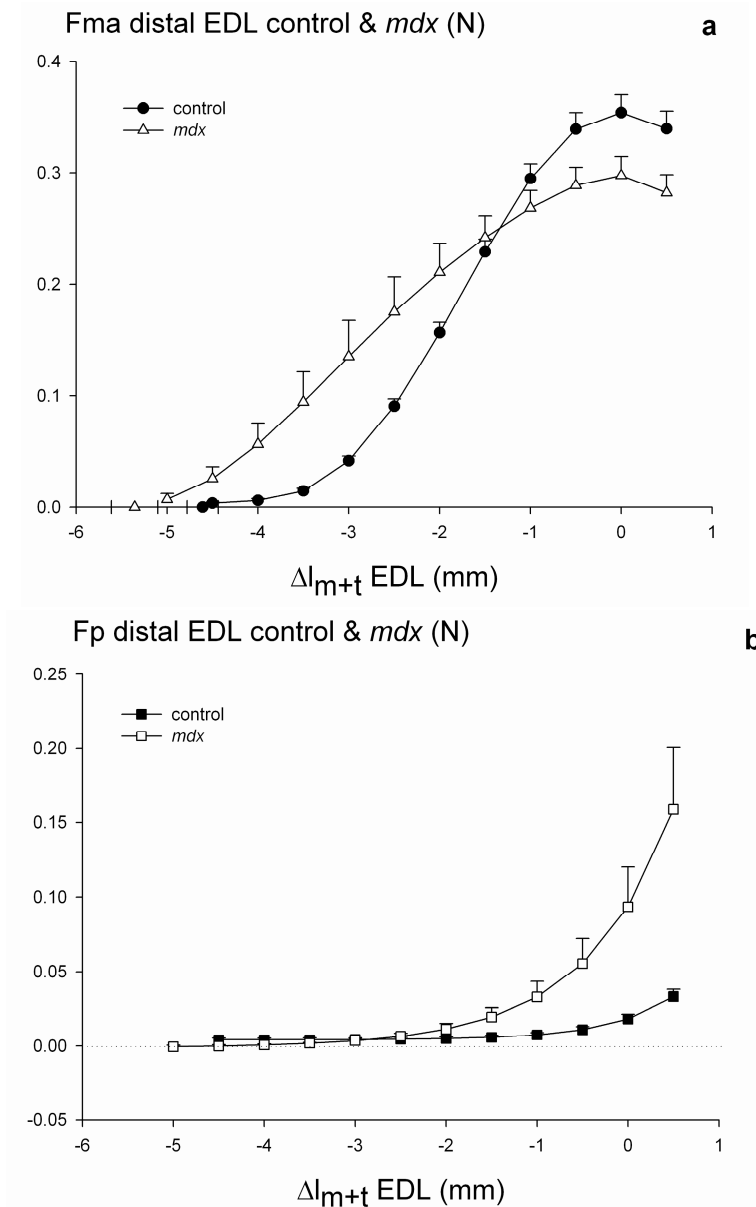
A comparison of effects of EDL length on the proximo-distal EDL force differences

For both dystrophic and control mice, significant differences in proximally and distally exerted active and passive EDL forces (Fig. 4) were found. Any proximo-distal force difference is taken as an indication that epimuscular myofascial force transmission occurs and a net epimuscular load is exerted upon the muscle (i.e. via non-myotendinous pathways). ANOVA showed main effects of length on the proximo-distal force active difference, but could not show significant effects of mouse strain. No interaction between mouse strain and EDL length was shown. It is concluded that EDL proximo-distal active force differences are certainly not smaller in *mdx* than in control mice. This means that the hypothesis that muscular dystrophy is exclusively a disease of epimuscular myofascial force transmission should be rejected. At low muscle lengths, the proximo-distal difference attains small negative values (Fig. 4a). An indicative of that a small net epimuscular load exerted on EDL in the distal direction. Such a net load is integrated in the force exerted at the proximal tendon. As EDL is lengthened at its distal tendon, the proximo-distal active force difference becomes positive, indicating that a net distally directed load is exerted on EDL at higher length.

For the EDL proximo-distal passive force difference, ANOVA showed a significant main effect of EDL length, but not for mouse strain. However, a significant interaction effect between EDL length and mouse strain was shown. Bonferroni posthoc tests showed that this interaction is located at $\Delta l_{m+t} \geq 0$. For that length range, the proximo-distal difference in passive EDL force is highest for dystrophic mice (Fig. 4b). Note that, for both mouse strains, the proximo-distal passive force difference is always positive, indicating that a net distally directed epimuscular myofascial load is exerted on EDL in both *mdx* and control mice.

It is concluded that the net epimuscular load on passive EDL in the *mdx* mouse is at least as high as in control mice, or even higher (at higher lengths). Therefore,

the passive length force characteristics are affected substantially by the deficiency in dystrophin and the simultaneous replacement of that molecule by utrophin in *mdx* mouse.

Figure 2. Comparison of *mdx* and control EDL length-distal active and passive length-force characteristics.**(a)** Effects of EDL length on distal active force. **(b)** Effects of EDL length on distal passive force.Length is expressed as a deviation (in mm) of distal EDL optimum muscle length. Values are expressed as mean + S.E., n = 6 for control mice, n = 7 for dystrophic mice.
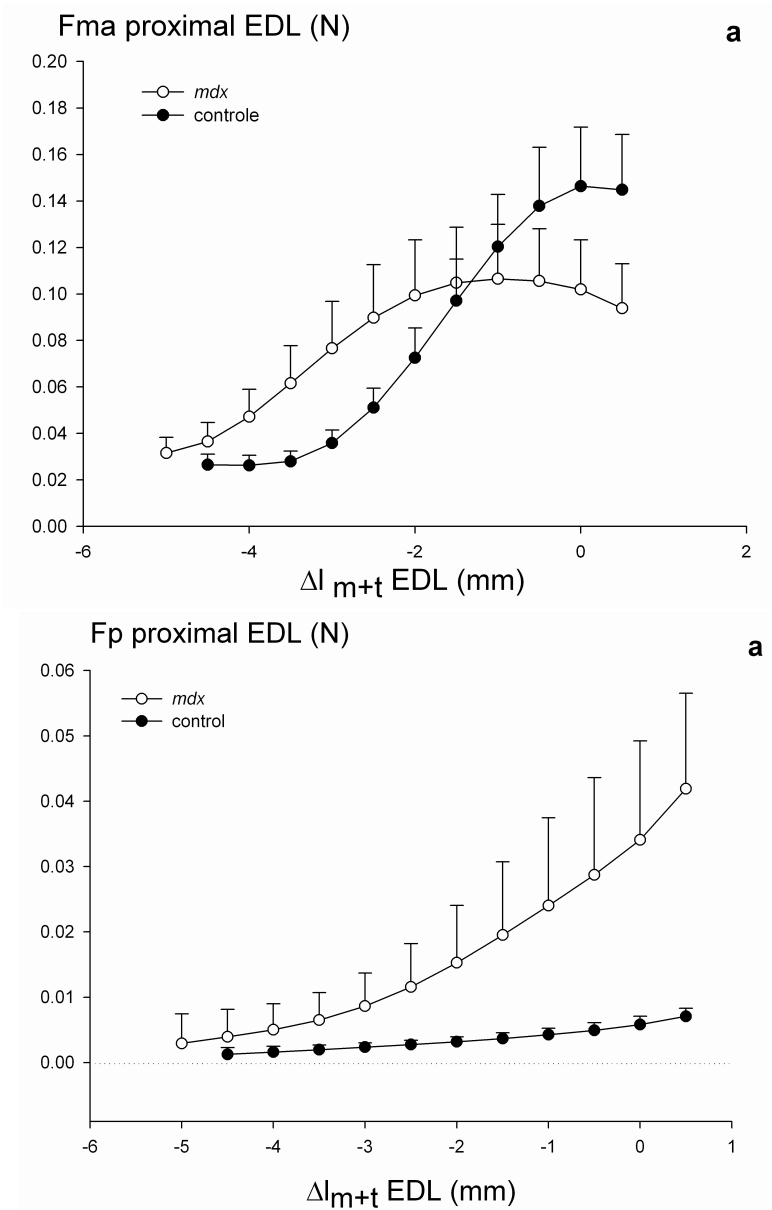
Figure 3. Comparison of mdx and control EDL length-proximal active and passive length-force characteristics. **(a)** Effects of EDL length on proximal active forces. **(b)** Effects of EDL length on proximal passive forces. Length is expressed as a deviation (in mm) of distal EDL optimum muscle length. Values are expressed as mean + S.E., n = 6 for control mice, n = 7 for dystrophic mice.
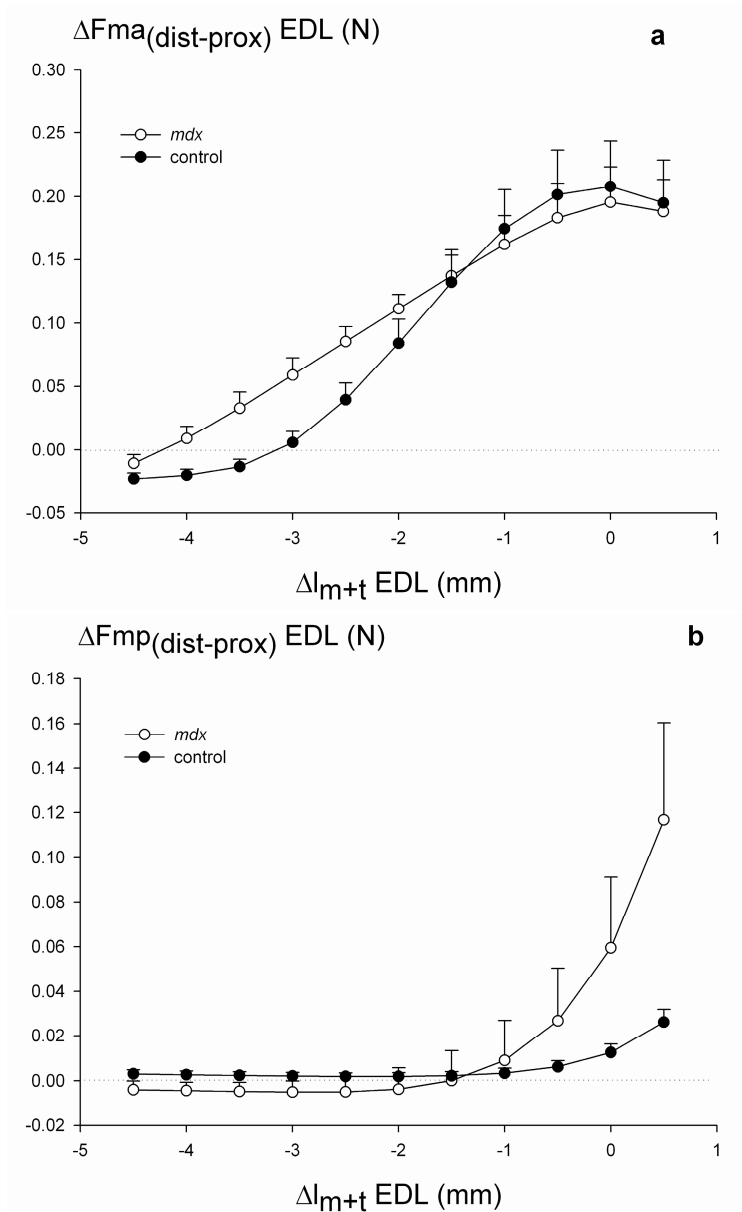
Figure 4. Comparison of *mdx* and control EDL proximo-distal active and passive force differences. (a) Effect of EDL length on absolute differences in proximally and distally exerted EDL active forces ($\Delta Fma_{dist-prox}$). (b) Effect of EDL length on absolute differences in proximally and distally exerted passive EDL forces ($\Delta Fmp_{dist-prox}$). Proximo-distal force differences are calculated as Fdist-Fprox. Length is expressed as a deviation (in mm) of distal EDL optimum muscle length. Values are expressed as mean + S.E., n = 6 for control mice, n = 7 for dystrophic mice.

Effects of EDL lengthening on active force of TA+EHL kept at constant length

Optimum forces of TA+EHL were found to be significantly higher in *mdx* than in control mice (mean ± SE: 1.38N ± 0.04 in *mdx* vs. 1.13N ± 0.05 in controls).

For distally exerted active TA+EHL forces, ANOVA showed significant main effects of EDL length, as well as mouse strain. However no significant interaction could be shown. Despite being left at a constant muscle-tendon complex length, TA+EHL active forces of both *mdx* and control mice decreased, as EDL was lengthened at the distal tendon (Fig. 5).

For control mice, lengthening of EDL decreased active TA+EHL force from 0.44N to 0.39N (i.e. a decrease by 11% of the initial active force). In contrast, in dystrophic mice, active TA+EHL force decreased from 0.49N to 0.40N (i.e. a decrease of 18%) as EDL was lengthened distally by 5 mm. It is concluded that the mechanical interaction between synergistic EDL and TA+EHL muscles is enhanced substantially by the deficiency in dystrophin and the simultaneous replacement of that molecule by utrophin in *mdx* mouse.

Figure 5. Comparison of effects of EDL length on TA+EHL forces in mdx and control mice. Active forces exerted by TA+EHL at constant muscle-tendon complex length are plotted as a function of EDL length in control and dystrophic mice. Length is expressed as a deviation (in mm) of distal EDL optimum muscle length. Values are expressed as mean + S.E., n = 6 for control mice, n = 7 for dystrophic mice.
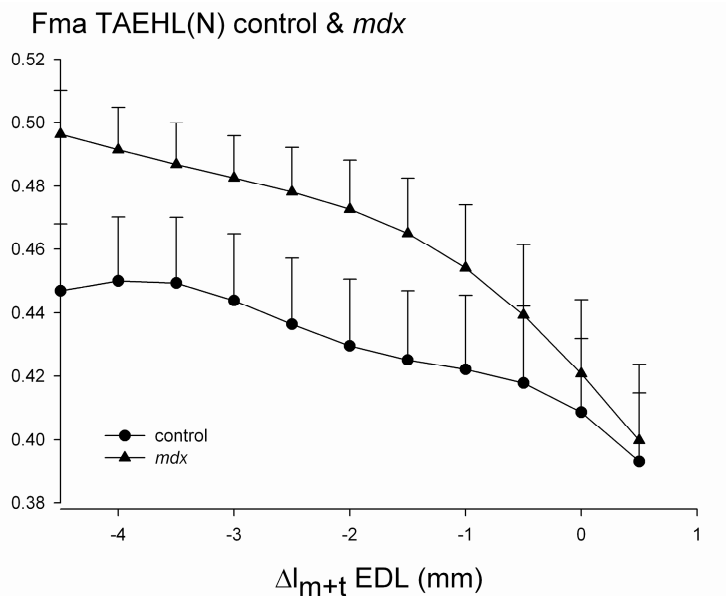
Discussion

The major and novel finding of this study is that epimuscular myofascial force transmission between EDL and its surrounding tissues in *mdx* mice is at least as high as in control mice and possibly higher. This is also true for the mechanical interaction by epimuscular myofascial force transmission between synergistic anterior crural muscles. A number of conceivable explanations should be considered for these phenomena:

(1) Neither dystrophin, nor utrophin, is involved at all in the transmission of muscle force via myofascial pathways from the muscle fibre cytoskeleton to the connective tissue stroma. In such a case the myofascial effects should be mediated by other (possibly as yet unknown) molecules. In such a case, the enhanced myofascial effects (for example in the passive state) are rather hard to explain, unless the muscular dystrophies are diseases involving much more complex primary changes than the deficiency of one molecule in the chains connecting cytoskeleton to the connective tissue stroma.

(2) The mechanical effects of dystrophin in the myofascial pathway are very effectively and possibly even more than completely taken over by utrophin. This explanation seems more likely. Enhanced myofascial effects would require stiffer connections between cytoskeleton and the connective tissue stroma. Considering the lack of knowledge of mechanical effects of utrophin, other than its possible role in anchoring the motor end plate to the muscle fibre (Blake *et al.* 1996), it is not surprising that it is not clear how utrophin should affect such changes in stiffness of trans-sarcolemmal myofascial paths in locations where otherwise dystrophin would act.

Effects on EDL length-force characteristics of replacing dystrophin by utrophin.

The differences in length-distal force characteristics for *mdx* mice are hypothesized to be the result of increased distributions in sarcomere lengths. The higher EDL distal active forces at the ascending limb ($\Delta l_{m+t} < -1.5$) of the *mdx* length-force curve indicates that a distal population of sarcomeres within EDL muscle fibres attain higher sarcomere lengths (presumably because of higher proximally directed epimuscular myofascial loads preventing the sarcomeres from shortening further). The decrease in active slack length could also be explained by such phenomena.

At higher muscle lengths (e.g. near optimum length), this distal population of sarcomeres within EDL muscle fibres would exert a lower force as they are already stretched to the length range of the descending limb.

Effects of dystrophin replacement by utrophin on EDL and TA+EHL active force levels

Unlike for human DMD patients, it has been reported that limb muscles of *mdx* mice, in spite of a lack of dystrophin, are able to maintain absolute force levels at that of age-matched control mice (Soleus and EDL) or above (TA) (Coulton *et al.* 1988; Dangain & Vrbova 1984; Dellorusso *et al.* 2001; Kometani *et al.* 1990; Lynch *et al.* 2001; Sacco *et al.* 1992). Our current results for TA+EHL optimal active force

agree with the findings that *mdx* TA force is higher than for controls. However, for *mdx* EDL, active forces are higher than controls at low muscle lengths, but around optimum muscle length, *mdx* active force is lower than controls (Fig. 2a). Note that our results can not be directly compared with most studies on *mdx* muscle (Dellorusso *et al.* 2001), as in these studies, muscles are fully dissected with only the blood supply left intact, or fully dissected, taken out of the body and suspended in a bath. Thus, most epimuscular myofascial pathways are removed. This would reduce the distributions in sarcomere lengths and optimum active force would increase at the expense of length range of active force exertion. This would explain part of the discrepancy between our current data for *mdx* EDL and reports from the literature. Also, several studies were performed around optimum muscle length whereas for a better understanding of the effects of dystrophin replacement by utrophin on active force exertion, the whole length range of active force exertion should be considered. In addition, age effects should be taken into account (Coulton *et al.* 1988). However, it remains unclear why in *mdx* mice, TA attains higher optimum active forces than in controls, whereas the opposite is true for EDL.

In conclusion, a preliminary analyses of epimuscular myofascial force transmission in healthy and *mdx* mice shows that epimuscular myofascial force transmission in *mdx* mice is at least as high as in healthy controls. Therefore, the observed pathologies in *mdx* muscle can not be caused by reduced myofascial force transmission.

Acknowledgements

7

Epimuscular myofascial force transmission in the mouse; are effects of synergist length different from those in the rat?

Introduction

Recently, it has been shown that muscle force is not only transmitted via the myotendinous pathway (Tidball 1991; Trotter 2002), but also via non-myotendinous connective tissue structures. Such transmission is referred to as *epimuscular myofascial force transmission* (Huijing *et al.* 1998; Huijing & Baan 2003). From the myofibril, transsarcolemmal connections with the extracellular matrix (Street & Ramsey 1965; Street 1983; Trotter 1990) allow intramuscular myofascial force transmission via the continuous intramuscular stroma (endomysium, perimysium and epimysium) (Jarvinen *et al.* 2003; Nishimura *et al.* 1996b; Passerieux *et al.* 2006). Via the epimysium, force can be transmitted onto other muscles via the continuous stroma of intramuscular connective tissues of adjacent muscles (i.e. intermuscular myofascial force transmission (Maas *et al.* 2001)), or onto extramuscular connective tissues, such as intermuscular septa, general fasciae, interosseal membranes and collagen fibre-reinforced blood and lymph vessels and nerves (i.e. extramuscular myofascial force transmission (Huijing *et al.* 2007; Rijkelijkhuizen *et al.* 2005)).

The phenomenon of epimuscular myofascial force transmission has been studied extensively in the rat (Huijing & Baan 2003; Maas *et al.* 2004), and has also been established for humans (Kreulen *et al.* 2003; Smeulders & Kreulen 2007) and even for amphibia (Huijing & Jaspers 2005). However, the most common animal model to study (human) muscle pathologies resulting from deficiencies in intra- and extracellular and transsarcolemmal molecules is the mouse (Aszódi *et al.* 1998; Grady *et al.* 1997; Mao *et al.* 2002; Sasaoka *et al.* 2003). Therefore, the goal of this study is to investigate the presence and extent of epimuscular myofascial force transmission in the mouse by determining the effect of tibialis anterior and extensor hallucis longus length (TA+EHL) on extensor digitorum longus (EDL) forces. It is hypothesized that due to the smaller size, effects of epimuscular myofascial force transmission are smaller in the mouse than in the rat.

Material and Methods

Surgical procedures

Six male C57BL10/ScSN mice obtained from Charles River Laboratories (body mass of 24,5 gr., SE = 0.6) were used. The mice were first sedated with 0.15cc Nembutal (6mg/ml) and then anaesthetized with urethane (12.5% solution, 125mg/ml, 1.2 ml/100 g body mass). Additional doses of Nembutal (0.3cc) were given when necessary, but after several hours, urethane injections were given to maintain deep anaesthesia. Surgical and experimental procedures were in compliance with the guidelines and regulations concerning animal welfare and experimentation set forth by Dutch law, and approved by the Committee on Ethics of Animal Experimentation at the Vrije Universiteit.

Immediately after all experiments, animals were killed using Euthestate solution (sodium pentobarbital solution), and double-sided pneumothorax was performed. During surgery and data collection, animals were placed on a heated water pad of approximately 37° C to prevent hypothermia. The skin and biceps femoris of the left hind limb were removed, exposing the anterior crural compartment. Only very limited fasciotomy was performed distally to severe the retinaculae (i.e. the transverse crural ligament and crural cruciate ligament). More proximally, connective tissues, particularly at the muscle bellies were left intact. Subsequently, the distal tendons of extensor digitorum longus (EDL) and tibialis anterior and extensor hallucis longus muscles were dissected. Markers were placed on the distal EDL, TA and EHL tendons to mark their corresponding positions in the reference position (corresponding to a knee angle of 110° and ankle angle of 180° plantar flexion). Subsequently, the distal tendons of EDL were tied together (Ethilon surgical suture) and severed distally of the knot. Also the distal tendons of TA and EHL were tied (polyester yarn) and severed from their insertions. Below, this complex will be referred to as TA+EHL complex. In the reference position, the position of the proximal tendon of EDL was marked by placing corresponding markers on the proximal EDL tendon and lateral collateral ligament, before cutting a small piece of the epicondylus lateralis of the femur comprising the proximal attachment of the EDL muscle. To insert a small clamp on the femur, small insertions were made in the musculature located anteriorly and posteriorly of the femur. The sciatic nerve was dissected free from surrounding tissues and severed as proximally as possible. The foot was firmly fixed to a plastic plate.

Experimental set-up

The animal was mounted with the femur clamped at a knee angle of 110° (Fig. 1). The foot, attached to a plastic plate, was fixed firmly to a rigid frame with the ankle in extreme plantar flexion, to allow free passage of the distal tendons at the ankle. The target tendons were connected to force transducers (ME-Meßsysteme GmbH, Germany, compliance of 0.025 mm/N) mounted on single-axis micropositioners by short (maximally 2.5 cm) Kevlar threads (4% elongation at a break load of 800N) and metal rods. This system was aligned with the muscles' line of pull. The sciatic nerve was placed on a pair of silver electrodes and prevented from dehydration by covering it with paper tissue saturated with isotonic saline and a thin piece of latex.

Experimental conditions

Ambient temperature (22° C ± 0.5) and air humidity (70 ± 2%) were kept constant by a computer-controlled air-conditioning system (Holland Heating, Waalwijk, the Netherlands). Muscle and tendon tissue was further prevented from dehydration by regular irrigation with isotonic saline. The proximal EDL tendon was set at a position 1 mm distal of the reference position (i.e. shorter muscle). Prior to excitation, all muscles were brought passively to the desired length and position by moving the distal force transducers.
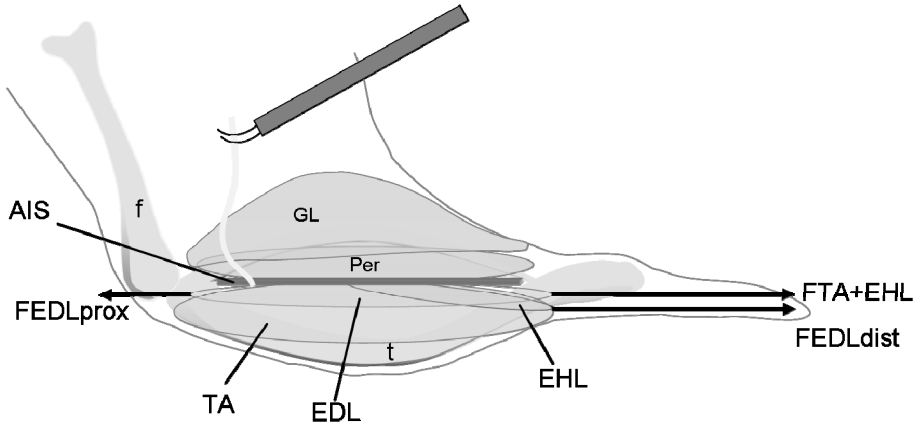
Figure 1. Schematic representation of the experimental set-up. Lateral view of mouse lower limb anatomy after removal of the skin and biceps femoris. The origin of the extensor digitorum longus (EDL) at the lateral condyle of the femur (f) and distal insertions of tibialis anterior (TA), extensor hallucis longus (EHL), and EDL on the foot are severed and connected to force transducers (represented by arrows). Both femur and foot were fixed within a rigid frame in the reference position, corresponding to knee angle of 110° and an ankle angle of 180° plantar flexion. Note that the anterior intermuscular septum (AIS) separates the anterior crural muscles from the peroneal muscles (Per). GL indicates lateral gastrocnemius muscle, t denotes the tibia.

Before acquiring the set of length-force data, EDL and TA+EHL, were preconditioned by isometric contractions at alternating high ($\Delta l_{m+t} = 0$) and low ($\Delta l_{m+t} = -3$) muscle lengths, until active forces at low length were reproducible (i.e. effects of previous activity at high length (Huijing & Baan 2001b) are minimized). Isometric contractions were performed at different EDL and TA+EHL lengths. The lengthening protocol was performed as follows; 1) EDL was passively brought to the desired length, while TA+EHL complex was left at a length at which it exerted zero active force (this lengthening condition will be from here on referred to as lengthening of EDL exclusively), and 2) EDL was brought passively to the desired length, and the TA+EHL complex was brought to a corresponding length by aligning the previously placed markers (condition referred to as added lengthening of TA+EHL).

Both TA+EHL and EDL muscles were lengthened distally at 0.5 mm increments. All muscles were activated by supramaximal stimulation using a constant current of the sciatic nerve (3 mA) and a stimulation frequency of 100 Hz (pulse width 0.5 ms). Two twitches were evoked, followed by a tetanic contraction of 300 ms. Timing of stimulation of the nerve and A/D conversion (12-bit A/D converter, sampling frequency 1000 Hz) was controlled by a special purpose microcomputer. After each tetanic contraction, the muscles were allowed to recover near active slack length for 2 minutes. Passive isometric force was measured prior to the tetanic contraction and total force was measured during the tetanic plateau of the muscle force.

Data treatment

Passive muscle force was fitted with an exponential curve using a least-squares criterion:

$$y = \exp(ax + b) + C$$

where y represents passive muscle force, x represents muscle-tendon complex length and a, b and C are fitting constants. Active muscle force (F_{ma}) was estimated by subtracting the calculated passive force (F_{mp}) for the appropriate length using the fitted function, from total force (F_m) measured. Active length-force data were obtained then fitted applying a stepwise polynomial regression procedure (also see statistics):

$$y = b_0 + b_1x + b_2x^2 + \dots b_nx^n$$

where y represents active muscle force, x represents active muscle force length and b_0 through b_n are fitting constants. Using the selected polynomials, mean and standard errors of active muscle force were calculated for given muscle lengths. Optimum muscle length was defined for each individual muscle as the active muscle length at which the fitted active force curve showed maximum force (F_{mao}). Active slack lengths for TA+EHL and distal tendon of EDL were estimated by selecting data at lower muscle lengths ($F_{ma} < 0.3x\ F_{mao}$) and extrapolated using the fitted curve;

$$y = \exp(b_0 x + b_1) + b_2$$

where y represents muscle active force, x represents active muscle force length and b_0 through b_n are fitting constants. For each individual muscle, active slack length was calculated by solving the roots for this equation. The group mean of active slack lengths is calculated for each muscle and is plotted with horizontal error bars.

For EDL, the differences in passive and active force between the distal and proximal tendon (respectively $\Delta Fmp_{dist-prox}$ and $\Delta Fma_{dist-prox}$) were calculated by subtracting proximal force from distal force.

Statistics

For curve fitting of active muscle force, the procedure starts with a first order polynomial and the power was increased up to a sixth order, as long as this yields a significant improvement of the statistical description of the length-active force data, as determined by one-way analysis of variance (ANOVA) (Neter *et al.* 1990). Two-way ANOVA's for repeated measurements were used to test for

a) effects of EDL muscle length and location of force exertion (proximal or distal) for 1) EDL active forces and 2) EDL passive forces

b) effects of anterior crural muscle length and location of force exertion on 1) EDL active forces and 2) EDL passive forces

c) effects of anterior crural muscle(s) length and lengthening condition (exclusive lengthening of EDL or added lengthening of TA+EHL) on 1) the EDL proximo-distal active force difference and 2) the EDL proximo-distal passive force difference

d) for effects of location of force exertion and lengthening condition on EDL optimum lengths (L_{mao}).

One-way ANOVA was used to test for 1) differences in EDL active slack lengths, 2) for effects of anterior crural muscles length on distal TA+EHL active forces, and 3) for effects of anterior crural muscles length on passive distal TA+EHL forces. Effects were considered significant at $P < 0.05$. If significant effects were found, Bonferroni post-hoc tests for multiple pair wise comparisons were used to locate differences.

Results

Dissection of the mouse anterior crural compartment revealed similarities to the anatomy of the anterior crural compartment in the rat. Tibialis anterior muscle almost completely envelopes the extensor hallucis longus and extensor digitorum longus muscles. The anterior crural compartment is delimited dorsally by the anterior intermuscular septum, and medially by the interosseal membrane and tibial periost. Proximally within the anterior crural compartment and the intersection between the septum and interosseal membrane, the anterior tibial artery and the deep branch of the common peroneal nerve enter to supply and innervate the anterior crural muscles.

Effects of EDL length on proximal and distal active and passive forces for lengthening of EDL exclusively

For distal lengthening of EDL exclusively, ANOVA showed main effects of muscle length and location of force exertion (proximal or distal) on EDL active forces, as well as a significant interaction. Proximally and distally measured active forces differed as a function of EDL muscle length (Fig. 2a). ANOVA did not show a significant difference in proximally and distally determined optimum lengths. At low muscle lengths ($\Delta l_{m+t} < -3,5$), proximally measured active force is higher than distally measured active force. At higher lengths obtained by distal lengthening, distal active force is always higher than proximal active force. Distal optimal force is 0.37N, whereas proximal optimal active force is 0.13N. Any difference in distally and proximally measured active forces is unequivocal proof of epimuscular myofascial force transmission between EDL and surrounding tissues. Note that any difference in force between the origin and insertion of a muscle means that additional forces, other than myotendinous ones, are exerted on the muscles.

Also for passive EDL forces, ANOVA showed main effects of muscle length and location of force exertion, as well as a significant interaction. Proximally and distally measured passive forces differ as a function of EDL muscle length. At all muscle lengths obtained by distal lengthening, distal passive force is higher than

proximal passive forces (Fig. 2a, grey lines). Peak distal passive force is 0.03N, whereas proximal peak passive force is maximally 0.007N. Thus also for passive EDL, differences in proximally and distally measured forces exits which are proof of myofascial loads being exerted on the muscle.

Length-force characteristics for the added lengthening of TA+EHL

For the added lengthening of TA+EHL, ANOVA showed a significant effect of anterior crural muscle length on TA+EHL active force (Fig. 3). TA+EHL distal active force increased with increasing muscle length until optimum muscle length at Δl_{m+t} = -0.5 (1.13N), and decreased at higher muscle lengths.
ANOVA also showed a significant main effect of anterior crural muscles length on passive TA+EHL force, which increased exponentially up to 0.2N with increasing muscle length.

Effects of the added lengthening of TA+EHL on EDL proximal and distal active and passive forces

After the added lengthening of TA+EHL, ANOVA showed main effects of anterior crural muscle length and location of force exertion, as well as significant interaction, for both distally and proximally measured EDL active forces. Also in this condition, distally and proximally measured EDL active forces differed as a function of anterior crural muscle length (Fig. 2b). At low muscle lengths, proximally measured active force is higher than distally measured active force. For Δl_{m+t} < -3, distal active force is always higher than proximally measured active force. Distal optimal active force is 0.32N, whereas proximal optimal active force is 0.19N. ANOVA showed no difference in proximal and distal optimum length.
For passive EDL forces (Fig. 2b, grey lines), ANOVA showed main effects of anterior crural muscle length and location of force exertion, as well as significant interaction. Proximal and distal passive forces differ as a function of anterior crural muscle length. At high muscle lengths, distal passive force is higher than proximal passive force. Distal passive force increases exponentially to a peak value of 0.04N, whereas proximal passive force peaks at 0.006N.

Effects of the added lengthening of TA+EHL on the EDL proximo-distal force differences, EDL optimum lengths and distal active slack lengths

For lengthening of EDL exclusively, as well as after the added lengthening of TA+EHL, significant differences in proximally and distally measured EDL active and passive forces were found (Fig. 4a). ANOVA showed main effects of length and lengthening condition on the EDL proximo-distal active force difference, as well as significant interaction. Only at the lowest muscle lengths the proximo-distal active force difference ($\Delta Fma_{dist-prox}$) is negative, albeit small. For this length range, $\Delta Fma_{dist-prox}$ is highest for the added lengthening of TA+EHL (-0.01586N ≈ -4,5% of distal optimum active force, Fig. 4a). A negative value for the proximo-distal force difference indicates that a *net* distally directed myofascial load is exerted on EDL, which is integrated in the force exerted at the proximal tendon.
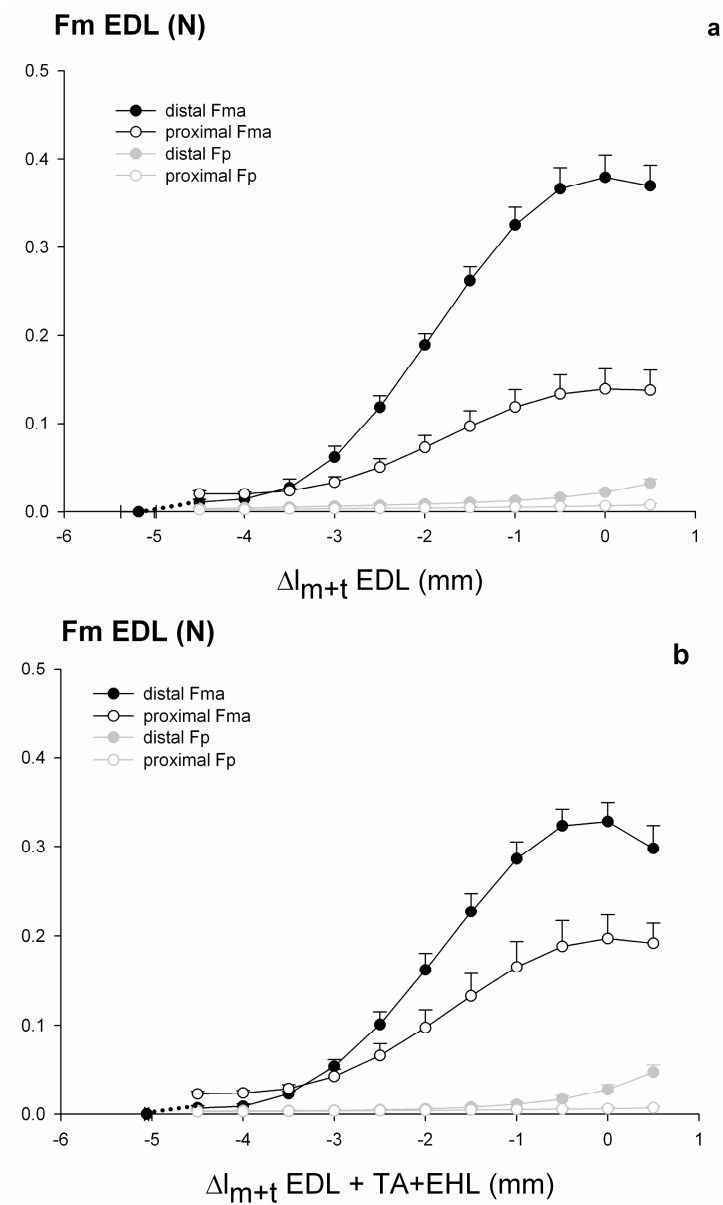
Figure 2. Effects of anterior crural lengthening condition on proximal and distal active and passive EDL forces. **(a)** Proximal and distal EDL active and passive forces as a function of EDL lengthening. **(b)** Proximal and distal EDL active and passive forces as a function of EDL + TA+EHL lengthening. Lengthening was obtained by moving the distal force transducer(s). All values are shown as mean + SE, n = 6.
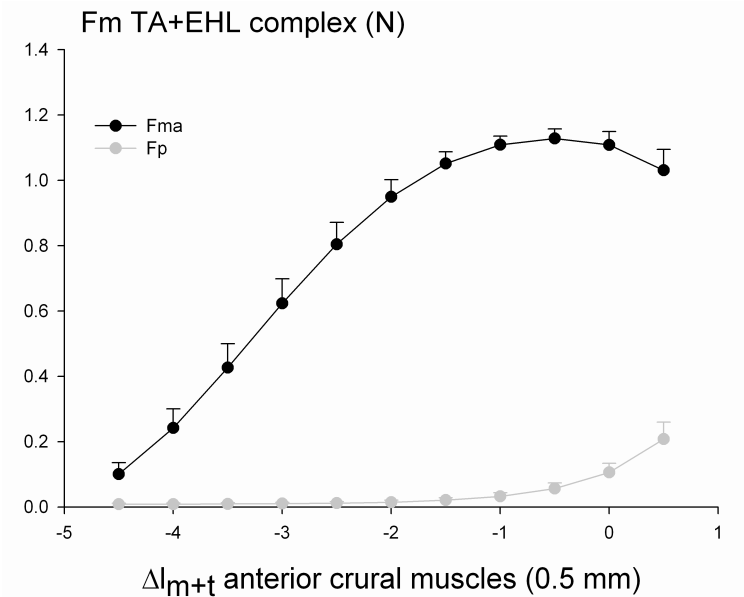
Figure 3. TA+EHL active and passive length-force characteristics as a function of EDL + TA+EHL lengthening. Lengthening was obtained by moving the distal force transducers. All values are shown as means + SE, n = 6.

As muscle length increases, $\Delta Fma_{dist-prox}$ becomes positive and increases for both lengthening conditions. A positive value for the proximo-distal force differences indicates a *net* proximally directed load exerted on the muscle, which is integrated in the force exerted at the distal tendon (Fig. 4a) Note that for $\Delta l_{m+t} > -3.5$, $\Delta Fma_{dist-prox}$ is significantly higher for lengthening of EDL exclusively: the maximum $\Delta Fma_{dist-prox}$ for lengthening of EDL exclusively is 0.24N (i.e. 62% of EDL distal optimum active force). The added lengthening of TA+EHL reduces this value to $\Delta Fma_{dist-prox} = 0.13N$ (i.e. 39% of distal optimum active force).

For the passive proximo-distal EDL difference ($\Delta Fp_{dist-prox}$), ANOVA also showed a main effect of anterior crural muscle length, but no effect of lengthening condition. However, significant interaction between these factors was found. Bonferroni posthoc tests, locating the interaction effect, showed that $\Delta Fp_{dist-prox}$ differed at $\Delta l_{m+t} = 0.5$, with the lengthening of EDL exclusively resulting in a lower proximo-distal difference in passive forces. For both lengthening conditions, $\Delta Fp_{dist-prox}$ attained only positive values, representing a *net* proximally directed myofascial load exerted on passive EDL at all muscle lengths studied. For $\Delta l_{m+t} \leq -1$, $\Delta Fp_{dist-prox}$ is slightly higher for lengthening of EDL exclusively. At $\Delta l_{m+t} > -1$, $\Delta Fp_{dist-prox}$ is highest for the lengthening of all anterior crural muscles.

ANOVA showed no difference in distally determined optimum length and distal active slack length between the two lengthening conditions. The same was true for proximally determined optimum lengths. Thus, the added lengthening of TA+EHL did not significantly alter distally and proximally determined optimum lengths, and did not alter distal active slack lengths.
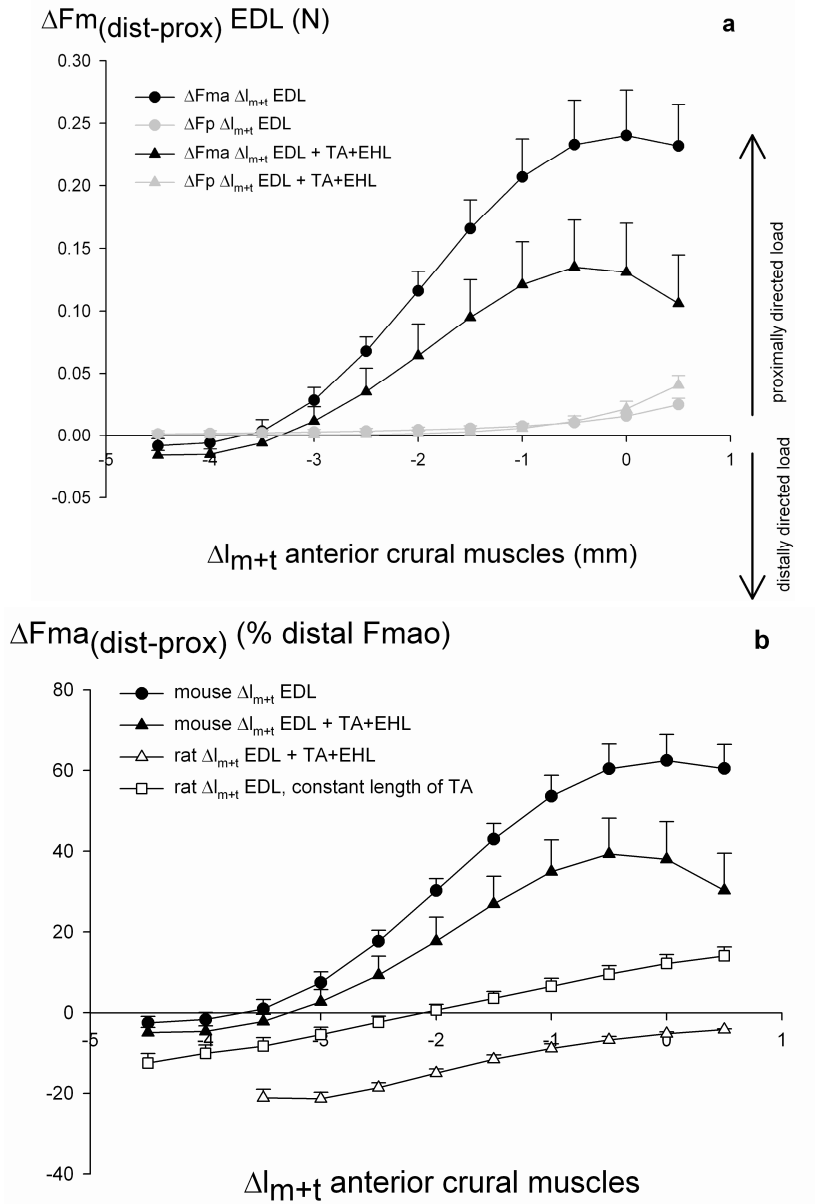
Figure 4. Effects of anterior crural lengthening condition on the EDL proximo-distal force differences. **(a)** ΔF, absolute differences between proximally and distally measured active and passive forces as a function of anterior crural muscle(s) length in the mouse. **(b)** ΔF, the proximo-distal difference in active force normalized for distal optimum active force as a function of anterior crural muscle(s) length for rat (open symbols) and mouse (closed symbols). Note that the Δlm+t indicates mm for the rat, and 0.5mm for the mouse. All values are shown as mean + SE, n = 6.

In conclusion, a *net* epimuscular myofascial load is exerted on EDL muscle for lengthening of EDL exclusively, as well as for the added lengthening of TA+EHL. However, the added lengthening of TA+EHL increases the distally directed *net* epimuscular myofascial load on active EDL at low muscle lengths, but reduces the *net* proximally directed epimuscular myofascial load at higher muscle lengths.

Discussion

The main finding of this study is the presence in the mouse of significant differences in proximally and distally measured active and passive EDL forces. Such differences are unequivocal proof of the transmission of forces via non-myotendinous connective tissue structures, i.e. epimuscular myofascial force transmission (Huijing *et al.* 1998; Huijing 2003). This study demonstrates the presence of epimuscular myofascial force transmission in the mouse, an animal species often used in the study of (neuro) muscular disorders (Anderson *et al.* 2005; Deconinck *et al.* 1997; Gillis 1996).

Effects of EDL length on the proximo-distal EDL force difference and pathways of myofascial force transmission

For the lengthening of EDL exclusively, the proximo-distal difference in active EDL force attains a negative, albeit small, value at low muscle lengths. At higher muscle lengths (i.e. Δl_{m+t} > -3,5), a *net* positive myofascial load is exerted on EDL of maximally 0,23N, which constitutes 60% of distal optimum active force. This means that the majority of the EDL distal active force originates within other muscles! The magnitude and direction of the myofascial load are affected by muscle length and the position of the muscle relative to its surroundings, i.e. muscle relative position (Maas *et al.* 2004; Yucesoy *et al.* 2006). Note that it is very well conceivable that conditions are imposed on muscles that involve loading of muscle by multiple, oppositely directed, myofascial pathways. Therefore, a *net* myofascial load (i.e. proximo-distal force difference) should generally be considered as the result of oppositely directed myofascial loads (Huijing 2007; Meijer *et al.* 2007).

At low muscle lengths, EDL active forces measured at the tendons are low, and consequently, also less force is transmitted myofascially. The small *net* distal load indicates that distally directed myofascial loads are slightly higher than proximally directed myofascial loads. During the experiment, a distal myofascial load is seen to be transmitted onto the TA+EHL complex by the distal parts of long compartmental and general fasciae, which are attached to the TA epimysium. As TA+EHL is short, these distal fasciae are stretched and exert a distally directed load on active TA+EHL. It is hypothesized that via epimuscular myofascial connections between TA+EHL and EDL, a fraction of this distal load is transmitted onto active EDL as well. Apparently, for the passive muscle, this distally directed load remains smaller than the proximally directed myofascial load on EDL resulting in a positive EDL proximo-distal difference in passive force

(figure 4a). However, upon activation, shortening of the TA+EHL and EDL muscle bellies lengthens the distal fasciae, and consequently, the distal load increases, resulting in a *net* distally directed load exerted and EDL.

Distal lengthening of EDL induces changes in the position of the muscle relative to surrounding connective tissues and other muscles, and these changes are most pronounced for the distal segment of the muscle. As a consequence, the direction of the *net* epimuscular load exerted on EDL by the myofascial connections is altered from a distal direction to a transmission proximal direction (Fig. 4a). As a result of distal lengthening of EDL, epimuscular myofascial connections between EDL and surrounding connective tissue and TA muscle belly may increase in length and stiffness, and the proximally directed load transmitted by these epimuscular myofascial connections increases.

For lengthening of EDL exclusively, i.e. as TA+EHL is kept at constant low length, the change in relative position between EDL and TA+EHL is substantial, and thus, intermuscular myofascial connections at the muscle-belly interface between TA+EHL and EDL are lengthened and increase in stiffness, exerting a proximally directed load on EDL. However, in addition to intermuscular myofascial pathways, distal lengthening of EDL also causes shearing of the neurovascular tract, an extramuscular myofascial pathway which is constituted by the collagen-reinforced network in which blood vessels and nerves supplying and innervating the muscles are embedded. The neurovascular tract is anchored to the walls of the compartment and lengthening of the muscles will shear it. This will cause the neurovascular tract to exert a proximally directed load on anterior crural muscles.

However, for lengthening of EDL exclusively, the contributions of each myofascial pathway to the *net* myofascial load exerted on EDL can not be distinguished. Therefore, it is argued that for the lengthening of EDL exclusively, both intermuscular and extramuscular pathways may contribute to the EDL proximo-distal difference in force.

Effects of TA+EHL length on the proximo-distal EDL force differences

At low muscle lengths, the added lengthening of TA+EHL increases the *net* distally directed load exerted on EDL by 2,2% of distal EDL optimum force (Fig. 4a). Note however that, as TA+EHL attains higher lengths, the length of the connections to the distal fasciae decreases and the distally directed load exerted by them on TA+EHL is smaller. Therefore, the distal fasciae can not account for the higher distal load exerted on EDL. For the added lengthening of TA+EHL, the relative position of EDL with regard to TA+EHL is different from that for lengthening of EDL exclusively. Therefore, it is argued that for the added lengthening of TA+EHL, intermuscular myofascial connections between EDL and TA+EHL at their muscle belly interface are stretched, and now exert a higher distal load on EDL.

At higher muscle lengths, the added lengthening of TA+EHL reduces the *net* proximal load exerted on EDL but leaves a myofascial load exerted on EDL (e.g. from 0.23N to 0.13N at optimum length, Fig. 4a). This decrease in the *net* myofascial load exerted on EDL can be also explained by the altered the relative

position between EDL and TA+EHL for the added lengthening of TA+EHL: intermuscular myofascial connections between TA+EHL and EDL are stretched and exert a distally directed load on EDL. Consequently, the *net* proximally directed myofascial load on EDL decreases. The most likely candidate for the transmission of a proximally directed myofascial load on EDL for the added lengthening of TA+EHL is the neurovascular tract. The view of the neurovascular tract as main contributor to proximo-distal EDL force differences is in agreement with results from studies on the rat (Huijing & Baan 2001b; Maas *et al.* 2005b) who found by dissection that not intermuscular, but extramuscular myofascial connections are the main contributor to any EDL proximo-distal difference in active force. The neurovascular tract is a branching structure that is anchored to compartmental walls of the anterior crural compartment, as well as to general fasciae and intermuscular septa. Distal lengthening of TA+EHL will lead to an overall higher loading of the neurovascular tract, but may simultaneously cause an unloading of the small EDL branch, thereby decreasing the proximal myofascial load exerted on EDL. If so, the decrease in the EDL proximo-distal active force difference for the added lengthening of TA+EHL is not only the result of changes in the direction of the force transmitted by the intermuscular myofascial pathway, but also of a decreased stiffness of the extramuscular myofascial pathway. Also for the added lengthening of TA+EHL, our current results do not allow for an unambiguous discrimination of the contribution of each pathway to the proximo-distal difference in EDL active force, although the neurovascular tract is hypothesized to play an important role. Further experimentation with progressive dissection of the myofascial pathways may yield enhanced insight in the relative importance of inter- and extramuscular myofascial pathways.

Note that for the added lengthening of TA+EHL, the passive proximo-distal force differences in EDL are at high muscle lengths higher than for lengthening of EDL exclusively. This may be caused by a non-linear increase in stiffness of a myofascial pathway exerting a proximally directed load. This pathway is likely to be the neurovascular tract.

Interspecies differences in myofascial force transmission?

The nature of the myofascial interaction between TA+EHL and EDL muscles in the mouse is in agreement with experiments on myofascial force transmission reported in the rat: synergistic muscle length is a major co-determinant for EDL forces. However, quantitatively, differences in the myofascial load between rat and mouse exist.

At low muscle lengths, the effect of the added lengthening of TA+EHL on *net* distal load exerted on EDL is considerably smaller for the mouse than for the rat (Meijer *et al.* 2007). Added lengthening of TA+EHL in the rat increased the *net* distal load at low muscle lengths to a value of 20% of distal optimum active force, versus 5% in the mouse. Also for the mouse, intact distal fasciae will exert a significant distal load on TA+EHL and EDL at low lengths. However, in the absence of a large *net* distal myofascial load exerted on EDL at low muscle lengths,

it is argued that in addition to a significant distal load, a large, oppositely directed (i.e. proximally directed) myofascial load is exerted on TA+EHL at low muscle lengths as well. Such a proximal load reduces the *net* distal myofascial load exerted on TA+EHL. Possible candidates for the transmission of a proximal load are the rather stiff extramuscular pathways, such as the neurovascular tract and proximal segments of compartmental and general fasciae.

At high muscle lengths, the reported normalized proximo-distal difference in active EDL force for lengthening of EDL exclusively and added lengthening of TA+EHL for the mouse are higher than any normalized proximo-distal force difference found for the rat (Fig. 4b). So far, experiments on myofascial force transmission in the rat have yielded proximo-distal force differences of maximally 35% of proximal optimal active force (Huijing & Baan 2003; Maas *et al.* 2001; Meijer *et al.* 2006). This is in contrast with our current results, where normalized proximo-distal active force differences were much higher (ranging from 40% for added lengthening of TA+EHL to 60% for lengthening of EDL exclusively, Fig. 4b). For murine EDL in the present experimental conditions, this means that the majority of the distally measured active force originates from other muscles!

There are two possible explanations for these differences between results of the rat and the mouse experiments: 1) differences in experimental conditions, or 2) interspecies differences in the stiffness of myofascial pathways, possibly as an effect of body size. Note that our present values for murine proximo-distal active force difference originate from repeated observations of a single group of animals, whereas our values for the rat were obtained comparing different groups of animals. Probably more important, experimental conditions were different for the added lengthening of TA+EHL in the rat and the mouse. In the rat experiments, the peroneal and triceps surae muscles were set at a constant length higher than corresponding to their present condition of maximal plantar flexion. Huijing et al. (2007) reported that distal lengthening of the peroneal complex of the rat increases the distal myofascial load exerted on EDL (kept at a constant length) by approximately 6% of the initial EDL active force. Thus, lengthening of the peroneal and triceps surae muscles in the mouse experiment would be expected to increase the distal load thus to decrease the *net* proximal myofascial load on EDL at high muscle lengths. However, assuming similar material properties for myofascial pathways in the mouse and rat, the effects of lengthening antagonistic muscles may be too small to shift the curve for the *net* myofascial load down to levels comparable to that in the rat (Fig. 4b). Therefore, we consider it unlikely that the difference in experimental conditions fully explains the large values for the mouse proximo-distal difference in EDL active force at high muscle lengths compared to the rat.

Apart from the difference in body mass (the rat being roughly 10 times that of the mouse), the gross anterior crural anatomy is similar in mice and rats. Pollock et al (1994) showed that for the digital extensors, tendon cross-sectional area exhibits negative allometry and tendon length scales isometrically with body mass, which means that smaller animals have relatively thicker tendons and a relatively higher

tendon stiffness. However, nothing is known regarding the scaling of myofascial connections and its material properties. For the fraction of the force transmitted myofascially to increase, it is required that the myofascial pathways are relatively more stiff than the myotendinous pathways. Thus, if tendon stiffness is higher in the mouse, the fraction of the force transmitted myofascially would increase only in combination with a yet even stiffer myofascial pathway. Assuming similar material properties, smaller distances between muscles and surrounding connective tissues and other muscles in the mouse may result in relatively shorter, stiffer myofascial connections. Such a hypothesis could explain the high proximally directed myofascial loads exerted on murine EDL: a shorter, stiffer neurovascular tract would result in a relatively stiffer extramuscular pathway and cause a higher fraction of force to be transmitted myofascially compared to the rat. Based on the present results, we consider it conceivable that interspecies differences in myotendinous and myofascial pathways between the rat and the mouse exist, which cause smaller animals to have relatively stiffer myofascial pathways, enhancing the transmission of muscle force via myofascial connections relatively to myotendinous pathways.

In conclusion, effects of epimuscular myofascial force transmission are substantial also in the mouse; length of synergistic muscle is a major co-determinant for EDL force. Effects of myofascial force transmission should be taken into account for the study of (neuro)muscular disorders in mice. Interspecies differences due to scaling may enhance myofascial force transmission in smaller rodents.

8

Epimuscular non-myotendinous force transmission in the invertebrate desert locust (*Schistocerca gregaria*)

Introduction

In vertebrates, muscle force is not only transmitted via the tendon, but can also be transmitted via non-tendinous connective tissue structures. Such transmission is referred to as epimuscular myofascial force transmission (Huijing & Baan, 1998). Myofascial force transmission has been shown to occur in various vertebrate species, i.e. in rat anterior crural muscles (Huijing *et al.* 2003; Maas *et al.* 2005b), frog tibialis anticus muscle (Huijing & Jaspers 2005) and human flexor carpi ulnari muscle (FCU) (Smeulders *et al.* 2002; Smeulders & Kreulen 2007). Pathways of myofascial force transmission are 1) intramuscular connective tissue, i.e. the stromata of endo-, peri- and epimysium (referred to as *intramuscular myofascial force transmission*), 2) the continuous stromata of intramuscular connective tissue of adjacent muscles (referred to as *intermuscular myofascial force transmission*), and 3) the non-muscular connective tissue structures such as compartmental fasciae and collagen-reinforced tracts of nerves and lymph and blood vessels (referred to as *extramuscular myofascial force transmission*). Note that for a muscle within its natural context of connective tissue, it is often not possible to distinguish between these latter pathways; in those cases, it is referred to as epimuscular myofascial force transmission.

Via epimuscular myofascial force transmission, additional forces are exerted on the muscle, other than those exerted by the myotendinous pathways. Therefore, forces exerted at the origin and insertion of a muscle need not necessary be equal, and a difference in forces measured at the muscles' origin and insertion is taken as an indication for epimuscular myofascial force transmission (Huijing *et al.* 1998). The transmission of forces via myofascial pathways results in length-force characteristics that differ from those described for fully dissected muscles (Maas *et al.* 2001; Yucesoy *et al.* 2003a). An continuous and intact network of connective tissues is essential for myofascial force transmission; disruption or removal of connective tissue structures decreases the stiffness of the myofascial network and reduces the transmission of force via these pathways (Huijing & Baan 2001a; Rijkelijkhuizen *et al.* 2005).

In contrast to vertebrate muscle, it has been reported that insects contain very little connective tissue (Ashhurst 1968; Hoyle 1955; Pond 1982). Such observations could indicate that myofascial force transmission is less important within insects.

The aim of this study is therefore to investigate whether non-myotendinous force transmission occurs in insect flight muscle. Focus of this study is the subalar muscle of the desert locust *Schistocerca gregaria*. This muscle was chosen because the exoskeletal origin and insertion (note that the direct attachments of the muscle onto the epidermis of the chitinous exoskeleton also classifies as a myotendinous pathway (Tiegs 1955)) can be severed from the body and attached to force transducers, which is a prerequisite for unequivocal proof of additional forces being exerted on the muscle via epimuscular myofascial force transmission.

Methods

Animal keeping

Adult male desert locusts (*Schistocerca gregaria*, Forskål 1775) were obtained from a breeding colony at the Laboratory of Entomology at Wageningen University (Nld.). The animals were housed in a glass terrarium, with a light/dark cycle of 16/8 and a room temperature of 25° C ± 0.5. The animals were fed on fresh grass ad libitum.

Surgical procedures

The animals (n=12) were anaesthetized with 0.2 cc abdominally injected 12, 5% urethane solution. The mesothoric wings and legs were cut and removed. The animals were pinned on their left side to be able to measure the muscle-tendon complex length of the right subalar muscle, a wing depressor (Albrecht, 1953, n° 129). The position of the origin and insertion with the metathoracic leg folded against the abdomen, and the metathoracic wing folded in is referred to as the reference position, and the length of the muscle-tendon complex in the reference position is referred to as lref. Subsequently, the length of the subalar muscle was measured with the metathoric wing deflected at an angle of 150°, which is the maximum deflection of the wing during flight (Weis-Fogh 1956). In addition, the length of the subalar muscle was measured for the maximum deflection of the metathoric leg during walking (Duch & Pflüger 1995) with the wing in the reference position. The differences between the lengths represent the *in vivo* length range of the subalar muscle.

Subsequently, the metathoric wings and legs were then removed as well. The wingbase of the metathoracic wing was detached from the surrounding scutum, so that only the subalar muscle was left attached to the wingbase. At the coxa of the right metathoric leg, a piece of the exoskeleton containing the insertion of the subalar muscle was cut out. Note that the exoskeleton covering the muscle was left intact. The wingbase, as well as the severed piece of coxa were attached to Kevlar threads to later allow attachment to the dorsally and ventrally located force transducers. The left side of the body of the animal was glued to a rigid Plexiglas frame

Experimental conditions and procedures

Ambient temperature (25° C ± 0.5) and air humidity (70 ± 2%) were kept constant by a computer-controlled air-conditioning system (Holland Heating, Waalwijk, the Netherlands). Before each experiment, the force transducers (ME-Meßsysteme GmbH, Germany, compliance of 0.025 mm/N, mounted on single-axis micropositioners) were calibrated in the experimental set-up. The ventral force transducer was suspended vertically and calibrated using weights. The ventral force transducer was then placed horizontally again and the dorsal force transducer was calibrated against the proximal one while being attached to it by a compliant spring. The animal fixed on the Plexiglas frame was mounted in the experimental set- up at an angle of approximately 45°C with its head down (Fig.

1b), so that the subalar muscle was horizontal and the two Kevlar threads were allowed free passage to the force transducers. The Kevlar threads were connected to force transducers and aligned with the muscles' line of pull. Copper wire electrodes were inserted into the subalar muscle at its dorso-anterior side and wrapped around the muscle at the ventral insertion (Fig. 1a). Prior to excitation, the muscle was brought to the desired length. The muscle was stimulated with a constant current (4mA). The stimulation protocol started with two twitches, followed by a pulse train of 300 ms at 50 Hz stimulation (pulse width of 0.5ms).
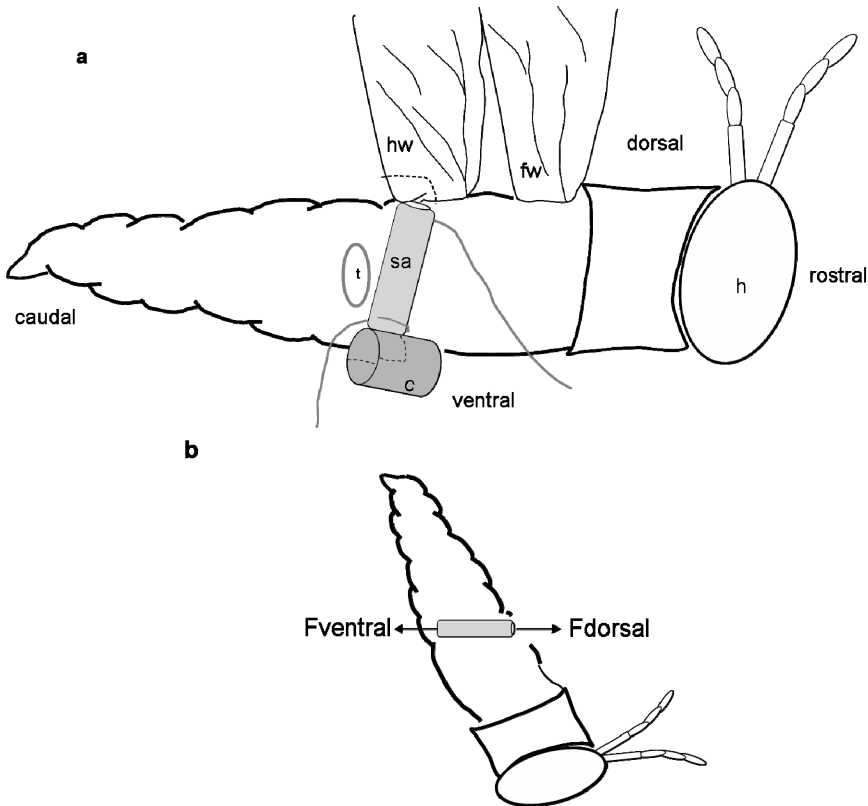
Figure 1. Schematic representation of the location and orientation of the subalar muscle and the experimental set-up. **(a)** Lateral view of the right side of the locust body after removal of the metathoric pleurite. The subalar muscle (sa) attaches ventrally on the caudal rim of the coxa, and dorsally on the wingbase of the hindwing. The dotted lines denote the pieces of hindwing and coxa attachments of the muscle that were cut and connected to the force transducers. t denotes tympanum, hw denotes hind wing, fw denotes forewing, h denotes head, and c denotes the coxa. Note that the fore and hindwings here have been lifted manually to show the attachment of the subalar muscle. Copper wire electrodes were inserted at its dorso-anterior side and wrapped around the muscle at the ventral insertion. **(b)** Schematic representation of the experimental set-up, in which the animal is tilted with its head down so that the subalar muscle is horizontal and aligned within the line of pull of the ventral and dorsal force transducers (represented by arrows).

Three experimental protocols were applied (represented schematically in Fig. 2). Note that in the reference position, the ventral force transducer is at $\Delta l_{ventral} = 0$ and the dorsal force transducer at $\Delta l_{dorsal} = 0$.

a) A lengthening protocol, in which the muscle was lengthened dorsally by 0.1 mm increments from a length 0.5 mm shorter than at reference position ($\Delta l_{dorsal} = -0.5$) until $\Delta l_{dorsal} = 0.5$. The position of the ventral force transducer was maintained with the muscle insertion at the reference position (Fig. 2a).

b) A lengthening protocol, in which the muscle was lengthened ventrally by 0.1 mm increments from a length 0.5 mm shorter than reference position ($\Delta l_{ventral} = -0.5$) until $\Delta l_{ventral} = 0.5$. Here, the position of the dorsal force transducer was maintained with the muscle origin at the reference position (Fig. 2b).

c) A protocol in which the muscle's position was changed relative to its surroundings but the muscle was kept at a constant length (i.e. lref). Initially, the muscle was set at a dorsal position, which corresponded to the position of the insertion at the dorsal maximum of the *in vivo* length range (see Fig. 2c). Subsequently, the muscle was moved in the ventral direction by moving the ventral and dorsal force transducers in steps of 0.1 mm, until position of the origin corresponded to the ventral maximum of the *in vivo* length range (see Fig. 2c).

The muscle lengths higher than reference length ($\Delta lref > 0$) fall within the length range encountered during flying and walking. For each animal, contractions were performed at the length range $-0.5 \leq$ lref ≥ 0 to study the effects of myofascial active force transmission in the locust.

Data processing and statistics

Dorsal and ventral passive force (Fp) were measured and averaged over an interval of 300 ms prior to contraction. Also, total force (Fm) was measured and averaged over an interval of 300 ms during contraction. For each individual animal, active force at each muscle length was then calculated by subtracting passive force from total force. Note that by subtracting passive force measured before the tetanic contraction from total force measured during the tetanic contraction, only an estimate of active force is obtained(MacIntosh & MacNaughton 2005).

The difference in dorsally and ventrally measured active ($\Delta Fma_{dors-ven}$) and passive forces ($\Delta Fmp_{dors-ven}$) was calculated by subtracting ventral force from dorsal force. For each muscle length and muscle relative position, mean dorsally and ventrally measured active and passive force, as well as the mean dorso-ventral force difference ($\Delta Fma_{dors-ven}$ and $\Delta Fmp_{dors-ven}$) and respective standard errors (SE) were calculated for the whole group of animals.
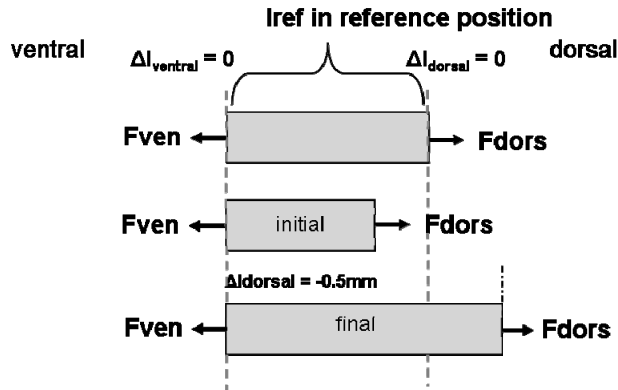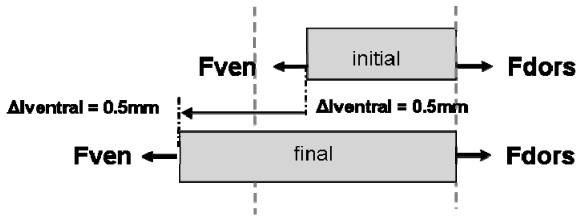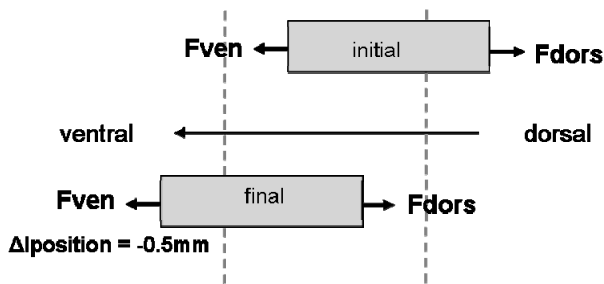
Figure 2. Schematic representation of conditions of experimental lengthening and muscular relative position. **(a)** The muscle is lengthened at the dorsal side from 0.5 mm below reference length to 0.5 mm over reference length. **(b)** The muscle is lengthened at the dorsal side from 0.5 mm below reference length to 0.5 mm over reference length. **(c)** The muscle remains at a constant muscle length, but starts at a dorsal position with respect to its surroundings, from where it is moved to a ventral position. Note that the extreme positions in the lengthening protocols correspond to the maximum lengths in vivo.

Two-way ANOVA for repeated measurements was used to test for main and interaction effects of muscle length and location of force exertion on (1) active force, and (2) passive force. In addition, two-way ANOVA for repeated measurements was used to test for main and interaction effects of muscle relative

position and the location of force exertion on (1) active force, and (2) passive force. One-way ANOVA was used to test for the effect of muscle-tendon complex length on (1) the dorso-ventral differences in active force, (2) the dorso-ventral differences in passive force, and for the effect of muscle relative position on (3) the dorso-ventral differences in active forces, and (4) the dorso-ventral differences in passive forces. Effects were considered significant at $P < 0.05$. If significant effects were found, Bonferroni posthoc tests were used to further locate these differences.

Results

Active force and dorso-ventral differences in active force

For the lengthening protocols as well as the position protocol, active forces are lower than passive forces at the same length. Over a large part of the length range: the dorsally and ventrally measured active forces are less than half of the respective passive forces at the same length (Figures 3a-b, 4a-b and 5a-b). Such low values are ascribed to our inability to excite the muscle maximally. Despite these low values for active forces, ANOVA showed significant main effects of location of force measurement on active forces indicating the presence of significant dorso-ventral force differences in the lengthening as well as the position protocols.

Effects of dorsal lengthening on dorsally and ventrally measured passive forces

ANOVA showed a significant main effect of length on passive forces, but did not indicate a significant effect of the location of force exertion. However, significant interaction between these factors was found. Bonferroni post-hoc tests showed that this interaction effect was present at $\Delta l_{dorsal} = -0.5$ and $\Delta l_{dorsal} \geq 0.3$, where ventral and dorsal passive forces differed significantly. Such differences in dorsally and ventrally exerted forces are indicative of epimuscular force transmission via non-myotendinous pathways. Both ventral and dorsal passive forces increase with increasing muscle lengths (Fig. 3b). At $\Delta l_{dorsal} > 0$, dorsal passive force is higher than ventral passive force. Dorsal passive force reaches a peak value of 43mN, whereas ventral passive force reaches 35mN. Note that the higher dorsal passive force indicates that an additional *net* load is exerted on the muscle in the ventral direction (Fig. 3c) and is integrated in the force measured at the dorsal insertion. ANOVA showed a significant effect of length on the dorso-ventral difference in passive forces. At low muscle lengths, the dorso-ventral difference in passive force is negative (indicative of a dorsally directed epimuscular load), but the difference decreases with increasing muscle length and attains positive values over $\Delta l_{dorsal} = 0.1$ (maximally 7mN at $\Delta l_{dorsal} = 0.5$). Note that positive values for the dorso-ventral force difference correspond to a ventrally directed myofascial load.

It is concluded that for dorsally lengthened passive locust subalar muscle, dorsally and ventrally exerted passive forces are significantly different as a result of the force transmission of additional forces via non-myotendinous pathways. The

direction and the magnitude of the *net* epimuscular load are dependent on muscle length.

Effect of ventral lengthening on dorsally and ventrally measured passive forces

For ventral lengthening of the muscle, ANOVA showed significant effects of muscle length and location of force exertion, as well as significant interaction between these factors. At low muscle lengths ($\Delta l_{ventral} \leq 0$), dorsally measured passive force dominates over ventrally exerted passive force: at $\Delta l_{dorsal = }$ -0.5, dorsal passive force being 10.6mN and ventral passive force 6.5mN (Fig. 4b). At higher muscle lengths, ventrally exerted passive force is higher than dorsally exerted passive force and ultimately increases up to 45mN, whereas dorsal passive force increases only to 32mN. This indicates that also for ventral lengthening of the muscle, additional epimuscular loads are exerted upon the subalar muscle. ANOVA showed an effect of muscle length on the dorso-ventral differences in passive forces (Fig. 4c). At low muscle length, the dorso-ventral difference in passive force attains positive values of maximally 3.9mN, representing a *net* myofascial load in the ventral direction. With increasing ventral muscle length the ventrally directed myofascial load decreases and reverses direction to a dorsally directed load of maximally 11mN.

It is concluded that also for ventral lengthening of the locust flight muscle, additional, i.e. epimuscular, loads are exerted on the passive muscle. The direction and the magnitude of the *net* load are affected by muscle length. Note however that the effects of ventral lenghtening are the reverse of those of dorsal lengthening despite the identical lengths being studied.

Effects of muscle relative position on dorsally and ventrally measured passive forces

Despite the fact that the subalar muscle was kept at a constant muscle length, ANOVA showed significant main effects of muscle relative position and of location of force exertion on passive muscle forces, as well as a significant interaction. Thus, ventrally and dorsally exerted passive forces differ as a function of muscle relative position. This is taken as evidence for epimuscular force transmission. Dorsal passive force decreased by more than half (from 28mN to 13 mN) when the muscle was moved from a dorsal to a ventral position. In contrast, ventral passive force increased from 13mN to 35mN as a result of the 1mm shift in relative position (Fig. 5b). ANOVA showed an effect of muscle relative position on the dorso-ventral difference in passive force. The net epimuscular load reverses from a dorsally directed load (peak value of14mN) to a ventrally directed load at ΔPosition ≤ 0.2 and increases up to 21mN.

It is concluded that, despite being kept at a constant length, dorsally and ventrally measured passive forces differ as a function of muscle relative position. Such effects are indicative of epimuscular force transmission.
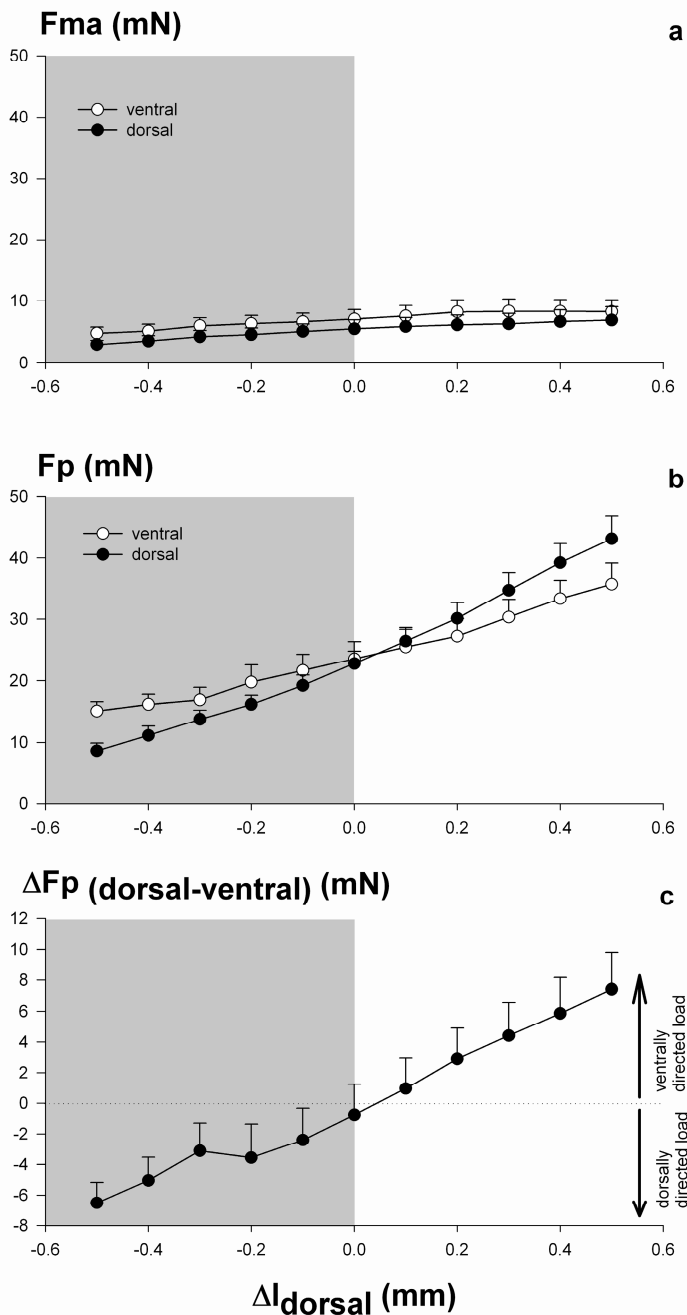
Figure 3. Ventrally and dorsally exerted active and passive forces for dorsal lengthening of the muscle. **(a)** Ventrally and dorsally exerted active forces (Fma) as a function of muscle length. **(b)** Ventrally and dorsally exerted passive forces (Fmp) as a function of muscle length. **(c)** The difference in dorsally and ventrally determined passive forces (ΔFmp) as a function of muscle length. Values are plotted as mean + SE, n = 12, and muscle length is expressed as a deviation (in mm) of the reference muscle length (lref). Grey areas indicate muscle length ranges that can not be attained during *in vivo* muscle functioning.
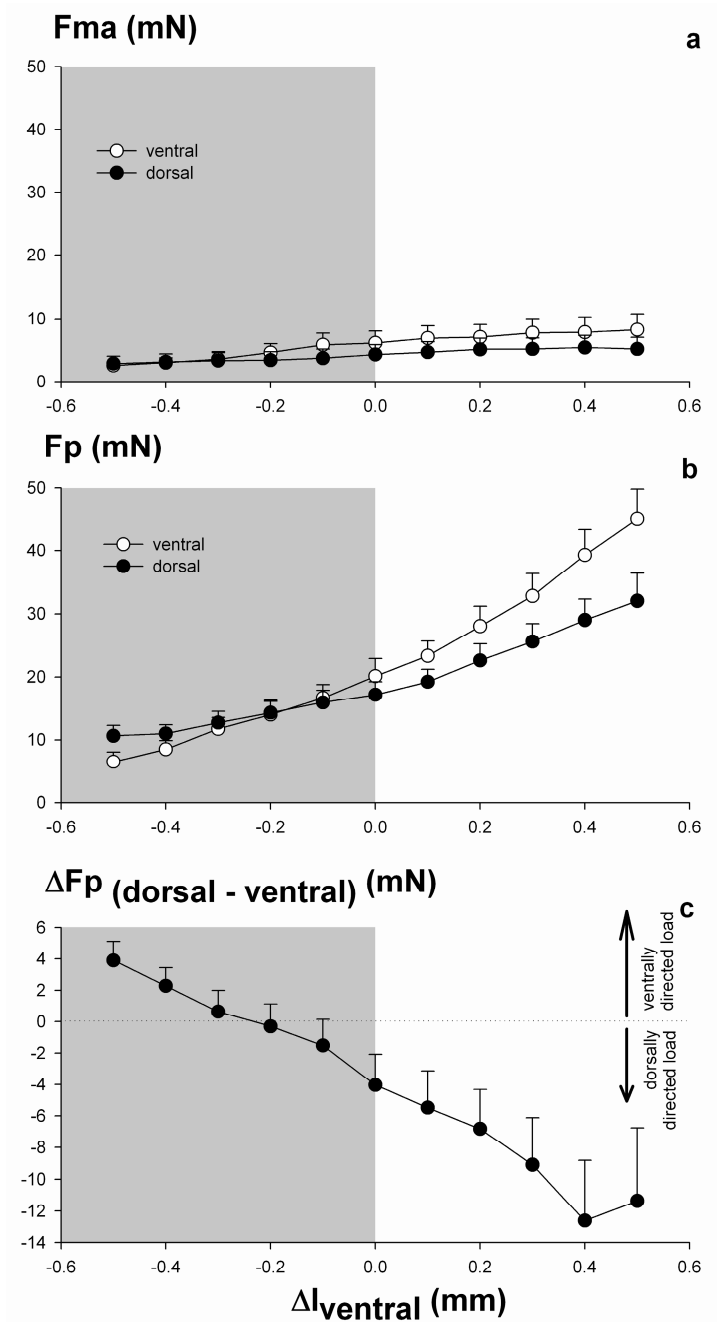
Figure 4. Ventrally and dorsally determined active and passive forces for ventral lengthening of the muscle. **(a)** Ventrally and dorsally determined active forces as a function of ventral muscle length. **(b)** Ventrally and dorsally determined passive forces as a function of ventral muscle length. **(c)** The difference in dorsally and ventrally determined passive forces (ΔFmp) as a function of ventral muscle length. All values are plotted as mean + SE, n = 12, and muscle length is expressed as a deviation (in mm) of the reference muscle length (lref). Grey areas indicate muscle length ranges that can not be attained during *in vivo* muscle functioning.
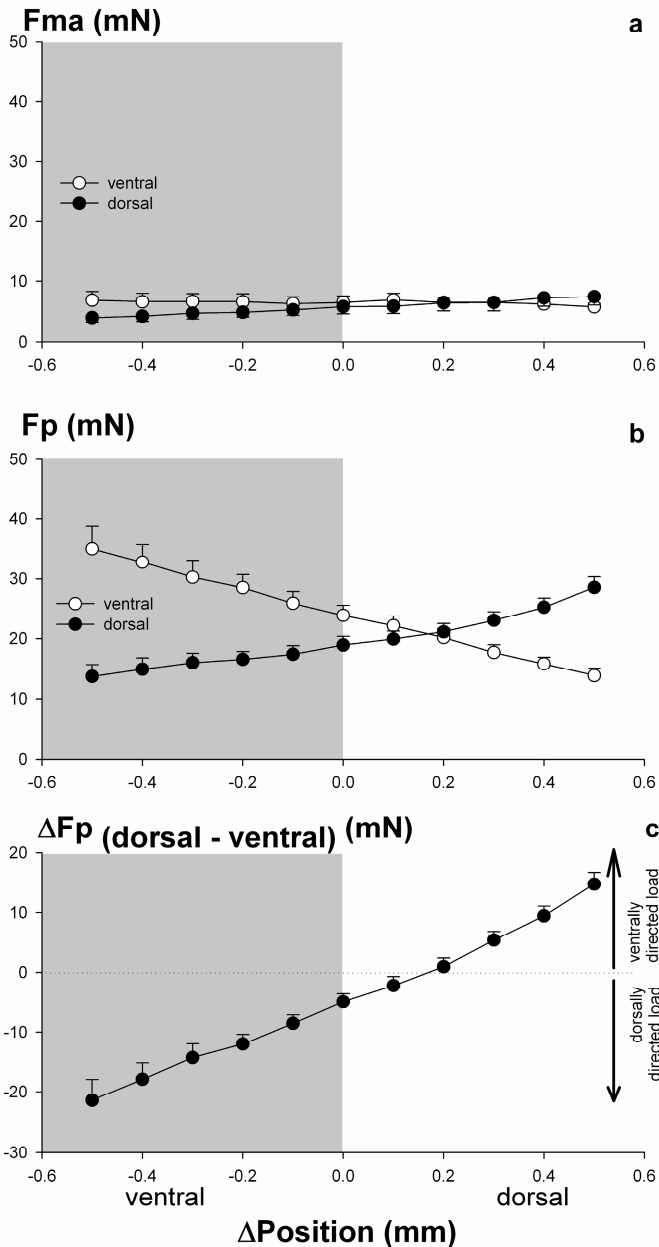
Figure 5. Ventrally and dorsally determined active and passive forces as a function of the relative position of the muscle. **(a)** Ventrally and dorsally determined active forces as a function of muscle relative position. **(b)** Ventrally and dorsally determined passive forces as a function of muscle relative position. **(c)** Dorso-ventral differences in passive and active forces as a function of muscle relative position. All values are plotted as mean + SE, n = 12, and muscle length is expressed as a deviation (in mm) of the reference muscle length (lref). Grey areas indicate muscle length ranges that can not be attained during *in vivo* muscle functioning.

Discussion

The main and novel finding of this study is the presence of epimuscular force transmission in the locust. Significant differences in ventrally and dorsally exerted passive forces are taken as unequivocal proof that, in addition to the loads exerted by the myotendinous connections; additional forces, other then myotendinous ones, are exerted on the muscle (Huijing *et al.* 1998),. These additional forces act as a loads on the muscle, and the *net* load is integrated in the force measured at the opposite tendon. This study is the first to demonstrate the presence of epimuscular force transmission in insects, an animal group distinctly different from vertebrates for which such transmission has already shown previously (Huijing *et al.* 1998; Huijing & Jaspers 2005; Huijing 2007).

Low levels of active force

There are two conceivable explanations for our present low values measured for the active forces; (1) Interference of the anesthetic with the excitation physiology of muscle and/or nerve. Anesthesia was used to remove pain stimuli and reduce the stress response of the animal, but the authors are not aware of any studies regarding possible effects of anesthetic agents on muscle functioning in insects. (2) We were unable to reach full excitation and thus full recruitment of the muscle during the contraction. This may have been the result of unforeseen movement of the electrodes during stimulation of the muscle or damage to the nerve resulting from the dissection of the muscles' origin and insertion. Force traces from the tetani show that the muscle was indeed not fully recruited nor activated constantly.

Despite the low levels of recruitment of the muscle, dorsally and ventrally exerted active forces were shown to differ significantly. This indicates that also at very low levels of recruitment, non-myotendinous, forces are exerted on the active muscle. However, because we were not able to obtain a constant stimulation of the muscle throughout the length and position trajectories, for the present work we refrain from drawing conclusions regarding the length-dependence of the non-myotendinous load exerted on the active muscle.

Effects of muscle length on ventrally and dorsally exerted forces.

For ventral as well as dorsal lengthening of the muscle, it was demonstrated that additional loads are exerted on the passive muscle (Fig. 3b-c & 4b-c). For a muscle within its natural context of connective tissues, the only candidates for the transmission of such loads are the tissues that form connections between the muscle and its surroundings (i.e. epimuscular connections).

For dorsal and ventral lengthening, the direction of the myofascial load reverses at a certain muscle length. Such a reversal is the combined effect of changes in muscle length and relative position of the muscle with respect to its surroundings, with concomitant changes in stiffness of the epimuscular structures. For dorsal lengthening at low muscle lengths (Fig. 3b, grey area), particularly the dorsal muscle segment has changed in position relative to the surrounding tissues.

Consequently, epimuscular connections between the dorsal muscle segment and its surroundings are stretched. This results in a stiffening of the connections which exert a *net* dorsally directed load on the muscle. This *net* load is integrated in the force measured at the ventral tendon (ventral passive force is higher than dorsal passive force, Fig. 3b). As the muscle is lengthened dorsally, initially the epimuscular connections of the dorsal segment of the muscle shorten and the dorsally directed load decreases. Further lengthening of the muscle first reverses the loading direction of the connections (at $\Delta lref_{dorsal} = 0$), exerting a ventrally directed *net* load on the muscle, and subsequently lengthens the connections, increasing the ventrally directed load. The ventrally directed *net* load is integrated in the force measured at the dorsal tendon; dorsal passive force is now higher than ventral passive force (Fig. 3b, white area). Note that for ventral lengthening, the opposite occurs: the most ventral segment of the muscle is now subject to the biggest changes in relative position at low muscle lengths. Consequently, a ventrally directed load is exerted on the muscle initially (dorsal passive force is higher than ventral passive force, grey area in fig. 4b), which reverses into an increasing dorsally directed load as the muscle is ventrally lengthened (Fig. 4c). As opposite effects are encountered for dorsal and ventral lengthening to identical lengths, an additional factor is active namely muscle relative position.

Effects of muscle relative position on ventrally and dorsally measured forces

Despite being left at a constant muscle length, passive forces are affected by the position of the muscle relative to its surroundings. So therefore, it is concluded that also for insect muscles, not only muscle length, but also muscle relative position is a co-determinant of muscle force. Such results are in agreement with experiments on vertebrate muscles (Huijing 2007; Maas *et al.* 2004; Rijkelijkhuizen *et al.* 2007; Yucesoy & Huijing 2007). The muscle length and muscle relative position dependence of the myofascial load in insects implies that the effects of epimuscular force transmission are not taxon-dependent, but are a general feature of the integration of muscles in a higher level of organization of the body.

As muscle relative position is changed, myofascial connections change in length and stiffness, and forces transmitted by these myofascial connections changes in magnitude and direction as well. In the initial position (ΔPosition = 0.5), the muscle has moved in dorsal direction with respect to its surroundings. As a consequence, myofascial connections at the dorsal segment, as well as the ventral segment of the muscle are stretched and exert a ventrally directed *net* load on the muscle, which is integrated in the force exerted at the dorsal tendon (i.e. dorsal passive forces are higher than ventral passive forces (Fig. 5)). Moving the muscle in the ventral direction initially decreases the length, and thus the stiffness, of the epimuscular connections. Further movement of the muscle in this direction reverses the direction of the loading of the epimuscular pathways and they now exert a dorsally directed load on the muscle.

Pathways of epimuscular force transmission and can such transmission be considered myofascial force transmission?

Insect muscle is thought to possess little connective tissues (Ashhurst 1968; Hoyle 1955; Pond 1982). Pond (1982) observed that

"[for adult insects] each muscle was anatomically distinct and only very loosely attached to adjacent muscles. Even its constituent fibres could easily be teased apart, and each one could, and apparently in life often did, contract independently of its neighbors."

However, several studies have shown the presence of collagenous connective tissues in insects (Ashhurst 1968; Ashhurst & Bailey 1980; Locke & Huie 1972), although connective tissues are more sparse in insects compared to other animal groups. Nevertheless, the current results (i.e. the difference in forces exerted at the muscles'' origin and insertion) prove unequivocally that force is transmitted via non-myotendinous pathways. Connective tissue structures are a good candidate for such transmission. In vertebrates, two types of connective tissues can be distinguished which could take part in the force transmission between muscles (Huijing 2003; Maas *et al.* 2001): 1) intermuscular connective tissue and 2) extramuscular connective tissue. Intermuscular connective tissues constitute by the continuous intramuscular stromata of adjacent muscles. Extramuscular connective tissues consist of non-muscular connective tissues such as compartmental fasciae, intermuscular septa, periost and connective tissues reinforcing blood vessels and nerves (the latter is often referred to as the neurovascular tract). It has been argued that extramuscular myofascial pathways are the most important epimuscular myofascial pathway via which force is transmitted (Maas *et al.* 2005b).

Despite several anatomical studies on locust flight muscles (Albrecht 1953; Hoyle 1955; Tiegs 1955), detailed knowledge regarding intra- and intermuscular connective tissues is lacking. Hoyle (1955) observed "muscle units", which he describes as groups of muscle fibres wrapped in a common membrane, but also notes that "there is virtually no connective tissue between these units". The aforementioned studies by Ashhurst (1968; Ashhurst & Bailey 1980) and Pond (1982) also suggest that intermuscular connective tissues are very scarce. Therefore, intermuscular myofascial force transmission via continuous networks of intramuscular stromata is expected to be of minor importance within the locust.

For vertebrates, an important extramuscular pathway is the collagen-reinforced system of blood and lymph vessels and nerves (Maas *et al.* 2005b). The sheet of collagen enveloping the blood and lymph vessels and nerves serves to protect these delicate structures and is sufficiently stiff to transmit force. However, in contrast to vertebrates, insects lack a closed circulation system. Therefore, blood vessels are absent. Instead the locust's organs and tissues are supplied with oxygen by the tracheal system, a complex branching network of tubes and air sacs that delivers oxygen to every organ in the body through diffusion (Maina 1989). The tracheae begin at the spiracles in the exoskeleton and branch repeatedly, eventually becoming small, delicate tracheoles. Trachea can also form airsacs. Several microscopical studies (Biserova & Pfluger 2004; Maina 1989; Tiegs 1955)

show that the smallest tracheoles are widely distributed between muscle fibres and even are surrounded by intracellular content by invaginations of the sarcolemma (similar to t-tubuli in vertebrates). To prevent the small tracheoles from collapsing during muscle contraction, they are reinforced with chitin in spiral structures called taenidiae. The tracheoles attached to the muscle fibres provide a potential pathway for force transmission. It should be noted that although transmission via the tracheal system is clearly non-myotendinous force transmission, it is not clear whether this potential pathway truly classifies as myofascial because of the chitin based mechanisms. Such a structure is hard to consider as a fascia. Albrecht (1953) observed that the subalar muscle is supplied by a trachea connected to an airsac located medio-dorsally within the body. Such a structure provides a potential pathway for the exertion of a dorsally directed load on the muscle. In addition, changing the relative position of the muscle from a dorsal to a ventral position will lengthen the tracheal system and increase the dorsally directed load on the muscle.

Motor nerves innervating the muscles are surrounded by sheath cells, a neural lamina and an outer membrane (Hoyle 1955). The neural lamina was found to contain collagen (Ashhurst 1968; Ashhurst & Bailey 1980; Locke & Huie 1972). Hoyle (1955) argued that "The sheet around the nerve trunks is far from being delicate and remarkably tough despite its thinness". It was even argued that the neural lamina may be continuous with the sarcolemma (Hoyle 1955; Tiegs 1955). Such observations indicate that the connective tissues reinforcing nerves are continuous with the muscle fibre and could be sufficiently stiff to transmit muscle forces, similar to the connective tissue reinforcement of nerves in vertebrates. Hoyles' observation on the toughness of the collagen-reinforced neural lamina raises the question whether such toughness can also be shown in collagen structures between adjacent muscles. The ganglia are located ventrally within the body, which means that the nerves approach the muscle from the ventral side. Consequently, the motor nerves innervating the subalar muscle may exert a ventrally directed myofascial load on the muscle.

Our current work does not allow for a proper distinction between the pathways involved in myofascial force transmission between the subalar muscle and its surroundings. Within vertebrates, progressive dissection is used to study how each pathway is involved in myofascial force transmission. However, for insects, such progressive dissection may be very complicated because of the vulnerability of the tracheal system which is closely associated with the muscle and its physiological function.

Functionality of epimuscular force transmission

Wilson (1962) noting that many of the locusts flight muscles were also attached to the coxa, argued that these muscles may also be involved in moving the legs, as well as the wings. A bi-articular muscle suits the concept of epimuscular force transmission; for the force necessary for movement at the insertion needs not to be equal to the force exerted at the origin. The presence of a epimuscular load on the passive muscle indicates that in flight, a force is exerted on the coxa to keep the leg

folded at all times regardless of the force exerted at the wings (i.e. upstroke or downstroke). Such an adaptation reduces energy and the need for separate mono-articulate muscles keeping the leg folded. This may be particularly favorable during extended periods of flight.

It is concluded that epimuscular force transmission is present within the locust and affects flight muscle forces. It is hypothesized that mostly extramuscular pathways, i.e. on the one hand the collagen-sheet around the nerves and on the other hand the tracheoles, are involved in the transmission of muscle force. The presence of a myofascial load may provide an advantageous adaptation during flight. The presence of myofascial force transmission within insects indicates that the concept of transmission of muscle force also via non-tendinous structures is a very conservative mechanism with significant advantages during locomotion.

9

General Discussion

The work presented in this thesis demonstrates unequivocally that myofascial force transmission significantly affects muscle forces exerted at their origin and insertion. Fundamental issues concerning myofascial force transmission (Chapters 2 – 5) were addressed in an experimental rat model, in which aspects of myofascial force transmission regarding its functional relevance were investigated. In addition, myofascial force transmission was studied in the dystrophin-deficient mouse, an animal model for muscular dystrophy (Chapter 6). Finally, comparative morphological studies were carried out to compare myofascial force transmission in two mammal species (Chapter 7), as well as to investigate myofascial force transmission in insects, an animal group distinctly different from mammals (Chapter 8). Based on the results, it is concluded that myofascial force transmission is a fundamental and evolutionary conserved mechanism of force transmission, inherent to the integration of muscle tissue into a higher hierarchy of tissue, and should therefore be reckoned with in studies on muscle functioning *in vivo.*

However, it should be made clear that our experiments were never designed to replicate the exact conditions under which muscles operate *in vivo*. Instead, single variables were chosen, such as firing frequency or lengthening condition of synergistic muscles within a compartment, to investigate their effect on myofascial force transmission. In chapter 5, two of these variables were combined to study their combined effects. Such an approach brings us a step closer to understanding the potential extent and functional relevance of myofascial force transmission in *in vivo* muscle functioning.

Designing experiments that exactly replicate the in vivo conditions should be considered idealistic and may be in fact impossible to realize. A major reason for this is the immense complexity of the physiological conditions under which muscles function. Besides firing frequency and synergist lengthening conditions, the two variables studied in the current work, factors such as shortening velocity, contraction type, level of recruitment, and length changes due to different joint angles and moment arms all affect muscle functioning. The simultaneous implementation of several of these factors within an experimental design would be too complex and leave little experimental control of variables. Another factor preventing us from exactly replicating the *in vivo* conditions is an inevitable consequence of anatomical study; any dissection upon an organism irreversibly alters the functional characteristics of its anatomy. This conflicts with the basic prerequisite for myofascial force transmission to occur, namely the integrity of the continuous network of myofascial structures connecting muscle(s) (fibres) to the surrounding matrix. Therefore, future research should focus on non-invasive techniques, such as magnetic resonance imaging (MRI) and high-resolution ultrasound, which provide a valuable tool for the study of myofascial force transmission *in vivo.*

Implications of the current work

Despite the gap between our experimental model(s) and the *in vivo* situation, the experimental work performed in this thesis has yielded important new insights regarding myofascial force transmission.

First, the enhanced importance of myofascial force transmission at submaximal firing frequencies is an important step in understanding myofascial force transmission under physiological conditions, for healthy muscles are hardly ever active maximally. For freely moving adult rats, Hennig and Lomo (1985) found that firing frequencies vary between 20 and 60 Hz. Despite the lower active muscle force at such submaximal activation, the fraction of active muscle force that is transmitted via myofascial pathways between synergistic EDL and TA+EHL is surprisingly larger than at maximal stimulation (Chapter 3). The enhanced myofascial force transmission on submaximally active EDL resulted in length-force characteristics which differ substantially from those described for fully dissected muscle fibres and muscles (Brown *et al.* 1999; Rack & Westbury 1969; Roszek & Huijing 1997). This means that also at submaximal levels of stimulation, myofascial force transmission is significant and even interferes with effects of intrinsic properties of muscles, such as the Ca++ dependent increase of force at lower firing frequencies. These results are in contrast to a very early account of myofascial force transmission between submaximally active muscles by Kronecker and Cash (1880), who noted that a passive muscle was shortened by its maximally shortening neighbour. For an intermediately shortening muscle, the passive muscle did not move at all. This suggests that at low levels of stimulation, myofascial force transmission is negligible. However, the experiments described in chapter 3 of this thesis prove otherwise.

Secondly, the substantial transmission of muscle force between antagonistic peroneal and triceps surae and anterior crural muscle groups (Chapter 4) demonstrates that length changes of a muscle may significantly affect *any other muscle within that limb segment*. The effects of such intercompartmental mechanical interaction are expected to be largest for antagonistic compartments, as the differences in relative position (i.e. the position of the muscle with respect to surrounding structures) between antagonistic muscles are greater than between synergistic muscles. Also for submaximally active antagonistic muscles, mechanical interaction via myofascial force transmission is substantial (Chapter 5). However, in contrast to the results described in Chapter 3, for lengthening of a group of synergists, submaximal firing frequencies resulted in decreased net myofascial force transmission (i.e. small EDL proximo-distal force differences) between synergistic muscles. These results would suggest that for lengthening of all synergists within a compartment (TA+EHL and EDL), myofascial force transmission between synergistic muscles is not enhanced at low firing frequencies. But in spite of the small myofascial load exerted on EDL, length-force characteristics for both TA+EHL and EDL at low firing frequencies, particularly for 10 Hz stimulation, deviate dramatically from length-force curves of fully dissected (i.e. with only the blood supply left intact) muscles. Fig. 1 shows the

143

TA+EHL length force characteristics as a function of lengthening of all anterior crural muscles and the hypothesized curve for 10 Hz active force based on data from fully isolated muscles. The grey area represents the increase in active force at the ascending limb for 10 Hz with respect to the hypothesized 10 Hz curve. Such additional, myofascial, load on the muscles increased distributions in mean fibre sarcomere length and altered length-force characteristics. Thus, despite a small proximo-distal difference in force at low firing frequencies, altered length-force characteristics indicate that significant myofascial loads are exerted on the muscle nonetheless. Note that also in the presence of larger proximo-distal force differences at submaximal firing frequencies (Chapter 3), EDL length-force characteristics also show deviations from those described for fully dissected muscles. Such results strengthen the conclusion that effects of myofascial force transmission are substantial at low firing frequencies, and affect synergistic, as well as antagonistic muscle groups.
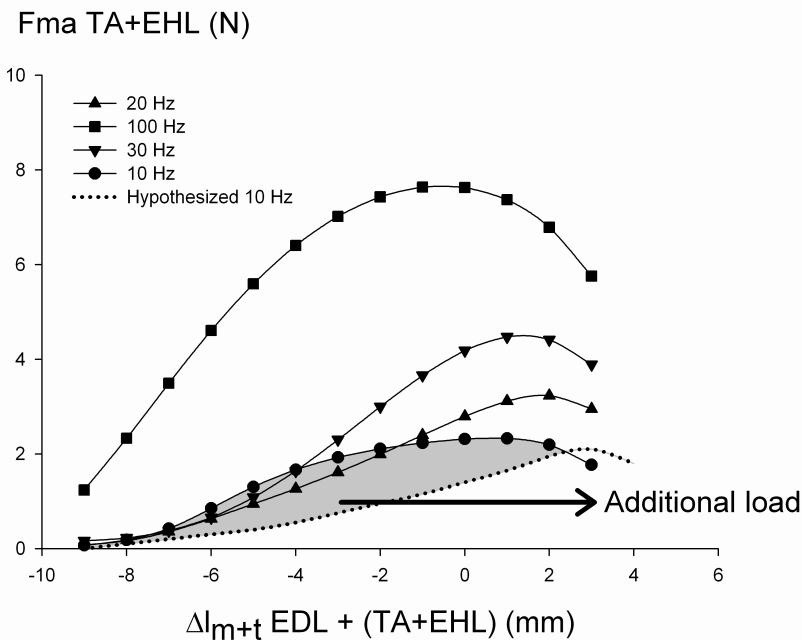
Figure 1. TA+EHL active forces as a function of EDL + TA+EHL length and stimulation frequency. The dotted line represents the hypothesized 10 Hz active force based solely on measurements on isolated muscles, whereas the closed circles represent the 10 Hz active force for lengthening of all synergistic muscles within an intact compartment. The shaded area indicates the additional load exerted on TA+EHL muscles for 10 Hz activation. It is thought that this additional load is exerted on the muscles via epimuscular myofascial pathways.

Indicators for myofascial force transmission and the concept of multiple myofascial loads

The results described in Chapter 5 challenge the concept of a difference in forces exerted at the origin and insertion of muscle as the sole indicator of the presence of force transmission via non-myotendinous pathways, since substantial effects of

myofascial force transmission on EDL length-force characteristics were demonstrated in the absence of a large proximo-distal difference in EDL active force. In previous work considering the presence of myofascial force transmission, a difference in forces exerted at the origin and insertion of a muscle has been taken as definite proof that additional loads are exerted on the muscle via non-myotendinous pathways (Huijing 1998; Huijing *et al.* 1998; Maas *et al.* 2004). This additional load may be fully or partially integrated in the force measured at the tendon opposite of the direction in which the myofascial load is applied, or may leave the muscle again via other myofascial pathways. Inadvertently, this may lead one to think that the difference in force at the origin and insertion is the result of a single myofascial load transmitted via a single pathway. Yet for a muscle within its natural context of connective tissues, many force-bearing myofascial connections exist which may be orientated in opposite directions (although their orientation is partially determined by muscle length and muscle relative position). For instance, a major proximally directed extramuscular myofascial pathway in the lower limb is the neurovascular tract, which forms a connection between multiple compartments. An extramuscular pathway capable of exerting a distally directed myofascial load is considered to be the compartmental and general fasciae, which are continuous with the muscles' epimysium. As the muscle attains a short length at its distal insertion, these fasciae consequently lengthen and are thought to exert a distally directed load on the muscle (Huijing 2007). At the proximal origin of the muscle, the compartmental and general fasciae are hypothesized to exert a proximally directed load as the muscle attains short lengths at its origin, but this has yet to be investigated. Thus, it is conceivable that loading of a muscle occurs simultaneously by more than one myofascial pathway, and in more than one direction. The exertion of multiple myofascial loads by multiple pathways complicates the analysis of the effects of myofascial force transmission, as the contribution of each pathway can not be readily distinguished.

Intersegmental myofascial force transmission?

The demonstration of myofascial force transmission, between maximally and submaximally active muscle compartments in Chapters 4 and 5 raises the question whether myofascial force transmission is limited to one segment only, or that myofascial forces can also be transmitted between adjacent segments, and possibly even further? In this thesis, the collagen-reinforced neurovascular tract is considered an important extramuscular myofascial pathway for the transmission of forces between antagonistic compartments (Chapters 2, 4 and 5). The continuation of the collagen reinforcement of the blood vessels and nerves proximal of the lower leg forms a possible pathway for intersegmental myofascial force transmission between lower leg muscles and the femoral segment (Huijing 2007). In work by Vleeming *et al.* (1995) on human cadavers, it was shown that the posterior layer of the thoracolumbar fascia may play an important role in force transmission between the spine, pelvis and legs, possibly contributing to rotation of the trunk and stabilization of the lower lumbar spine. Also the continuity of

intramuscular stroma of the rectus femoris with adjacent knee flexors as well as with the capsular connective tissues (as interpreted from data by Riewald and Delp (1997)) suggest that muscle force can be transmitted from one segment onto another segment in series via epimuscular myofascial pathways.

Limitations of the current work

The work described in this thesis has enhanced our understanding of myofascial force transmission and its potential effects for *in vivo* muscle functioning. However, issues regarding its functional relevance remain to be considered.

The use of low firing frequencies has been provided new insights in myofascial force transmission. However, it can be argued that an asynchronous stimulation of the nerve following Rack and Westbury (1969), rather than the synchronous stimulation used, provides a better approach to the *in vivo* situation. Asynchronous stimulation results in more smooth contractions at low forces as the forces of the individual twitches are summed. Unfortunately, the use of a distributed stimulation protocol is not possible within our current experimental set-up, as it would involve dissection of the sciatic nerve very close to the muscle to be able to stimulate each nerve branch independently, a procedure that is interferes with the integrity of the myofascial network. Although dissection of the sciatic nerve more proximally may resolve this issue, the procedure of splitting the nerve to obtain separate nerve branches is very difficult and the nerves are easily damaged. The effects of firing frequency result from mainly intracellular mechanisms (the Ca^{++} - dependence of force, for instance), and the major effects of firing frequency as described by Rack and Westbury (1969) are present within our results. Therefore, the use of a distributed stimulation protocol is unlikely to bring us much closer to the *in vivo* condition.

In addition to varying firing frequency (Person & Kudina 1972), muscle force can also be regulated by varying the number and size of motor units recruited (Hennemans size principle, (Henneman *et al.* 1965)). Within the experiments described in this thesis, all motor units were recruited and only firing frequency was varied (chapters 3 and 5). Reducing the number of recruited motor units is expected to decrease the stiffness of the epimuscular myofascial connections, and consequently, less force is transmitted out of the muscle via epimuscular myofascial pathways. It is therefore necessary to investigate the effects of recruitment as an altered stiffness of epimuscular myofascial connections, may lead to altered distributions in sarcomere lengths throughout the muscle.

It can be argued that the lengthening conditions imposed within our experiments, for instance lengthening of only one muscle (EDL, chapter 3) or very low and very high muscle lengths, are too deviant from the in vivo conditions, because muscles *in vivo* are thought to be seldom subjected to such conditions. Nevertheless, performing contractions at the whole length range of the muscle provides insights in the fundamental mechanisms of myofascial force transmission. Also, the lengthening conditions imposed in chapters 4 and 5 provide a better

approximation of the *in vivo* situation, as plantar flexion of the ankle lengthens not just one but all anterior crural muscles. However, it should be noted that in chapters 4 & 5 the relative position between synergistic TA+EHL and EDL was kept constant, while changes in relative position are expected due to different moment arms of TA+EHL and EDL (Lieber 1997). Also, *in vivo* lengthening of synergists is always accompanied by simultaneous shortening of antagonistic peroneal and triceps surae muscles. In the experiments reported in chapters 4 and 5, peroneal and triceps surae muscles were kept at a constant, rather low, length, but these lengths were chosen arbitrarily. Simultaneous shortening of antagonistic peroneal and triceps surae muscles and lengthening of synergistic anterior crural muscles is hypothesized to increase myofascially transmitted forces as the relative position between these two muscle groups is enhanced. Thus, for this aspect of the *in vivo* condition, myofascial force transmission is expected to be even more substantial between oppositely moving antagonistic muscle groups.

In the current experimental work, muscle force was measured during isometric contractions. However, for a full understanding of myofascial force transmission *in vivo,* it is necessary to investigate myofascial force transmission in dynamic conditions, i.e. eccentric and concentric contractions. During such contractions, epimuscular myofascial force transmission is not only affected by series-elastic aspects of the myofascial connections, but also by their visco-elasticity. For repeated dynamic contractions of only a single head (III) of EDL, it was already reported that forces exerted at the distal and proximal EDL tendons were unequal (Maas & Huijing 2005). However, no effect on adjacent TA+EHL force was observed. Further research should focus on epimuscular force transmission in dynamic conditions. Maas et al. (2005a) also showed that repeated dynamic shortening of the head III of multi-tendoned EDL, results in damaged muscle fibres located closely to inter- and extramuscular myofascial pathways. This suggests that frequent loading of myofascial structures causes damage, possibly leading to injuries such as repetitive strain injury.

Consequences and evolutionary origins of myofascial force transmission

Consequences of myofascial force transmission

The presence of myofascial force transmission within several animal groups, such as mammals, amphibia and insects suggests that epimuscular force transmission is not limited to a certain group of animals but is widespread in the animal kingdom. This implies that myofascial force transmission is a fundamental mechanism inherent to the integration of muscle tissue into a higher level of organization. So far, research has barely touched upon the possible effect(s) of myofascial force transmission, but there are several indications that its presence is essential in maintaining healthy muscle functioning:

Joint stability is a prerequisite for efficient locomotion and preventing injury. Joint stability has been assumed to be determined by the stiffness of the attaching musculature and ligaments (Solomonow & Krogsgaard 2001). However, also by

myofascial structures should be taken into account when considering factors affecting joint stiffness and moments exerted. For instance, the interosseal membranes and intermuscular septa are continuous with the periost. Also, the joint capsule and capsular ligaments are continuous with the intramuscular connective tissue of the musculature arranged in series with them. Via these myofascial paths, forces as well as moments are transmitted onto the bone, in addition to myotendinal ones, that contribute to joint stability. The joint-stabilizing function of myofascial force transmission may be of particular use in joints which are frequently loaded or in the limb joints of heavy animals, i.e. large animals tend to have unusually thick fasciae (J. Hutchinson, *personal communication*).

In addition, it has been argued before that myofascial force transmission may also be relevant for motor control. Huijing (2007) argues that muscle spindles may not only be length and velocity receptors, but possibly also 'misalignment receptors'. Their location in the perimysium enables them to detect shear strains resulting from different relative positions of adjacent fascicles. This suggests that the proprioceptive information sent back to the central nervous system also contains information regarding the muscles' relative position. Also, it was argued that the length-force characteristics of individual motor units were also determined by the state of contraction of surrounding motor units (Monti *et al.* 2001). Thus, it is possible that effects of myofascial force transmission are considered in the control of movement. However, more research is needed to establish the relationship between myofascial force transmission and the neural control of movement.

In humans, severe (muscle) pathologies result from the absence of molecules that anchor the contractile apparatus to the collagen IV reinforcement of extracellular matrix (ECM), such as dystrophin, laminin and adhalin (α-sarcoglycan) (Fig. 1 in Introduction). The authors interpret this as a clear indication that an intact myofascial pathway between the cytoskeleton and the ECM is essential in maintaining healthy muscle cells. The muscular dystrophies are a very heterogeneous group of genetic hereditary muscle disorders. Despite the variability in phenotype, there seems to be a tendency for muscular dystrophies to become more severe when the deficient protein is located closer to the contractile apparatus. The absence of dystrophin (Duchenne Muscular Dystrophy), located at the intracellular side of the sarcolemma, leads to severe and progressive muscle wasting, and results in early death (Hoffman *et al.* 1987). To the contrary, patients with a deficiency in laminin α2 (merosin-deficient congenital muscular disorder (CMD) (Pegoraro *et al.* 1996)) and adhalin(α-sarcoglycan)-deficient patients (limb girdle muscular dystrophy (Duggan *et al.* 1997)) show milder phenotypes. If it is indeed true that muscular dystrophies are more severe when the deficient protein is located closer to the contractile apparatus, then the location of the protein in the cytoskeleton-ECM linkage is a co-determinant for the severity of the muscular dystrophy. It is not clear why this would be the case. It is possible that the molecules located more closely to the contractile apparatus, such as dystrophin, may also perform vital roles in other cellular processes such as signal transduction.

It is argued that myofascial force transmission is important in maintaining healthy muscles and movement, though more research is much needed to clarify the mechanisms responsible for such a role of myofascial force transmission.

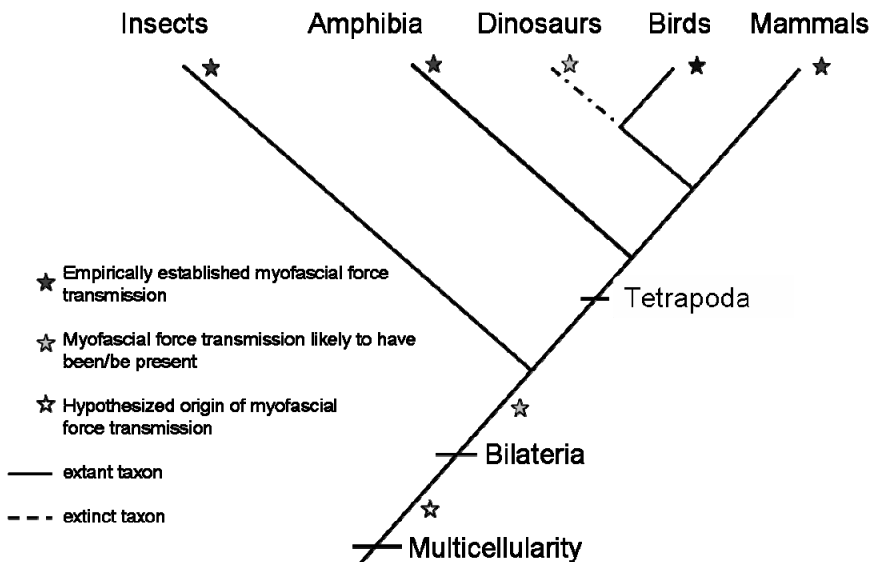*Evolutionary origin of myofascial force transmission*

Extensive research has been performed on the fundamentals of myofascial force transmission within mammals, i.e. rat (Huijing *et al.* 2003; Maas *et al.* 2003b), mouse (this thesis) and humans (Smeulders & Kreulen 2007). Also, Huijing and Jaspers (2005) reported the presence of myofascial force transmission in the amphibian *Xenopus laevis.* Finally, the work presented in chapter 8 has shown the presence of epimuscular force transmission within a species of insects, a group of invertebrate animals with a segmented body and lacking an endoskeleton. Especially these latest results shed an interesting light regarding the origin and evolution of myofascial force transmission, as this is the first time that epimuscular myofascial force transmission has been recorded outside vertebrates. The presence of myofascial force transmission in such diverse groups of animals suggests that the presence of myofascial force transmission presents an evolutionary advantageous trait conserved within several animal lineages.

The assessment of myofascial force transmission in insects, mammals and amphibians suggests either that epimuscular force transmission has arisen several times independently, or evolved once at the base of these taxa. In the study of evolution, the presence of a characteristic, either anatomical, physiological, behavioural or genetic, within several groups of organisms indicates that this characteristic is a synapomorphy; a derived or specialized characteristic shared by two or more groups and most likely to have originated in their last common ancestor. When epimuscular force transmission is to be considered to be a synapomorphic trait, judged by its presence in insects, mammals as well as amphibians, the most parsimonious hypothesis is that epimuscular force transmission found its origin at the base of these three groups, within the (last) common ancestor of these three animal groups. The last common ancestor of insects, mammals and amphibians is thought to be found within the Bilateria (Fig. 2), a group of multicellular organisms comprising 99% of all described living animals and classified by o.a. three different germ layers and bilateral symmetry. Note that very primitive bilaterians (such as the extant acoelomorph flatworm (Bagun & Riutort 2004)) do not posses any supportive skeletal systems or appendages, which arose much later in evolution. In the absence of tendons and bony structures, the transmission of force generated by muscle fibres onto other cells and connective tissues (such as the extracellular matrix must) was a prerequisite for movement to occur. Such reasoning indicates that epimuscular force transmission predates myotendinous force transmission.

However, the protein complexes that provide pathways for force transmission from the muscle cell tot the ECM (the integrins and the DGC) are also involved in biochemical signalling purposes at the cellular level. With the rise of multicellular organisms, cell adhesion became crucial in assembling individual cells into three-

dimensional animals (for a review, please refer to Gumberin (1996)). Mechanical signals from the physical adhesion interact with classical signal transduction pathways to help control cell growth and differentiation. It is therefore hypothesized that epimuscular force transmission originated as a signal transduction pathway and later became also useful for transmitting forces when unicellular organisms lived together to become multicellular organisms. Note that in the absence of fasciae, the definition of myofascial force transmission should be broadened to also include non-muscle cell-to-cell transmission of force via only the extracellular matrix.

Such a hypothesized origin of myofascial force transmission predates the Cambrian explosion, a radiation of life recorded in the fossil record and which lays out most of the animal body plans seen today. To investigate the step(s) from signal transduction to signal- and mechanotransduction in transsarcolemmal pathways, an interesting organism of study could be *Dictyostelium discoideum*, a social amoeba which grows as separate, independent cells but interact to form multicellular structures when challenged by adverse conditions such as starvation.

Figure 2. Hypothesized evolutionary history of myofascial force transmission. Black stars denote animal lineages in which myofascial force transmission has been established experimentally (see text for references), grey stars denote lineage presumed presence of myofascial force transmission, and the white star denotes the hypothesized origin of myofascial force transmission as force transmission via extracellular pathways after the rise of multicellularity.

Implications of myofascial force transmission for the use of muscle force-based reconstructions in vertebrate palaeontology

Myofascial force transmission enables forces to be transmitted from and onto muscle without passing at least one tendon, and as a consequence, force exerted at the tendons may be different from the force generated solely by the muscle attached to the tendon itself. Gregor et al.(1988) reported that the for feline soleus muscle during treadmill locomotion, force measured *in vivo* at its tendon was much higher than their expectations based on *in situ* experiments involving maximal excitation. Experimental work within this thesis demonstrates that in certain conditions, up to 60% of active muscle force exerted at the tendon may originate outside the muscle (chapter 7). In chapters 4 and 5, we reported that active muscle forces exerted at the tendons of triceps surae and peroneal muscles even decreases by sometimes as much as 30% as a result of myofascial force transmission. Such effects of myofascial force transmission may have substantial consequences for the reconstruction of extinct animals based on intrinsic muscle properties determined *in situ*.

In the slow process of fossilization, vast amounts of anatomical information are lost with the destruction of soft tissues. Within the field of paleobiology, vertebrate palaeontologists therefore often rely on muscle attachment sites on bones to reconstruct the biology of extinct animals. Such muscle attachment sites, or entheses, may represent either a direct or 'fleshy' attachment where the muscles' connective tissue merges with the periost, or a tendinous attachment in which the muscle attaches to the bone via a tendon or aponeurosis (Bryant & Seymour 1990). Entheses exhibit significant morphological variation both within and between species (Bryant & Seymour 1990; McGowan 1982), and as the area of a surface is proportional to the mechanical stress experienced by that surface, larger or more 'obvious' attachment sites have been thought to reflect increased muscle mass and/or muscle use. This assumed relationship has been used to reconstruct the biology of animals long extinct, based on variations in size, shape and complexity of muscle attachment sites on (sub) fossil bones (Berta *et al.* 1989; Maglio 1973; Sumida 1989).

Enthesis size is determined by closely studying the bone surface, relying on microscopical details to distinguish entheses from non-entheses. Such research methods are suitable for establishing the absence/presence and gross dimensions of the attaching musculature, especially in combination with the extant phylogenetic bracket (EPB) method (Witmer 1995), in which one relies on examination of extant and fossil related species. In other words, observations are placed within a phylogenetic context and data from extant taxa are used to constrain inferences concerning soft tissue structures. A good example of such work by Hutchinson (Carrano & Hutchinson 2002; Hutchinson 2001a; Hutchinson 2001b) in which careful use of the EPB and different levels of inferences results in reliable conclusions regarding the musculature of extinct animals.

However, the functional significance of enthesis morphology in determining muscle size and muscle force has been questioned (Bryant & Seymour 1990;

Zumwalt 2006). It has been argued that the visible features on bony surfaces do not fully or reliably reflect the actual extent of muscle attachment, and that the degree to which such bony features reflect soft tissue attachment appears to vary between vertebrate lineages (Bryant & Seymour 1990). Factors such as sex or age (Wilczak 1998) on the observed variation in enthesis morphology are largely ignored. In addition, the relationship between enthesis morphology and loading is poorly understood (Zumwalt 2006). Another complicating factor is that the interface between tendon or muscle and bone is likely to be designed to buffer the underlying bone from the local strain created by the muscle, either by a gradual change in tissue type at the sites of tendon attachments, or by expansion of the attachment site over a large area (Zumwalt 2006).

So far, effects of myofascial force transmission have been left out of the equation, but it is clear that myofascial force transmission further obscures the relationship between enthesis size and the attaching musculature. Zumwalt (2006) studied the effects of endurance training on the size and complexity of several muscle attachments sites. Despite hypertrophy of the muscles, no effects were found on the enthesis itself. It was argued that protective mechanisms may have reduced the influence of muscle activity on the underlying bone, such that variations in muscle activity and size are not necessarily transferred into variations in enthesis morphology. One such protective mechanism is thought to be the gradual change in tissue type at the tendon attachment (Zumwalt 2006). However, an increase in myofascially transmitted forces, possibly via an increase in connective tissue (a factor not investigated in the study), out of the muscle may have prevented the enthesis from being exposed to higher muscle forces resulting from hypertrophy. Thus, effects of myofascial force transmission should be taken into account when considering the relationship between enthesis size and complexity and muscle size.

Despite the poorly understood effects of muscle force and myofascial force transmission on enthesis size, effects of myofascial force transmission on the reconstruction of fossil animals can be investigated by adapting existing models.

Subject of much debate are the running abilities of the large predatory dinosaur *Tyrannosaurus rex*; some argue that it was capable of at best slow running (Alexander 1985) while others support much faster speeds (Paul 2000). Hutchinson and Garcia (2002) estimated the minimum extensor muscle mass needed per leg for fast running, and it compared to data from living alligators and chicken. First, they estimated the required moments at the hip, knee, ankle and toe joints to maintain static equilibrium during mid-stance. The minimum muscle mass required to produce each joint moment was then calculated for each joint, and total extensor muscle mass *T* i.e. the total of the muscle masses per joint was calculated. Their model results showed that *T. rex* would have needed an unreasonable high mass of extensor muscles of amounting to at least 86% of body mass (43% per leg), to support its own body mass during running. Values for total extensor muscle mass of 50% are thought to indicate very poor running ability (Hutchinson & Garcia 2002). Hutchinson and Garcia therefore concluded that

"*Tyrannosaurus* had very little, if any, running ability [......] but if *T. rex* was indeed an adept runner, it must have had many musculoskeletal specializations that available data do not suggest". Such a musculoskeletal specialization may have been myofascial force transmission, although the term 'specialization' is superfluous as myofascial force transmission has been shown to be a general feature of muscle (Huijing 2007). Via myofascial pathways, additional forces may be exerted on the muscle belly and/or connective tissue surrounding the tendons. These myofascial forces are born by the muscle and integrated in the force measured at the tendons. So far, experimental research has only shown the presence of myofascial force transmission in amphibia, insects and mammals, but myofascial force transmission is likely to have been present in dinosaurs, as they are grouped with amphibians and mammals within the Tetrapoda (Fig. 2). Other evidence for the presence of myofascial force transmission in dinosaurs are preliminary observations on passive myofascial force transmission in chicken (Bender & Hawkins 2004), as birds are the living representatives of dinosaurs, and the finding of collagen in *T. rex* (Schweitzer *et al.* 2007). Therefore, it is argued by the present authors that in order to estimate minimum extensor muscle mass in *T. rex*, effects of myofascial force transmission should be considered.

In the equation to calculate the minimum extensor muscle mass per joint, muscle stress was entered at 3.0×10^5 kg m^{-3} based on data from mostly fully dissected vertebrate muscles and muscle fibres (Johnston 1985). However, for muscles within an intact compartment, force exerted may be greater than based solely on its cross-sectional area, as additional forces are exerted on the muscle and its tendon via myofascial pathways. Experiments on EDL in the rat show that for lengthening of EDL at its distal tendon, sometimes as much as 30% of the force exerted at the distal tendon originates from outside the muscle. Also, Gregor et al. (1988) reported that for cat soleus muscle, the force output from the submaximally active muscle *in vivo* was greater than under maximal stimulation *in situ*. In the model of running *T. rex,* during mid stance phase, extensor muscles are stretched at their distal tendon and their muscle bellies have shifted in relative position with regard to their antagonists. It is therefore argued that significant myofascial loads in the proximal direction are exerted upon the extensor muscles, and that these myofascial loads are integrated at the forces exerted at the distal tendons, resulting in forces higher than assumed in the model. A conservative estimate of such effect (based on data presented in this thesis as well as earlier work by Maas and Huijing) is that force exerted at the distal tendon is increased by 20%, resulting in a muscle stress of 3.6×10^5 kg m^{-3}. When entered in the equation to estimate minimum extensor muscle mass gives a total extensor muscle mass per leg of 34.8%, resulting in $T = 70.6\%$. Our value for T is 16% lower than that of Hutchinson & Garcia, but the implementation of myofascial force into the model does not make *T. rex* a better runner. Using a combination of different parameters, Hutchinson and Garcia were able to reduce the value for T to 26%, promoting *T. rex* to the 'uncertain running ability' category. Implementation of myofascial force transmission in this model reduces T to 21% (10.5% per leg). This estimate is in agreement with scaling data, which suggest that a 6000 kg *T. rex* had 7-10% of

extensor muscle mass per leg (Alexander *et al.* 1981; Bennett 1996). Thus, on theoretical grounds, implementation of effects of myofascial force transmission into the model by Hutchinson and Garcia would enable *T. rex* to run.

Conclusions

From the work presented in this thesis, the overall conclusion is that muscular interaction via myofascial force transmission is inherent to the integration of muscles in a higher level of tissue organization. Muscle force and length-force characteristics are affected by myofascial force transmission at low levels of activation and for lengthening of a group of synergistic muscles. Evidence was also found that epimuscular myofascial pathways enable mechanical interaction between muscles located at opposite sites of a limb segment, and it is considered likely that such interaction may even extend beyond the segment. A preliminary analysis of epimuscular myofascial force transmission in healthy and dystrophin-deficient *mdx* mice shows that epimuscular myofascial force in *mdx* mice is at least as high as in healthy mice. The observed pathologies in *mdx* muscle do not result from reduced myofascial force transmission.

The presence of myofascial force transmission in a variety of animals indicates a very early evolutionary origin for the transmission of force via non-myotendinal pathways.

References

- References -

Albrecht, F. O. 1953 *The anatomy of the migratory loucst*. Athlone Press, London.

Alexander, R. M., Jayes, A. S., Maloiy, G. M. O. & Wathuta, E. M. 1981. Allometry of the leg muscles of mammals. *J Zool* **194**, 539 - 552.

Alexander, R. M. 1985. Mechanics of posture and gait of some large dinosaurs. *Zool J Linn Soc* **83**, 1 - 25.

Almdahl, S. M. & Samdal, F. 1989. Fasciotomy for chronic compartment syndrome. *Acta Orthop Scand* **60**, 210-211.

Anderson, J. L., Head, S. I. & Morley, J. W. 2005. Synaptic plasticity in the dy2J mouse model of laminin alpha2-deficient congenital muscular dystrophy. *Brain Res* **1042**, 23-28.

Asakawa, D. S., Blemker, S. S., Gold, G. E. & Delp, S. L. 2002. In vivo motion of the rectus femoris muscle after tendon transfer surgery. *J Biomech* **35**, 1029-1037.

Ashhurst, D. E. 1968. The connective tissue of insects. *Annu Rev Entomol* **13**, 45 - 74.

Ashhurst, D. E. & Bailey, A. J. 1980. Locust Collagen: Morphological and Biochemical Characterization. *Eur J Biochem* **103**, 75-83.

Aszódi, A., Pfeifer, A., Wendel, M., László, H. & Fässler, R. 1998. Mouse models for extracellular matrix diseases. *J Mol Med* **76**, 238 - 252.

Babri, A. S., Kippers, V. & Bennett, M. (2003). Longitudinal excursion of peripheral nerves of the human lower limb. In *International Society of Biomechanics XIXth Congress*, ed. P. Milburn, B. Wilson & T. Yanai, Dunedin, New Zealand

Bagun, J. & Riutort, M. 2004. The dawn of bilaterian animals: the case of the acoelomorph flatworms. *BioEssays* **26**, 1046 - 1057.

Bender, C. J. & Hawkins, D. (2004). Quantitative characterization of lateral force transmission in passive skeletal muscle. In *American Society of Biomechanics 28th Annual Meeting*, ed. Portland, Oregon, USA

Bennett, M. B. 1996. Allometry of the leg muscles of birds. *J Zool* **238**, 435 - 443.

Berta, A., Ray, C. E. & Wyss, A. R. 1989. Skeleton of the oldest known pinniped, *Enaliarctos mealsi*. *Science* **244**, 60 - 62.

Berthier, C. & Blaineau, S. 1997. Supramolecular organization of the subsarcolemmal cytoskeleton of adult skeletal muscle fibers. A review. *Biol Cell* **89**, 413 - 434.

Biserova, N. M. & Pfluger, H. J. 2004. The ultrastructure of locust pleuroaxillary "steering" muscles in comparison to other skeletal muscles. *Zoology* **107**, 229 - 242.

Blake, D. J., Tinsley, J. M. & Davies, K. E. 1996. Utrophin: a structural and functional comparison to dystrophin. *Brain Pathol* **6**, 37-47.

Bloch, R. J. & Gonzalez-Serratos, H. 2003. Lateral Force Transmission Across Costameres in Skeletal Muscle. *Exerc Sport Sci Rev* **31**, 73 - 78.

Bojsen-Moller, J., Hansen, P., Aagaard, P., Svantesson, U., Kjaer, M. & Magnusson, S. P. 2004. Differential displacement of the human soleus and medial gastrocnemius aponeuroses during isometric plantar flexor contractions in vivo. *J Appl Physiol* **97**, 1908-1914.

Brown, I. E., Cheng, E. J. & Loeb, G. E. 1999. Measured and modeled properties of mammalian skeletal muscle. II. The effects of stimulus frequency on force-length and force-velocity relationships. *J Muscle Res Cell Motil* **20**, 627-643.

Bryant, H. N. & Seymour, K. L. 1990. Observations and comments on the reliability of muscle reconstruction in fossil vertebrates. *J Morphol* 109 - 117.

Bulfield, G., Siller, W. G., Wight, P. A. L. & Moore, K. J. 1984. X chromosome-linked muscular dystrophy (*mdx*) in the mouse. *Proc Natl Acad Sci U S A* **81**, 1189 - 1192.

Carrano, M. T. & Hutchinson, J. R. 2002. Pelvic and hindlimb musculature of *Tyrannosaurus rex* (Dinosauria:Theropoda). *J Morphol* **253**, 207 - 228.

- References -

Coulton, G. R., Curtin, N. A., Morgan, J. E. & Partridge, T. A. 1988. The mdx mouse skeletal muscle myopathy: II. Contractile properties. *Neuropathol Appl Neurobiol* **14**, 299-314.

Dangain, J. & Vrbova, G. 1984. Muscle development in mdx mutant mice. *Muscle Nerve* **7**, 700-704.

Deconinck, A. E., Rafael, J. A., Skinner, J. A. *et al.* 1997. Utrophin-Dystrophin-Deficient mice as a model for Duchenne Muscular Dystrophy. *Cell* **90**, 717 - 727.

Dellorusso, C., Crawford, R. W., Chamberlain, J. S. & Brooks, S. V. 2001. Tibialis anterior muscles in *mdx* mice are highly susceptible to contraction-induced injury. *J Muscle Res Cell Motil* **22**, 467 - 475.

Duch, C. & Pflüger, H. J. 1995. Motor patterns for horizontal and upside down walking and vertical climbing in the locust. *J Exp Biol* **198**, 1963 - 1976.

Duggan, D. J., Gorospe, J. R., Fanin, M., Hoffman, E. P. & Angelini, C. 1997. Mutations in the sarcoglycan genes in patients with myopathy. *N Engl J Med* **336**, 618-624.

Ettema, G. J. & Huijing, P. A. 1994a. Frequency response to rat gastrocnemius medialis in small amplitude vibrations. *J Biomech* **27**, 1015-1022.

Ettema, G. J. & Huijing, P. A. 1994b. Effects of distribution of muscle fiber length on active length-force characteristics of rat gastrocnemius medialis. *Anat Rec* **239**, 414-420.

Garfin, S. R., Tipton, C. M., Mubarak, S. J., Woo, S. L., Hargens, A. R. & Akeson, W. H. 1981. Role of fascia in maintenance of muscle tension and pressure. *J Appl Physiol* **51**, 317-320.

Gillis, J. M. 1996. Membrane abnormalities and Ca homeostasis in muscles of the mdx mouse, an animal model of the Duchenne muscular dystrophy: a review. *Acta Physiol Scand* **156**, 397-406.

Gillis, J. M. 1999. Understanding dystrophinopathies: an inventory of the structural and functional consequences of the absence of dystrophin in muscles of the mdx mouse. *J Muscle Res Cell Motil* **20**, 605-625.

Grady, R. M., Teng, H., Nichol, M. C., Cunningham, J. C., Wilkinson, R. S. & Sanes, J. R. 1997. Skeletal and cardiac myopathies in mice lacking utrophin and dystrophin: a model for Duchenne Muscular Dystrophy. *Cell* **90**, 729 - 738.

Gregor, R. J., Roy, R. R., Whiting, W. C., Lovely, R. G., Hodgson, J. A. & Edgerton, V. R. 1988. Mechanical output of the cat soleus during treadmill locomotion: *in vivo* vs *in situ* characteristics. *J Biomech* **21**, 721 - 732.

Gumbiner, B. M. 1996. Cell adhesion: the molecular basis of tissue architecture and morphogenesis. *Cell* **84**, 345 - 357.

Henneman, E., Somjen, G. & Carpenter, D. O. 1965. Functional Significance Of Cell Size In Spinal Motoneurons. *J Neurophysiol* **28**, 560-580.

Hennig, R. & Lomo, T. 1985. Firing patterns of motor units in normal rats. *Nature* **314**, 164 - 166.

Hoffman, E. P., Brown, R. H. & Kunkel, L. M. 1987. Dystrophin: the protein product of the Duchenne Muscular Dystrophy locus. *Cell (Cambridge, Mass)* **51**, 919 - 928.

Hoffman, E. P. & Dressman, D. 2001. Molecular pathophysiology and targeted therapeutics for muscular dystrophy. *Trends Pharmacol Sci* **22**, 465-470.

Hoyle, G. 1955. The anatomy and innervation of locust skeletal muscle. *Proc R Soc London, B* **143**, 281 - 292.

Huijing, P. A. 1995. Parameter independence and success of skeletal muscle modelling. *Human Movement Sciences* **14**, 443 - 486.

Huijing, P. A. 1996. Important experimental factors for skeletal muscle modelling: non-linear changes of muscle length force characteristics as a function of degree of activity. *Eur J Morphol* **34**, 47-54.

- References -

Huijing, P. A. 1998. Muscle, the motor of movement: properties in function, experiment and modelling. *J Electromyogr Kinesiol* **8**, 61 - 77.

Huijing, P. A., Baan, G. C. & Rebel, G. T. 1998. Non-myotendinous force transmission in rat extensor digitorum longus muscle. *J Exp Biol* **201**, 683-691.

Huijing, P. A. 1999a. Muscle as a collagen fiber reinforced composite: a review of force transmission in muscle and whole limb. *J Biomech* **32**, 329 - 345.

Huijing, P. A. 1999b. Muscular force transmission: a unified, dual or multiple system? A review and some explorative experimental results. *Arch Physiol Biochem* **107**, 292-311.

Huijing, P. A. & Baan, G. C. 2001a. Myofascial force transmission causes interaction between adjacent muscles and connective tissue: effects of blunt dissection and compartmental fasciotomy on length force characteristics of rat extensor digitorum longus muscle. *Arch Physiol Biochem* **109**, 97 - 109.

Huijing, P. A. & Baan, G. C. 2001b. Extramuscular myofascial force transmission within the rat anterior tibial compartment: proximo-distal differences in muscle force. *Acta Physiol Scand* **173**, 297-311.

Huijing, P. A. 2002. Intra-, extra-, and intermuscular myofascial force transmission of synergists and antagonists: effects of muscle length as well as relative position. *J Mech Med Biol* **2**, 405 - 419.

Huijing, P. A. 2003. Muscular force transmission necessitates a multilevel integrative approach to the analysis of function of skeletal muscle. *Exerc Sport Sci Rev* **31**, 167-175.

Huijing, P. A. & Baan, G. C. 2003. Myofascial force transmission: muscle relative position and length determine agonist and synergist muscle force. *J Appl Physiol* **94**, 1092 - 1107.

Huijing, P. A., Maas, H. & Baan, G. C. 2003. Compartmental Fasciotomy and Isolating a Muscle from neighboring muscles interfere with myofascial force transmission within the rat anterior crural compartment. *J Morphol* 306 - 321.

Huijing, P. A. (2004). Myotendinous and myofascial force transmission in skeletal muscle: An introduction to the symposium on force transfer. In *European Society of Biomechanics, Netherlands*, ed.

Huijing, P. A. & Jaspers, R. T. 2005. Adaptation of muscle size and myofascial force transmission: a review and some new experimental results. *Scand J Med Sci Sports* **15**, 349-380.

Huijing, P. A. 2007. Epimuscular myofascial force transmission between antagonistic and synergistic muscles can explain movement limitation in spastic paresis. *J Electromyogr Kinesiol* in press.

Huijing, P. A., van de Langenberg, R. W., Meesters, J. & Baan, G. C. 2007. Extramuscular myofascial force transmission also occurs between synergistic muscles and antagonistic muscles. *J Electromyogr Kinesiol* in press.

Hutchinson, J. R. 2001a. The evolution of femoral osteology and soft tissues on the line of extant birds (Neornithes). *Zool J Linn Soc* **131**, 169 - 197.

Hutchinson, J. R. 2001b. The evolution of pelvic osteology and soft tissues on the line to extant birds (Neornithes). *Zool J Linn Soc* **131**, 123 - 168.

Hutchinson, J. R. & Garcia, M. 2002. Tyrannosaurus was not a fast runner. *Nature* **415**, 1018-1021.

Jarvinen, T. A., Jozsa, L., Kannus, P., Jarvinen, T. L. & Jarvinen, M. 2002. Organization and distribution of intramuscular connective tissue in normal and immobilized skeletal muscles. An immunohistochemical, polarization and scanning electron microscopic study. *J Muscle Res Cell Motil* **23**, 245-254.

- References -

Jarvinen, T. A., Jozsa, L., Kannus, P. *et al.* 2003. Mechanical loading regulates the expression of tenascin-C in the myotendinous junction and tendon but does not induce de novo synthesis in the skeletal muscle. *J Cell Sci* **116**, 857-866.

Johnston, I. A. 1985. Sustained force development: specializations and variation among the vertebrates. *J Exp Biol* **115**, 239-251.

Julian, F. J. & Morgan, D. L. 1979. Intersarcomere dynamics during fixed-end tetanic contractions of frog muscle fibres. *J Physiol* **293**, 365-378.

Kawakami, Y. & Lieber, R. L. 2000. Interaction between series compliance and sarcomere kinetics determines internal sarcomere shortening during fixed-end contraction. *J Biomech* **33**, 1249-1255.

Kometani, K., Tsugeno, H. & Yamada, K. 1990. Mechanical and energetic properties of dystrophic (mdx) mouse muscle. *Jpn J Physiol* **40**, 541 - 549.

Kreulen, M., Smeulders, M. J., Hage, J. J. & Huijing, P. A. 2003. Biomechanical effects of dissecting flexor carpi ulnaris. *J Bone Joint Surg Br* **85**, 856-859.

Kreulen, M., Smeulders, M. J. & Hage, J. J. 2004. Restored flexor carpi ulnaris function after mere tenotomy explains the recurrence of spastic wrist deformity. *Clin Biomech (Bristol, Avon)* **19**, 429-432.

Kronecker, H. & Cash, T. 1880. Ueber die Beweglichkeit der Muskeln in ihrem naturlichen Zusammenhange. *Archiv fur Physiologie, Physiologische Abteilung des Archives fur Anatomie und Physiologie* 179- 180.

Lieber, R. L. 1997. Muscle fiber length and moment arm coordination during dorsi- and plantarflexion in the mouse hindlimb. *Acta Anatomica (Basel)* **159**, 84-89.

Locke, M. & Huie, P. 1972. The fiber components of insect connective tissue. *Tissue Cell* **4**, 601 - 612.

Lynch, G. S., Hinkle, R. T., Chamberlain, J. S., Brooks, S. V. & Faulkner, J. A. 2001. Force and power output of fast and slow skeletal muscles from *mdx* mice 6-28 months old. *J Physiol (Lond)* **535.2**, 591 - 600.

Maas, H., Baan, G. C. & Huijing, P. A. 2001. Intermuscular interaction via myofascial force transmission: effects of tibialis anterior and extensor hallucis longus length on force transmission from rat extensor digitorum longus muscle. *J Biomech* **34**, 927 - 940.

Maas, H., Baan, G. C., Huijing, P. A., Yucesoy, C. A., Koopman, B. H. & Grootenboer, H. J. 2003a. The relative position of EDL muscle affects the length of sarcomeres within muscle fibers: experimental results and finite-element modeling. *J Biomech Eng* **125**, 745-753.

Maas, H., Jaspers, R. T., Baan, G. C. & Huijing, P. A. 2003b. Myofascial force transmission between a single muscle head and adjacent tissues: length effects of head III of rat EDL. *J Appl Physiol* **95**, 2004-2013.

Maas, H., Yucesoy, C. A., Baan, G. C. & Huijing, P. A. 2003c. Implications of muscle relative position as a co-determinant of isometric muscle force: a review and some experimental results. *J Mech Med Biol* **3**, 145 - 168.

Maas, H., Baan, G. C. & Huijing, P. A. 2004. Muscle force is determined also by muscle relative position: isolated effects. *J Biomech* **37**, 99 - 110.

Maas, H. & Huijing, P. A. 2005. Myofascial force transmission in dynamic muscle conditions: effects of dynamic shortening of a single head of multi-tendoned rat extensor digitorum longus muscle. *Eur J Appl Physiol* **94**, 584-592.

Maas, H., Lehti, T. M., Tiihonen, V., Komulainen, J. & Huijing, P. A. 2005a. Controlled intermittent shortening contractions of a muscle-tendon complex: muscle fibre damage and effects on force transmission from a single head of rat EDL. *J Muscle Res Cell Motil* **26**, 259-273.

- References -

Maas, H., Meijer, H. J. M. & Huijing, P. 2005b. Intermuscular interaction between synergists in rat originates from both intermuscular and extramuscular myofascial force transmission. *Cells Tissues Organs* **181**, 38 - 50.

MacIntosh, B. R. & MacNaughton, M. B. 2005. The length-dependence of muscle active force: considerations for parallel elastic properties. *J Appl Physiol* **98**, 1666 - 1673.

Maglio, V. J. 1973. Origin and evolution of the Elephantidae. *Trans Am Phil Soc, new series* **63**, 1 - 149.

Maina, J. N. 1989. Scanning and transmission electron microscopic study of the tracheal air sac system in a grasshopper Chrotogonus senegalensis (Kraus) - Orthoptera: Acrididae:Pyrgomorphinae. *Anat Rec* **223**, 393 - 405.

Malaiya, R., McNee, A. E., Fry, E. L. C., Gough, M. & Shortland, A. P. 2007. The morphology of the medial gastrocnemius in typically developing children and children wiht spastic hemiplegic cerebral palsy. *J Electromyogr Kinesiol* in press.

Mao, J. R., Taylor, G., Dean, W. B. *et al.* 2002. Tenascin-X deficiency mimics Ehlers-Danlos syndrome in mice through alteration of collagen deposition. *Nat Genet* **30**, 421-425.

McGowan, C. 1982. The wing musculature of the Brown kiwi *Apteryx australis mantelli* and its bearing on ratite affinities. *J Zool* **197**, 173 - 219.

Meijer, H. J. M., Baan, G. C. & Huijing, P. A. 2006. Myofascial force transmission is increasingly important at lower forces: firing frequency-related length-force characteristics of rat extensor digitorum longus. *Acta Physiol (Oxf)* **186**, 185-195.

Meijer, H. J. M., Rijkelijkhuizen, J. M. & Huijing, P. A. 2007. Myofascial force transmission between antagonistic rat lower limb muscles: effects of single muscle or muscle group lengthening. *J Electromyogr Kinesiol* in press.

Mela, P., Veltink, P. H., Huijing, P. A., Salmons, S. & Jarvis, J. C. 2002. The optimal stimulation pattern for skeletal muscle is dependent on muscle length. *IEEE Trans Neural Syst Rehabil Eng* **10**, 85-93.

Monti, R. J., Roy, R. R. & Edgerton, V. R. 2001. Role of motor unit structure in defining function. *Muscle Nerve* **24**, 848-866.

Neter, J., Wasserman, W. & Kutner, M. E. 1990 *Applied linear statistic models: regression, analysis of variance and experimental design*. Irwin, Homewood, IL.

Nishimura, T., Hattori, A. & Takahashi, K. 1996a. Arrangement and identification of proteoglycans in basement membrane and intramuscular connective tissue of bovine semitendinosus muscle. *Acta Anat (Basel)* **155**, 257-265.

Nishimura, T., Ojima, K., Liu, A., Hattori, A. & Takahashi, K. 1996b. Structural changes in the intramuscular connective tissue during development of bovine semitendinosus muscle. *Tissue Cell* **28**, 527-536.

Passerieux, E., Rossignol, R., Chopard, A. *et al.* 2006. Structural organization of the perimysium in bovine skeletal muscle: Junctional plates and associated intracellular subdomains. *J Struct Biol* **154**, 206-216.

Pasternak, C., Wong, S. & Elson, E. 1995. Mechanical function of dystrophin in muscle cells. *J Cell Biol* **128**, 355-361.

Pastoret, C. & Sebille, A. 1993. Further aspects of muscular dystrophy in mdx mice. *Neuromuscul Disord* **3**, 471-475.

Paul, G. S. 2000. Limb design, function and running performance in ostric-mimics and tyrannosaurs. *Gaia* **15**, 257 - 270.

Pegoraro, E., Mancias, P., Swerdlow, S. H. *et al.* 1996. Congenital muscular dystrophy with primary laminin alpha2 (merosin) deficiency presenting as inflammatory myopathy. *Ann Neurol* **40**, 782-791.

- References -

Person, R. S. & Kudina, L. P. 1972. Discharge frequency and discharge pattern of human motor units during voluntary contraction of muscle. *Electroencephalogr Clin Neurophysiol* **32**, 471-483.

Petrof, B., Shrager, J. B., Stedman, H. H., Kelly, A. M. & Sweeney, H. L. 1993. Dystrophin protects the sarcolemma from stresses developed during muscle contraction. *Proc Natl Acad Sci U S A* **90**, 3710 - 3714.

Pollock, C. M. & Shadwick, R. E. 1994. Allometry of muscle, tendon, and elastic energy storage capacity in mammals. *Am J Physiol Regul Integr Comp Physiol* **266**, 1022 - 1031.

Pond, C. M. 1982. The importance of connective tissue within and in between muscles. *Behav Brain Sci* **5**, 562.

Rack, P. M. & Westbury, D. R. 1969. The effects of length and stimulus rate on tension in the isometric cat soleus muscle. *J Physiol (Lond)* **204**, 443 - 460.

Rando, R. A. 2001. The dystrophin-glycoprotein complex, cellular signaling, and the regulation of cell survival in te muscular dystrophies. *Muscle Nerve* **24**, 1575 - 1594.

Riewald, S. A. & Delp, S. L. 1997. The action of the rectus femoris muscle following distal tendon transfer: does it generate knee flexion moment? *Dev Med Child Neurol* **39**, 99-105.

Rijkelijkhuizen, J. M., Baan, G. C., de Haan, A., de Ruiter, C. J. & Huijing, P. A. 2005. Extramuscular myofascial force transmission for in situ rat medial gastrocnemius and plantaris muscles in progressive stages of dissection. *J Exp Biol* **208**, 129-140.

Rijkelijkhuizen, J. M., Meijer, H. J. M., Baan, G. C. & Huijing, P. A. 2007. Myofascial force transmission also occurs between antagonistic muscles located within opposite compartments of the rat lower hind limb. *J Electromyogr Kinesiol* in press.

Roszek, B. & Huijing, P. A. 1997. Stimulation frequency history alters length-force characteristics of fully recruited rat muscle. *J Electromyogr Kinesiol* **7**, 161 - 177.

Sacco, P., Jones, D. A., Dick, J. R. & Vrbova, G. 1992. Contractile properties and susceptibility to exercise-induced damage of normal and mdx mouse tibialis anterior muscle. *Clin Sci (Lond)* **82**, 227-236.

Sasaoka, T., Imamura, M., Araishi, K. *et al.* 2003. Pathological analysis of muscle hypertrophy and degeneration in muscular dystrophy in gamma-sarcoglycan-deficient mice. *Neuromuscul Disord* **13**, 193-206.

Schweitzer, M. H., Suo, Z., Avci, R. *et al.* 2007. Analyses of soft tissue from Tyrannosaurus rex suggest the presence of protein. *Science* **316**, 277-280.

Sicinski, P., Geng, Y., Ryder-Cook, A. S., Barnard, E. A., Darlison, M. G. & Barnard, P. J. 1989. The molecular basis of muscular dystrophy in the mdx mouse: a point mutation. *Science* **244**, 1578-1580.

Smeulders, M. J., Kreulen, M., Hage, J. J., Baan, G. C. & Huijing, P. A. 2002. Progressive surgical dissection for tendon transposition affects length-force characteristics of rat flexor carpi ulnaris muscle. *J Orthop Res* **20**, 863-868.

Smeulders, M. J. & Kreulen, M. 2007. Myofascial force transmission and tendon transfer for patients suffering from spastic paresis: A review and some new observations. *J Electromyogr Kinesiol*

Solomonow, M. & Krogsgaard, M. 2001. Sensorimotor control of knee stability. A review. *Scand J Med Sci Sports* **11**, 64-80.

Stephenson, D. G. & Williams, D. A. 1982. Effects of sarcomere length on the force-pCa relation in fast- and slow-twitch skinned muscle fibers from the rat. *J Physiol (Lond)* **333**, 637 - 653.

- References -

Stephenson, D. G. & Wendt, I. R. 1984. Length dependence of changes in sarcoplasmic calcium concentration and myofibrillar calcium sensitivity in striated muscle fibers. *J Muscle Res Cell Motil* **5**, 243 - 272.

Street, S. F. & Ramsey, R. W. 1965. Sarcolemma: Transmitter of active tension in frog skeletal muscle. *Science* **149**, 1379 - 1380.

Street, S. F. 1983. Lateral transmission of tension in frog myofibers: a myofibrillar network and transverse cytoskeletal connections are possible transmitters. *J Cell Phys* **114**, 346-364.

Sumida, S. S. 1989. The appendicular skeleton of the early permian genus *Labidosaurus* (Reptilia, Captorhinomorpha, Captorhinidae) and the hind limb musculature of captorhinid reptiles. *J Vert Pal* **9**, 295 - 313.

Tidball, J. G. 1991. Force transmission across muscle cell membranes. *J Biomech* **24**, 43-52.

Tiegs, O. W. 1955. The flight muscles of insects - their anatomy and histology; with some observations on the structure of striated muscle in general. *Philos Trans R Soc Lond B Biol Sci* **238**, 221 - 348.

Tinsley, J., Deconinck, N., Fisher, R. *et al.* 1998. Expression of full-length utrophin prevents muscular dystrophy in *mdx* mice. *Nat Med* **4**, 1441 - 1444.

Trotter, J. A., Hsi, K., Samora, A. & Wofsy, C. 1985. A morphometric analysis of the muscle-tendon junction. *Anat Rec* **213**, 26-32.

Trotter, J. A. 1990. Interfiber tension transmission in series-fibered muscles of the cat hindlimb. *J Morphol* **206**, 351-361.

Trotter, J. A. & Purslow, P. P. 1992. Functional morphology of the endomysium in series fibered muscles. *J Morphol* **212**, 109-122.

Trotter, J. A. 2002. Structure-function considerations of muscle-tendon junctions. *Comp Biochem Physiol A Mol Integr Physiol* **133**, 1127-1133.

Vleeming, A., Pool-Goudzwaard, A. L., Stoeckart, R., van Wingerden, J. P. & Snijders, C. J. 1995. The posterior layer of the thoracolumbar fascia. Its function in load transfer from spine to legs. *Spine* **20**, 753-758.

Weis-Fogh, T. 1956. Biology and Physics of Locust Flight. II. Flight performance of the desert locust (Schistocerca gregaria). *Philos Trans R Soc Lond B Biol Sci* **239**, 459 - 510.

Wilczak, C. 1998. Consideration of sexual dimorphism, age and asymmetry in quantititative measuremetns of muscle insertion sites. *Int J Osteoarchaeol* **8**, 311 - 325.

Willems, M. E. & Huijing, P. A. 1994. Heterogeneity of mean sarcomere length in different fibres: effects on length range of active force production in rat muscle. *Eur J Appl Physiol Occup Physiol* **68**, 489-496.

Williams, M. W. & Bloch, R. J. 1999. Extensive but coordinated reorganization of the membrane skeleton in myofibres of dystrophic (*mdx*) mice. *J Cell Biol* **144**, 1259 - 1270.

Wilson, D. M. 1962. Bifunctional muscles in the thorax of grasshoppers. *J Exp Biol* **39**, 669 - 677.

Witmer, L. M. 1995 The extant phylogenetic bracket and the importance of reconstructing soft tissues in fossils. In: J. J. Thomason (eds) *Functional morphology in vertebrate paleontology*, pp. 19 - 33. Cambridge University Press, Cambridge, U.K.

Yucesoy, C. A., Koopman, B. H., Huijing, P. A. & Grootenboer, H. J. 2002a. Three-dimensional finite element modeling of skeletal muscle using a two-domain approach: linked fiber-matrix mesh model. *J Biomech* **35**, 1253-1262.

Yucesoy, C. A., Maas, H., Koopman, H. F. J. M., Grootenboer, H. J. & Huijing, P. A. 2002b. Finite element modeling of the effects of relative position of a muscle with intact extramuscular connections. *J Mech Med Biol* **2**,

Yucesoy, C. A., Koopman, B. H., Baan, G. C., Grootenboer, H. J. & Huijing, P. A. 2003a. Effects of inter- and extramuscular myofascial force transmission on adjacent synergistic muscles: assessment by experiments and finite-element modeling. *J Biomech* **36**, 1797-1811.

Yucesoy, C. A., Koopman, B. H. F. J. M., Baan, G. C., Grootenboer, H. J. & Huijing, P. A. 2003b. Extramuscular Myofascial Force Transmission: Experiments and Finite Element Modeling. *Arch Physiol Biochem* **111**, 377 - 388.

Yucesoy, C. A., Koopman, B. H. F. J. M., Baan, G. C., Grootenboer, H. J. & Huijing, P. A. (2003c). Inter- and extramuscular myofascial force transmission function as a major determinant of muscle force and length range of force exertion. In *International Society of Biomechanics XIXth Congress*, ed. P. Milburn, B. Wilson & T. Yanai, Dunedin, New Zealand

Yucesoy, C. A., Baan, G. C., Koopman, B. H. F. J. M., Grootenboer, H. J. & Huijing, P. A. 2005. Pre-strained epimuscular connections cause muscular myofascial force transmission to affect properties of synergistic EHL and EDL muscles of the rat. *J Biomech Eng* **127**, 819 - 828.

Yucesoy, C. A., Maas, H., Koopman, B. H., Grootenboer, H. J. & Huijing, P. A. 2006. Mechanisms causing effects of muscle position on proximo-distal muscle force differences in extra-muscular myofascial force transmission. *Med Eng Phys* **28**, 214-226.

Yucesoy, C. A. & Huijing, P. A. 2007. Substantial effects of epimuscular myofascial force transmission on muscular mechanics have major implications on spastic muscle and remedial surgery. *J Electromyogr Kinesiol* in press.

Zumwalt, A. 2006. The effect of endurance exercise on the morphology of muscle attachment sites. *J Exp Biol* **209**, 444-454.

Summary & Samenvatting

Aspects of epimuscular myofascial force transmission; a physiological, pathological and comparative-zoological approach

In addition to the transmission of muscle force via the sarcomeres in series and the myotendinous junction (myotendinous force transmission), muscle force can also be transmitted via non-myotendinous connective tissue pathways. Such transmission is referred to as myofascial force transmission. In this thesis, physiological, pathological and comparative-zoological aspects of myofascial force transmission are investigated.

The purpose of **Chapter 2** is to study the origin of mechanical interactions between rat extensor digitorum longus muscle (EDL) and the tibialis anterior and extensor hallucis longus muscles (TA+EHL). EDL is kept at a constant muscle-tendon complex length, while the TA+EHL complex is lengthened distally. Intermuscular interaction is tested in two conditions: (1) after full longitudinal compartmental fasciotomy, and (2) after blunt dissection of the intermuscular connective tissues between EDL and the TA+EHL complex. In the initial condition, distal lengthening of the TA+EHL complex decreases distal EDL active force by 11.8% and increases proximal EDL active force by 9.5%. After blunt dissection, TA+EHL and EDL distal active forces are decreased at low TA+EHL lengths, whereas proximal EDL active force is decreased for all TA+EHL lengths. It is concluded that mechanical interaction between synergists originates from both inter- and extramuscular myofascial pathways, but the highest contribution should be ascribed to the latter one.

In **Chapter 3**, effects of submaximal stimulation frequencies on myofascial force transmission are investigated for anterior crural muscles within the rat lower limb. The TA+EHL complex is kept at a constant length while (EDL) is lengthened distally. All muscles are activated simultaneously at 10, 20, 30 and 100 Hz. At all firing frequencies studied, proximally and distally measured EDL forces differe significantly. Absolute EDL proximo-distal active force difference are highest at 100 Hz ($\Delta Fma_{dist-prox}$ = 0.4N), whereas the normalized difference (i.e. the fraction of force transmitted myofascially) increases with progressively lower firing frequencies (30% of F_{dist} at 10 Hz vs. 15% at 100 Hz). Also, TA+EHL complex active isometric force decreases with increasing distal EDL length. The highest absolute decrease is found at 100 Hz, but the highest normalized decrease is found at 10 Hz. It is concluded that low firing frequencies as encountered *in vivo* enhance the relative importance of epimuscular myofascial force transmission with respect to myotendinous force transmission.

In **Chapter 4,** effects of lengthening of the whole group of anterior crural muscles on myofascial force transmission between synergistic EDL and TA+EHL complex, as well as on myofascial force transmission between anterior crural and antagonistic peroneal muscles are investigated. The peroneal complex is left at a constant length, whereas EDL and TA+EHL are lengthened simultaneously. The lengthening of all anterior crural muscles significantly alters the curve for the EDL proximo-distal active force difference; at all muscle lengths, a distally directed net load is exerted onto EDL. This distally directed net load decreases with increasing

anterior crural muscle length. Also, despite being kept at a constant length, distal peroneal force decreases by 26% of the initial force as a function of distal lengthening of all anterior crural muscles. It was concluded that lengthening of all anterior crural muscles alters the epimuscular load exerted on EDL, and increases the effects of extramuscular myofascial force transmission on antagonists.

Chapter 5 describes the effects of firing frequency on the above described effects of muscle group lengthening on myofascial force transmission between synergists and between antagonistic muscles. The peroneal complex and triceps surae muscles are left at a constant length, whereas EDL and TA+EHL are lengthened simultaneously. All muscles are activated simultaneously at 10, 20, 30 and 100 Hz. At low firing frequencies, the distally directed net myofascial load on EDL is reduced. However, EDL as well as TA+EHL complex length-force characteristics at low firing frequency are altered from those described for fully dissected muscles; especially at 10 Hz stimulation, active forces at the ascending limb of the length-force curve are higher and optimum muscle length occurs at a lower muscle length than expected. In addition, effects of extramuscular myofascial force transmission on antagonistic peroneal and triceps surae muscles are substantial at low firing frequencies. It is concluded that also for lengthening of all anterior crural muscles, effects of myofascial force transmission on EDL as well as antagonists are substantial.

In Duchenne Muscular Dystrophy (DMD), the absence of dystrophin, a protein thought to play a role in stabilization of the membrane during shear stress, results in severe muscle degeneration and ultimately death. In contrast to human patients, dystrophin-deficient *mdx* mice show elevated levels of utrophin, a dystrophin homologue, and a less severe phenotype. In **Chapter 6**, the hypothesis is tested that in *mdx* mice, epimuscular myofascial force transmission is decreased due to less stiff intramuscular myofascial pathways. In healthy and *mdx* mice, EDL is distally lengthened and the TA+EHL is kept at a constant length. For dystrophic mice, the net myofascial load exerted on EDL is at least as large as in healthy controls. Also distal TA+EHL active force decreases significantly as a function of distal EDL length in control and *mdx* mice, with the largest decrease found in *mdx* mice. It is concluded that epimuscular myofascial force transmission in *mdx* mice is not decreased. However, it remains unclear what causes the observed muscle pathologies.

In **Chapter 7**, it is investigated whether effects of myofascial force transmission are smaller within smaller animals. Therefore, effects of the TA+EHL complex length are studied in both the rat and mice. EDL was lengthened distally while the TA+EHL complex was either left at a length at which it exerted zero active force, or brought to a corresponding length (as determined by previously placed markers) . Also for the mouse, effects of TA+EHL complex length on EDL active forces are substantial; synergistic muscle length is also a co-determinant for EDL forces in the mouse. However, at high muscle lengths, the normalized proximo-distal force differences in mouse EDL active force are higher (40%– 60% of distal optimum active force) than any normalized proximo-distal force difference found for the rat (maximally 35%). It is considered conceivable that interspecies

differences in myotendinous and myofascial pathways between the rat and the mouse exist, which cause smaller animals to have relatively stiffer myofascial pathways.

Pond (1982) suggested that insects have very little intermuscular connective tissue, which would suggest that within this group of animals, myofascial force transmission is of less importance. In **Chapter 8**, the presence and extent of myofascial force transmission in the flight muscles of the migratory locust is investigated. Active and passive forces measured at the ventral origin and dorsal insertion of the muscle differ significantly. Ventrally and dorsally measured passive forces differ as a function of muscle length and the position of the muscle relative to surrounding tissues. It is concluded that myofascial force transmission is present in locusts and may be of relevance in flying and walking. Therefore, the occurrence of myofascial force transmission in an invertebrate species suggests that is a conserved and evolutionary functional design.

The final chapter of this thesis, **Chapter 9**, discusses the experimental results of this thesis, as well as their implications regarding our understanding of healthy and pathological muscles. In addition, the possible evolutionary origin and consequences of myofascial force transmission will be dealt with. Finally, in an attempt to integrate multiple scientific disciplines, the role of myofascial force transmission in reconstructing animals long gone extinct (the field of vertebrate palaeontology, a major interest of the author) are explored.

Aspecten van epimusculaire myofasciale krachttransmissie; een fysiologische, pathologische en vergelijkend-zoologische benadering

Naast de transmissie van spierkracht via de sarcomeren in series en de myotendineuze junctie (myotendineuze krachttransmissie), kan spierkracht ook worden overgedragen via niet-tendineuze bindweefsel paden. Dit noemt men myofasciale krachttransmissie. In dit proefschrift worden een aantal fysiologische, pathologische en vergelijkend-zoologische aspecten van myofasciale krachttransmissie bestudeerd.

Het doel van **Hoofdstuk 2** is het bestuderen van de origine van de mechanische interactie tussen de extensor digitorum longus (EDL) en tibialis anterior en extensor hallucis longus (TA+EHL) spier complex. De spier-pees complex lengte van EDL wordt constant gehouden, terwijl het TA+EHL complex verlengd werd aan de distale zijde. Intermusculaire myofasciale interactie werd bestudeerd in twee condities: (1) na volledige longitudinale fasciotomy, en (2) na blunt dissection van de intermusculaire bindweefsel structuren tussen EDL en TA+EHL spier complex. In de eerste conditie daalt de distaal gemeten actieve EDL kracht met 11.8% als gevolg van het distaal verlengen van het TA+EHL spiercomplex. De proximaal gemeten actieve EDL kracht stijgt met 9.5%. Na blunt dissection dalen de distale actieve krachten van EDL en het TA+EHL spiercomplex gemeten op lage lengtes van het TA+EHL spiercomplex, terwijl de proximaal gemeten actieve EDL kracht voor alle lengtes van het TA+EHL spiercomplex daalt. We concluderen dat de mechanische interactie tussen synergisten voortkomt uit zowel inter- als extramusculaire myofasciale paden, maar dat de hoogste bijdrage moet worden toegeschreven aan het laatste pad.

In **Hoofdstuk 3** worden de effecten van submaximale vuurfrequentie op myofasciale krachttransmissie tussen spieren uit het anterior cruraal compartiment van de rat bestudeerd. Het TA+EHL spiercomplex blijft nu op een constante lengte terwijl de EDL distaal wordt verlengd. Alle spieren zijn simultaan actief op achtereenvolgend 10, 20, 30 en 100 Hz. Voor elke vuurfrequentie worden significante verschillen tussen de distaal en proximaal EDL krachten, een indicatie voor myofasciale krachttranmissie, gemeten. Het absolute proximo-distale verschil in actieve EDL kracht is het grootst op 100 Hz ($\Delta Fma_{dist-prox}$ = 0.4N), maar het genormaliseerde proximo-distale verschil in actieve EDL kracht (de fractie van de kracht die overgedragen wordt via myofasciale paden) neemt toe op lagere vuurfrequentie (30% van F_{dist} op 10 Hz vs. 15% op 100 Hz). De actieve kracht van het TA+EHL spiercomplex daalt als gevolg van distale verlenging van de EDL. De grootste daling in actieve TA+EHL kracht vindt plaats op 100 Hz, maar de grootste genormaliseerde daling vindt plaats op 10 Hz. Deze bevindingen hebben geleid tot de conclusie dat op lage vuurfrequenties, zoals die ook voorkomen *in vivo*, epimusculaire myofasciale krachttransmissie relatief belangrijker wordt ten opzichte van myotendineuze krachttransmissie.

In **Hoofdstuk 4** zijn de effecten beschreven van het verlengen van een groep van anterior crurale spieren op myofasciale krachttransmissie tussen de EDL en het TA+EHL spiercomplex, en op myofasciale krachttransmissie tussen anterior crurale spieren en het antagonistische peroneus spiercomplex. De EDL en het

TA+EHL spiercomplex worden simultaan verlengd, terwijl het peroneus spiercomplex op een constante lengte werd gehouden. Als gevolg van het verlengen van alle anterior crurale spieren verandert de curve van het proximo-distale verschil in actieve EDL kracht; op elke spierlengte wordt een netto distaal gerichte kracht op de EDL uitgeoefend. Deze distaal gerichte netto kracht neemt af met toenemende lengte van de anterior crurale spieren. Ondanks het feit dat het peroneus spiercomplex op een constante lengte wordt gehouden, daalt de distaal gemeten peroneus kracht met 26% van het beginniveau als gevolg van het verlengen van alle anterior crurale spieren. Er wordt geconcludeerd dat als gevolg van het verlengen van alle anterior crurale spieren, de epimusculaire krachten uitgeoefend op EDL veranderen. De effecten van extramusculaire myofasciale krachttransmissie op antagonistische spieren neemt toe.

Hoofdstuk 5 beschrijft de effecten van vuurfrequentie op de myofasciale krachttransmissie tussen synergisten en antagonisten voor verlenging van alle anterior crurale spieren. Het peroneus spiercomplex en de triceps surae spieren worden op een constante lengte gehouden, terwijl de EDL en het TA+EHL spiercomplex simultaan distaal verlengd worden. Alle spieren worden gelijktijdig geactiveerd op achtereenvolgend 10, 20, 30 en 100 Hz. Op lage vuurfrequenties neemt de distale gerichte myofasciale kracht op EDL af. Ondanks deze schijnbaar kleine myofasciale kracht op EDL, vertonen de lengte-kracht karakteristieken van zowel EDL als het TA+EHL spiercomplex afwijkingen in vergelijking met de lengte-kracht karakteristieken van geïsoleerde spieren. In het bijzonder voor 10 Hz is de actieve kracht op het stijgende deel van de lengte-kracht relatie hoger, en schuift optimum spierlengte naar een lagere lengte, in vergelijking met geïsoleerde spieren. Ook de antagonistische peroneus spiercomplex en triceps surae spieren vertonen significante effecten van extramusculaire myofasciale krachttransmissie; op alle vuurfrequenties daalt zowel de peroneus als triceps surae actieve kracht, ondanks het feit dat ze op een constante spier-pees complex werden gehouden. De conclusie is dan ook dat ook op lage vuurfrequenties substantiële epimusculaire myofasciale krachttransmissie op de EDL, alsmede tussen antagonisten bestaat als gevolg van het verlengen van alle anterior crurale spieren.

In Duchenne Muscular Dystrophy (DMD) leidt de afwezig van dystrophine, een eiwit dat wordt gedacht een rol te spelen bij het stabiliseren van het membraan tijdens afschuifstress, tot spierdegeneratie and uiteindelijk een vroege dood. In tegenstelling tot menselijke DMD patiënten, vertonen dystrophine-deficiënte *mdx* muizen verhoogde niveaus van utrophin, een homoloog van dystrophine. Ook de symptomen van de ziekte zijn minder erg dan in menselijke DMD patiënten. In **Hoofdstuk 6** wordt de hypothese getest dat in *mdx* muizen, epimusculaire krachttransmissie lager is als gevolg van minder stijve intramusculaire myofasciale paden door het ontbreken van dystrophine. Deze hypothese wordt getest door in gezonden muizen als in *mdx* muizen de EDL distaal te verlengen, terwijl het TA+EHL spiercomplex op een constante lengte wordt gehouden. In *mdx* muizen bleek dat de epimusculaire myofasciale kracht op EDL minstens net zo groot is als in gezonde muizen. Voor het TA+EHL spiercomplex blijkt dat de

daling in kracht als gevolg van het distaal verlengen van de EDL in *mdx* muizen zelfs groter is dan in gezonde muizen. Epimusculaire myofasciale krachttransmissie is dus niet lager in *mdx* muizen in vergelijking met gezonde muizen, en de geobserveerde spierdegeneratie in *mdx* muizen kunnen niet verklaard worden door minder epimusculaire krachttransmissie.

In **Hoofdstuk 7** wordt onderzocht of de effecten van epimusculaire myofasciale krachttransmissie kleiner zijn in kleinere dieren. Daarvoor worden de effecten van de lengte van het TA+EHL spiercomplex op epimusculaire krachttransmissie op de EDL onderzocht in de rat en de muis. De lengte-kracht karakteristieken van de EDL worden daarom bepaald in twee condities: (1) terwijl het TA+EHL spiercomplex of op een zeer korte spierlengte gehouden wordt zodat de actieve TA+EHL kracht nul is, en (2) terwijl het TA+EHL spiercomplex simultaan met de EDL distaal verlengd word. De effecten van de lengte van het TA+EHL spiercomplex zijn ook substantieel in de muis, en dus ook voor de muis geld dat synergist lengte een co-determinant is voor spierkracht. Op hoge spierlengte is het genormaliseerde proximo-distale verschil in actieve EDL kracht (40% - 60% van distale optimum kracht) hoger dan elk genormaliseerd proximo-distale verschil in actieve EDL kracht ooit gevonden in de rat (maximaal 35%) . Het wordt daarom niet onwaarschijnlijk geacht dat er verschillen bestaan in de myotendineuze en myofasciale paden tussen de rat en de muis, waardoor kleinere dieren relatief stijvere myofasciale paden bezitten.

In 1982 suggereerde Pond dat insecten weinig tot geen intermuscular bindweefsel bezaten. Dit zou betekenen dat in insecten, myofasciale krachttransmissie een minder grote rol zou spelen. In **Hoofdstuk 8** wordt de aanwezigheid en grootte van myofasciale krachttransmissie in de woestijnsprinkhaan bestudeerd. Actieve en passieve kracht gemeten aan de dorsale en ventrale aanhechtingen van een van de vliegspieren zijn significant verschillend en duiden op myofasciale krachtoverdracht. De ventraal en dorsaal gemeten passieve krachten verschillen als een functie van zowel spierlengte als de positie van de spier t.o.v. omringend weefsel. We concluderen daarom dat myofasciale krachttransmissie ook voorkomt bij insecten en dat het misschien voordelig kan zijn tijdens vliegen en lopen. Dit is de eerste keer dat myofasciale krachttransmissie is aangetoond in een ongewerveld dier, en men kan de conclusie trekken dat myofasciale krachttransmissie een evolutionair geconserveerd mechanisme is.

In het laatste hoofdstuk van dit proefschrift, **Hoofdstuk 9**, worden de experimentele resultaten uit dit proefschrift, evenals hun implicaties voor ons begrip van gezonde en pathologische spieren besproken. Daarnaast wordt ingegaan op de mogelijke evolutionaire oorsprong en voordelen van myofasciale krachttransmissie. Tenslotte wordt, in een poging om meerdere wetenschappelijke disciplines te verenigen, de mogelijkheden van myofasciale krachttransmissie in de reconstructies van lang uitgestorven dieren (een grote interesse van de auteur) besproken.

Dankwoord

In de afgelopen jaren hebben veel mensen op allerlei manieren bijgedragen aan het goede verloop van mijn onderzoek alswel aan mijn persoonlijke welbevinden.

Allereerst mijn promotor Peter Huijing. Peter, jouw kennis van anatomie en je aanstekelijke enthousiasme voor het spieronderzoek zijn een enorme motivatie geweest tijdens mijn promotietraject. Na onze wekelijkse besprekingen kwam ik dan ook vaak weer met frisse moed naar buiten. Aan je kritische blik ontsnapte niets e. Ik waardeer het heel erg dat je mij de ruimte gegeven om, na de eerste stappen in het promotietraject die vanaf het begin vast lagen, mijn eigen ideeën en interesses binnen het onderzoek te ontwikkelen. Wie had ooit gedacht dat je een proefschrift over myofasciale krachttransmissie zou kunnen afsluiten met een discussie over *Tyrannosaurus rex*!

Guus Baan, zonder jou waren veel van mijn experimenten simpelweg niet mogelijk geweest. Jouw jarenlange ervaring in de praktische kant van het spieronderzoek, je vakkundigheid en niet te vergeten creativiteit en improvisatievermogen hebben ervoor gezorgd dat mijn experimenten allemaal succesvol zijn afgerond. Menig experiment wat dreigde te mislukken werd door jou tot een goed einde geleid.

Ondanks het feit dat Guus me de geheimen van solderen en schroefdraad tappen onthulde, had ik nooit zonder de hulp van de volgende mensen mijn opstellingen in elkaar kunnen knutselen. Frans den Boer, bedankt voor je ondersteuning van ons project en het soms op het laatste moment uitvoeren van veranderingen aan meetapparatuur. Erik Clay, bedankt voor de verbeterde programmatuur voor het uitvoeren van onze metingen. Peter Verdijk, bedankt voor je hulp bij het DAV programma. Henk Cretier van de instrumenten makerij, bedankt voor het fabriceren van alle balken, staven, blokjes en voetjes van onze opstellingen. Tinelies Busé-Pot wil ik graag bedanken voor haar steun tijdens verdovingsperikelen. Veel dank ben ik ook verschuldigd aan de medewerkers van het UPC voor hun hulp en flexibiliteit bij de huisvesting van mijn proefdieren.

Judith van Deutekom en Sjef de Kimpe van Prosensa Holding B.V. wil ik graag bedanken voor het delen van hun kennis over Duchenne spierdystrofie en *mdx* muizen, hun advies over de experimenten uit hoofdstuk 6, en de inspiratie die voortkwam uit onze gesprekken hierover.

Mijn (oud)kamergenootjes kan ik niet genoeg bedanken voor de gezelligheid en broodnodige ontspanning tijdens en naast het soms frustrerende promotieonderzoek. Josina, Marijke, Ronald, Teatske, Astrid en Jan-Willem, vele uurtjes werden gevuld met het bediscussiëren van promotieperikelen. Maar de dingen die ik me het meest zal herinneren zijn gelukkig luchtiger van aard, zoals de kerstklassieker-singalong, het uitvoerig bespreken van de dramatische levens van Net 5 personages, en gelukkig heel erg veel grappen en grollen. Jongens, ontzettend bedankt voor de leuke en gezellige tijd en jullie steun in donkere dagen, ik zal jullie missen! Ook de mede-koffiedrinkers van het lab op de 4[de] etage, bedankt voor de gezelligheid.

Ook buiten de VU waren er veel mensen begaan met mij en mijn promotietraject. Allereerst John de Vos. Beste John, mijn wetenschappelijke vorming is ooit bij jou begonnen, en je bent me altijd tot voorbeeld geweest. Als ik mijn spieronderzoek eens helemaal zat was, was er altijd tijd om met een kopje koffie eens lekker over fossielen te praten. Ik ben dan ook erg blij dat je, als vertegenwoordiger van de paleontologie-wereld, zitting neemt in mijn opponentencommissie! Ook de rest van het bestuur en de leden van de Werkgroep Pleistocene Zoogdieren (WPZ) wil ik graag bedanken voor de gezelligheid en hun interesse in het wel en wee van mijn onderzoek. André Veldmeijer en Erno Endenburg, bedankt voor alle gezellige en hilarische etentjes waar de drank altijd rijkelijk vloeide, de soms felle discussies over wetenschap en natuurlijk de inspiratie voor onze ambitieuze onderzoeksprojecten. Ik hoop nog lang samen met jullie PalArch te maken. Lieve Minke, ik vind het altijd weer leuk om met jouw vrolijke persoontje af te spreken! Peter, we zijn inmiddels Klik 8 ver ontgroeid, maar je blijft mijn favoriete oud-huisgenoot! En zonder jou was hoofdstuk 6 er nooit geweest. Penny, Monique en Janine, eens *fabulous,* altijd *fabulous!*

Een bijzonder dank je wel voor groep van biologen en adoptiebiologen die zich de afgelopen jaren als een schijnbaar zooitje ongeregeld toch elke vrijdagmiddag weer wist te verzamelen rond een tafel in het Keizertje, en met wie ik vele kerstborrels, barbecues, foute dansavondjes en voetbalwedstrijdjes heb doorgebracht. De vrijdagmiddag is voor mij uitgegroeid tot een moment waarop ik alle werkstress van me af kan laten glijden en kan genieten van de mensen om me heen. Marieke, Chris, Ilse, Patrick, Ira, Merijn, Arjan, Eugenia, Jon, Donna, Danielle, Remco, Machteld, Erik, Vincent, Daniël, Chamindi, Chris S., Monique, Marjolein en Barbara, bedankt!! Zonder jullie waren de afgelopen vier jaar een stuk minder leuk geweest. Hopelijk mag deze traditie nog lang blijven voortbestaan! En lieve Marieke, na 9 jaar vol vriendschap en ontzettend veel plezier ben ik heel erg blij dat je mijn paranimf wilt zijn!

Lieve pap en mam en Marloes en Roel, jullie zijn altijd heel erg geïnteresseerd geweest in wat ik deed, en dat was tijdens de afgelopen jaren niet anders. Bedankt voor al jullie steun en liefde! Mijn lieve Urville, je was, bent en blijft de stille kracht achter mij.

List of publications

van den Bergh, G.D., **Meijer, H.J.M.**, Rokus Due Awe, Szabó, K., van den Hoek Ostende, L.W., Morwood, M.J., Sutikna, T., Saptomo, E.W., Piper, P. & Dobney, K.M. 2007. The Liang Bua faunal remains: a 95 kyr sequence from Flores, East Indonesia. The Journal of Human Evolution, *accepted for publication.*

Veldmeijer, A.J., Signore, M. & **Meijer, H.J.M**., 2007. Description of two pterosaurian (Pterodactyloidae) from the lower Cretaceous of Brazil. DEINSEA, *accepted for publication*

Meijer, H.J.M., Rijkelijkhuizen, J.M. & Huijing, P.A. 2007. Myofascial force transmission between antagonistic rat lower limb muscles: effects of single muscle or muscle group lengthening. Journal of Electromyography and Kinesiology, *in press.*

Rijkelijkhuizen, J.M., **Meijer, H.J.M.**, Baan, G.C. & Huijing, P.A., 2007. Myofascial force transmission also occurs between antagonistic muscles located within opposite compartments of the rat lower hind limb. Journal of Electromyography and Kinesiology, *in press.*

Meijer, H.J.M., Baan, G.C. & Huijing, P.A., 2006. Myofascial force transmission is increasingly important at lower forces: firing frequency-related length-force characteristics of rat extensor digitorum longus. Acta Physiologica (Oxford) 186: 185 – 195.

van Geel, B., van de Steeg, J.F. & **Meijer, H.J.M.**, 2006. Flora en fauna van 'Holt und Haar'; gegevens uit een Weichseliën-groeve gecombineerd. Cranium 23(2): 15 – 24.

Veldmeijer, A.J., **Meijer, H.J.M**. & Signore, M., 2006. *Coloborhynchus* from the Lower Cretaceous Santana Formation, Brazil (Pterosauria, Pterodactyloidae, Anhangueridae), and update. PalArch's Journal of Vertebrate Paleontology 3(2).

Veldmeijer, A.J., Signore, M.& **Meijer, H.J.M**., 2005. *Brasileodactylus*, (Pterosauria, Pterodactyloidae, Anghangueridae), an update. Cranium 22(1): 45 – 56.

Maas, H., **Meijer, H.J.M.** & Huijing, P.A., 2005. Intermuscular interaction between synergists in rat originates from both intermuscular and extramuscular myofascial force transmission. Cells Tissues Organs 181: 38 – 50.

Veldmeijer, A.J., Signore, M. & **Meijer, H.J.M.**, 2005. Description of two pterosaur (Pterodactyloidae) mandibles from the lower Cretaceous Santana Formation, Brazil. DEINSEA 11: 67 – 86.

Meijer, H.J.M., 2004. The first record of birds from Mill (the Netherlands). PalArch's Journal of Vertebrate Palaeontology 1(2).

Dutta, H. & **Meijer, H.J.M.**, 2003. Sublethal effects of the pesticide Diazinon on the structure of the testis of bluegill, *Lepomis macrochirus*: A microscopic analysis. Environmental Pollution 125: 355 – 360.

Meijer, H.J.M., 2002. Pleistocene vogels; de ornithofauna van 'Holt und Haar' (Dld.) Cranium 19(2): 135 – 145.

Meijer, H.J.M., 2001. Mammoeten moeten ook drinken. Een nieuwe visie op een laat-Pleistoceen ecosystem. Cranium 18(2): 17 – 26.

Abstracts

Meijer, H.J.M., Rijkelijkhuizen, J.M. & Huijing, P.A., 2007. Effects of single muscle or muscle group lengthening on myofascial force transmission between synergists and antagonists. Proceedings of the XXIth Congress of the International Society of Biomechanics, Taipei, Taiwan.

Maas, H., **Meijer, H.J.M**. & Huijing, P.A., 2005. The origin of mechanical interactions between adjacent synergists in rat. Proceedings of the XXth Congress of the International Society of Biomechanics, Cleveland, USA.

Meijer, H.J.M., Baan, G.C. & Huijing, P.A., 2005. Myofascial force transmission is more important at low-frequency stimulation. Proceedings of the XXth Congress of the International Society of Biomechanics, Cleveland, USA.